



UNIVERSIDADE FEDERAL DO RIO GRANDE DO SUL
FACULDADE DE FARMÁCIA
PROGRAMA DE PÓS-GRADUAÇÃO EM CIÊNCIAS FARMACÊUTICAS



ÉCOLE DOCTORALE PICARDIE SCIENCES ET SANTÉ
UNIVERSITÉ DE PICARDIE JULES VERNE
FACULTÉ DE PHARMACIE

Planejamento e Síntese de Novos Compostos Derivados
de Agliconas Triterpênicas de Espécies de *Ilex* visando à
Atividade Antimalárica

Tese

Simone Cristina Baggio Gnoatto

PORTO ALEGRE, 2007.



UNIVERSIDADE FEDERAL DO RIO GRANDE DO SUL
FACULDADE DE FARMÁCIA
PROGRAMA DE PÓS-GRADUAÇÃO EM CIÊNCIAS FARMACÊUTICAS



ÉCOLE DOCTORALE PICARDIE SCIENCES ET SANTÉ
UNIVERSITÉ DE PICARDIE JULES VERNE
FACULTÉ DE PHARMACIE

Planejamento e Síntese de Novos Compostos Derivados
de Agliconas Triterpênicas de Espécies de *Ilex* visando à
Atividade Antimalárica

Tese apresentada por

Simone Cristina Baggio Gnoatto

para obtenção do GRAU DE DOUTOR

em Ciências Farmacêuticas

Orientadores: Prof. Dr. Grace Gosmann

Prof. Dr. Pascal Sonnet

PORTO ALEGRE, 2007.

Thesis presented at Programa de Pós-graduação em Ciências Farmacêuticas -
Faculdade de Farmácia - Universidade Federal do Rio Grande do Sul and
approved in 11.07.2007, by the jury:

Dr. Jean Guillon

Université Victor Segalen Bordeaux 2, France.

Dr. Suely Lins Galdino

Universidade Federal de Pernambuco, Brazil.

Dr. Vera Lucia Eifler Lima

Universidade Federal do Rio Grande do Sul, Brazil.

G572p Gnoatto, Simone Cristina Baggio

Planejamento e síntese de novos compostos derivados de agliconas
triterpênicas de espécies de *Ilex* visando à atividade antimalárica /
Simone Cristina Baggio Gnoatto – Porto Alegre : UFRGS, 2007. – 234
p.: il., tab., graf.

Tese (doutorado). UFRGS. Faculdade de Farmácia. Programa de
Pós-Graduação em Ciências Farmacêuticas.

Trabalho realizado em co-tutela internacional com a École Doctorale
Picardie Science et Santé. Faculté de Pharmacie. Université de Picardie
Jules Verne.

1. Ácido ursólico : Derivados. 2. Extração. 3. Semi-síntese. 4.
Farmacomodulação. 5. Análogos triterpênicos. 6. Atividade antimalárica.
7. Inibição de b-hematina. I Gosmann, Grace. II. Sonnet, Pascal. III.
Título.

CDU: 615.2.011

Bibliotecária responsável:

Margarida Maria Cordeiro Fonseca Ferreira, CRB 10/480

This thesis in *cotutela* was accomplished through the *Accord CAPES/COFECUB 418/03* between Universidade Federal do Rio Grande do Sul (UFRGS), Porto Alegre, Brazil, and Université de Picardie Jules Verne (UPJV), Amiens, France.

The project was conducted at *Laboratório de Fitoquímica* from Faculdade de Farmácia (UFRGS), Brazil, and *Laboratoire de Chimie Organique et Thérapeutique* (DMAG, EA 3901) from Faculté de Pharmacie (UPJV), France.

The experimental part accomplished in France was enabled through the financial support from *Coordenação de Aperfeiçoamento de Pessoal de Nível Superior* (CAPES, Brazil) and *Comité Français d'Evaluation de la Coopération Universitaire et Scientifique avec le Brésil* (COFECUB, France).

The experimental part accomplished in Brazil was enabled through the financial support from *Conselho Nacional de Desenvolvimento Científico e Tecnológico* (CNPq, Brazil) and from *Coordenação de Aperfeiçoamento de Pessoal de Nível Superior* (CAPES, Brazil).

ACKNOWLEDGEMENTS

I would like first to thank my examiners, who honored me by accepting to examine this thesis:

Dr. Jean Guillon, *Maître de Conférences*, HDR at *Université Victor Segalen Bordeaux 2, Laboratoire de Chimie Physique et Minérale – EA 2962 – Pharmacochimie, UFR des Sciences Pharmaceutiques*, France.

Dr. Suely Lins Galdino, *Professor Associado I* at *Universidade Federal de Pernambuco, Centro de Ciências Biológicas, Departamento de Antibióticos*, Brazil.

Dr. Vera Lucia Eifler Lima, *Professor Adjunto III* at *Universidade Federal do Rio Grande do Sul Faculdade de Farmácia, Departamento de Produção de Matéria-Prima*, Brazil.

Dr. Grace Gosmann, *Professor Associado I* at *Universidade Federal do Rio Grande do Sul, Faculdade de Farmácia, Departamento de Produção de Matéria-Prima*, Brazil.

Dr. Pascal Sonnet, *Professeur* at *Université de Picardie Jules Verne, Faculté de Pharmacie, Laboratoire de Chimie Organique et Thérapeutique – EA 3901 – DMAG*, France.

I would also like to thank to my Advisors, Dr. Grace Gosmann for passing me many leads, discussing human factors points, and helping to set up the project in the first place, and Dr. Pascal Sonnet for his enthusiastic supervision providing resources and subjects, and offering direction and penetrating criticism.

I thank to Dr. Alexandra Dassonville, *Maître de Conférences*, for the relevant discussions on the organic reactions and spectral data, and Sophie Da Nascimento, Pharmacist, for the help with mass measurements and technical

discussions. Thanks to all the rest of the academic group of the *Laboratoire de Chimie Organique et Thérapeutique* at the *Université de Picardie Jules Verne*, particularly, Julien Pécher and Viviane Pires for their assistance with all types of problems - at all times. Thanks to Claiton Lencina and Fillipo De Simone for all serious discussion and the routine mutual aid.

I am grateful to all my friends from Amiens, France, for being the surrogate family during the days I stayed there and for their continued moral support there after.

Thanks are also due to several researchers at *Laboratório de Síntese Orgânica Medicinal* at *Universidade Federal do Rio Grande do Sul* that I frequented in the initial stages of this study: Prof. Dr. Vera Lucia Eifler Lima, Patricia Amaral, and Cedric Graebin for their help with experimental set up and general advice.

This work would not have been possible without the support, numerous stimulating discussions and encouragement from my past and present colleagues and friends, Carla Kauffmann, Gustavo Provensi, Aline Zimmer, Juliane Fleck, Simone Quintana de Oliveira and Luciana Dalla Vecchia. Thanks also to Fernanda De Costa, Anna Yendo, Everton Moraes and Gisele Barbon.

I would particularly like to thank to Prof. Dr. Hugo Verli, *Faculdade de Farmácia*, UFRGS, for detailed discussion and encouragement in the area of modeling techniques.

For financial support, I thank the CNPq and CAPES in Brazil and, COFECUB in France.

Finally, I am forever indebted to my family for their understanding, endless patience, encouragement and love when it was most required, especially my husband Edlus. I dedicate this thesis to my children Filipe and Mateus.

CONTENTS

	Page
List of Abbreviations.....	xi
List of Figures.....	xv
List of Tables.....	xvii
Resumo.....	xix
Resumé.....	xxi
Abstract.....	xxiii
I Introduction.....	01
II Aims of this study.....	07
III Literature Review.....	11
III.1 The malaria.....	13
III.1.1 Malaria Treatment.....	15
III.1.1.1 Quinine and related compounds.....	15
III.1.1.2 Antifolate combination drugs.....	16
III.1.1.3 Artemisinin compounds.....	16
III.1.1.4 Miscellaneous compounds.....	17
III.1.2 Mechanism of action of antimalarial drugs.....	18
III.1.2.1 Haeme detoxification systems of <i>P. falciparum</i>	19
III.1.2.2 Quinolines- mechanism of action, spectroscopic and computational features.....	22
III.1.3 Resistance to antimalarial drugs.....	26
III.1.3.1 Dihydrofolate reductase (<i>dhfr</i>).....	27
III.1.3.2 Dihydropteroate synthase (<i>dhps</i>).....	28
III.1.3.3 <i>P. falciparum</i> chloroquine-resistance transporter (<i>pfcr</i>).....	28
III.1.3.4 <i>P. falciparum</i> multidrug-resistance gene 1 (<i>pfmdr1</i>).....	29
III.1.3.5 Cytochrome <i>b</i>	30
III.1.4 Targets for antimalarial chemotherapy.....	31
III.2 Derivatives and antimalarial activity.....	33
III.2.1 Synthesis of aminoquinoline derivatives.....	33
III.2.2 Synthesis of bisquinoline derivatives.....	35
III.2.3 Synthesis of bisacridine derivatives.....	35
III.2.4 Synthesis of ferrocene derivatives.....	36
III.2.5 Synthesis of piperazine derivatives.....	44
III.2.6 Synthesis of benzylpiperaziny flavone derivatives.....	51
III.2.7 Triterpene derivatives.....	52
III.2.7.1 Natural triterpenoids.....	53
III.2.7.2 Synthesis of triterpenoid derivatives.....	56
III.2.7.3 Mechanism of action of antimalarial triterpenoid compounds.....	62
IV Results and discussion.....	65
IV.1 Extraction and isolation of aglycones and triterpenic saponins from <i>Ilex paraguariensis</i> and <i>Ilex dumosa</i>	67
IV.1.1 Identification of compound 1	69
IV.1.2 Identification of matesaponins.....	71
IV.1.3 Identification of compound 5	74

IV.2 Design and synthesis of antimalarial compounds.....	75
IV.2.1 Synthesis of ursolic and oleanolic acid derivatives with modifications in the cycle A.....	76
IV.2.1.1 Oxidation at C-3.....	76
IV.2.1.2 Acetylation at C-3.....	77
IV.2.1.3 Inversion of OH configuration at C-3.....	78
IV.2.1.4 Beckmann rearrangement (Cycle A expansion).....	80
IV.2.2 Synthesis of ferrocene derivatives from ursolic acid.....	84
IV.2.2.1 Ferrocene coupling at C-3.....	85
IV.2.2.1.1 Benzoylation of ursolic acid.....	89
IV.2.2.2 Ferrocene coupling at C-28.....	91
IV.2.3 Synthesis of piperazine derivatives from ursolic acid.....	93
IV.2.3.1 Synthesis of <i>N</i> -[1,4-bis(3-aminopropyl)piperazinyl]-3-O- acetylursol-amide 180	94
IV.2.3.2 Reductive amination reactions to obtain tertiary amines.....	98
IV.2.3.2.1 Identification of aromatic compounds.....	102
IV.2.3.2.2 Identification of aliphatic compounds.....	104
IV.2.3.2.3 Identification of 197	106
IV.2.3.3 Reductive amination reactions to obtain secondary amines.....	106
IV.3 Biological results.....	110
IV.3.1 Antimalarial activity assay.....	110
IV.3.1.1 <i>In vitro P. falciparum</i> Culture and Drug Assays.....	110
IV.3.1.2 Compounds with modifications in the cycle A.....	112
IV.3.1.3 Compounds with ferrocene moiety.....	114
IV.3.1.4 Compounds with piperazine moiety.....	115
IV.3.1.5 Assays using <i>P. falciparum</i> chloroquine-sensitive strain Thai and MRC-5 cells.....	117
IV.3.2 Inhibition of β -hematin formation test.....	118
IV.4 The antimalarial activity of ursolic acid derivatives and their structure-activity relationships (SAR).....	121
IV.4.1 Design.....	121
IV.4.1.1 Modifications at cycle A.....	122
IV.4.1.2 Modifications at C-28.....	122
IV.4.2 Structure-Activity Relationships.....	124
IV.4.3 Quantitative Structure-Activity Relationships to the piperazinyl analogues of ursolic acid– Preliminary studies.....	125
IV.4.3.1 Validation of the test set.....	131
IV.4.4 Molecular Modeling.....	132
V Concluding remarks	137
VI Experimental part	141
VI.1. Généralités.....	143
VI.1.1. Réactifs et Solvants.....	143
VI.1.2. Chromatographies.....	143
VI.1.3. Instrumentation.....	144
VI.2 Plant material.....	145
VI.2.1 Extraction.....	145
VI.2.2 Acid Hydrolysis of aqueous extracts.....	145
VI.2.3 Isolation of matesaponins.....	146
VI.2.4 Identification of aglycons and saponins.....	146
VI.3. Méthodes Générales.....	147

VI.3.1. Réactions d'amination réductrice.....	147
VI.3.1.1. Méthode A.....	147
VI.3.1.2. Méthode B.....	147
VI.3.1.3. Méthode C.....	147
VI.3.2. Réaction de déprotection d'une fonction amine protégée par un groupement Boc.....	148
VI.3.3. Réaction de déprotection d'une fonction alcool protégée par un groupement acétyle.....	148
Synthesis of compounds.....	149
VII References.....	205
VIII Annexes.....	225
VIII.1. Structures numbering.....	227
VIII.2. General Reactions Scheme.....	228
IX Biography of the author.....	231

LIST OF ABBREVIATIONS (English / Français):

AcOEt : ethyl acetate
Ala : alanine
Ara: arabinose
Arg : arginine
Asn: asparagine
Asp: aspartic acid
Bel-7402 : human hepatoma cell line
BHIA: β -haematin inhibitory activity
Bn : benzyl
Boc : *t*-butyloxycarbonyl
Boc₂O: di-*tert*-butyldicarbonate
CC : cytotoxicity concentration
CDCl₃ : chloroform-d
Cp et Cp' : cyclopentadienyl group
CQ: chloroquine
Cys: cysteine
DDT : dichloro-diphenyl-trichloroethane
DEAD: diethyl azodicarboxylate
Dhfr: dihydrofolate reductase
Dhps: dihydropteroate synthase
DIAD : Diisopropyl azodicarboxylate
DIBAL: diisobutylaluminium hydride
DMF : *N,N*-Dimethylformamide
DMSO : dimethylsulfoxide
DNDI: Drugs for Neglected Diseases Initiative
equiv. equivalent / éq : équivalent
Et₂O : Diethyl ether
EtOH : ethanol
Fc : ferrocenyl group
Fe(III)PPIX : ferroprotoporphyrin IX
FV: food vacuole
Gal: galactose
Glc: glucose

Gln: glutamine

Gly : glycine

GSH: glutathione

Hela : cervical cancer immortal cell line

HMBC: Heteronuclear Multiple Bond Correlation

HMQC: Heteronuclear Multiple-Quantum Coherence Experimental

HPLC : High performance Liquid chromatography / CLHP: chromatographie
liquide haute performance

HRMS : high resolution masse spectrometry / SMHR : spectrométrie de masse
haute résolution

IC : inhibition concentration / CI : concentration inhibitrice

Ile:isoleucine

IR: infrared

IR-ATR: infrared spectroscopy in the Attenuated Total Reflection Mode

L5178Y: lymphoma cells line

Leu: leucine

Lys : lysine

m-CPBA : *m*-Chloroperoxybenzoic acid

MD: molecular dynamics simulations

MDSA: molecular dynamics simulated annealing

MeOH: methanol

MEP: molecular electrostatic potential

Met: methionine

MIC : minimum inhibitory concentration

MM : molar mass

MM: molecular mechanics

MMV: Medicines for Malaria Venture

Mp : melting point / pF : point de fusion

MR: molar refractivity

MRC-5: human diploid embryonic lung cell line

MSF: Médecins Sans Frontières

n-BuOH: butanol

NMM : *N*-Methylmorpholine

NMR : Nuclear magnetic resonance / RMN : résonance magnétique nucléaire

PABA: *para*-aminobenzoic acid

PCC : Pyridinium chlorochromate

Pfcr1: *P. falciparum* chloroquine-resistance transporter
pfmdr1: *P. falciparum* multidrug-resistance gene 1
QSAR: Quantitative Structure-Activity Relationship
RBM: Roll Back Malaria Partnership
Rdt : yield / rendement
Rha: rhamnose
RI: resistance index
 R_t : retention time / t_r : temps de rétention
rt : room temperature / TA : température ambiante
SAR : structure-activity relationships
Sc: subcutaneous
Ser : serine
SI: selective index
SN : nucleophilic substitutions
TDR: Research in Tropical Diseases
TEA: Triethylamine
TFA : trifluoroacetic acid
THF : Tetrahydrofuran
Thr : threonine / thréonine
TLC : thin layer chromatography / CCM: chromatographie sur couche mince
VAR: vacuolar accumulation ratios

STRAINS OF *PLASMODIUM FALCIPARUM*

3D7: Chloroquine sensitive
D6: Chloroquine sensitive
Dd2: Chloroquine resistant
FcB1: Chloroquine resistant
FCM17: Chloroquine resistant
FCM6: Chloroquine resistant
FCR3: Chloroquine resistant
FG1: Chloroquine resistant
FG2: Chloroquine sensitive
FG3: Semi-chloroquine-resistant
FG4: Chloroquine sensitive
HB3: Chloroquine sensitive
K1: Chloroquine resistant and pyrimethamine resistant
NF-54: Chloroquine resistant
SGE2: Chloroquine sensitive
T9-96: Chloroquine sensitive and pyrimethamine sensitive
W2: Chloroquine resistant

LIST OF FIGURES

Figure 1. IC ₅₀ against <i>P. falciparum</i> Ghana and cytotoxicity (MRC-5 cells) of <i>Ilex</i> compounds.....	5
Figure 2. Life Cycle of <i>Plasmodium sp.</i> in man and the mosquito.....	14
Figure 3. Schematic representation of haemoglobin catabolism in the malaria parasite <i>P. falciparum</i>	20
Figure 4. Free haeme detoxification systems in malaria parasite.....	16
Figure 5 Chloroquine stacking in μ -oxo-oligomeric haematin.....	23
Figure 6. Chloroquine bound to (001) β -hematin crystal highlighting energetically favorable interactions.....	25
Figure 7. Mechanism of antimalarial activity of chloroquine.....	33
Figure 8. Proposed structure-function relationships in chloroquine.....	34
Figure 9. Proposed structure-activity relationships for ferroquine.....	43
Figure 10. Natural products obtained from <i>Ilex</i>	112
Figure 11. Derivatives with pharmacomodulations at cycle A.....	113
Figure 12. Ferrocenyl derivatives of ursolic acid.....	114
Figure 13. Graphic of experimental activity values (Log1/IC ₅₀) versus calculated activity values for the model.....	128
Figure 14. Graphic of experimental activity values (Log1/IC ₅₀) versus calculated.....	130
Figure 15. Graphic of experimental activity values versus predicted activity values for the test set.....	131
Figure 16. Orientation of haeme molecules observed to occur in solution from a 10.0 ns MD simulation, starting from random orientations.....	133
Figure 17. Side and front views of complexes between haematin and chloroquine (blue), bispyrrolo[1,2- α]quinoxaline derivative (Guillon <i>et al.</i> , 2004) (red), 182 (cyan), 195 (orange) and 185 (purple).....	134
Figure 18. Interactions (black dashes) between haematin and chloroquine (blue), the bispyrrolo[1,2- α]quinoxaline derivative (Guillon <i>et al.</i> , 2004) (red), 182 (cyan), 195 (orange) and 185 (purple).....	135

LIST OF TABLES

Table 1. Targets for antimalarial chemotherapy.....	31
Table 2. In vitro sensitivity of <i>P. falciparum</i> strains to Chloroquine and Ferroquine 24	37
Table 3. In vitro antimalarial activity of chloroquine and ferroquine 24 against <i>P. falciparum</i> strains.....	37
Table 4 In vitro antimalarial activity of artemisinin derivatives against <i>P. falciparum</i> strains.....	41
Table 5. In vitro sensitivity of <i>P. falciparum</i> strains to bisacridine 45	45
Table 6. In Vitro Sensitivity of <i>P. falciparum</i> FcB1 Strain to Compounds 47-66 (Series A), 67-86 (Series B), and 87-106 (Series C).....	46
Table 7. <i>In vitro</i> Cytotoxicity of Compounds 47-66 (Series A), 67-86 (Series B), and 87-106 (Series C) on MRC-5 cells.....	48
Table 8. <i>In vitro</i> Inhibition of β -haematin Formation of a Few Compounds from Series A-C.....	48
Table 9. <i>In vitro</i> Sensitivity of <i>P. falciparum</i> Strains and <i>in vitro</i> Cytotoxicity on Mammalian L6 Cells.....	50
Table 10. ^{13}C -NMR Chemical Shifts of matesaponin 1, and peracetylated compounds matesaponin 2, and matesaponin 3.....	73
Table 11. Structural data for 3-epioleanolic acid 157	80
Table 12. Results of <i>N</i> -Boc protection of 177 under various conditions.....	94
Table 13. Compounds 183-190 obtained by reductive amination reactions from 180	100
Table 14. Compounds 191-196 obtained by reductive amination reactions from 180	101
Table 15. Compound 197 obtained by reductive amination reactions from 180	101
Table 16. ^1H and ^{13}C NMR spectral data of the aromatic groups of compounds 183 to 190	103
Table 17. Compounds 198-200 obtained by reductive amination from 180	107
Table 18. ^1H and ^{13}C NMR spectral data of the aromatic groups of compounds 198 and 199	108
Table 19. <i>In vitro</i> sensitivity of <i>P. falciparum</i> FcB1 to Ursolic 1 and oleanolic 5 acids, saponins 2 and 3 , and peracetylated saponins 151-153	112
Table 20. <i>In vitro</i> Sensitivity of <i>P. falciparum</i> FcB1 to Compounds 147 , 154 , 157-160	113
Table 21. <i>In vitro</i> Sensitivity of <i>P. falciparum</i> FcB1 to Compounds 170-172 and 175	114
Table 22. <i>In vitro</i> Sensitivity of <i>P. falciparum</i> FcB1 Strain to Compounds 180-200	116
Table 23. <i>In vitro</i> Sensitivity of <i>P. falciparum</i> Thai Strain and MRC-5 cells.....	118
Table 24. Inhibition of β -hematin formation.....	119
Table 25. Experimental values of IC_{50} calculated by the Equation 1, according to model, and the π values calculated for R.....	127
Table 26. Experimental values of $\text{Log}1/\text{IC}_{50}$ calculated by Equation 1, according to the model, and the respective errors.....	128
Table 27. Experimental values of IC_{50} calculated by the Equation 3,	

according to model, and the π values calculated for R.....	129
Table 28. Experimental values of IC_{50} predicted by Equation 3, for the test set, and the respective errors.....	131

RESUMO

A Malária é uma doença endêmica que representa um grave problema de saúde pública na África, Ásia, Oceania e América Latina. Na América latina as principais áreas endêmicas estão na Bacia Amazônica e, infelizmente, são registrados cem mil novos casos clínicos no Brasil anualmente. Atualmente, mesmo nos Estados Unidos e no Oeste da Europa, o número de casos de malária tem aumentado a cada ano devido aos viajantes que vêm de áreas de risco. Este trabalho apresenta a síntese de compostos visando aumentar a atividade antimalárica de triterpenos através de farmacomodulação, especialmente em C-3 e em C-28 dos ácidos ursólico e oleanólico. Sete produtos naturais foram obtidos a partir das espécies sul-americanas *Ilex paraguariensis* e *Ilex dumosa*: os triterpenos ácido ursólico e ácido oleanólico e as matessaponinas 1 e 3, bem como, os derivados peracetilados das matessaponinas 1, 2 e 3. Três séries de derivados triterpênicos foram sintetizadas: derivados dos ácidos ursólico e oleanólico com modificações no ciclo A, derivados ferrocênicos e derivados piperazínicos do ácido ursólico. Estes compostos foram testados *in vitro* frente a cepas de *Plasmodium falciparum*. Os derivados piperazínicos do ácido ursólico foram os mais ativos. Sete novos análogos apresentaram atividade em concentrações na ordem de nanomolar (IC₅₀ 78 a 964 nM), enquanto que a cloroquina apresentou IC₅₀ de 130 nM. Baixos índices de resistência cruzada com a cloroquina foram observados. Este estudo também contribuiu para o melhor entendimento da relação estrutura-atividade (REA) para a classe de derivados piperazínicos do ácido ursólico. Desta forma, foi demonstrada a importância do esqueleto triterpênico e do grupamento acetila em C-3 para a atividade antimalárica. O grupamento piperazina foi identificado como farmacóforo nesta série de compostos. Foi caracterizada a importância de substituintes hidrofílicos no nitrogênio terminal da cadeia lateral bis-(3-aminopropil)piperazina através de um estudo de relação estrutura-atividade quantitativa (QSAR). O possível mecanismo de ação destes compostos foi sugerido via inibição da formação de β-hematina a partir de testes *in vitro* e de modelagem molecular.

Palavras chave: derivados do ácido ursólico, extração, semi-síntese, farmacomodulação, análogos triterpênicos, atividade antimalárica, inibição de β-hematina.

RESUMÉ

Conception et synthèse de nouveaux dérivés de génines triterpéniques d'*Ilex* à visée antipaludique

Le paludisme est une maladie endémique sérieuse qui représente une menace importante de santé publique en Afrique, en Asie, Océanie, et en Amérique latine. En Amérique latine, les régions touchées sont principalement centrées autour de l'Amazonie brésilienne. En effet, le Brésil enregistre, chaque année, 100 000 nouveaux cas de paludisme. Aujourd'hui, même les Etats-Unis et l'Europe de l'ouest, qui ne sont pourtant pas des secteurs endémiques, enregistrent un nombre important et croissant de nouveaux cas, essentiellement dus à des voyageurs. Il y a également une recrudescence de la résistance du parasite, à l'origine du paludisme, aux molécules actuellement commercialisés. Par conséquent, la recherche de nouvelles molécules antipaludiques est un enjeu primordial. Nous avons observé que l'acide ursolique, extrait d'espèces sud américaines *Ilex paraguariensis* et *Ilex dumosa*, possédait une activité antipaludique intéressante. Ce travail de thèse a pour but l'extraction, l'hémisynthèse d'analogues de l'acide ursolique et enfin l'évaluation de l'activité antipaludique des composés ainsi obtenus. Le but de ce travail est d'augmenter l'activité antipaludique de l'acide ursolique, initialement décrite, par pharmacomodulation du noyau triterpénique en position 3 et 28. Sept produits naturels ont été extraits et purifiés à partir d'espèces sud américaines *Ilex paraguariensis* et *Ilex dumosa*. Il s'agit des triterpènes de l'acide ursolique et de l'acide oléanolique et les saponosides matésaponines peracétylées ou non. L'optimisation de l'activité antipaludique, par la synthèse de nouveaux analogues triterpéniques, a été basée sur l'hypothèse que l'activité antipaludique initialement observée était due à un mécanisme d'inhibition de la formation de la β -hémazoïne par l'acide ursolique. Ces analogues peuvent être classés selon trois séries : acides ursolique et oléanolique avec des modifications au niveau du cycle A, dérivés ferrocéniques de l'acide ursolique et dérivés pipéraziniques de l'acide ursolique. Les meilleures activités ont été observées pour les dérivés pipéraziniques de l'acide ursolique. En effet, sept nouveaux analogues ont démontré des activités intéressantes de l'ordre de nanomolaire (IC_{50} 78 to 964 nM). Les activités obtenues représentent ainsi un gain d'activité au moins d'un facteur 100 par rapport à celle de l'acide ursolique. Une étude de structure-activité a été réalisée sur ces dérivés pipéraziniques de l'acide ursolique. Ainsi, nous avons démontré l'importance du noyau triterpénique et du groupement acétyle en C-3 pour l'activité antipaludique. De même, l'importance des substitutions au niveau de l'azote terminal de la chaîne bis-(3-aminopropyl)pipérazine, notamment de groupements hydrophiles, a aussi été réalisée par une étude de relation structure activité quantitative (QSAR). Enfin, l'hypothèse que ces composés agissent sur l'inhibition de la formation de β -hémazoïne a été confirmée par des études *in vitro* (inhibition de la formation de la β -hématine) et de modélisation moléculaire.

Mots-clés : dérivés de l'acide ursolique, extraction, hémisynthèse, pharmacomodulation, analogues de triterpènes, antipaludique, β -hématine.

ABSTRACT

Design, Synthesis and Antimalarial Activity of new Triterpenoid Derivatives from *Ilex*

Malaria is a serious endemic disease that represents a major threat to public health in Africa, Asia, Oceania, and Latin America. In Latin America endemic areas are mainly centered throughout the Brazilian Amazonia and unfortunately, Brazil registers 100 thousands of new clinical cases annually. Nowadays, even in the United States and Western Europe, which are not endemic areas, an important number of malaria infections are carried by travelers came from areas of high risk, and it increases each year. The present study describes efforts to synthesize compounds in order to increase the antiplasmodial activity of triterpene by pharmacomodulation, especially at C-3 and C-28 of ursolic and oleanolic acids. Seven natural products, namely the triterpenes ursolic and oleanolic acids, and matesaponins and peracetylated matesaponins were obtained from the South American species *Ilex paraguariensis* and *Ilex dumosa*. Through a rational design, based on the known molecular mechanism of the malaria disease, a series of new derivatives of ursolic and oleanolic acids were successfully synthesized. These compounds could be divided in three series: ursolic and oleanolic acids with modifications at cycle A, ferrocene derivatives from ursolic acid and piperazine derivatives from ursolic acid. The best activity was observed with piperazinyl derivatives. Indeed, seven new piperazinyl analogues of ursolic acid showed significant activity in the order of nano molar range (IC_{50} : 78 to 964 nM), while chloroquine presented IC_{50} 130 nM. Low levels of cross-resistance to chloroquine were observed. This study had also contributed to provide better knowledge on structure-activity relationships (SAR) of these piperazine derivatives from ursolic acid. In this way, it was demonstrated the importance of the triterpene skeleton and the acetyl group at C-3 for antimalarial activity; piperazine was identified as a pharmacophore in this series. The importance of the hydrophilic framework attached at *N* terminal of the bis-(3-aminopropyl)piperazine joined to the triterpene ring was also characterized by quantitative structure-activity relationships (QSAR) approaches. A possible mechanism of interaction implicating binding of these compounds to β -haematin was supported by *in vitro* tests and molecular modeling.

Keywords: ursolic acid derivatives, extraction, hemisynthesis, pharmacomodulation, triterpenes analogues, antimalarial activity, β -haematin inhibition.

I INTRODUCTION

Malaria is a serious endemic disease that represents a major threat to public health in more than 100 countries, distributed in Africa, Asia, Oceania, and Latin America (WHO, 2006a). In Latin America endemic areas are mainly centered throughout the Brazilian Amazonia. Brazil registers 100 thousands new clinical cases annually (<http://portal.saude.gov.br/portal/svs>). Today, even in the United States and Western Europe, which are not endemic areas, an important number of malaria infections are carried by travelers came from areas of high risk, and it increases each year.

Malaria has resisted to all efforts of eradication and control for over a century. The two major approaches consisted on killing the parasite and killing the parasite vector. In addition, various attempts to develop antimalarial vaccines were carried out. The first large multilateral initiative was the WHO Malaria Eradication Program (1955-1969), which aimed at the total eradication of malaria mainly by vector control (particularly by using DDT). This effort failed but achieved regional eradication in Southern Europe and some countries in North Africa and Middle East. Subsequent important initiatives were the creation of the Special Program in Training and Research in Tropical Diseases (TDR) in 1975, the Multilateral Initiative on Malaria (MIM) in 1997, the Roll Back Malaria Partnership (RBM) launched in 1998 by the WHO, the Medicines for Malaria Venture (MMV) in 1999, the Global Fund, created in 2002, and Drugs for Neglected Diseases Initiative (DNDI) in 2003 (Martin *et al.*, 2004).

In relation to the participation of Brazil and France in these efforts, it is important to emphasize that Drugs for Neglected Diseases Initiative (DNDI) is an not-for-profit drug development initiative established in 2003 by five public-sector research organizations- Kenya Medical Research Institute, Indian Council of Medical Research, Oswaldo Cruz Foundation Brazil, Malaysian Ministry of Health, and France's Institut Pasteur and Médecins Sans Frontières (MSF) (www.dndi.org).

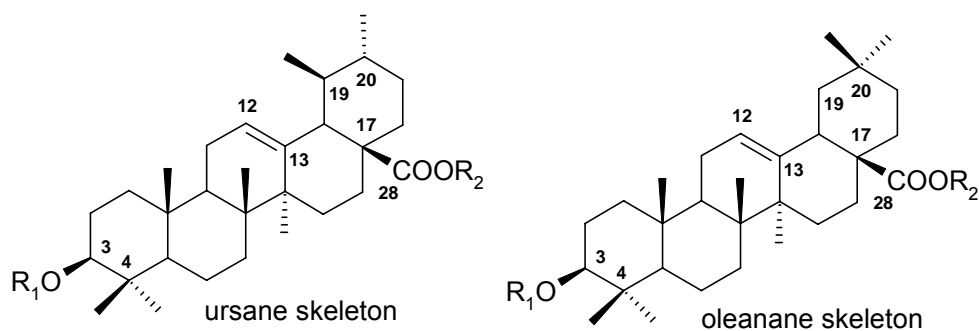
Moreover, the rapidly growing resistance of the malaria parasite to the available drugs represents a significant role in the occurrence and severity of epidemics and a challenge to be surpassed. Chloroquine, and mefloquine resistance was reported in Brazil (Alecrim *et al.*, 1999) as well as sulfadoxine-

pyrimethamine resistance (Wongsrichanalai *et al.*, 2002). It is also spreading over Amazon basin of Peru bordering Brazil and Colombia (Magill *et al.*, 2004).

Considering these facts, the need for novel chemotherapeutic compounds in the fight against the resistant *Plasmodium falciparum* pathogen is unquestionable. In this sense, natural products continue to be rich sources of novel antimalarial scaffolds. One of the challenges inherent in addressing drug resistance today is to start with natural products which had already demonstrated antimalarial activities (Caniato and Puricelli, 2003, Biot and Chibale, 2006).

Our two laboratories worked together since many years and are partners in the search of new natural products prototypes through isolation and synthetic modifications. This collaboration had resulted in the structural elucidation of several triterpene compounds. More recently, we have decided to begin a new project which is consisting in chemical modifications and pharmacological studies of some triterpenes in the antimalarial area.

Indeed, in our preliminary work, some triterpenic compounds had demonstrated interesting antimalarial activities. These compounds extracted from South American *Ilex* species exhibited *in vitro* inhibitory activity on strain *P. falciparum* Ghana, without toxic effects on human MRC-5 cell lines (Figure 1). These tests were developed in cooperation with World Health Organization (WHO) (data not yet published). The saponins **2** to **4** are ursolic acid **1** derivatives and were obtained from *Ilex paraguariensis*, while compounds **6** to **8** were extracted from *Ilex dumosa* and are oleanolic acid **5** derivatives (Figure 1). Ursolic and oleanolic acids are position isomers. These compounds presented a modest, but promising activity, especially aglycon **1**. Consequently, the systematic modification of ursolic acid **1** represents a promising strategy to identify new active antimalarial compounds.



	N°	R ₁	R ₂	IC ₅₀ (μM)	Cytotoxicity (μM)
Ursane derivatives	1	H	H	7	4
	2	β-D-glc-(1-3)- α-L-ara	β-D-glc	11	>32
	3	β-D-glc-(1-3)- α-L-ara	β-D-glc-(1-6)- β-D-glc	21	>32
	4	β-D-glc-(1-3)- [α-L-rha-(1-2)-ara]	β-D-glc-(1-6)- β-D-glc	32	>32
Oleanane derivatives	5	H	H	NT	NT
	6	β-D-glc-(1-2)- β-D-gal	H	29	>32
	7	β-D-glc-(1-2)- β-D-gal	β-D-glc	24	>32
	8	α-L-ara-(1-2)- β-D-gal	β-D-glc	5	>32
Chloroquine				0.02	NT

Figure 1. IC₅₀ against *P. falciparum* Ghana and cytotoxicity (MRC-5 cells) of *Ilex* compounds (NT: not tested)

The present study describes efforts to synthesize compounds in order to increase the antiplasmodial activity of this triterpene skeleton. We report here the synthesis, pharmacological and structure-activity relationship studies of new triterpene derivatives. The rationale for this work was, first, to synthesize these compounds by pharmacomodulation, especially at C-3 and C-28 positions of ursolic **1**; second, to evaluate the antimalarial activities of these compounds; third, to establish the mechanism of action (inhibition of β-haematin formation and modeling studies) and the relationship studies of some derivatives.

We hope to contribute for the development of a new class of antimalarial drugs, and so, to sum to the world wide efforts carried out in order to stop this mortal disease.

II AIMS OF THIS STUDY

The overall aim of this study was:

- ❖ Obtention antimalarial compounds using the triterpene ursolic acid as prototype.

In order to obtain this objective it was decided:

- ❖ To obtain saponins and their aglycons from the South American species: *Ilex paraguariensis* and *Ilex dumosa*.
- ❖ To synthesize analogues of ursolic and oleanolic acids with modifications in the cycle A using reactions as: oxidation, acetylation, inversion of hydroxyl configuration at C-3, and an expansion of this cycle via Beckmann rearrangement.
- ❖ To synthesize analogues of ursolic acid having a ferrocene moiety at C-3 or C-28.
- ❖ To synthesize analogues of ursolic acid possessing the *N*-1,4-bis(3-aminopropyl)piperazine moiety at C-28.
- ❖ To synthesize analogues of *N*-[1-(4-(3-aminopropyl)piperazinyl)-propyl]-3-*O*-acetylursolamide with different substituents at the terminal amine.
- ❖ To assay *in vitro* these synthesized compounds against *P. falciparum* together with studies of cytotoxicity activity and inhibition of β -haematin formation.
- ❖ To establish structure-activity relationships and exploring them through molecular dynamics simulations.

III LITERATURE REVIEW

III.1 The Malaria

Nowadays, malaria is one of the most geographically widespread and devastating infections in humans. Every year, 300-500 million people suffer from this disease and approximately 2-3 million people die of malaria. Three-quarters of these fatalities are children under the age of 5 years (WHO, 2006a; Breman, 2001).

Malaria is caused by the *Plasmodium* parasite which spends its life in both humans and certain species of mosquitoes. Four species of *Plasmodium* cause malaria in humans: *P. falciparum*, *P. vivax*, *P. malariae* and *P. ovale*. Of these, *P. falciparum* is the most important in most parts of the tropics and is responsible for most severe illnesses and deaths (WHO, 2006a).

Malaria parasites are transmitted by female mosquitoes belonging to the genus *Anopheles*. The life cycle of the malaria parasite is divided into three different phases – one in the mosquito (the **sporogonic cycle**) and two in the human host: the **erythrocytic cycle** (in human blood cells) and the **exo-erythrocytic cycle** (outside the blood cells) (Klan and Waters, 2004) (Figure 2).

The male and female gametocytes of the parasite are ingested by the mosquito when taking a blood meal, and they will form male and female gametes within the mosquito's stomach (midgut). Both gametes generate zygotes which can move and they are called the ookinetes (10). The ookinete penetrates the wall of the midgut and becomes a round oocyst (11). Inside the oocyst, the nucleus divides repeatedly with the formation of a large number of sporozoites. When the sporozoites are fully formed, the oocyst bursts, releasing the sporozoites into the mosquito's body cavity (haemocoel) (12). The sporozoites migrate to the salivary glands from where they will be inoculated into a new human host. The time necessary for the development of the sporozoites varies with temperature and to a smaller extent with the species of the malaria parasite and with humidity, but generally it is about 8-15 days (Braga and Fontes, 2000; Klan and Waters, 2004; WHO, 2006c).

The human cycle begins with the inoculation of the sporozoites (the infective stage of *Plasmodium*) (1) that infect liver cells (2). Over a period of 7-

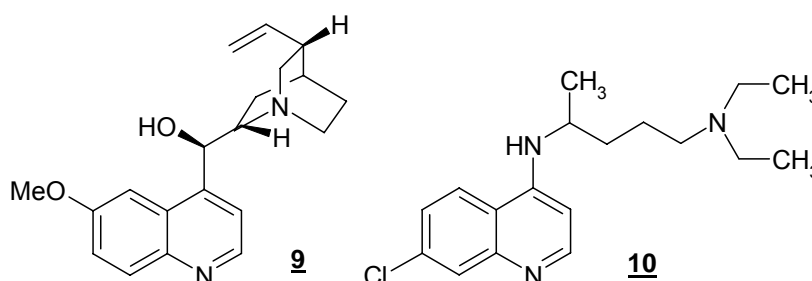
infecting and destroying red blood cells (anaemia) and by clogging the capillaries that carry blood to the brain (cerebral malaria) or other vital organs. Malaria, together with HIV/AIDS and Tuberculosis, is one of the major public health challenges undermining development in the poorest countries in the world (Tracy and Webster, 2003; WHO, 2006c).

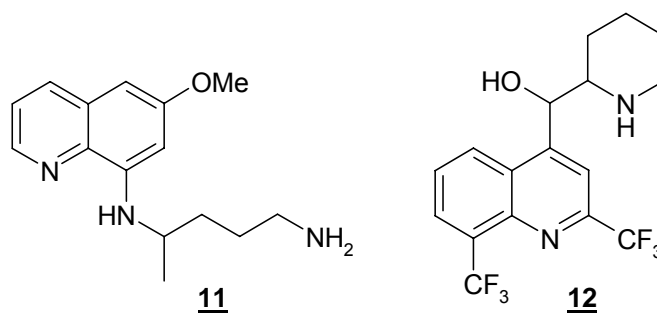
III.1.1 Malaria Treatment

There are only a limited number of drugs which can be used to treat or prevent malaria. The most widely used are quinine and its derivatives and antifolate combination drugs.

III.1.1.1 Quinine and related compounds

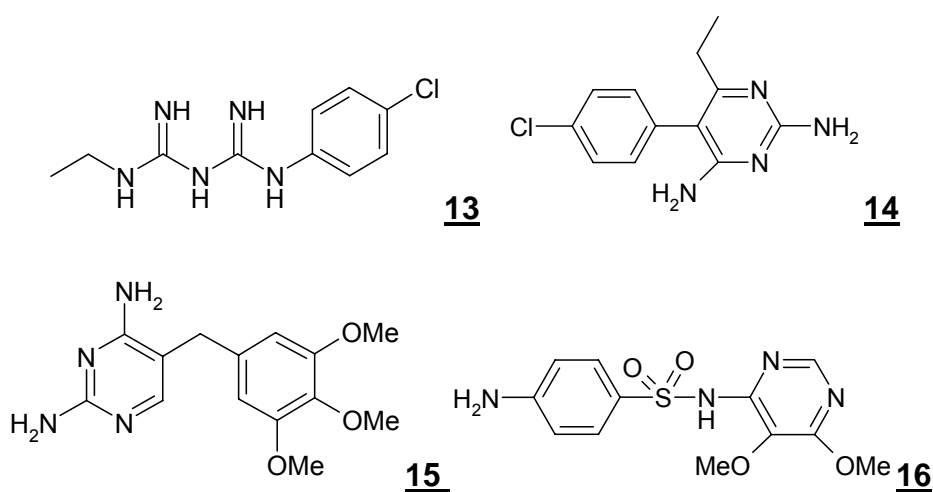
Quinine **9**, an alkaloid from *Cinchona sp*, has been the drug of last resort for the treatment of malaria, especially severe disease. Chloroquine **10** is a 4-aminoquinoline derivative of quinine first synthesized in 1934 and has since been the most widely used antimalarial drug. Historically, it has been the drug of choice for the treatment of non-severe or uncomplicated malaria and for chemoprophylaxis, although drug resistance has dramatically reduced its usefulness. Other quinine-related compounds in common use include primaquine **11** (specifically used for eliminating the exoerythrocytic forms of *P. vivax* and *P. ovale* that cause relapses), and mefloquine **12** (a quinoline-methanol derivative of quinine) (Bell, 2005; Williams and Lemke, 2002, WHO, 2006a).





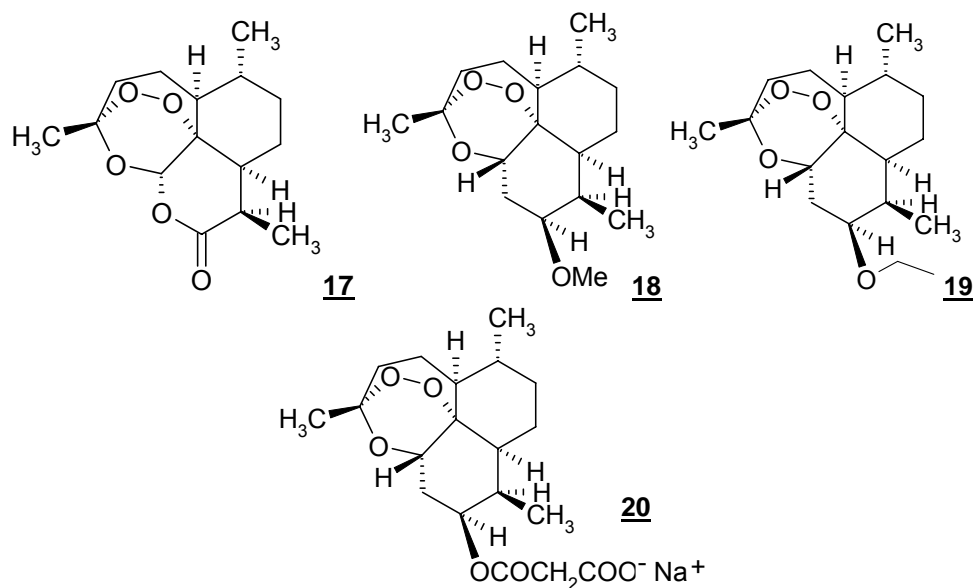
III.1.1.2 Antifolate combination drugs

These drugs are various combinations of dihydrofolate-reductase inhibitors (proguanil **13**, pyrimethamine **14**, and trimethoprim **15**) and sulfa drugs (sulfadoxine **16** and others). Although these drugs have antimalarial activity when used alone, parasitological resistance can develop rapidly (Winstanley *et al.*, 2004). When used in combination, they produce a synergistic effect on the parasite and can be effective even in the presence of resistance to the individual components. Typical combination is sulfadoxine/pyrimethamine (Williams and Lemke, 2002; Winstanley *et al.*, 2004; WHO, 2006a).



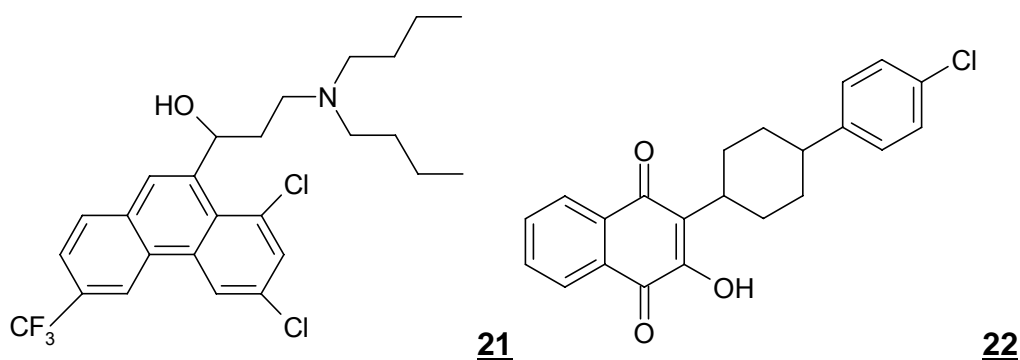
III.1.1.3 Artemisinin compounds

A number of sesquiterpene lactone compounds have been obtained or synthesized from the plant *Artemisia annua* (artemisinin **17**, artemether **18**, arteether **19** and artesunate **20**). These compounds are used for treatment of severe malaria and have shown very rapid parasite clearance times and faster fever resolution than occurs with quinine (Williams and Lemke, 2002, Li *et al.*, 2006).



II.1.1.4 Miscellaneous compounds

Halofantrine **21** is a phenanthrene-methanol compound with activity against the erythrocytic stages of the malaria parasite. Its use has been especially recommended in areas with multiple drug-resistant *P. falciparum* (Bell, 2005). Atovaquone **22** is a hydroxynaphthoquinone that is currently being used most widely for the treatment of opportunistic infections in immunosuppressed patients. It is effective against chloroquine-resistant *P. falciparum* but because, when used alone, resistance develops rapidly, atovaquone is usually given in combination with proguanil **13** (Williams and Lemke, 2002, WHO, 2006a).



Since the beginning of 2007, it is found in the market an association of artesunate and amodiaquine approved by WHO due the resistance of antimalarial drugs.

III.1.2 Mechanism of action of antimalarial drugs

The mechanisms of action of key antimalarial drugs are not completely understood.

The mode of action of artemisinin and related 1,2,4-trioxanes involves the cleavage of endoperoxide bridge homolytically by haeme to give a reactive free radical intermediate that alkylate vital parasite protein molecules. Artesunate acts via inhibiting cytochrome oxidase and DNA synthesis by blocking the purine synthesis (Vangapandu *et al.*, 2007).

In relation to antifolates, parasites cannot use exogenously supplied folic acid to synthesize folate co-factors, rather, they need to synthesize these co-factors *de novo* starting with the condensation of pteridine with *para*-aminobenzoic acid (PABA) to form dihydropteroic acid. These are the basis of selective toxicity to parasites of PABA antagonists and inhibitors of dihydrofolate reductase (Vangapandu *et al.*, 2007). Antifolates attack all growing stages of the malaria parasite.

Quinolines are thought to prevent effective formation of haemozoin by binding to haem through π - π stacking of their planar aromatic structures, resulting in toxicity to the parasite. Primaquine **11** (8-aminoquinoline) possesses little activity against the erythrocytic form of the malaria parasite. Its activity is due to an oxidative stress mechanism. In contrast to chloroquine, primaquine does not inhibit haematin polymerization although it does bind to haematin μ -oxo dimer with modest affinity (Vangapandu *et al.*, 2007).

In order to understand the mechanism of action of quinolines, it will be presented, initially, a brief explanation of the mechanism of haeme

detoxification of the parasite. Following, the studies related to the mechanism of action, specially, of chloroquine will be presented.

III.1.2.1 Haeme detoxification systems of *P. falciparum*

Malaria parasite possesses efficient haeme detoxification mechanisms to protect itself from haeme-induced oxidative stress, one of them, via haemozoin formation in the food vacuole (FV) of parasite (Fitch, 2004; Kumar *et al.*, 2007).

During its blood stages, within infected erythrocytes, *P. falciparum* consumes 50-80% (molar concentration of 5 mM in the erythrocyte's volume of $88.4 \mu\text{m}^3$) of the cytosolic haemoglobin during a 48 h period releasing an equivalent of 10-16 mM free haeme (Moore *et al.*, 2006). The parasite uses this haemoglobin as its primary food source. In the lysosomal vacuole, haemoglobin is digested by the aspartic proteases enzymes plasmepsin I, II and IV and histo-aspartic protease, by the cysteine proteases falcipain 1, 2 and 3 and by the zinc protease, falcilysin (Salas *et al.*, 1995; Eggleston *et al.*, 1999; Shenai *et al.*, 2000; Sijwali *et al.*, 2001; Banerjee *et al.*, 2002; Rosenthal *et al.*, 2002). Haeme (containing Fe (II)) is oxidized to haematin (containing Fe(III)) by O_2 and originates a toxic action against the parasite. For survival, the parasite compartmentalizes haematin in the lysosomal vacuole (volume of $4 \mu\text{m}^3$, resulting in an estimated 22-fold increase in concentration reaching 350-400 mM), where it is polymerized into insoluble haemozoin (malaria pigment), overcoming the lack of the haeme oxygenase, the defensive mechanisms used by vertebrates (Aikawa *et al.*, 1966; Krugliak *et al.*, 2002; Egan *et al.*, 2002). The degradation process is summarized in Figure 3.

By converting haematin to haemozoin, the parasite removes it permanently from solution and deposits haematin in a relatively innocuous solid form.

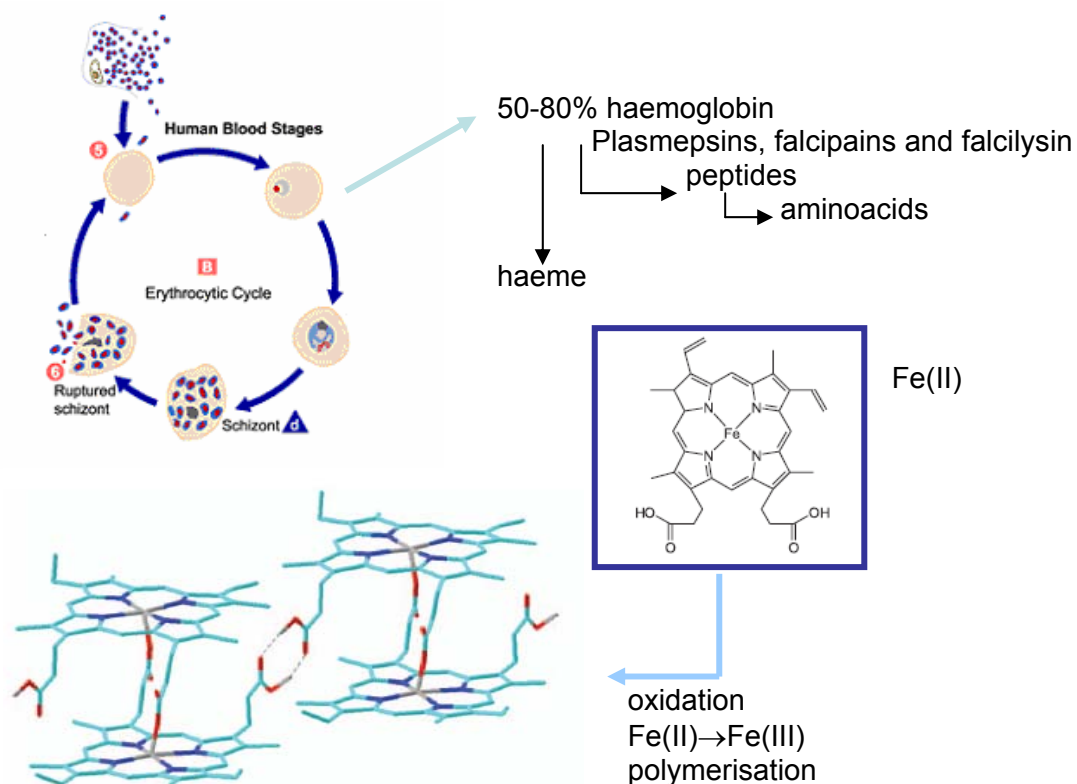


Figure 3. Schematic representation of haemoglobin catabolism in the malaria parasite *P. falciparum*.

Haemozoin is a polymer of haeme units linked through an iron-carboxylate bond between the central iron of one haeme and the propionate side chain of the other one (Sullivan *et al.*, 1996; Pagola *et al.*, 2000). The conversion of ferriprotoporphyrin IX (haematin) to β -haematin (haemozoin) can occur in the absence of biological material in acetate salts solutions, and recently it was demonstrated that the conversion does occur under physiologic conditions (Egan *et al.*, 2006). Despite an extensive search, an enzyme with haematin dimerizing activity has not been found (Fitch, 2004). Haemozoin formation appears to be a type of biomineralisation process (Egan *et al.*, 2006), but recently it was pointed that it may also be mediated by proteins or lipids (Ziegler *et al.*, 1999; Egan *et al.*, 2001, Fitch, 2004; Kumar *et al.*, 2007). Since malaria parasite is enriched with linoleic acid, it is probable that linoleate or a derivative is the principal lipid promoting haematin dimerizing (Fitch, 2004).

Fitch (2004), in his review, also pointed to the evidence of a second target in addition to haematin. This author indicated evidences that malaria parasites recognize two subclasses of quinoline antimalarial drugs, the 4-aminoquinoline (as chloroquine **10**) and quinoline-4-methanol (as quinine **9** and mefloquine **12**). One of these evidences is that mutations of *pfcr1* cause chloroquine resistance in *P. falciparum* and it is associated with increased susceptibility to quinine and mefloquine. Moreover, mefloquine binds with high affinity to membrane and purified phospholipids, as phosphatidylinositol and phosphatidylserine, on the contrary, chloroquine does not bind to them with high affinity. Based on the difference in responses of malaria parasites to chloroquine, quinine and mefloquine and on the high affinity of phospholipids for mefloquine, it is probable that malaria parasite possess one or more phospholipids targets for quinoline-4-methanol antimalarial drugs.

Other systems of detoxification are situated mainly in the cytosol, such as detoxification by glutathione (GSH), haeme binding proteins and degradation of free haeme by H_2O_2 as Figure 4 (Kumar *et al.*, 2007).

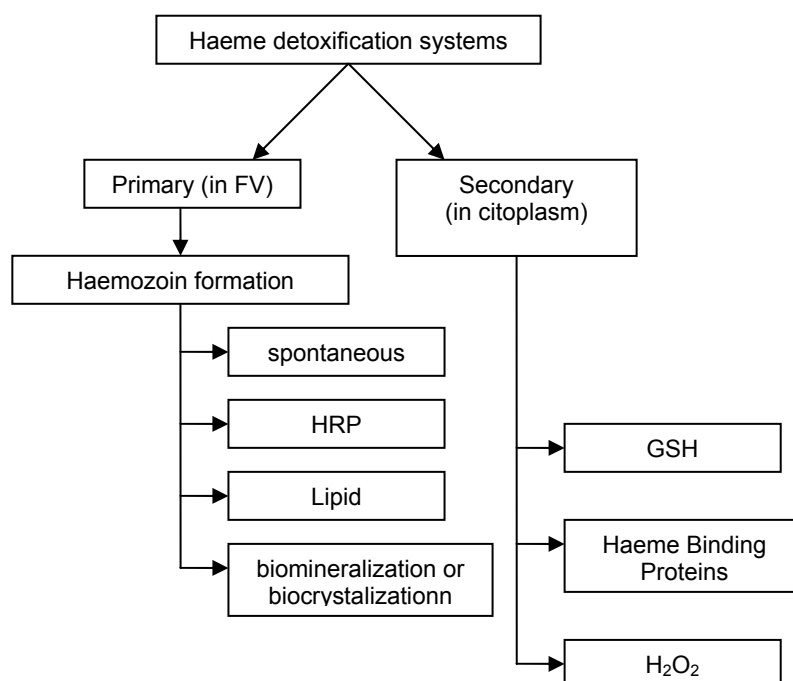


Figure 4. Free haeme detoxification systems in malaria parasite (Kumar *et al.*, 2007).

III.1.2.2 Quinolines-mechanism of action, spectroscopic and computational features

The 4-aminoquinoline derivative chloroquine **10** is the prototype of this therapeutic class and has been studied extensively. It is believed to exert its antimalarial activity by inhibiting a process of haematin polymerization in the lysosomal vacuole of the parasite.

There are considerable evidences suggesting that the site of action of chloroquine and chloroquine-related compounds is the digestive vacuole of the parasite. It can be proposed about the drug: **i.** it enters the digestive vacuole, possibly via diffusion of the free base across intervening membranes; **ii.** it accumulates in the digestive vacuole, at least in part due to pH trapping of the protonated drug at the low pH of the vacuole (Homewood *et al.*, 1972) (this process involves diffusion of only the free base across the digestive vacuole membrane; increased protonation of the drug at the low pH of the vacuole results in inflow of more drug until free base concentrations are equal on both sides of the membrane); **iii.** it forms a complex (Moreau *et al.*, 1985; Constantinidis and Satterlee, 1988) with haematin inhibiting the formation of haemozoin; and **iv.** it exerts a toxic effect on the parasite in the form of the haematin-drug complex (Egan *et al.*, 2000).

The complex formation between chloroquine and haematin was first reported in the 1960s by Cohen and co-workers. The authors observed changes in the UV-visible spectrum of Fe(III)PPIX upon addition of chloroquine. A considerable hypochromic effect in the Soret band of Fe(III)PPIX upon interaction with chloroquine in mixed aqueous solution (40% v/v aqueous DMSO) and in absolute ethanol was reported by Egan *et al.*, 1997 and Egan and Ncokazi, 2004.

Chou and co-workers (1980) proposed that haematin is the molecular drug target of chloroquine and other 4-aminoquinoline and quinoline methanol antimalarials and they further examined the equilibrium association of these compounds with haematin.

The knowledge of the structures of haematin-quinoline complexes derives from NMR and computational evidences. Moreau *et al.* (1985) were the first to attempt to elucidate these structures. Shifts in ^1H NMR spectra of chloroquine and quinine were monitored as a function of haematin and uroporphyrin concentration. Assuming a co-planar arrangement of the quinoline and porphyrin rings and using a mathematical ring-current model, the authors proposed a structure for the chloroquine **10** and quinine **9** complexes with uroporphyrin. They suggested that the quinoline ring is centered over the porphyrin ring, with the bulky Cl atom of chloroquine and the OCH_3 group of quinine as well as the side-chains of both compounds being held away from the porphyrin core. Considerations of ^{13}C NMR shifts, upon interaction of chloroquine and quinine with uroporphyrin, led Constantinidis and Satterlee (1988) to reach similar conclusions in the case of the chloroquine complex. However, in the case of quinine, they proposed that the drug is located towards the edge of the porphyrin. Both groups of authors suggested that chloroquine and quinine is sandwiched between two metalloporphyrins in the case of Fe(III)PPIX (haematin) and $\text{Fe(III)uroporphyrin}$ (Figure 5).

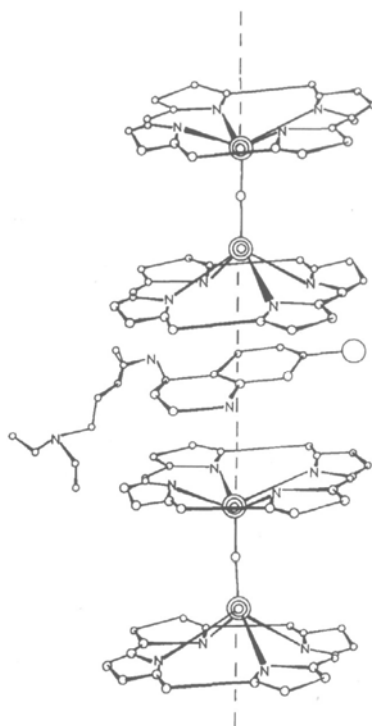


Figure 5. Chloroquine stacking in μ -oxo-oligomeric haematin (Moreau *et al.*, 1985)

Using molecular mechanics (MM) and molecular dynamics simulated annealing (MDSA) modeling an approximately co-planar arrangement of the quinoline and porphyrin rings was observed by Marques and co-workers (1996) and O'Neill and co-workers (1997). These later authors suggested, also, that the side chains are oriented away from the porphyrin nucleus and interacts with the negative charged propionate group, via positively charged protonated *t*-butylamino side chain by salt-bridge like interaction.

The main features of the proposed quinoline interaction with the porphyrin core have subsequently been supported by NMR-constrained MDSA calculations (Leed *et al.*, 2002). The NMR study obtained ^1H -Fe(III) distances from the effect of the paramagnetic center on T_1 ^1H -relaxation rates using the Solomon-Bloembergen equation. These distances were used as restraints in the calculations. In this study the quinoline nitrogen of chloroquine was found to be oriented towards the periphery of the porphyrin, while the 4-amino group was located closer to the Fe(III) center and the side chain was found to interact with the porphyrin. The NMR study demonstrated the dynamic nature of the complex and suggested that the quinoline ring is not entirely co-planar with the porphyrin ring, but is significantly tilted in most cases. Leed *et al.* (2002) proposed different distance between the terminal *N* and Fe(III)PPIX for the complex formed between unprotonated chloroquine (4.7 Å), monoprotonated chloroquine (5.3 Å) or diprotonated chloroquine molecule (4.6 Å). In the last case, the repulsion between *N* protonated and iron was decreased by the π - π interaction. In both of these models, Fe(III)PPIX was assumed to exist as a μ -oxo-dimer.

An alternative approach to understanding the structural aspects of Fe(III)PPIX-quinoline interactions was to explore features of the surfaces of both the quinoline and metalloporphyrin crystals. Buller and co-workers (2002), by making use of the crystal structure of β -haematin, have described a theoretical growth of β -haematin and proposed a noncovalent binding site for the quinoline family at the end face of the fastest-growing direction of β -haematin. Chloroquine form hydrogen bond between (aromatic)*N* and HC=C (vinyl) (2.4 Å), and a CCl interaction with CH₃ of the porphyrin (3.0 Å), and NH with C=C (2.7 Å) (Figure 6). These results are in agreement with those of

Solomonov and co-workers (2007), when an effect of the presence of quinine or chloroquine was observed on the β -haematin growth morphology. The authors showed by IR-ATR and Raman spectra that β -haematin growth in the presence of quinoline drugs embodies molecular based differences from pure β -haematin. The obtained results suggest modifications of surface and bulk propionic acid linkages and aggregation perturbation within the crystal.

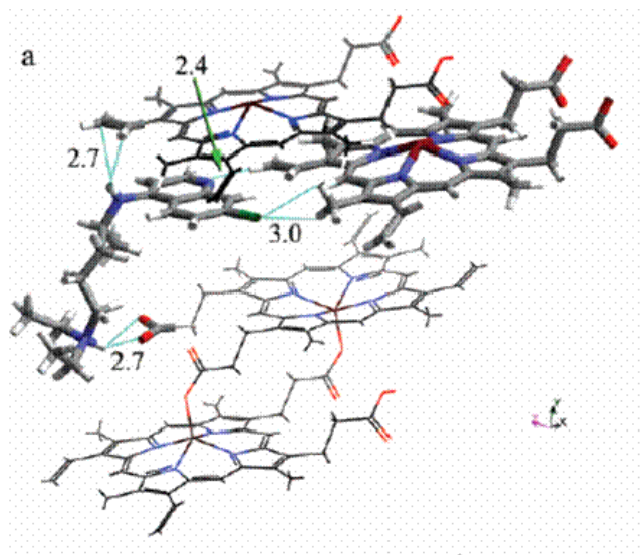


Figure 6. Chloroquine bound to (001) β -haematin crystal highlighting energetically favorable interactions (Buller *et al*, 2002).

Vippagunta and co-workers (1999), assuming a sandwich type structure in which the quinoline is located between two Fe(III)PPIX μ -oxo-dimers, found that the electron rich part of the quinoline, indicated by a molecular electrostatic potential (MEP) surface determined by *ab initio* calculation at the 6-31G** level of theory, could be comfortably situated over the core of the metalloporphyrin, which is electron poor. The electron density of the quinoline was found to be located towards the edge containing the quinoline nitrogen and C-8. This electronic arrangement has been supported by a subsequent study using density functional theory (Portela *et al.*, 2004). This confirms that in the neutral quinolines, the edge of the ring containing the *N* and C-8 has strong negative character, while that to which the 4-amino group is attached is electron poor. This study has proposed that the electron poor region interacts with the porphyrin core, which this study suggested to be electron rich. These authors

further proposed that two points of electron density on the electron rich edge of the quinoline interact with the Fe(III)PPIX propionate protons that are electron deficient. Biot and co-workers (2005) showed that protonation of the chloroquine *N* causes a major change in the distribution of electron density. The area around the Cl atom is the least positive area of the chloroquine dication, while the three *N* atoms exhibit the most positive character.

Despite the significant advances in our understanding of Fe(III)PPIX–quinoline interactions, the relationship between formation of such complexes and the ability of the quinoline to inhibit β -haematin formation remains elusive. In addition, correlations between Fe(III)PPIX–quinoline interactions in solution and biological activity have also remained elusive. By contrast, there is significant correlation between β -haematin inhibition and biological activity (Egan, 2006).

III.1.3 Resistance to antimalarial drugs

Resistance of *P. falciparum* to chloroquine appeared almost simultaneously in Colombia and on the frontier between Thailand and Cambodia. In Asia, chloroquine resistance was initially confined to the Indochinese peninsula, until the 1970's, when it spread westwards and towards the neighboring islands in the south and east. The advent of chloroquine resistance in Africa occurred much later, and it took a decade to cross the continent. Today, only countries in Central America north of the Panama Canal and on the island of Hispaniola have not documented chloroquine-resistant *P. falciparum* malaria (Wongsrichanalai *et al.*, 2002; WHO, 2006b).

The sulfadoxine–pyrimethamine combination was used as a replacement for chloroquine in most countries. At the beginning of the 1980's, however, that treatment became almost totally ineffective in Thailand and neighboring countries, and resistance to the treatment spread rapidly in South America. In 1993, Malawi was the first country in East Africa to change from chloroquine **10** to the sulfadoxine–pyrimethamine combination as the first-line drug, and other African countries followed this example in the late 1990's. Because of extensive

use of this combination, however, resistance also spread in East Africa (Alecrim *et al.*, 1999; Wongsrichanalai *et al.*, 2002; WHO, 2006b).

Resistance to mefloquine **12** is found mostly in Cambodia, Myanmar, Thailand and Viet Nam. Sporadic cases of prophylactic failure of mefloquine in travellers and therapeutic failure have been reported in Africa, other Asian countries and South America. Several studies have shown a diminution in sensitivity *in vitro*, and studies *in vitro* in West Africa showed the existence of strains with decreased sensitivity to mefloquine even before its introduction into the region for therapeutic use. Resistance to quinine **9** is often overestimated, as the dosage of 24 mg base per kg for 7 days is rarely respected, and the threshold for resistance *in vitro* has not been clearly defined (Wongsrichanalai *et al.*, 2002; WHO, 2006b).

So far, no resistance to artemisinin **17** or artemisinin derivatives has been reported, although some decrease in sensitivity *in vitro* has been reported in China and Viet Nam (WHO, 2006b).

The genetic mechanisms of *P. falciparum* drug resistance have not been completely elucidated. Five parasite genes that appear to play a role in regulation of resistance to the principal chemical families of antimalarials in current use have been identified. These are briefly discussed in the following.

III.1.3.1 Dihydrofolate reductase (*dhfr*)

Several studies on the *dhfr* gene have provided solid proof of the fundamental importance of a point mutation at the Ser108Asn codon in the pyrimethamine-resistant phenotype of *P. falciparum*. Additional point mutations at the Asn51Ile, Cys59Arg or Ile164Leu positions increase the level of resistance to antifolates. Not only there is an almost perfect correlation between the presence of a mutant codon 108 and resistance to pyrimethamine **14** *in vitro*, but also the level of resistance increases with the number of mutations (Basco and Ringwald, 2000).

Triple mutations at codons 108, 51 and 59 are seen in South-East Asia and Africa. A quadruple mutant represents the severest form of resistance and is responsible for a high level of resistance to the sulfadoxine–pyrimethamine combination (Hankins *et al.*, 2001; Krudsood *et al.*, 2005).

III.1.3.2 Dihydropteroate synthase (*dhps*)

The mechanism of resistance to sulfadoxine **16** is also associated with point mutations. Five sites of point mutation, on the Ser436Ala/Phe, Ala437Gly, Lys540Glu, Ala581Gly and Ala613Thr/Ser codons of the *dhps* gene, have been reported. It is unclear which mutation is the key, as a mutation at codon 108 is in *dhfr*, and mutations at 436, 437 and 540 may confer some degree of resistance. A higher level of resistance requires multiple mutations. The 581 and 613 mutations are rare or absent in Africa but could lead to a high level of resistance to sulfadoxine–pyrimethamine (Wang *et al.*, 1997; Ndounga *et al.*, 2001; Mberu *et al.*, 2002).

III.1.3.3 *P. falciparum* chloroquine-resistance transporter (*pfcr*t)

The *pfcr*t gene is situated on chromosome 7 and it codes for a protein transport in the vacuolar membrane (Fidock *et al.*, 2000). Experimental studies with clones and transfected parasites have shown that the *pfcr*t gene plays a major role in determining the phenotype of chloroquine **10** resistance, when lysine has been replaced at codon 76 by threonine. This mutation is generally not isolated but is associated, depending on the geographical setting, with mutations at other codons, Cys72Ser, Met74Ile, Asn75Glu, Ala220Ser, Gln271Glu, Asn326Ser, Ile356Thr and Arg371Ile, the role of which is not well defined. Clinical studies have confirmed that the Lys76Thr mutation is present in all isolates of *P. falciparum* after treatment failure with chloroquine (Djimbe *et al.*, 2001; Basco *et al.*, 2002). However, these studies also showed that this mutation can be present in chloroquine-sensitive isolates, suggesting that other mutations in the *pfcr*t gene or other genes may be involved (Basco, 2002;

Thomas *et al.*, 2002; Chen *et al.*, 2002; Mappi *et al.*, 2003; Ngo *et al.*, 2003; Vathsal *et al.*, 2004; Casey *et al.*, 2004; Durrand *et al.*, 2004).

III.1.3.4 *P. falciparum* multidrug-resistance gene 1 (*pfmdr1*)

The *cg2* gene was initially suggested to be the key gene for chloroquine resistance, but its association with chloroquine resistance is probably artefactual and related to the fact that it is situated on chromosome 7 close to the *pfcr1* gene (Su *et al.*, 1997). The *pfmdr1* gene, situated on chromosome 5 and coding for the P-glycoprotein homologue 1, has also generated keen interest, because of two observations. In some mammalian cancer cells, over expression of *mdr* genes encoding P-glycoprotein is directly correlated with an increased efflux of anti-cancer drugs from drug-resistant cells. Drug efflux can be inhibited by several pharmacological entities that are not anticancer agents, so that drug-resistant cancer cells are killed by the drug against which they are resistant. A similar phenomenon has been observed *in vitro* with chloroquine-resistant *P. falciparum* exposed to resistance modulators (e.g. verapamil modulates drug resistance in both cancer cells and malaria parasites). The Asn86Tyr mutation has been associated with chloroquine resistance, but studies conducted *in vivo* and *in vitro* in parallel have produced discordant results (Gomez-Saladin *et al.*, 1999; Nagesha *et al.*, 2001; Basco and Ringwald, 1997; Basco and Ringwald, 1998; Bhattacharya and Pillai, 1999; Bhattacharya *et al.*, 1997; von Seidlein *et al.*, 1997; Grobusch *et al.*, 1998; Flueck *et al.*, 2000).

Several other compensatory mutations have also been described: as Tyr184-Phe, Ser1034Cys, Asn1042Asp and Asp1246Tyr. Linkage disequilibrium between the Lys76Thr mutation on the *pfcr1* gene and the Asn86Tyr mutation on the *pfmdr1* gene have been observed in studies in Burkina Faso, Nigeria and Sudan, providing a supplementary argument for the hypothesis that polymorphisms have to converge before emergence of a phenotype that is strongly chloroquine-resistant (Adagut and, 2001; Babiker *et al.*, 2001; Tinto *et al.*, 2003). All highly chloroquine-resistant isolates have at least the Lys76Thr and Ala220Ser mutations in the *pfcr1* gene, generally

associated with the Asn86Tyr mutation in the *pfmdr1* gene (Howard *et al.*, 2002). An additional mechanism of chloroquine resistance suggested for *pfmdr1* is gene amplification, which was observed in some chloroquine-resistant reference clones. In laboratory-adapted clones selected for drug resistance *in vitro*, gene amplification might play a role in determining the drug resistance phenotype, although amplification does not appear to be the main mechanism of chloroquine resistance in field isolates.

The *pfmdr1* gene has also been implicated in resistance to amino alcohols and artemisinin. Transfection studies have raised the possibility that the Asn86Tyr, Ser1034Cys, Asn1042Asp and Asp1246Tyr mutations are associated with quinine resistance as well as increased sensitivity to mefloquine **12**, halofantrine **21**, lumefantrine and artemisinin derivatives. Field studies have yielded contradictory results (Zalis *et al.*, 1998; Reed *et al.*, 2000; Duraisingh *et al.*, 2000a; Duraisingh *et al.*, 2000b; Basco and Ringwald, 2002; Pillai *et al.*, 2003).

III.1.3.5 Cytochrome *b*

When atovaquone **22**, a hydroxynaphthoquinone, is administered as monotherapy, resistant parasites are rapidly selected. In order to delay the emergence and spread of atovaquone resistance, the synergistic combination atovaquone–proguanil has been developed (Looareesuwan *et al.*, 1999). Molecular analysis of recrudescence isolates demonstrated that atovaquone resistance was linked to a single mutation at the cytochrome *b* gene codon (Tyr268Asn or Tyr268Ser), inducing an approximately 10,000-fold increase in the atovaquone IC₅₀ (Fivelman *et al.*, 2002; Gil *et al.*, 2003). This mutation appeared to provide a sufficient explanation of the treatment failures observed with the atovaquone–proguanil combination.

III.1.4 Targets for antimalarial chemotherapy

Most antimalarial drugs in use nowadays were developed through serendipitous identification of the therapeutic activity of natural products (as quinine **9** and artemisinin **17**), its derivatives (as cloroquine **10** and artesunate **20**), or compounds used to other infectious (as antifolates and tetracyclines). Recently, the advanced of molecular biology techniques improved the understanding of the biochemistry of malaria parasites concurring to the identification of potential targets for new drugs (Fidock *et al.*, 2004).

These targets could be related to the functions of the parasite organelles structures. So, in Table 1, it can be seen the possible targets to be explore. Some of them are currently projects in development. It is emphasized the interest on the lysosomal food vacuole (site of the haemoglobin degradation), the apicoplast (a plastid organelle) and the mitochondrion (Macreadie *et al.*, 2000; Fidock *et al.*, 2004).

Table 1. Targets for antimalarial chemotherapy (Fidock *et al.*, 2004).

Target location	Mechanism	Target molecule	Existing therapies	New compounds
Cytosol	Folate metabolism	Dihydrofolate reductase Dihydrofolate synthase	pyrimethamine, proguanil sulphadoxine, dapsone	Chlorproguanil
	Glycolysis	Thymidylate synthase Lactate dehydrogenase Peptide deformylase		
	Protein synthesis Glutathione metabolism	Heat shock protein 90 Glutathione reductase	artemisinine	5-fluoroorotate Gossypol deriv. Actinonin Geldanamycin Enzyme inhibit Oxindole derive.
	Signal transduction Unknown	Protein kinases Ca ²⁺ ATPase		
Parasite membrane	Phospholipid synthesis	Choline transporter	quinolines	G25 Dinucleoside dimers Hexoxe deriv.
	Membrane transport	Unique channels Hexose transporter		
Food vacuole	Haem polymerization	Haemazoin	chloroquine	New quinolines Protease inhibitors Protease inhibitors New peroxides
	Haemoglobin hydrolysis	Plasmepsins Falcipains unknown		
Mitochondrion	Free radica generation	Cytochrome c Oxidoreductase	artemisinins atavaquone	
	Electron transport			
Apicoplast	Protein synthesis	Apicoplast ribosome	tetracyclines, clindamycin quinolines rifampin	Thiolactomycin Triclosan Fosmidomycin Peptidomimetics
	DNA synthesis	DNA gyrase		
	Transcription	RNA polymerase		
	Type II fatty acid biosynthesis	FabH FabI/PfENR		
	Isoprenoid synthesis	DOXP reductoisomerase		
Extracellular	Protein famesylation	Famesyl transferase		
	Erythrocyte invasion	Subtilisin serine proteases		

It is important to emphasize that to explore these potential targets it will be necessary to get standardized *in vivo* and *in vitro* screens in order to evaluate new compounds.

It is clear that new antimalarial drugs are needed. In this sense, exploration of natural products through medicinal chemistry and lead optimization should contribute to obtain more effective and less toxic medicines (Fidock *et al.*, 2004; Liu, 2005).

In this thesis, the synthesized compounds were designed based on the β -haematin inhibition as their mechanism of action having chloroquine as antimalarial drug prototype.

In resume, chloroquine is a weakly basic molecule and accumulated inside the food vacuole. It interacts with the μ -oxo dimer form of oxidized haeme and prevents the haemozoin formation. The π - π interaction between chloroquine and the electronic system of haematin governs the formation of adducts. Free haeme and haeme-chloroquine complexes kill parasites by including oxidative stress and this oxidative stress may lead to peroxidation of parasite membrane lipids, damage of DNA, oxidation of protein and finally parasite death (see Figure 7) (Kumar *et al.*, 2007).

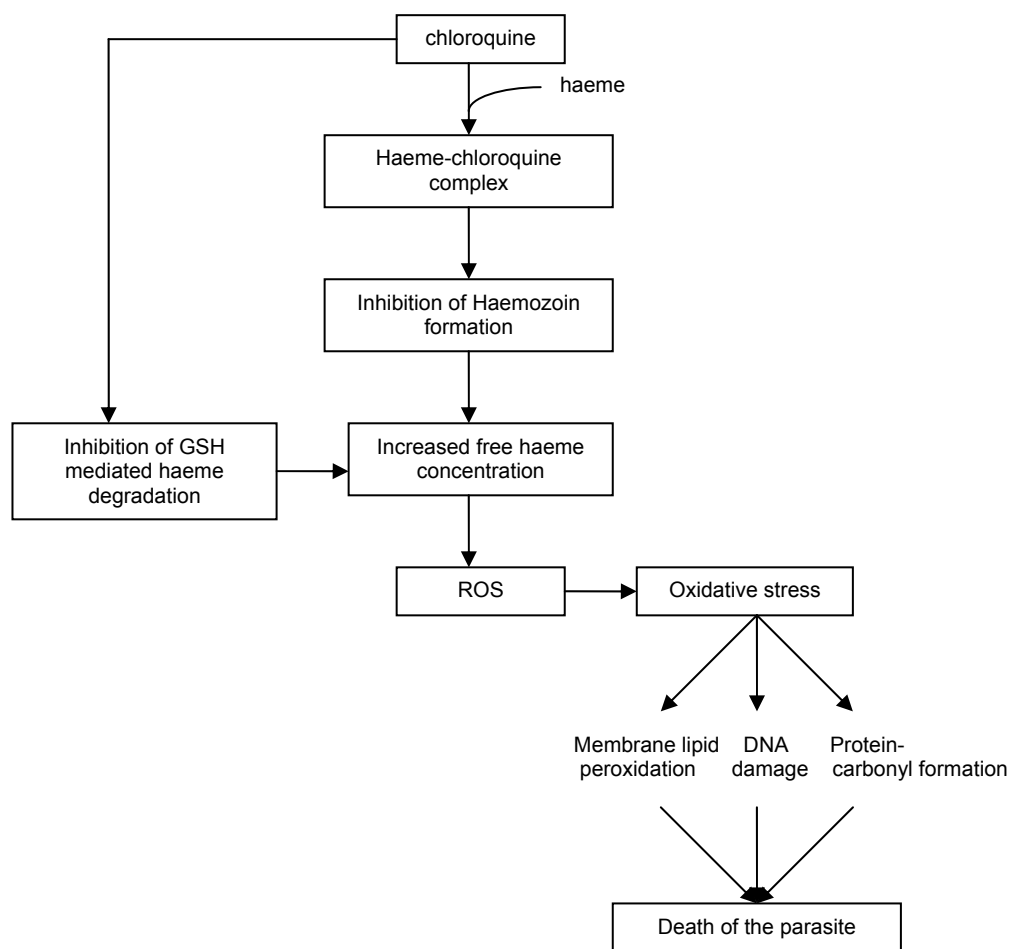


Figure 7. Mechanism of antimalarial activity of chloroquine (Kumar *et al.*, 2007).

III.2 Derivatives and antimalarial activity

III.2.1 Synthesis of aminoquinoline derivatives

Egan and co-workers (2000) presented the comparison of nineteen aminoquinolines in relation of Fe(III)PPIX complexation, β -haematin inhibition and antiplasmodial activity, in order to probe the effect of amino group position and of chlorination at the 7-position on the activities of these compounds with the aim of establishing a detailed structure-activity profile (SAR) of chloroquine. Through the presented results, these authors were able to propose a model of SAR in chloroquine according to Figure 8. First, the 4-aminoquinoline nucleus provides an Fe(III)PPIX complexing template but is not sufficient for inhibition of haemozoin formation; second, introduction of the 7-chloro group is responsible

for inhibition of haemozoin formation but probably has little influence on the strength of association with Fe(III)PPIX; and, finally, the aminoalkyl side chain is a requirement for strong antiplasmodial activity. These findings are in accordance with the investigations of De and co-workers (1998). It appears that changes in the side chain alone overcome chloroquine resistance without having to make changes to the quinoline nucleus.

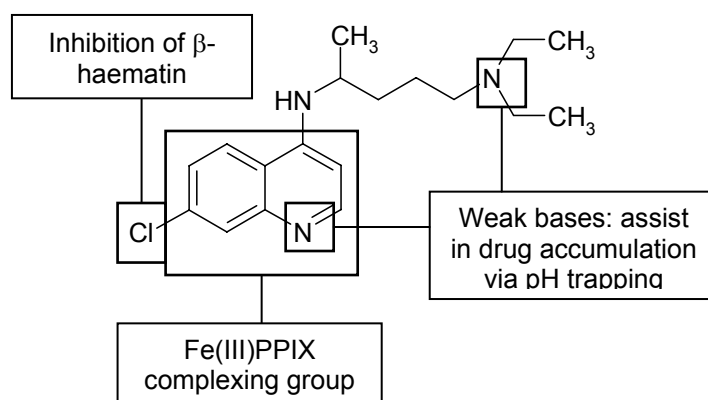


Figure 8. Proposed structure-function relationships in chloroquine (Egan *et al.*, 2000).

In continuation to the work discussed above, Kaschula and co-workers (2002) studied the role of the group at the 7-position of 4-aminoquinoline antiplasmodials. The tested groups at the 7-position were NH₂, OH, OCH₃, H, CH₃, halogens, CF₃ and NO₂. The β -haematin inhibitory activity of these derivatives appears to correlate with both the haematin-quinoline association constant and the electron-withdrawing capacity of the group at the 7-position (Hammett constant). Moreover, for the compounds under investigation, the haematin association constant is in turn influenced by the lipophilicity of the group at the 7-position. It can be reasoned that accumulation of the free aminoquinoline through pH trapping is therefore essential to drive the equilibrium toward complex formation.

III.2.2 Synthesis of bisquinoline derivatives

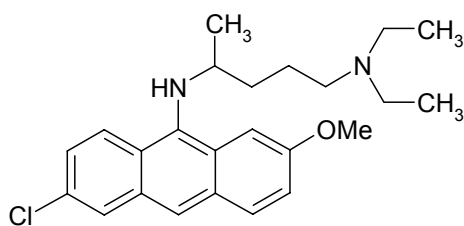
Biochemical studies indicate that isolates of the chloroquine-resistant parasite accumulate fewer drugs in the food vacuole than their more sensitive counterparts. However, opinions remain divided upon this mechanistic explanation. One possibility to overcome this resistance is to design quinoline-based drugs which are not recognized by the proteins involved in drug efflux. In this regard, bulky bisquinolines were synthesized and suggested to be extruded with difficulty by a proteinaceous transporter (Vennerstrom *et al.*, 1992).

Later, it was reported that some novel bisquinoline compounds comprising 4-(4-diethylamino-1-methylbutyl)aminoquinoline units joined by different linkers inhibited β -haematin formation with an efficiency similar to that of chloroquine (Ayad *et al.*, 2001).

There are other experiments at piperazine derivatives, see III.2.5.

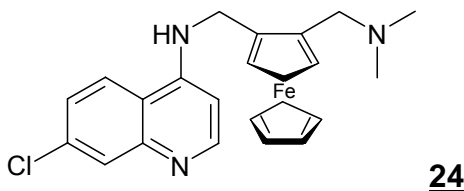
III.2.3 Synthesis of bisacridine derivatives

Acridine derivatives have been considered as potential antiprotozoal agents, and quinacrine **23**, the 9-amino-6-chloro-2-methoxyacridine analogue of chloroquine, was used clinically before chloroquine. Bisacridines may represent, along with bisquinolines, an alternative method to avoiding the efflux mechanism. However, the presence of an acridine moiety in a molecule can lead to stronger interactions with DNA and generate cytotoxicity. In this sense, Girault and co-workers (2000) had undertaken the synthesis of three series of bisacridines having alkanediamines and polyamines as linkers. These compounds were assayed to antimalarial, antitrypanosomal and antileishmanial activities. In relation to antimalarial activity, the introduction of a piperazine moiety to the linker resulted in a strong and selective activity (see again in piperazine derivatives, III.2.5).

**23**

III.2.4 Synthesis of ferrocene derivatives

The ferroquine **24**, a ferrocenic compound mimicking chloroquine, was synthesized by Biot and co-workers (1997). In this compound the lateral carbon chain of chloroquine was replaced by the hydrophobic ferrocenyl group where the four atoms between the two exocyclic *N* atoms were maintained.

**24**

The compound **24** was active *in vitro* against chloroquine-resistant strains of *P. falciparum* (FCM6, FCM7, and FG1), as well against *P. berguei* N and *P. yoelii* NS *in vivo*. The results summarized in Table 2 indicate that **24** and chloroquine have similar activity against the chloroquine-sensitive strains SGE2, FG2, and FG4. Furthermore, against the semi-chloroquine-resistant FG3 strain, **24** was more active than chloroquine. Also, ferroquine **24** was more active against the highly chloroquine resistant strains FCM6, FCM7, and FG1. In fact, the ratio of IC₅₀ indicated that compound **24** was about 22 times more effective against the parasite than chloroquine.

In continuation, the same authors submitted the above compounds to the blood schizontocidal assay in mice infected by *P. berguei* N and *P. yoelii* NS. Compound **24** (at 10 mg/kg/day, s.c.) was as efficient as chloroquine (at 10 mg/kg/day) against the two strains in a 4-day test. The survival study until 60 days indicated that all animals treated with **24** were cured from *P. berguei* N.

infection and only 20% of mice showed a recrudescence of *P. yoelii* NS infection. However, recrudescence occurred in all animals treated with chloroquine.

Table 2. *In vitro* sensitivity of *P. falciparum* strains to Chloroquine and Ferroquine **24**. n= number of experiments.

<i>P. falciparum</i> strains	IC ₅₀ (µg/mL)			
	Chloroquine	<i>n</i>	Ferroquine 24	<i>n</i>
SGE2	0.194 ± 0.175	8	0.160 ± 0.141	5
FG2	0.091 ± 0.065	3	0.059 ± 0.003	4
FG4	0.048 ± 0.009	4	0.057 ± 0.002	5
FG3	0.501 ± 0.139	3	0.095 ± 0.051	4
FCM6	1.241 ± 0.937	9	0.061 ± 0.013	8
FCM17	2.813 ± 2.189	5	0.177 ± 0.151	3
FG1	2.620 ± 0.175	3	0.067 ± 0.008	3

Delhaes and co-workers (2001) confirmed the *in vitro* antimalarial activity of **24** upon the *P. falciparum* chloroquine-sensitive strain HB3 and the CQ-resistant strains FCR3 and Dd2 (see Table 3). The better antimalarial activity of **24**, in comparison to chloroquine, was even more significant when comparing the IC₉₀ values. Regarding the *P. falciparum* chloroquine-resistant strain FCR3, IC₉₀ of **24** was six-fold smaller than the chloroquine one. In particular, Dd2, which is a mefloquine- and chloroquine-resistant strain, was as sensitive as HB3 to ferroquine.

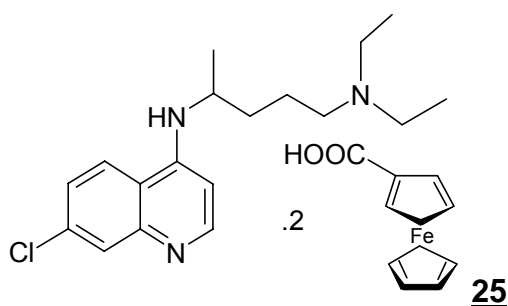
Table 3 *In vitro* antimalarial activity of chloroquine and ferroquine **24** against *P. falciparum* strains.

<i>P. falciparum</i> strains	IC ₅₀ (nM)	
	Chloroquine	Ferroquine 24
HB3	27.0 ± 1.1	17.6 ± 0.6
FCR3	152.2 ± 28.6	20.8 ± 8.7
Dd2	122.7 ± 0.9	14.1 ± 0.4
	IC ₉₀ (nM)	
HB3	43.5 ± 4.6	24.8 ± 0.9
FCR3	268.0 ± 49.5	42.0 ± 17.0

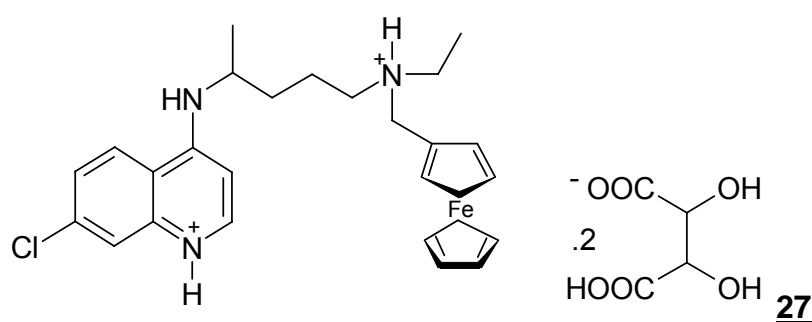
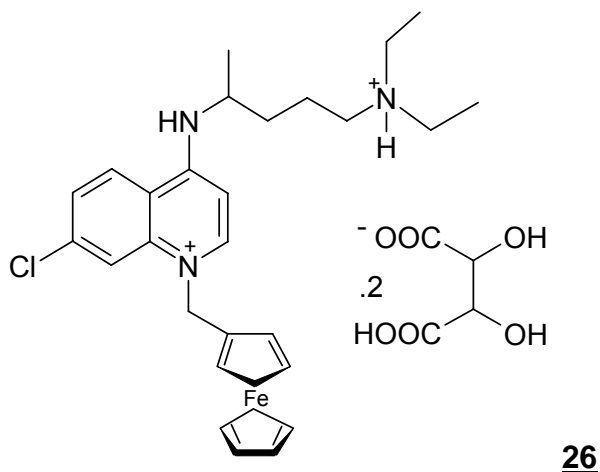
Ferroquine **24** completely inhibited the *in vivo* development of both chloroquine-resistant and sensitive *P. vinckei* strains and protected mice from lethal infection at a dose of 8.4 mg/kg/day subcutaneously or orally during 4 days. This curative effect was 5-20 times more potent than chloroquine. These compounds were tested to *in vitro* toxicity using lymphoma cells (L5178Y). Ferroquine was more toxic than chloroquine, nevertheless, the ferroquine security index remained about 700 to *P. falciparum* resistant strain, while the chloroquine security index dropped from 1,852 to 400 to *P. falciparum* chloroquine-sensitive and resistant strains, respectively (Delhaes *et al*, 2001).

The *in vitro* activity of ferroquine **24** was also evaluated using 103 *P. falciparum* cultures isolated from infected children from Gabon (Pradines *et al*, 2001). The IC₅₀ values of ferroquine were in the range of 0.43-30.9 nM and the geometric mean IC₅₀ for the 103 isolates was 10.8 nM, while the geometric mean for chloroquine, quinine, mefloquine, amodiaquine and primaquine were 370 nM, 341 nM, 8.3 nM, 18.1 nM and 7600 nM, respectively.

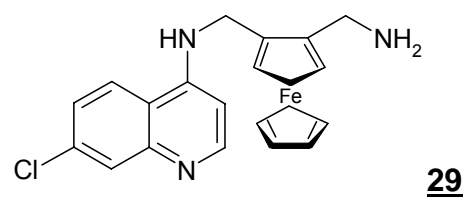
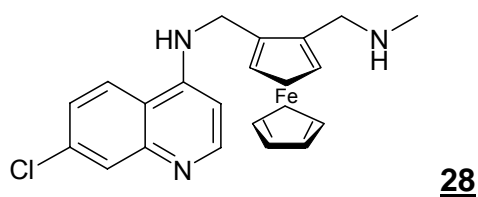
Through the synthesis of **25**, Domarle and co-workers (1998) demonstrated that the ferrocene molecule needs to be bound covalently to the chloroquine to inhibit the resistance of the parasite. Thus, the ferrocene by itself does not have an antimalarial activity but enhances the effectiveness of chloroquine when it is enclosed inside the molecule.



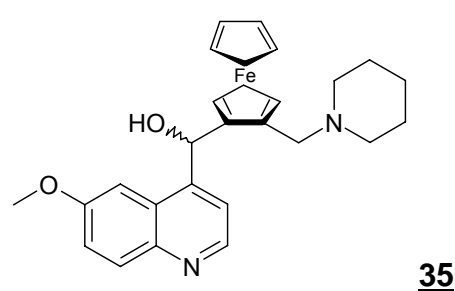
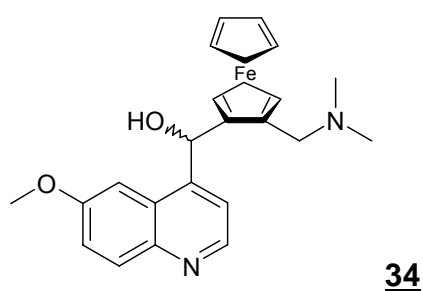
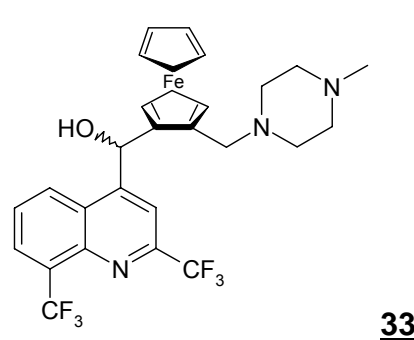
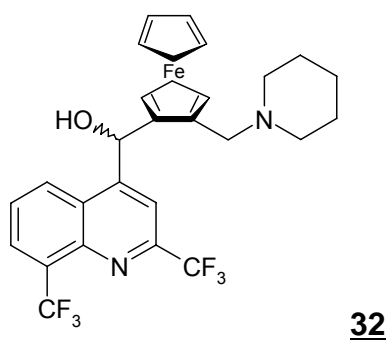
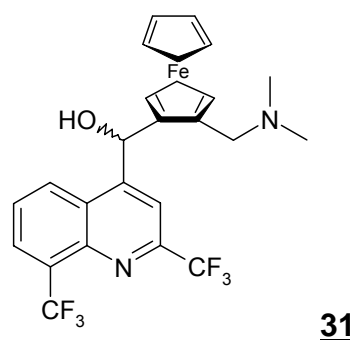
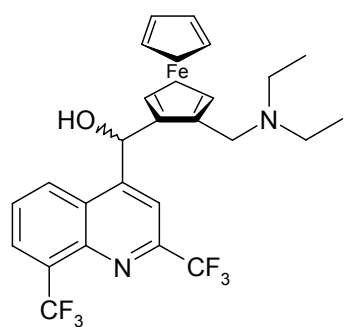
The position of the ferrocene group has also a significant importance. The compound **26** was less active than chloroquine and **27** was less active than ferroquine **24** when submitted to *in vitro* assays against *P. falciparum* strains HB3, Dd2, FG3, FG4, FCR3, and FG1 (Biot *et al*, 1999).



The two major metabolites of chloroquine are monodesethylchloroquine and didesethylchloroquine. By analogy, Biot and co-workers (1999) synthesized and evaluated two amino derivatives of ferroquine possessing terminal secondary or tertiary amine. Desmethylferroquine **28** possessed antimalarial activity comparable to that of the parent compound, against *P. falciparum* strains HB3 and Dd2. Didesmethylferroquine **29** was less potent against Dd2 strain, and as potent against HB3 strain as ferroquine **24**. These results are similar to those obtained for chloroquine and its major metabolites and suggest that, if the metabolization pathway of ferroquine is similar to that of chloroquine, the resulting products would remain more active than chloroquine against *P. falciparum*.



The strategy used to the synthesis of new ferrocene-antimalarial analogues, which replaced the carbon chain of chloroquine by ferrocenyl moiety, was applied to amino-alcohols by Biot and co-workers (2000) to afford new synthetic ferrocenic mefloquine **30** to **33** and quinine **34** and **35** analogues. These compounds were evaluated against *P. falciparum* HB3 and Dd2 strains and exhibited a lower antimalarial activity than mefloquine or quinine themselves.



Some artemisinin derivatives containing a ferrocenic nucleus (**36**, **37**, **38**, and **39**) were prepared and tested *in vitro* against *P. falciparum* strains (HB3, SGE2 and Dd2) by Delhaes and co-workers (2000) (see Table 4). Compound **38** was the most active against *P. falciparum* Dd2 strain (chloroquine-resistant), which activity was similar to artemisinin. Notably, it was the only compound to possess an amine function.

The authors also showed that **38** had capacity to bind with ferroprotoporphyrin IX, presenting an stoichiometry ferroprotoporphyrin IX:compound **38** of 2:1 at equilibrium. This result seems to demonstrate the role of adducts between artemisinin derivatives and haeme in the mechanism of action of these compounds.

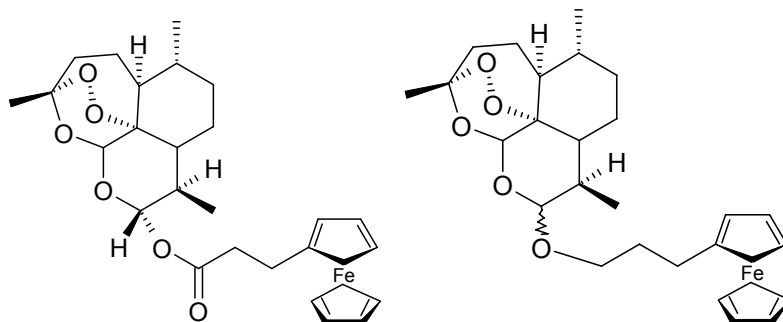
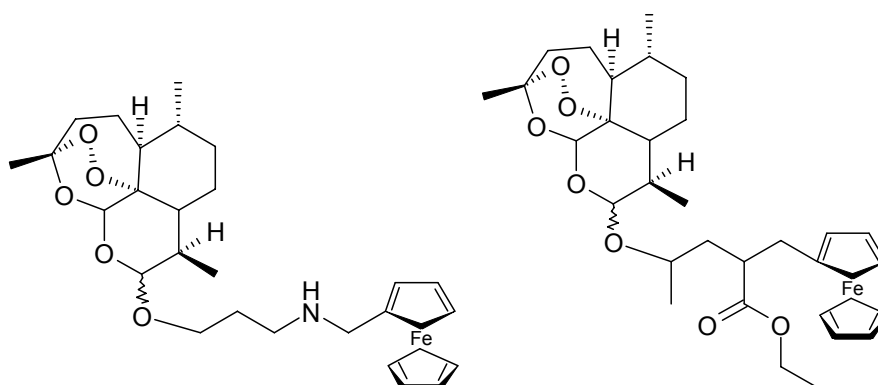
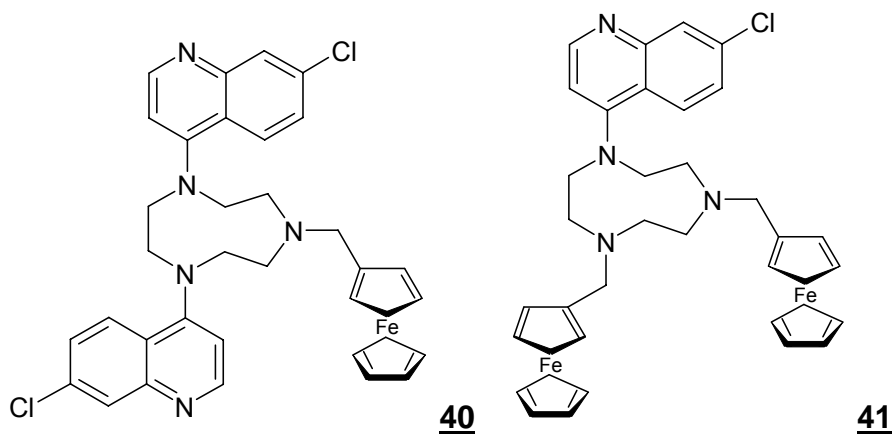
**36****37****38****39**

Table 4. *In vitro* antimalarial activity of artemisinin derivatives against *P. falciparum* strains.

Compounds	IC ₅₀ (nM)		
	HB3	SGE2	Dd2
36	10 ± 3	19 ± 9	32 ± 7
37	36 ± 6	49 ± 13	86 ± 15
38	12 ± 2	11 ± 5	14 ± 2
39	21 ± 5	31 ± 9	45 ± 5
artemisinin	7 ± 1	9 ± 4	13 ± 3
dehydroartemisinin	5 ± 1	9 ± 1	5 ± 2

Biot and co-workers (2004) synthesized the chloroquine-like bisquinoline **40** and bisferrocene **41**, considering that bisquinolines had already been active upon *P. falciparum*. The *in vitro* activity of the ferrocenic compounds **40** and **41** was monitored against two *P. falciparum* strains, HB3 and Dd2. Compound **40** was more active upon Dd2 strain ($IC_{50} = 62$ nM) than chloroquine although this compound was less active on the chloroquine-sensitive strain HB3, than chloroquine and ferroquine.



The physicochemical properties of ferroquine **24** were investigated by analogy with chloroquine in order to obtain information about its mechanism of action (Biot *et al*, 2005). Like chloroquine, ferroquine form complexes with haematin in solution ($\log K = 5.52$ and 4.95 , respectively). This is also demonstrated by the disappearance of the peaks at 1662 and 1209 cm^{-1} at the infrared spectrum of the compounds-haematin complexes which peaks are characteristics of β -haematin (Egan *et al*, 1994; 1999). The inhibition of β -haematin formation by diprotonated ferroquine was also quantified and related to that of chloroquine using the BHIA (β -haematin inhibitory activity) assay. The quantitative BHIA assay is based on the different solubility of haemin and β -haematin in DMSO and NaOH solution, respectively. The method determines the 50% inhibitory concentration for β -haematin inhibition in equivalents of compounds to haemin ($BHIA_{50}$). The ferroquine is a stronger inhibitor of β -haematin formation ($BHIA_{50} = 0.78$) than chloroquine ($BHIA_{50} = 1.9$).

However, both the basicity and lipophilicity of ferroquine was significantly different from those of chloroquine. The lipophilicity of ferroquine and chloroquine were similar when protonated at the putative food vacuole pH of 5.2

(log $D = -0.77$ and -1.2 , respectively), but differ markedly at pH 7.4 (log $D = 2.95$ and 0.85 , respectively) (Biot *et al.*, 2005).

In addition, the pK_a values of ferroquine were lower ($pK_{a1} = 8.19$ and $pK_{a2} = 6.99$) than those of chloroquine (10.03 and 7.94, respectively). This suggests that there would be a somewhat less vacuolar accumulation of ferroquine compared to chloroquine but this behavior could be partly compensated by its stronger β -haematin inhibition (Biot *et al.*, 2005). So, the authors concluded that the presence of the ferrocene moiety with different shape, volume, lipophilicity, effects on basicity and electronic profile dramatically modifies the pharmacological behavior of the parent drug. However, ferroquine appears to present reduced affinity for the postulated transporter related to chloroquine resistance (*pfCRT*) which seems to be extremely structure specific (Figure 9).

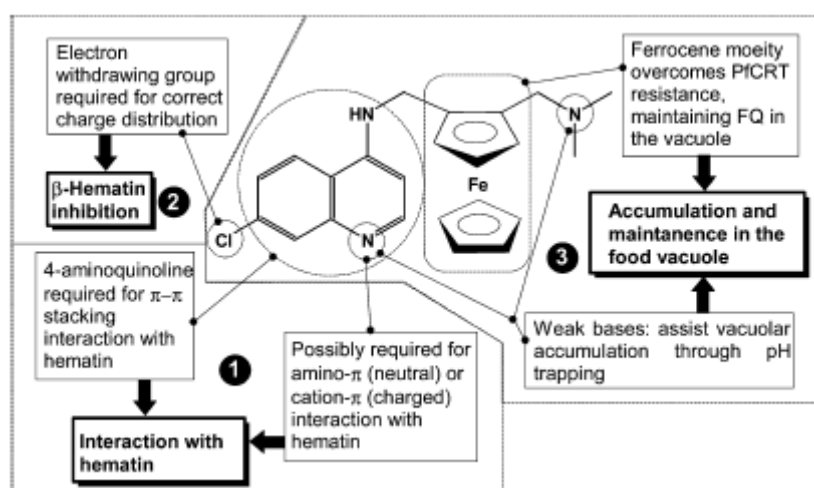
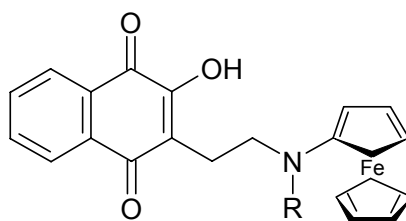


Figure 9. Proposed structure-activity relationships for ferroquine (Biot *et al.*, 2005)

Three ferrocenyl aminohydroxynaphthoquinones, **42**, **43**, and **44**, analogues of atovaquone which possess activity against *Toxoplasma gondii* *in vitro*, were evaluated against *P. falciparum* strains (3D7 and Dd2) by Baramée and co-workers (2006). However, these compounds were less active than atovaquone.



III.2.5 Synthesis of piperazine derivatives

Resistance to CQ may involve several mechanisms but its reversal by molecules such as verapamil and chlorpromazine suggests that an enhanced CQ efflux by a multi-drug-resistant mechanism may be implicated (Reed *et al* 2000). One possibility to overcome this mechanism is to design quinoline-based drugs which are not recognized by the proteins involved in the drug efflux. Considering this, several series of quinolines and acridines where aromatic rings are joined by a variety of polyamines were studied. Among them, the piperazine derivatives displayed antimalarial activity (Ryckebusch *et al.*, 2003).

In this regard, a series of bisacridine derivatives was prepared by Girauld and co-workers (2000). From this series, the bisacridine derivative **45**, having a bisaminopropylpiperazine linker, was tested to *in vitro* antimalarial activity upon the *P. falciparum* CQ-resistant strain FcB1R and, subsequently, to other seven strains (see Table 5). Compound **45** displayed a low *in vitro* cytotoxicity (CC₅₀= 25 μM) on MRC-5 cells and it was considered a potential antimalarial agent.

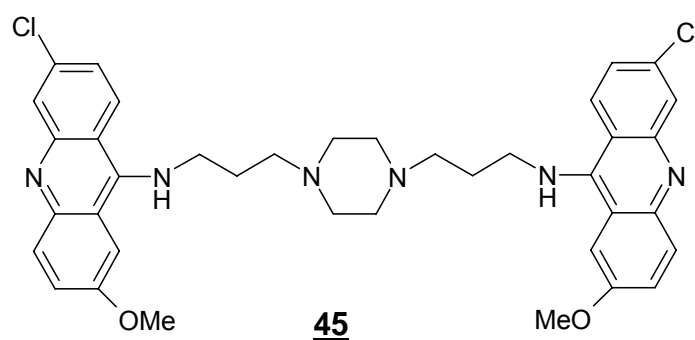
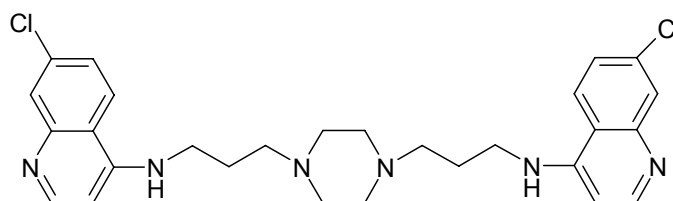


Table 5. *In vitro* sensitivity of *P. falciparum* strains to bisacridine **45**.

<i>P. falciparum</i> strains	IC ₅₀ (nM)		
	Chloroquine	Mefloquine	45
FcB1R			17.0 ± 10.0
3D7	20.0 ± 4.0	40.0 ± 10.0	13.0 ± 3.0
F32a	22.0 ± 2.0	62.0 ± 6.0	8.0 ± 2.0
GP1	39.0 ± 2.0	17.0 ± 3.0	11.0 ± 5.0
FCR3	102.0 ± 6.0	36.0 ± 15.0	18.0 ± 6.0
FCM29	216.0 ± 25.0	8.0 ± 3.0	13.0 ± 6.0
W2	219.0 ± 16.0	30.0 ± 3.0	12.0 ± 2.0
K1	267.0 ± 42.0	12.0 ± 1.0	16.0 ± 5.0

Continuing the efforts to design new series of 4-aminoquinoline derivatives active on resistant *P. falciparum* strains, the same authors synthesized bis-, tris- and tetra-quinolines using different spacers (Girauld *et al*, 2001). One of these derivatives, compound **46**, possessing a piperazine linker, displayed a good activity whatever the degree of CQ resistance of the *P. falciparum* strains tested (e.g., on FcB1 strain, IC₅₀ = 23 nM) (Rychebusch *et al*, 2002).

**46**

However, while the compound **46** containing two quinolines moieties was cytotoxic at 1 μM on human MRC-5 cells and mouse peritoneal macrophages, its bisacridine counterpart **45** was totally devoid of cytotoxicity at 25 μM. In order to explore the influence of the terminal group of 4-aminoquinoline derivatives on their biological properties and cytotoxicity, Rychebusch and co-workers (2003) designed compounds with terminal aromatic and aliphatic substituents. Three series of compounds were synthesized possessing amide (A series), secondary amine (B series), and tertiary amine (C series) terminal links.

In Table 6, it is presented the *in vitro* sensitivity of *P. falciparum* FcB1 Strain to Compounds **47-66** (Series A), **67-86** (Series B), and **87-106** (Series C).

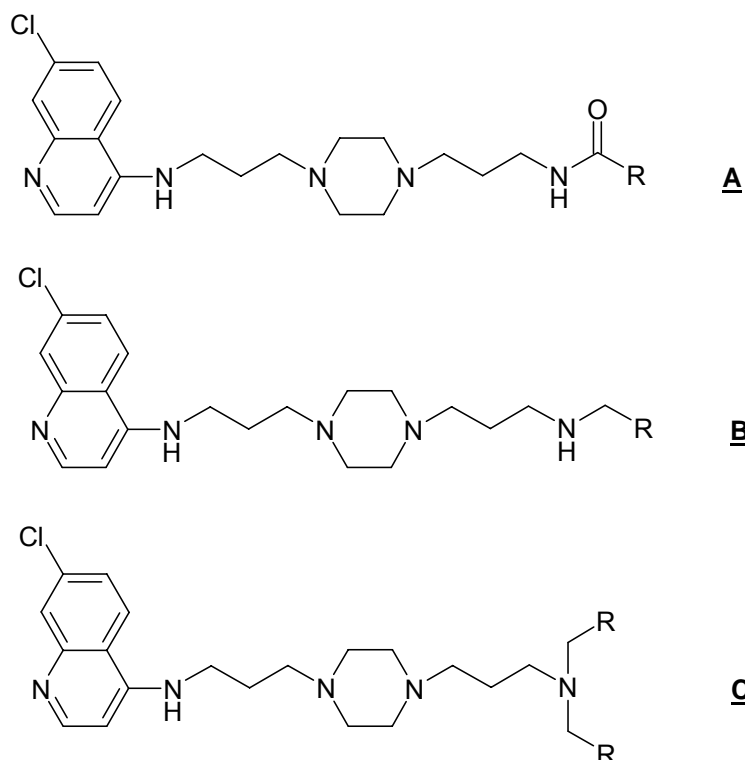


Table 6. *In Vitro* Sensitivity of *P. falciparum* FcB1 Strain to Compounds **47-66** (Series A), **67-86** (Series B), and **87-106** (Series C). (NT: not tested)

R	Series A	IC ₅₀ (nM)	Series B	IC ₅₀ (nM)	Series C	IC ₅₀ (nM)
CQ		126 ± 26,0				
4-quinolinyl	47	20.1 ± 2.3	67	74.1 ± 6.1	87	142.1 ± 8.5
1-naphthyl	48	155 ± 17	68	26.6 ± 5.1	88	215 ± 46.4
phenyl	49	80.6 ± 5.8	69	16.5 ± 4.6	89	54.4 ± 10.6
3-thiophenyl	50	112.1 ± 36	70	11.4 ± 0.9	90	62.8 ± 8.4
3-phenoxyphenyl	51	20.8 ± 5.9	71	19.8 ± 1.3	91	260.5 ± 16.2
4-chlorophenyl	52	16.7 ± 5.2	72	16.6 ± 3.7	92	NT
4-methoxyphenyl	53	20.2 ± 1.3	73	19.4 ± 0.7	93	9.6 ± 1
4-fluorophenyl	54	48.9 ± 11.5	74	18.7 ± 1.2	94	NT
4-nitrophenyl	55	12.2 ± 0.9	75	5.9 ± 1.3	95	46.1 ± 5.7
4-hydroxyphenyl	56	416 ± 18.3	76	55.2 ± 12	96	45.5 ± 12.6
benzyl	57	67.4 ± 8.4	77	18.5 ± 0.5	97	26.2 ± 5.6
phenethyl	58	82 ± 3,1	78	25.9 ± 7.8	98	40.1 ± 2.6
cyclohexyl	59	215.9 ± 15.9	79	43 ± 9.8	99	16 ± 4.3
cyclopropyl	60	289.2 ± 25.8	80	10.2 ± 7.6	100	8.8 ± 1.7
hexyl	61	34.7 ± 3.1	81	9.5 ± 0.3	101	37.8 ± 12.3
propyl	62	73.4 ± 3.7	82	24.8 ± 4.2	102	7.5 ± 2.8
ethyl	63	276.7 ± 8.1	83	36.1 ± 1.5	103	2.2 ± 1.1
methyl	64	396 ± 116.2	84	58 ± 13.2	104	5 ± 0.8
<i>tert</i> -butyl	65	163.2 ± 4.2	85	9.7 ± 0.4	105	NT
isopropyl	66	149 ± 9.3	86	18.8 ± 0.8	106	0.9 ± 0.1

It is generally admitted that a stronger basicity of the molecule increases the antimalarial activity due to a better uptake in the vacuole owing to the pH gradient between the cytosol and the acidic vacuole. By taking this into account, series B and C were designed to evaluate the influence of the introduction of a fourth basic nitrogen on the antimalarial activity, while the amide link, being of inherent weak base properties and flexibility, played the role of control (Ryckebusch et al., 2003).

The activity of the tertiary amines is very dependent on the R group, which suggests that steric hindrance and basicity of the amine play a role in the activity of this series. With the exception of **93** and **96**, compounds possessing aromatic groups (**87-98**) proved to be less active than their monosubstituted counterparts. For aliphatic R groups (**99-106**), an elongation of the chain tends to decrease the activity of the compounds. In this last series, several compounds were considered as good antimalarial candidates, particularly the compounds **100** and **102-106**.

The following order of cytotoxicity was observed: series A (18 compounds with CC_{50} values above 15 μ M) < series B (4 compounds with CC_{50} values above 15 μ M) < series C (none compound with CC_{50} value above 15 μ M) (see Table 7) (Ryckebusch *et al.*, 2003).

Aliphatic compounds from series C were more cytotoxic than their secondary amine and amide counterparts. Among all compounds assayed, eleven of them (**47**, **61**, **80**, **82-85**, **100**, **102**, and **106**) revealed selectivity index (ratio CC_{50}/IC_{50}) superior to that of CQ and a large number of substitutions lead to compounds having reduced cytotoxicity when compared to bisquinoline **46** ($CC_{50} < 1\mu$ M).

Studies of some compounds revealed that they were better inhibitors of β -haematin formation than chloroquine (Table 8) (Ryckebusch et al., 2003).

Table 7. *In vitro* Cytotoxicity of Compounds **47-66** (Series A), **67-86** (Series B), and **87-106** (Series C) on MRC-5 cells (selectivity index are given in parentheses).

R	Series A	CC ₅₀ (μM)	Series B	CC ₅₀ (μM)	Series C	CC ₅₀ (μM)
CQ		50.0 (397)				
4-quinoliny	47	16.4 (816)	67	1.2 (16)	87	5.6 (39)
1-naphthyl	48	4.0 (26)	68	5.5 (224)	88	4.0 (19)
phenyl	49	15.6 (194)	69	5.0 (303)	89	1.0 (18)
3-thiophenyl	50	20.5 (183)	70	1.0 (88)	90	1.0 (16)
3-phenoxyphenyl	51	5.0 (240)	71	1.0 (51)	91	4.0 (15)
4-chlorophenyl	52	1.0 (60)	72	1.0 (60)	92	1.0 (nd)
4-methoxyphenyl	53	4.0 (198)	73	4.0 (206)	93	1.0(104)
4-fluorophenyl	54	6.8 (139)	74	>3.1 (>165)	94	>3.1 (nd)
4-nitrophenyl	55	3.9 (320)	75	>3.1 (>525)	95	>3.1 (>67)
4-hydroxyphenyl	56	>25 (>60)	76	21 (380)	96	14.0 (308)
benzyl	57	4.0 (59)	77	5.0 (303)	97	1.0 (38)
phenethyl	58	4.0 (49)	78	1.0 (39)	98	1.0 (25)
cyclohexyl	59	4.0 (19)	79	5.5 (128)	99	5.1 (319)
cyclopropyl	60	16.0 (55)	80	16.0 (1569)	100	4.0 (455)
hexyl	61	14.5 (418)	81	>3.1 (>326)	101	> 3.1 (>82)
propyl	62	16.0 (218)	82	16.0 (645)	102	5.1 (864)
ethyl	63	32.0 (116)	83	16.0 (443)	103	0.1 (45)
methyl	64	32.0 (81)	84	32.0 (552)	104	0.1 (20)
<i>tert</i> -butyl	65	20.5 (126)	85	4.1 (423)	105	>3.1 (nd)
isopropyl	66	17.0 (114)	86	4.0 (213)	106	8.5 (9444)

Table 8. *In vitro* Inhibition of β-haematin Formation of a Few Compounds from Series A-C.

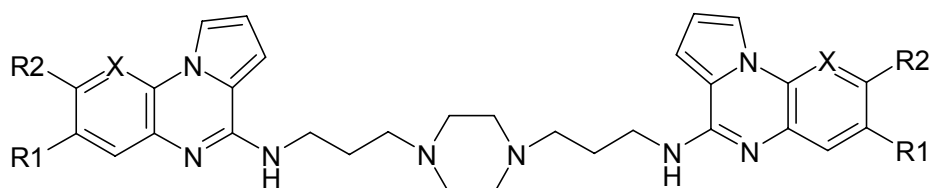
Compound	R	IC ₅₀ (μM) β-haematin formation
chloroquine		76.5
47	4-quinoliny	50.6
67	4-quinoliny	42.5
87	4-quinoliny	43.4
51	3-phenoxyphenyl	79
71	3-phenoxyphenyl	37.5
91	3-phenoxyphenyl	74.9
133	4-methoxyphenyl	34.2
73	4-methoxyphenyl	61.4
93	4-methoxyphenyl	47.8
55	4-nitrophenyl	35.6
75	4-nitrophenyl	40
95	4-nitrophenyl	15
60	cyclopropyl	34
80	cyclopropyl	23.3
100	cyclopropyl	27.1
61	propyl	40.2
81	propyl	50.9
101	propyl	6.7

Differences shown for some compounds in the IC_{50} values of β -haematin formation cannot explain the large differences in their *in vitro* antimalarial activities. Thus, in order to evaluate the contribution of the compound accumulation in the food vacuole to antimalarial activity, lipophilicity measurements ($\log D$ at vacuolar and cytosolic pH) and *in silico* vacuolar accumulation ratios (VAR) based on a week-base model were carried out by the authors. Compounds of series B and C, as expected, accumulated 4 to 200 times more than those of series A. For example, compounds **60** and **100** have a comparable inhibition of β -haematin formation (around 30 μ M). However, **100** (VAR = 6062×10^3 , $\log D_5 < -2.78$, $\log D_{7.4} = 1.16$) displayed a greater accumulation than compound **60** (VAR = 30×10^3 , $\log D_5 < -0.23$, $\log D_{7.4} = 2.78$), being 30 times more active than **60**.

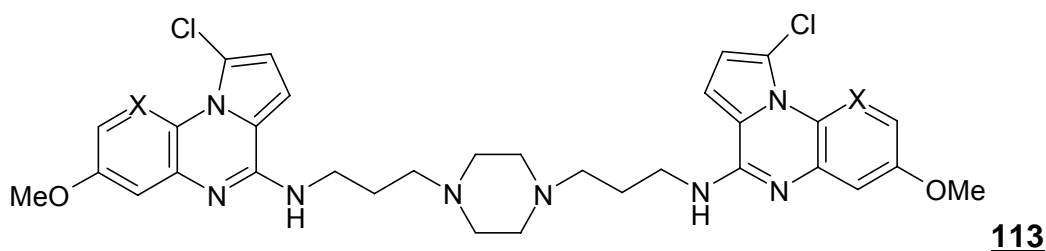
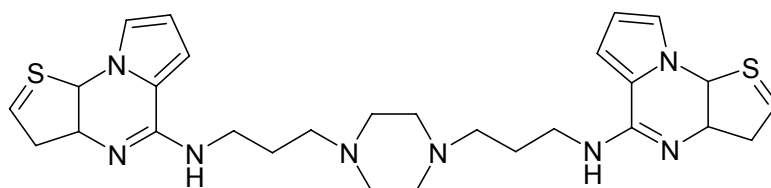
In addition, both compounds **100** and **103** provoked a 100% reduction of parasitemia at day 11 in the murine *P. berguei* model at 20 mg/kg by intraperitoneal route (Ryckebusch et al., 2003).

Pursuing their efforts, Ryckebusch and co-workers (2005) showed that lipophylic substituents (for example propylene-carbamic acid *tert*-butyl ester or butylcyanide) could be introduced in the place of one of the cyclopropyl methylene moieties in compound **100** but while maintaining a high antimalarial activity its toxicity was augmented.

Pyrroloquinoxalines were synthesized using various substituted nitroanilines or nitropyridines and their *in vitro* activity upon *P. falciparum* strains were tested (Guillon et al., 2004). The compounds having a bis(3-aminopropyl)piperazine linker (**107-114**) were generally more active than their counterparts possessing bis(3-aminopropyl)methylamine or bis(3-aminopropyl)amine linkages.



107	R1 = H	R2 = H	X = C
108	R1 = H	R2 = Cl	X = C
109	R1 = CH ₃ O	R2 = H	X = C
110	R1 = H	R2 = CH ₃ O	X = C
111	R1 = H	R2 = H	X = N
112	R1 = H	R2 = CH ₃ O	X = N

**114**

These compounds showed cytotoxicity upon mammalian L6 cells in the micromolar range and the index of selectivity for **110** was greater than 50 (Table 9).

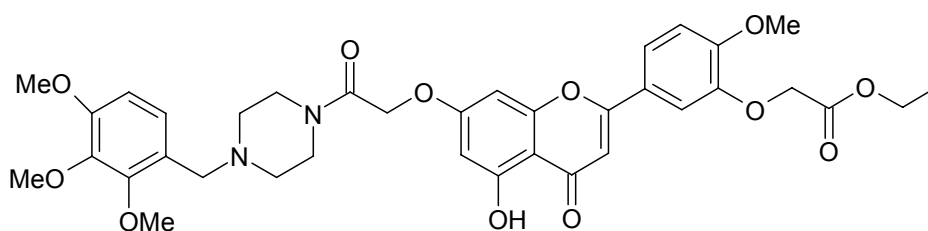
Table 9. *In vitro* Sensitivity of *P. falciparum* Strains and *in vitro* Cytotoxicity on Mammalian L6 Cells (NT = not tested).

Compound	IC ₅₀ (μM)			mammalian L6 cells	Index of Selectivity
	<i>P. falciparum</i> strains				
	Thai	FcB1	K1		
107	0.08 ± 0.01	0.29 ± 0.02	0.37 ± 0.15	5.04 ± 0.19	13.6
108	0.28 ± 0.05	0.64 ± 0.04	0.48 ± 0.09	4.01 ± 0.66	8.2
109	0.03 ± 0.01	0.13 ± 0.01	0.08 ± 0.02	1.32 ± 0.09	17.4
110	0.04 ± 0.01	0.13 ± 0.01	0.08 ± 0.01	4.06 ± 0.72	52.7
111	NT	1.09 ± 0.01	NT	NT	NT
112	NT	0.60 ± 0.02	NT	NT	NT
113	0.25 ± 0.05	0.72 ± 0.03	0.33 ± 0.01	3.07 ± 0.69	9.3
114	NT	0.93 ± 0.03	NT	NT	NT

In other important result from this group, using molecular modeling studies, it was proposed interactions by salt-bridge between the protonated piperazine *N* atom and the carboxylate group of haematin.

III.2.6 Synthesis of benzylpiperazinyl flavones derivatives

Auffret and co-workers (2007) reported the synthesis of 27 flavonoid derivatives containing a piperazinyl chain that were submitted to antimalarial evaluation. It was observed some structure-activity relationships of flavones as: polymethoxylation pattern of the benzylpiperazinyl chain at the 7-phenol group and an increased lipophilic flavone moiety were favorable to the activity. The most active compounds were those having a 2,3,4-trimethoxybenzylpiperazinyl chain attached to the flavone at the 7-phenol group (**115**).



115

In conclusion, as presented in this literature review until now, it can be seen the importance of some pharmacophores as bicycles, ferrocenyl and piperazinyl moieties. It is proposed that antimalarial compounds may interact differently according these pharmacophores: a. or through intercalation in the haematin; b. or through π - π stacking between the aromatic nucleus, and c. through interactions by salt-bridge between the protonated piperazine *N* atom and the carboxylate group of haematin. Also, physico-chemicals parameters may play a role in this activity, as lipophilicity and pKa. Ferrocene and piperazine moieties improve the lipophilicity of compounds, and this may facilitate their membrane transporting. Also, the pK_a values may be very important considering that accumulation of the free aminoquinoline through pH trapping is essential to drive the equilibrium toward complex formation (Kaschula *et al.*, 2002). Moreover, ferroquine appears to present reduced

affinity for the postulated transporter related to chloroquine resistance (*pfcr*) which seems to be extremely structure specific.

Considering that the ursolic acid **1** presented potential antimalarial activity, and that its triterpene skeleton may play a role in this activity (by intercalation, for example), and considering, also, its good lipophilicity, we decided to study the influence of several chemical modifications to the antimalarial activity using compound **1** as prototype.

In the following, it will be presented the literature about the synthesis and the antimalarial activity of triterpenes.

III.2.7 Triterpene derivatives

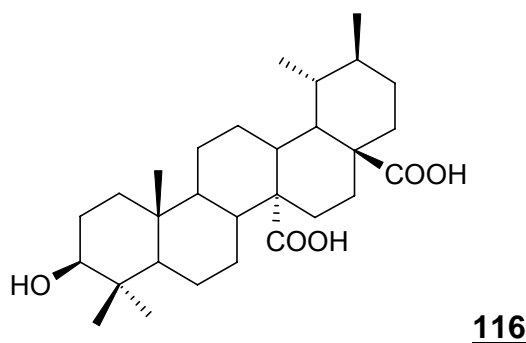
Among natural products, the terpenoid class of compounds represents a very important class of bioactive compounds. Among these, there are many studies on the chemical and biological properties of lupane and ursane triterpene type of compounds, such as betulinic and ursolic acids and their derivatives. Saponins are natural amphiphilic compounds having an aglycone (triterpenoidal or steroidal) with sugar chains attached by an ether or ester linkage. Saponins as well as triterpenes have been investigated for numerous biological activities as anti-inflammatory, antimalarial and HIV-activities, hepatoprotective effects and on cardiovascular system (Hostettmann and Marston, 1995, Liu, 1995, 2005; Mahato and Garai, 1998; Steele *et al.*, 1999).

Thus, these triterpenoid scaffolds provide an interesting pharmacophore in view of more potent therapeutic agents. The study of plant-derived drugs as prototypes should contribute to more effective and less toxic medicines.

In the following, it will be present natural and modified triterpenoids assayed to antimalarial activity. In the sequence, common reactions reported to modify the triterpene skeleton will also be described.

III.2.7.1 Natural triterpenoids

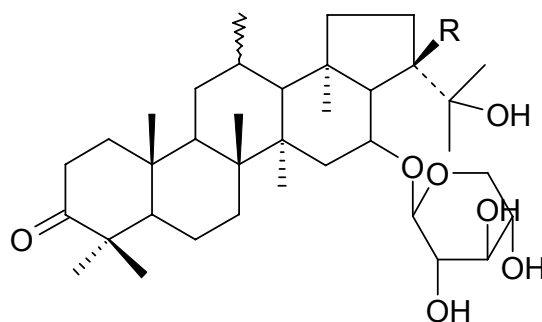
In the search to find new antimalarial compounds, Lamidi and co-workers (1996) studied *Nauclea diderrichii*, an evergreen tree used in West and Central Africa. The phytochemical analysis of the bark revealed that it is a source of alkaloids and saponins. Eleven glycosides from quinovic acid **116** were isolated. The saponins fraction and the monodesmosidic saponins fraction were evaluated *in vitro* against *P. falciparum* chloroquine sensitive (D6) and chloroquine-resistant (W2) strains. The monodesmosidic fraction presented an IC_{50} about 50 $\mu\text{g/mL}$ against both strains while the saponins fraction presented the same IC_{50} against W2 strain. In the same conditions the IC_{50} of chloroquine was 57 ng/mL for strain W2 and 3 ng/mL for strain D6, respectively.



Traore-Keita and co-workers (2000) studied *in vitro* the antimalarial activity and the cytotoxicity to macrophages (BABL/c mouse) of four plants used in traditional medicine in Mali for treating periodic fevers: *Mitragyna inermis*, *Nauclea latifolia*, *Glinus oppositifolius* and *Trichilia roka*. Leaves, roots and stem barks were submitted to aqueous, hydromethanol and chloroform extractions and antimalarial activity was assessed against the chloroquine-sensitive strain 3D7 and the chloroquine-resistant strain W2 of *P. falciparum*. The antimalarial action of chloroquine (IC_{50}) reached 9 ng/mL in the 3D7 strain and 55 ng/mL in the W2 strain. Nevertheless, ursolic acid **1**, purified from the hydromethanol extract of *M. inermis*, reduced parasite proliferation (IC_{50} = 15 $\mu\text{g/mL}$ in the 3D7 strain and 18 $\mu\text{g/mL}$ in the W2 strain). Only the extract provided from *N. latifolia* was toxic at a concentration of 50 $\mu\text{g/mL}$.

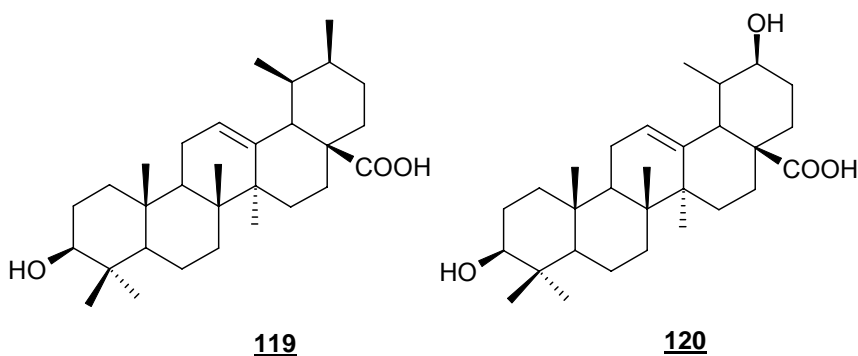
In continuation, two triterpenoid saponins having the hopane skeleton, glicosides A **117** and B **118**, were isolated from aerial parts of *Glinus*

oppositifolius (Traore et al., 2000). The antiplasmodial activity was assessed against two strains of *P. falciparum* (3D7 and W2). The small quantity of **118** did not allow the assessment of its antiplasmodial activity but the results showed that the fraction with both compounds had a better activity ($IC_{50} = 31.80 \mu\text{g/mL}$) than pure glicoside A **117** ($IC_{50} = 42.30 \mu\text{g/mL}$).



R = OH glicosídeo A **117**
R = H glicosídeo B **118**

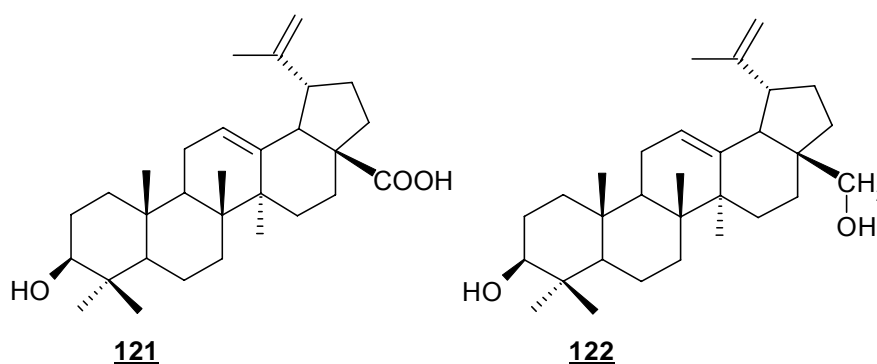
Ursolic acid **1** and two derivatives, tomentosolic acid **119** and 3 β ,20 β -dihydroxyurs-12-en-28-oic acid **120** were isolated from *Spathodea campanulata*, a plant used in traditional medicine for the management of malaria (Amusan et al., 1996). These three triterpenoids demonstrated antimalarial activity against *P. falciparum berghei berghei* in mice. Each compound demonstrated a dose-dependent market suppression of parasitemia and high mean survival times. Ursolic acid was the most active; it produced 97% suppression of parasitemia in mice and a mean survival period of 25 days at 60 mg/kg/day. This was comparable to the action of 10 mg/kg/day of chloroquine.



The lupane-type betulinic acid **121** was isolated from an ethanol extract of the root bark of *Uapaca nitida*, a Tanzanian tree used as a treatment for malaria (Steele et al., 1999). The *in vitro* antiplasmodial IC₅₀ values of betulinic acid **121** against *P. falciparum* chloroquine-resistant (K1) and sensitive (T9-96) strains were found to be 19.6 µg/mL and 25.9 µg/mL, respectively.

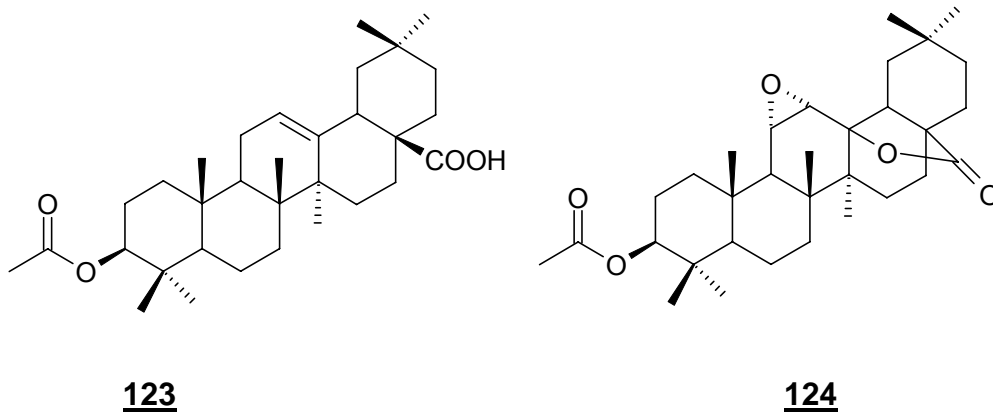
In a previous communication, Bringmann and co-workers (1997) reported a moderate *in vitro* antiplasmodial activity of betulinic acid **121** against *P. falciparum* NF-54 (IC₅₀ = 10.46 µg/mL).

The *in vitro* activities of several related triterpenes were also evaluated by Steele and co-workers (1999). Ursolic acid **1** exhibited similar potency with IC₅₀ values of 36.5 µg/mL (K1 strain) and 28.0 µg/mL (T9-96 strain), however, oleanolic acid **5** presented IC₅₀ values of 88.8 µg/mL (K1 strain) and 70.6 µg/mL (T9-96 strain). Betulin **122** (C-17 β-CH₂OH) was shown, in contrast, to be devoid of activity at the greatest concentration tested (500 µg/mL) against both strains of *P. falciparum* (Alakurtti et al., 2006). Betulinic acid **121**, ursolic acid **1** and oleanolic acid **5** presented the same activity against both *P. falciparum* chloroquine-resistant and CQ-sensitive strains, suggesting that their activities are unaffected by the mechanism of chloroquine resistance. The lack of activity of betulin at 500 µg/mL suggests that structural change at the C-28 position dramatically alters activity. The activity of chloroquine diphosphate against *P. falciparum* K1 strain was 0.15 µg/mL and against *P. falciparum* T9-96 strain was 0.01 µg/mL.



A bioactivity-guided fractionation of roots and leaves extracts from *Cajanus cajan*, one of the major legume crop of the tropical world, yielded eight compounds. Antiplasmodial assay was performed using *P. falciparum* chloroquine-sensitive 3D7 strain. Only betulinic acid **121** presented an important activity ($IC_{50} = 19 \mu\text{M}$) (Duker-Eshun *et al.*, 2004).

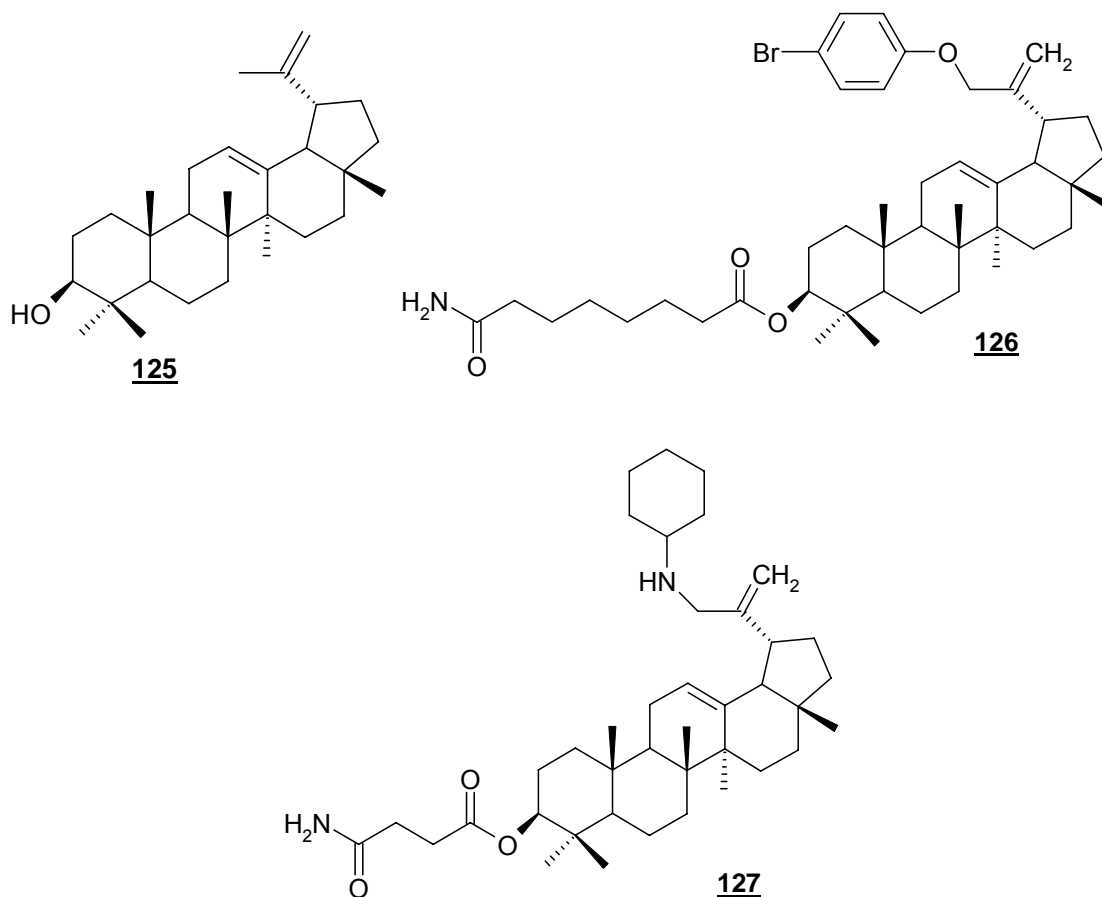
Two triterpenoids, β -acetylolean-12-en-olic acid **123** and 3β -O-acetyl- $11\alpha,12\alpha$ -epoxyolean-28,13-olide **124** were isolated from the roots and stems of *Prismatomeris fragrans*, a tree found in the Northeastern, Eastern and South-eastern parts of Thailand and in the Northwest of Laos. These compounds were evaluated to antimalarial activity against *P. falciparum* K1 strain, a multidrug resistant strain. Only compound **123** was active presenting IC_{50} value of $5.9 \mu\text{g/mL}$ (Kanokmedhakul *et al.*, 2005).



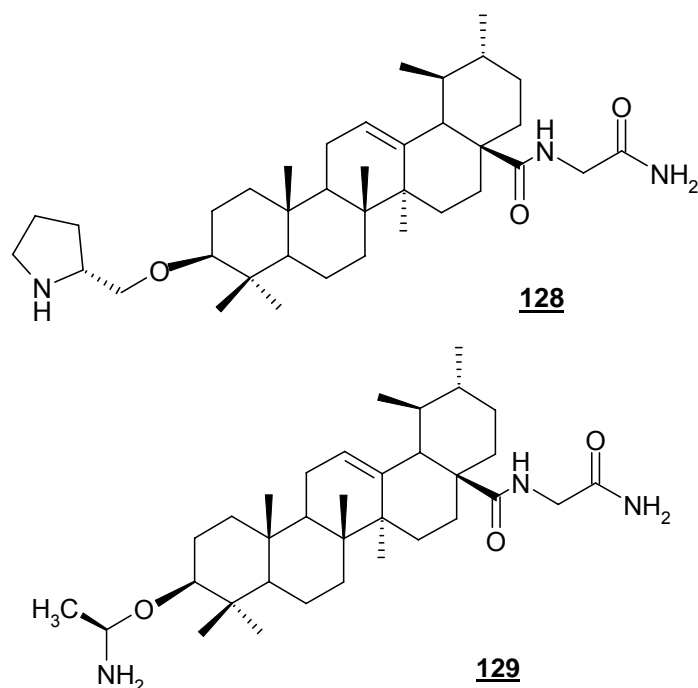
III.2.7.2 Synthesis of triterpenoid derivatives

In literature, it is found very few reports about the hemi-synthesis of triterpenic derivatives with the purpose to obtain antimalarial compounds. In one of these studies a library with 96 compounds was described using the triterpenoid lupeol as scaffold. Lupeol was anchored to a solid support (Rink amide/Sieber amide) through aliphatic dicarboxylic acid moieties, which also served as a site for introducing diversity. The antiparasitic activities of compounds were assessed by evaluating the minimum inhibitory concentration

(MIC) against *P. falciparum* (NF-54 strain) *in vitro*. From the 96 compounds screened, 15 compounds were found to be more active than lupeol **125** (117 μM) in a range of 13.07 to 16.0 μM (compounds **126** and **127**, respectively), others were inactive or equipotent to lupeol (Srinivasan *et al.* 2002).



Solid phase synthesis and antimalarial screening of novel libraries based on betulinic acid **121** and ursolic acid **1** derivatives were described by Pathak and co-workers (2002). Screening against *P. falciparum* NF-54 led to the identification of compounds with a more important biological activity in comparison to the parent one. For example, compounds **128/129** presented MIC= 10 $\mu\text{g/ml}$, while that of ursolic acid was 50 $\mu\text{g/ml}$, and that of chloroquine was 0.04 $\mu\text{g/ml}$.

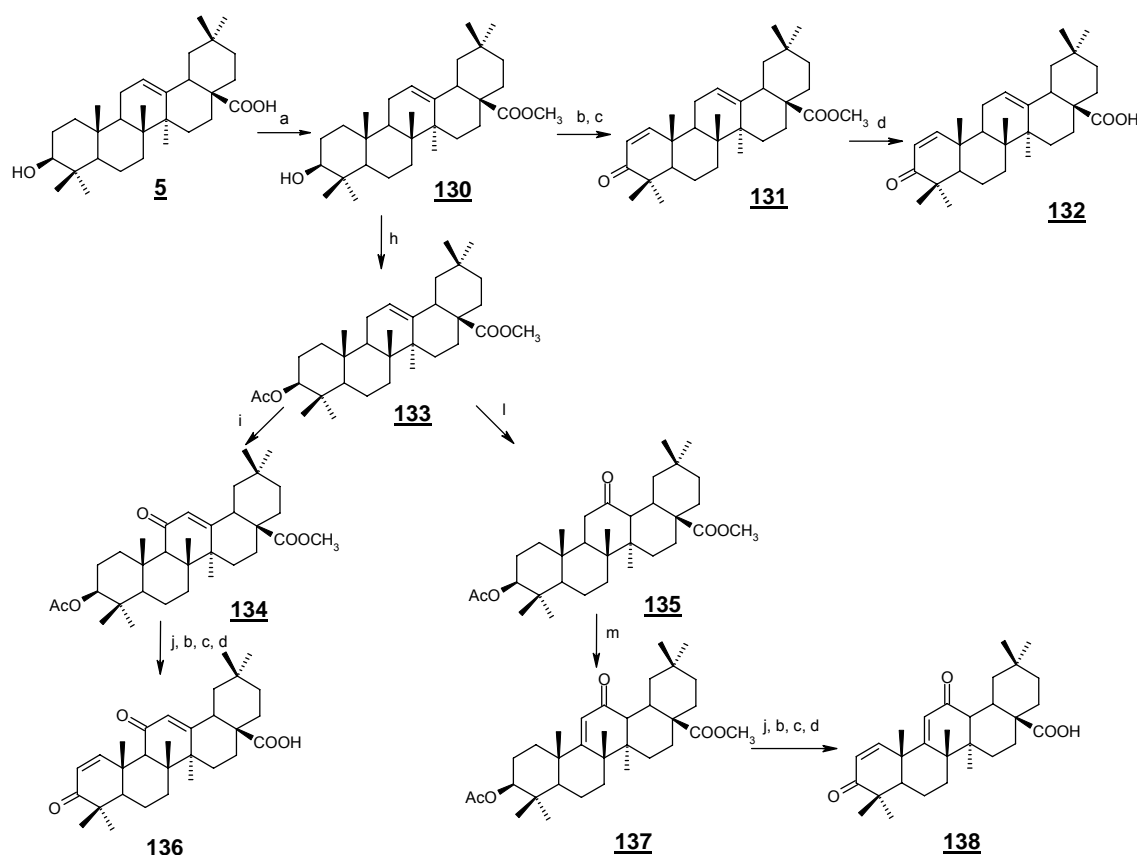


Additionally, some reactions used to modify the triterpene skeleton will be presented.

Honda and co-workers (1997) synthesized a series of oleanolic and ursolic acid derivatives aiming to obtain anti-inflammatory compounds. The synthesis of the oxidized oleanolic acid derivatives is illustrated in Scheme 1. This series of new derivatives of 3-oxo-olean-1-en-28-oic acid have significant inhibitory activity against interferon- γ induced NO production in mouse macrophages, especially compound **138** had the highest activity (IC_{50} 0.9 μ M). The compound **131** was obtained by Jones oxidation of methyl oleanolate **130**, followed by introduction of a double bond at C-1 with phenylselenenyl chloride in ethyl acetate and sequential addition of 30% hydrogen peroxide (PhSeCl- H_2O_2). The enone **132** was synthesized by halogenolysis of **131** with lithium iodide (LiI) in dimethylformamide (DMF). Bis-enone **136** was synthesized by alkaline hydrolysis of acetate **134**, which was prepared from **133**, using the same reaction conditions (sequential Jones oxidation, introduction of a double bond at C-1, and halogenolysis). Bis-enone **137** was synthesized from C-12 ketone **135** according to the same synthetic route as for **136**. This series of new derivatives of 3-oxo-olean-1-en-28-oic acid presented significant inhibitory

activity against interferon- γ induced NO production in mouse macrophages, especially compound **138** had the highest activity (IC_{50} 0.9 μ M).

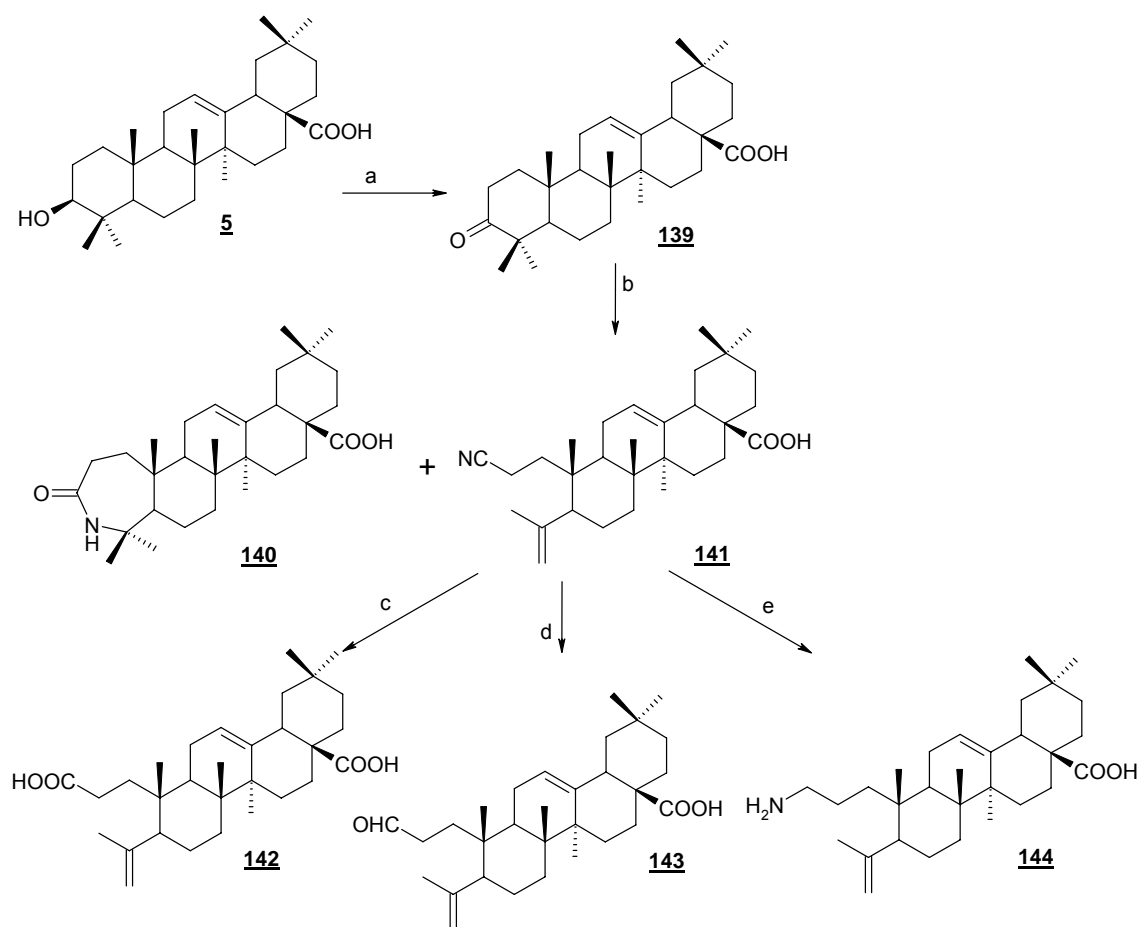
Scheme 1.



a: $CH_2N_2/Et_2O, THF$, b: Jones, c: $PhSeCl/ AcOEt, 30\%H_2O_2/THF$, d: LiI/DMF , h: Ac_2O/py , i: $CrO_3/py/CH_2Cl_2$, j: $KOH/MeOH$, l: $30\%H_2O_2/AcOH$, m: $Br_2/HBr/AcOH$

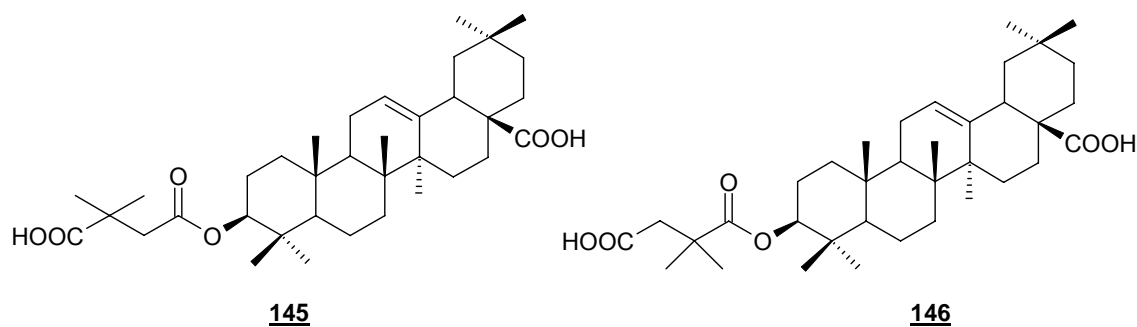
Synthesis of various novel A-ring cleaved oleanane analogs are described by Finlay and co-workers (1997). Jones oxidation of oleanolic acid **5** furnished intermediate ketone **139**, which was cleaved using Schmidt reaction conditions. A-ring cleaved nitrile **141** was obtained in 35% yield after separation from the lactam by-product. The nitrile was subsequently converted to the corresponding carboxylic acid **142** by a tetrafluorophthalic acid melt, to the aldehyde **143** by DIBAL reduction, and to the related primary amine **144** by hydrogenation over catalytic 10% palladium on activated charcoal (Scheme 2).

Scheme 2

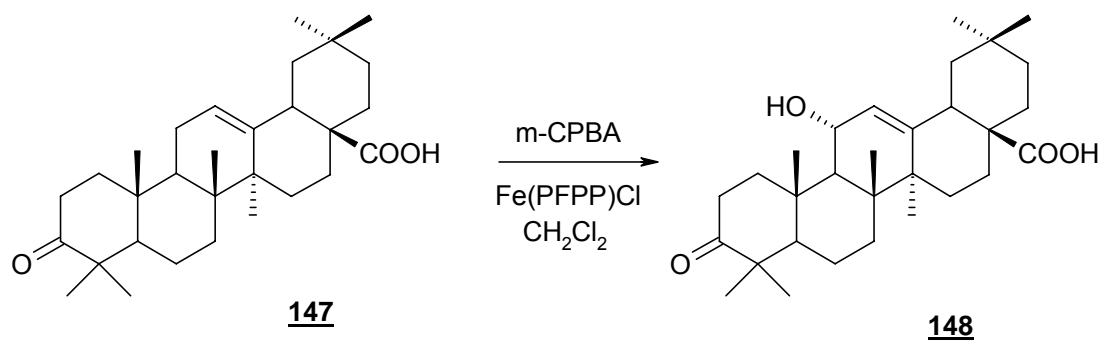


a: Jones, b: $\text{NaN}_3/\text{AcOH}/\text{H}_2\text{SO}_4$, c: tetrafluorophthalic acid/ $160\text{ }^\circ\text{C}$, d: 2,0 eq. DIBAL/ $-30\text{ }^\circ\text{C}/\text{THF}$, e: $\text{H}_2/10\% \text{ Pd/C}/\text{EtOH}/10\% \text{ HCl}$

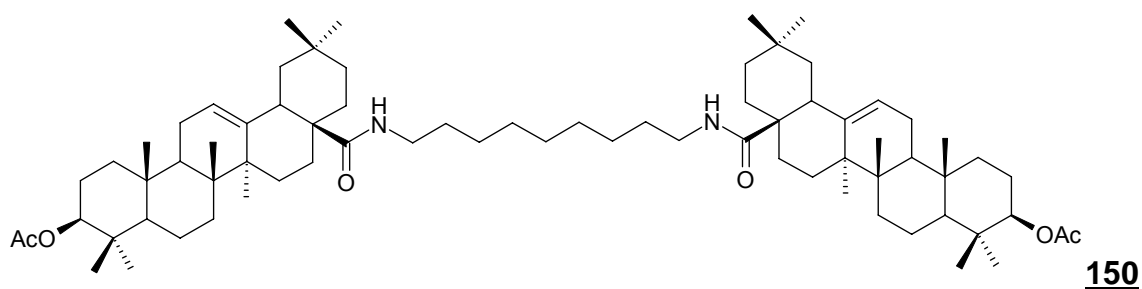
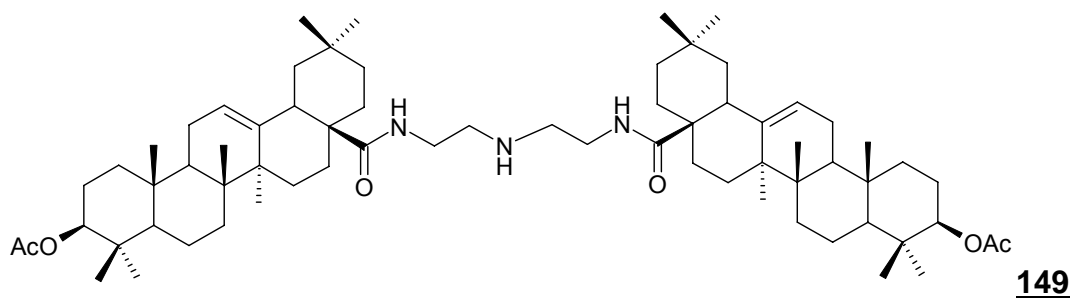
Kashiwada and co-workers (1998) prepared oleanolic acid derivatives and evaluated their anti-HIV activity. Oleanolic acid 3-O-3',3'-dimethylsuccinate **145** and its isomer **146** was obtained by oleanolic acid reflux overnight with the succinic anhydride, and (dimethylamino)pyridine in pyridine.



A allylic hydroxylation of oleanolic acid by *m*-CPBA, catalyzed by Fe(PFPP)Cl (3 mol%) at -78 °C during 4,5 h, was described by Konoike and co-workers (1999) (yield 67%).



Structural modifications were performed on the C-3 and C-28 of ursolic acid **1** and, the growth inhibitory activity of these derivatives against four tumor cell lines, HL-60, BGC, Bel-7402 and Hela, was evaluated by Ma and co-workers (2005). Significant improvement of cytotoxicity against HL-60 cell line was observed when amino alkyl groups were introduced to position 28, whether or not the 3-OH group was free or acetylated. In the case of dimeric compounds with a secondary amino alkyl group (compound **149**), selective cytotoxicity was observed only against HL-60 line cells. The 3-acetylated dimeric compound **150** possessing amide but no amino alkyl group in position 28 was inactive. These compounds were synthesized from 3-O-acetyl-ursolic acid using oxalyl chloride coupling agents.



III.2.7.3 Mechanism of action of antimalarial triterpenoid compounds

In relation to the antimalarial activity, the mechanism of action of several triterpenoid compounds is unknown. In this thesis we worked with the assumption that the synthesized compounds may have their antimalarial activity through inhibition of β -haematin.

Recently, Ziegler and co-workers (2004) presented a correlation between the erythrocyte membrane effect of betulinic acid analogues and their *in vitro* inhibition of *P. falciparum* growth. The authors demonstrated that hydrogen bonding properties of pentacyclic triterpenes determine their mode of incorporation into the erythrocyte membrane, and that this incorporation into the lipid bilayer of erythrocytes is prohibitive with respect to malaria parasite invasion and growth. There was a very good qualitative correlation between the extent of membrane shape alterations and the observed IC_{50} values for the inhibition of proliferation of malaria parasites. Thus, the erythrocyte membrane and the parasite vacuolization process might be a possible novel target for antimalarial therapy.

Considering the reported antimalarial activity of triterpenoid derivatives, the potential of ursolic acid and oleanolic acid as antimalarial compounds, we

decided to obtain several ursolic acid derivatives through synthetic modifications at the positions C-3 and C-28, and at the cycle A (see IV.2). These compounds were designed in order to study the electronic effects and steric hindrance in this series in relation to antiplasmodial activity. Moreover, after being assayed to antimalarial and cytotoxicity activities, structure-activity relationships (SAR) of these compounds will be proposed together with modeling studies.

IV RESULTS AND DISCUSSION

IV.1 Extraction and isolation of aglycons and triterpenic saponins from *Ilex paraguariensis* and *Ilex dumosa*

Ilex paraguariensis and *Ilex dumosa* are South American native trees belonging to the Aquifoliaceae family.

The dried leaves and twigs from *I. paraguariensis* are used to prepare a tea known as maté, being one of the most commonly consumed beverages in several Southern American countries, including Brazil, Uruguay, Paraguay and Argentina. The leaves of *Ilex paraguariensis* contain xanthines (mainly caffeine), flavonoid glycosides (as rutin), caffeoylquinic acid derivatives (chlorogenic acids) and a significant amount of triterpenoid saponins (around 10%) having as main aglycone the ursolic acid **1** (Alikaridis, 1987, Schenkel *et al.*, 1997).

In previous investigations, our research group reported the structure of eleven saponins, *i.e.* **matesaponin 1** (ursolic acid 3-O- $\{\beta$ -D-glucopyranosyl-(1-3)- α -L-arabinopyranosyl)-(28-1)- β -D-glucopyranosyl ester) (compound **2**) (Gosmann *et al.*, 1989). **matesaponin 2** (ursolic acid 3-O- $\{\beta$ -D-glucopyranosyl-(1-3)- $[\alpha$ -L-rhamnopyranosyl-(1-2)]- α -L-arabinopyranosyl)-(28-1)- β -D-glucopyranosyl ester) (compound **3**). **matesaponin 3** (ursolic acid 3-O- $\{\beta$ -D-glucopyranosyl-(1-3)- α -L-arabinopyranosyl)-(28-1)- $\{\beta$ -D-glucopyranosyl-(1-6)- β -D-glucopyranosyl ester) (compound **4**); **matesaponin 4** (ursolic acid 3-O- $\{\beta$ -D-glucopyranosyl-(1-3)- $[\alpha$ -L-rhamnopyranosyl-(1-2)]- α -L-arabinopyranosyl)-(28-1)- $\{\beta$ -D-glucopyranosyl-(1-6)- β -D-glucopyranosyl ester) (Gosmann *et al.*, 1995). **matesaponin 5** (ursolic acid 3-O- $\{\beta$ -D-glucopyranosyl-(1-3)- $[\alpha$ -L-rhamnopyranosyl-(1-2)]- α -L-arabinopyranosyl)-(28-1)- $[\beta$ -D-glucopyranosyl-(1-4)- β -D-glucopyranosyl-(1-6)- β -D-glucopyranosyl ester) (Kraemer *et al.*, 1996).

Also, the monodesmosidic and more apolar saponins were isolated: **saponin J1a** (ursolic acid 3-O- $[\alpha$ -L-rhamnopyranosyl-(1-2)]- α -L-arabinopyranosyl-ester); and its isomer **saponin J1b** (oleanolic acid acid-3-O- $[\alpha$ -L-rhamnopyranosyl-(1-2)]- α -L-arabinopyranosyl-ester); **saponin J2a** (ursolic acid 3-O- $\{\beta$ -D-glucopyranosyl-(1-3)- α -L-arabinopyranosyl ester); and **saponin**

J2b (oleanolic acid 3-*O*-{ β -*D*-glucopyranosyl-(1-3)- α -*L*-arabinopyranosyl} ester). Finally, the isomers **saponin J3a** (ursolic acid 3-*O*-{ α -*L*-rhamnopyranosyl-(1-2)}- α -*L*-arabinopyranosyl]-(28-1)- β -*D*-glucopyranosyl ester); and **saponin J3b** (oleanolic acid 3-*O*-{ α -*L*-rhamnopyranosyl-(1-2)}- α -*L*-arabinopyranosyl]-(28-1)- β -*D*-glucopyranosyl ester) were also isolated (Schenkel *et al.*, 1996, 1997).

More recently, Martinet and co-workers (2001) identified two minor saponins in the methanolic extract of the leaves of *Ilex paraguariensis*: **guaianicin B** (oleanolic acid 3-*O*-{ β -*D*-glucopyranosyl-(1-3)- α -*L*-arabinopyranosyl]-(28-1)- β -*D*-glucopyranosyl ester) and **nudicaucin C** (oleanolic acid 3-*O*-{ β -*D*-glucopyranosyl-(1-3)-[α -*L*-rhamnopyranosyl-(1-2)]}- α -*L*-arabinopyranosyl]-(28-1)- β -*D*-glucopyranosyl ester). Both are isomeric forms of the matesaponin 1 and 2 and differ only by the nature of the aglycon.

Ilex dumosa is reported as a maté adulterant. Our research group reported the structure of nine saponins isolated from its aerial parts. These saponins have oleanolic acid **5** as their main aglycon: oleanolic acid 3-*O*- β -*D*-glucopyranosyl-(1-2)- β -*D*-galactopyranosyl; oleanolic acid 3-*O*- α -*L*-arabinopyranosyl-(1-2)- β -*D*-galactopyranosyl; oleanolic acid 3-*O*- β -*D*-glucopyranosyl-(1-2)- β -*D*-galactopyranosyl-(28-1)- β -*D*-glucopyranosyl ester; oleanolic acid 3-*O*- α -*L*-arabinopyranosyl-(1-2)- β -*D*-galactopyranosyl-(28-1)- β -*D*-glucopyranosyl ester (Heinzmann and Schenkel, 1995). Also, oleanolic acid 3-*O*- β -*D*-glucuronopyranosyl-(28-1)- β -*D*-glucopyranosyl ester; the oleanolic acid 3-*O*- β -*D*-6-*O*-methylglucuronopyranosyl-(28-1)- β -*D*-glucopyranosyl ester; 29-hydroxyoleanolic acid 3-*O*- β -*D*-glucopyranosyl-(1-2)- β -*D*-galactopyranosyl-(28-1)- β -*D*-glucopyranosyl ester; oleanolic acid 3-*O*- α -*L*-arabinopyranosyl-(1-2)- α -*L*-arabinopyranosyl-(28-1)- β -*D*-glucopyranosyl ester, and oleanolic acid 3-*O*- β -*D*-galactopyranosyl-(1-2)- β -*D*-glucopyranosyl (Pires *et al.*, 1997).

In this thesis, air-dried powdered leaves of *I. paraguariensis* and *I. dumosa* were submitted, separately, to extraction by maceration using 70% EtOH using a plant:solvent relationship of 15%. After evaporation of ethanol under vacuum, the aqueous solution was extracted using cyclohexane in order to eliminate the lipophilic compounds (for example chlorophylls). One part (5 L)

of the resulting aqueous solution from both plants was submitted, separately, to acid hydrolysis in order to obtain the aglycones that were purified through crystallization (Gnoatto *et al.*, 2005) (Schemes 3 and 4).

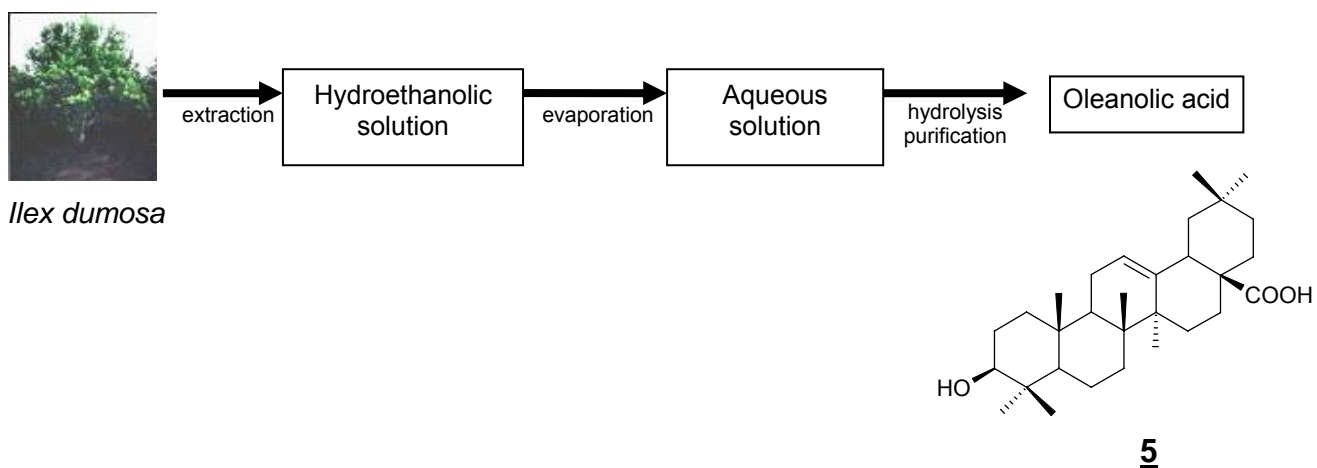
Another part (1 L) of the resulting aqueous solution from *I. paraguariensis* was submitted to extraction with *n*-BuOH. The saponins, due its amphiphilic character, are very soluble in this solvent. The *n*-BuOH residue, obtained after evaporation under vacuum, yielded 10 g that was column chromatographed in order to obtain the major saponins. Fractions with similar TLC profile were joined. Pure **matesaponin 1** (compound **2**) and **matesaponin 3** (compound **4**) were isolated in native form. Enriched fraction containing other saponins was submitted to acetylation and the compounds **151**, **152** and **153** (the peracetylated **matesaponins 1**, **2** and **3**) were obtained after column chromatography. These compounds were identified by spectroscopic methods and by comparison with literature data (Gosmann *et al.*, 1989; 1995) (Scheme 4).

The purification and acid hydrolysis of the hydroethanolic extract of *I. paraguariensis* led to isolation of ursolic acid **1** (8 g) with 10% yield. Its purity was determined by HPLC in which ursolic acid presented $R_t = 15$ min and purity > 95% (Gnoatto *et al.*, 2005).

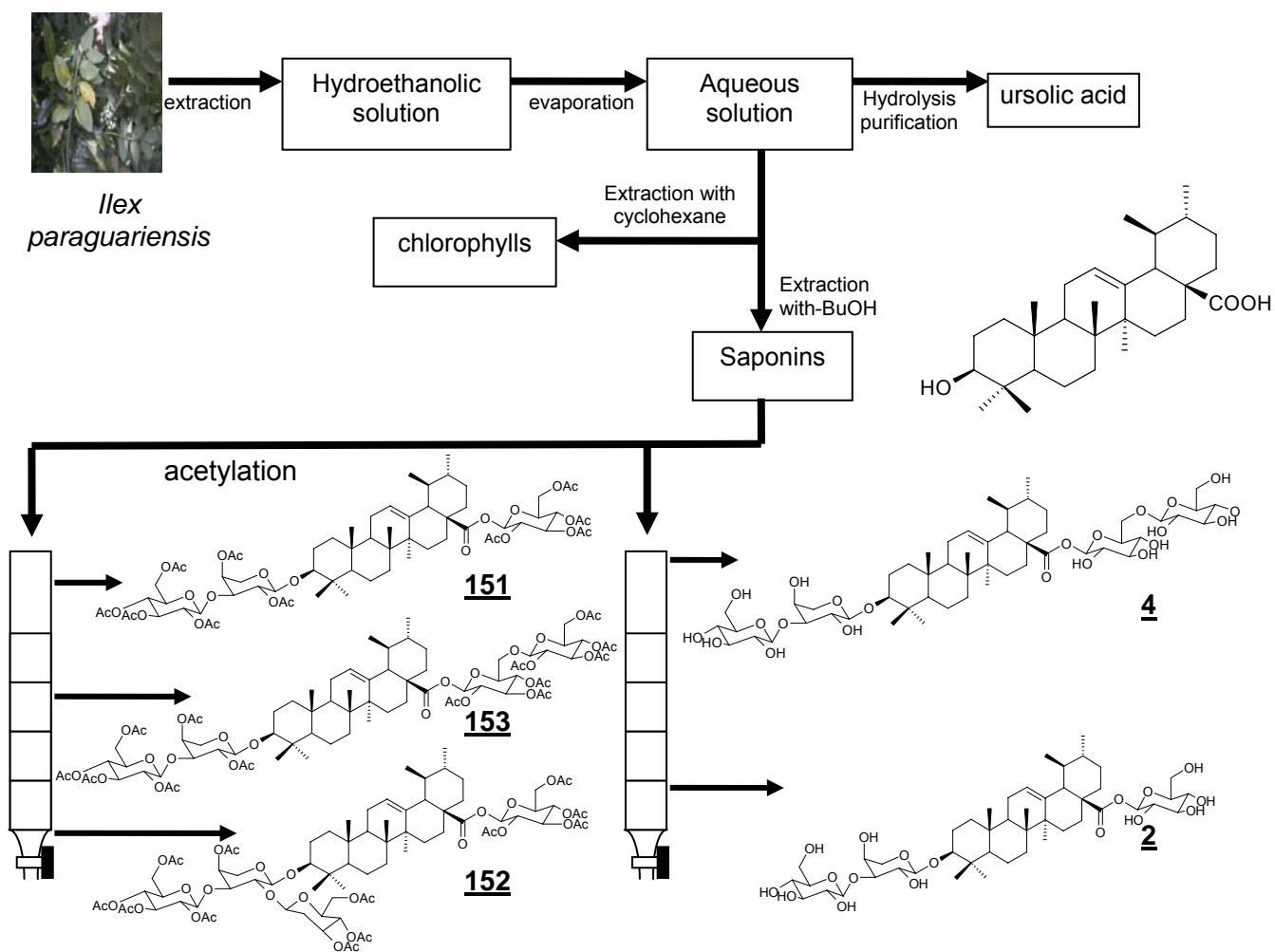
IV.1.1 Identification of compound **1**

Compound **1** was obtained as a white amorphous solid and had the molecular formula $C_{30}H_{47}O_3$ as deduced from the HRMS (observed m/z 455.3522 $[M+H]^+$), with mp 237–240 °C and optical rotation equal +72.5 (MeOH, c 0.4). Its IR spectrum showed characteristic absorption bands of one hydroxyl group at 3562 cm^{-1} and a carbonyl group at 1697 cm^{-1} .

Scheme 3.



Scheme 4.



NMR spectral data of **1** showed signals corresponding to a triterpenic skeleton. The ^1H NMR spectrum displayed signals for five methyl groups (δ 0.73, 0.76, 0.87, 0.93 and 1.04) together with signals corresponding to methyl protons of H-30 (δ 0.82, 3H, d, $^3J= 6.4$ Hz) and H-29 (δ 0.91, 3H, d, $^3J= 6.0$ Hz). The signal at δ 2.14 was attributed to H-18 (1H, d, $^3J= 11.3$ Hz) while H-3 α signal was observed at δ 3.20 (1H, dd). Finally, at δ 5.40 was observed a large triplet attributed to H-12.

Attribution of all resonances displayed on the ^{13}C NMR spectrum of **1** was accomplished by direct comparison with literature data (Mendive, 1940, Gosmann *et al.*, 1989, Mahato and Kundu, 1994; Tkachev *et al.*, 1994). Thus compound **1** was identified as ursolic acid, the major aglycon of *I. paraguariensis*.

IV.1.2. Identification of matesaponins

The compounds, **matesaponin 1** (compound **2**) and **matesaponin 3** (compound **4**), and **peracetylated matesaponins 1** (compound **151**), **2** (compound **152**) and **3** (compound **153**) were identified by spectroscopic methods and by comparison with literature data (Gosmann *et al.*, 1989; 1995).

The molecular mass of **matesaponin 1** (compound **2**) was shown to be 912 through fabms, which exhibited molecular ion peaks at m/z 935 $[\text{M}+\text{Na}]^+$. The ^1H NMR spectrum of the acetyl derivative of matesaponin 1 showed three anomeric proton signals at δ 4.63 ppm (d, $J = 8.0$ Hz) and δ 4.31 ppm (d, $J = 8.0$ Hz) attributed to glucose and arabinose, respectively, at C-3, and at δ 5.53 ppm (d, $J = 8.0$ Hz) corresponding to glucose at C-28. These assignments were supported by the ^{13}C -NMR spectrum of matesaponin 1, which showed three anomeric proton signals at δ 107.2 ppm, 106.0 ppm, and 95.5 ppm, the latter in full agreement with the presence of a β -glucopyranose linked in the form of an ester. The β configuration for the two glucopyranosyl units and the α configuration for the arabinopyranoside were inferred from the J values of the respective anomeric protons. The interglycosidic linkage was determined by the

observed downfield shift ($\Delta\delta$ 9.3) for C-3 of the inner α -L-arabinose, by comparing with the corresponding methylglycoside. This deshielding clearly indicated that the terminal glycosyl unit is attached at this position; the rest of the carbons were unaffected (Table 10).

After column chromatography, it was possible to isolate the peracetylated matesaponins 1 (compound **151**), 2 (compound **152**) and 3 (compound **153**) in a sufficient amount to allow NMR characterization and biological assays. Through careful comparison of the ^{13}C NMR spectrum of peracetylated matesaponin 2 (compound **152**) and matesaponin 3 (compound **153**) with that of native matesaponin 1, as well as with literature data (Gosmann *et al.*, 1995), it was to identify these compounds.

The fabms spectrum of **matesaponin 2** peracetylated (compound **152**) displayed an ion peak at m/z 1585 $[\text{M}+\text{Na}]^+$. The presence in the ^1H and ^{13}C NMR spectra of matesaponin 2 acetylated, compared to the ^1H and ^{13}C NMR spectra of the peracetylated derivative of matesaponin 1 (compound **151**), of one extra anomeric signal [δ (H-1) 5.35; δ (C-1) 96.0] and one extra methyl signal [δ (CH_3) 1.48; δ (CH_3) 16.7] established, together with observations from the fabms data, that matesaponin 2 (compound **3**) was substituted by one more rhamnose unit than matesaponin 1 (compound **2**). Thus, as in the case of matesaponin 1, a terminal glucose residue was linked at C-28 via an ester bond while an arabinose, glucose, rhamnose-constituted oligosaccharide was substituted at C-3 (Table 10).

The fabms spectrum of **matesaponin 3** exhibited at m/z 1097 $[\text{M}+\text{Na}]^+$, indicating a molecular formula of $\text{C}_{53}\text{H}_{86}\text{O}_{22}$, confirmed by a peak at m/z 1643 $[\text{M}+\text{Na}]^+$ in the fabms of matesaponin 3 peracetylated (compound **153**). This molecular formula was consistent with the presence of one arabinose and three glucose residues. Thus, matesaponin 3 was submitted to esterification at C-28 by a glucose-glucose chain. The interglycosidic linkage of this disaccharide was deduced to be glu(1-6)glu from the deshielding in the ^{13}C NMR spectrum of matesaponin 3 peracetylated of one of the two CH, units of this moiety (δ 67.9), indicating its substituted character (Table 10).

Table 10. ¹³C-NMR Chemical Shifts of matesaponin 1, and peracetylated compounds matesaponin 2, and matesaponin 3. (500 MHz)

Carbon	matesaponin 1 (δ ppm) pyridine- <i>d</i> ₅	matesaponin 2 peracetylated (δ ppm), CDCl ₃	matesaponin 3 peracetylated (δ ppm), CDCl ₃
aglycon			
C-3	88.6	89.1	90.0
C-12	125.9	125.8	126.1
C-13	138.3	136.8	137.0
C-28	176.1	175.0	175.2
3-O-sugar			
ara-1	107.2	104.1	103.7
ara-2	71.7	72.5	73.1
ara-3	83.9	79.0	76.9
ara-4	69.1	72.0	73.1
ara-5	66.7	63.8	64.3
rha-1		96.0	
rha-2		68.2	
rha-3		70.3	
rha-4		70.7	
rha-5		66.0	
rha-6		16.7	
glc-1	106.0	99.1	100.6
glc-2	75.5	69.5	70.1
glc-3	78.1	72.0	72.1
glc-4	71.4	66.8	68.4
glc-5	78.4	72.3	71.6
glc-6	62.5	61.2	61.7
28-O-sugar			
glc'-1	95.5	91.2	91.5
glc'-2	73.9	69.5	70.3
glc'-3	78.7	72.0	72.1
glc'-4	71.0	66.7	68.5
glc'-5	78.9	72.0	71.3
glc'-6	62.1	60.8	67.9
glc''-1			100.9
glc''-2			71.2
glc''-3			72.9
glc''-4			69.1
glc''-5			72.9
glc''-6			62.1

IV.1.3 Identification of compound 5

In continuation, the hydrolysis and purification of the hydroethanolic extracts of *I. dumosa* led to isolation of oleanolic acid 5 (5 g) with 6% yield.

Compound 5 was obtained as a white amorphous solid. The HRMS showed a molecular ion $[M+H]^+$ at m/z 455.3522 providing the molecular formula of $C_{30}H_{47}O_3$. Its melting point was greater than 250 °C and the optical rotation was equal +106 (MeOH, c 0.4). The IR spectrum was similar to that of 1. The only major difference was the presence of the bands around 1200 cm^{-1} from the geminal dimethyl in C-20.

The 1H NMR shifts of methyl groups of 5 were observed, differently to ursolic acid, as seven singlets at δ 0.82 (CH₃-25), 0.83 (CH₃-24), 0.96 (CH₃-26), 0.99 (CH₃-23), 1.05 (CH₃-27), and at δ 0.97 the CH₃-30 and at δ 1.19 the CH₃-29. The multiplicity of the signal attributed to the H-18 is also different from the oleanolic acid one. While to the ursolic acid is observed a doublet at δ 2.13 ($^3J = 11.3$ Hz), the H-18 oleanolic acid is observed as a double doublet at δ 2.88 ($^3J = 13.8; 4.2$ Hz) due the coupling of H-18 and H-19 (2H). These data, together with those from ^{13}C NMR spectrum, were in agreement with literature (Price *et al.*, 1987; Mahato *et al.*, 1988; Wang and Jiang, 1992, Mahato and Kundu, 1994), thus, compound 5, obtained from *I. dumosa*, was identified as oleanolic acid.

IV.2 Design and synthesis of antimalarial compounds

In this thesis we decided to synthesize new compounds with antimalarial activity through a rational design, based on the actual knowledge of the molecular mechanism of the malaria disease.

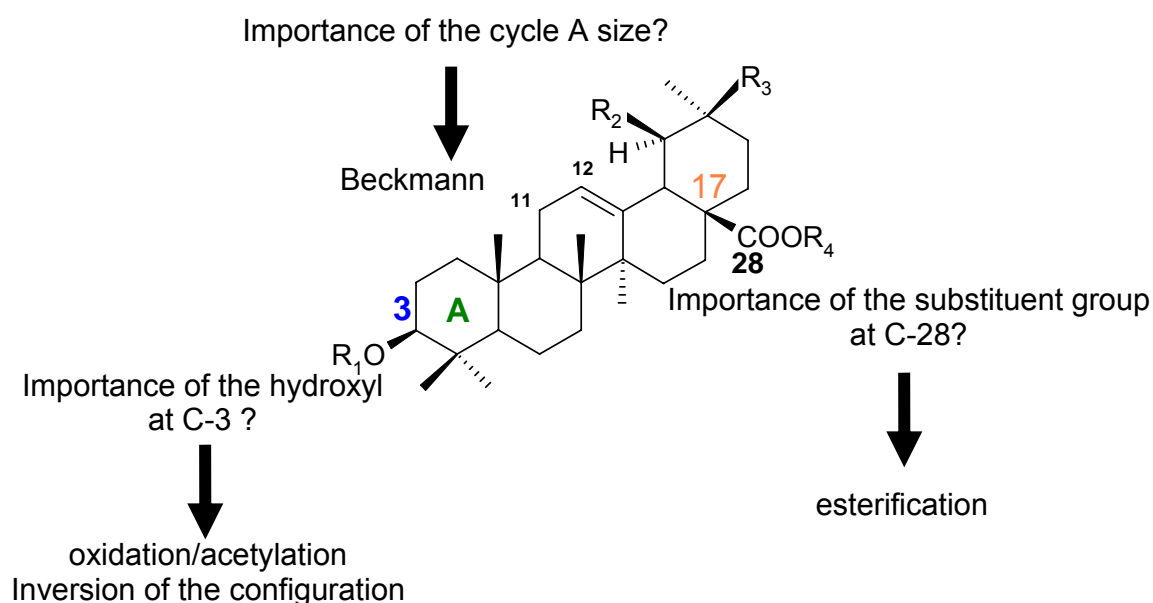
We used two strategies for the optimization of the already detected potential antimalarial activity of the ursolic acid:

1. Changes at the hydroxyl group at C-3, and in the size of cycle A.

In the first case, the role of the hydroxyl in the antimalarial activity was evaluated by carrying out an acetylation and an oxidation, and the influence of the β -configuration was evaluated by an inversion of the configuration. In the second case, a ring extension by reaction of Beckmann was performed.

2. **Changes at C-28.** The C-28 carboxylic group was replaced by substituted amides. This amide was substituted by the pharmacophoric groups: a. *N*-1,4-bis(3-aminopropyl)piperazine and b. ferrocenyl framework.

Scheme 5.



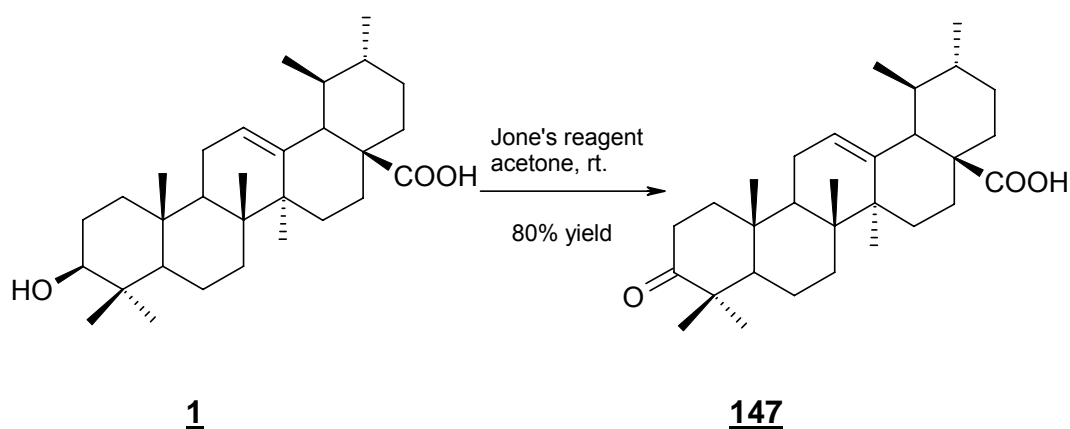
IV.2.1 Synthesis of ursolic and oleanolic acid derivatives with modifications in the cycle A

In order to investigate the structure-activity relationships for the antiplasmodial activity, several analogues of **1** and **5** with modifications in the cycle A were synthesized.

The 3-oxo-ursolic acid **147** was synthesized using Jones's reagent while 3-acetyl-ursolic acid **154** was obtained using acetic anhydride and pyridine in usual manner. Compound 3-epioleanolic acid **157** was obtained by Mitsunobu reaction. In addition, Beckmann rearrangement was applied to afford lactam **159**, 3 α -azo-3-oxo-ursolic acid.

IV.2.1.1 Oxidation at C-3

The oxidation of the secondary hydroxyl group of **1** proceeded with enough selectivity to afford the required product **147** in 80% yields, after purification in silica gel column chromatography, together with the starting material. It was used the Jones's reagent in acetone, during 1 h at room temperature (Furniss *et al.*, 1989).

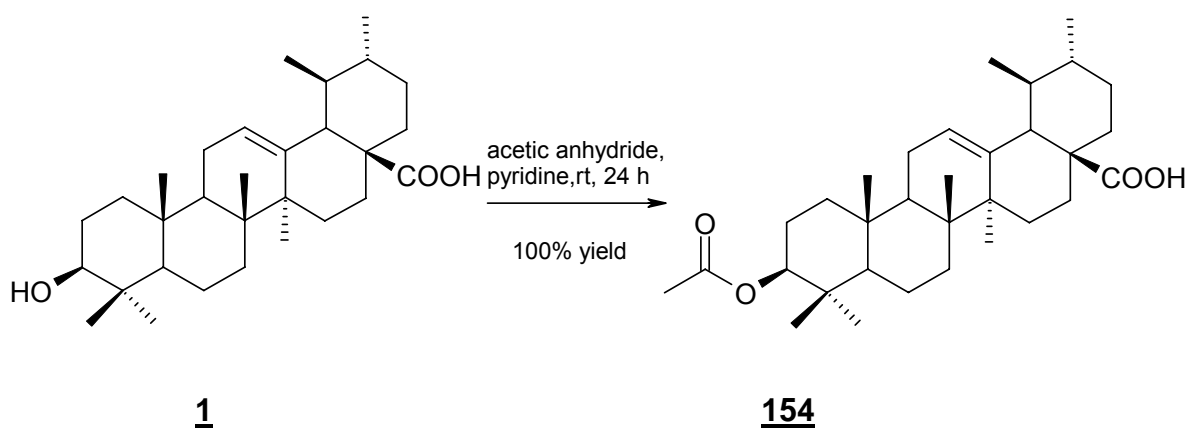


Compound **147** was obtained as a white amorphous solid and the HRMS gave a peak at m/z 477.3339 $[M+Na]^+$ consisted with the molecular formula $C_{30}H_{45}O_3Na$. The IR spectrum showed characteristic absorption bands of the carbonyl (COOH-28) at 1697 cm^{-1} and a carbonyl of ketone (C-3) at 1705 cm^{-1} .

The only major difference observed between the ^1H NMR spectra of **1** and **147** was the lack of the signal at δ 3.20 attributed to H-3 of **1**. Evidence for the ketone group was observed in the ^{13}C NMR spectrum by the signal at δ 217.7. These data allowed the identification of **147** as 3-oxo-ursolic acid, the starting material for the Beckmann reaction.

IV.2.1.2 Acetylation at C-3

Acid anhydrides are highly reactive acylating agents and react rapidly with alcohols. Typically, this reaction is conducted under basic conditions, using bases such as pyridine to improve the alcohol acidity in order to attack the carbonyl group from anhydride. This attack gives an unstable intermediate, which undergoes an elimination reaction, losing a carboxylate anion, to give an ester. Thus, treatment of **1** with acetic anhydride and pyridine at room temperature gave the 3-acetylursolic acid **154** in quantitative yield.



The HRMS of **154** showed a molecular ion at m/z 497.3636 consistent with the molecular formula $\text{C}_{32}\text{H}_{49}\text{O}_4$. The ^1H NMR spectrum showed the presence of one additional methyl group as a singlet signal at δ 2.10 suggesting that acetylation had occurred. Also, as expected the H-3 signal was observed at δ 4.55, in lower field relating the ^1H NMR spectrum of **1**. Evidence for the methyl and carbonyl acetyl groups was observed in the ^{13}C NMR spectrum at δ 21.6 and 171.7, respectively.

Compound **154**, 3-acetylursolic acid, was also the starting material for the synthesis of piperazine derivatives.

IV.2.1.3 Inversion of OH configuration at C-3

In order to determine the importance of stereochemistry at C-3, we prepared the synthesis of 3-epioleanolic acid using the Mitsunobu reaction.

The Mitsunobu reaction was used to replace OH at C-3 by another OH with inversion of configuration. Discovered in 1967, this mild reaction converts a hydroxyl group into a potent leaving group that is able to be displaced by a wide variety of nucleophiles (Mitsunobu, 1981). The mechanism was the subject of some debate centering on the identity of the intermediates and the role(s) they may play (Camp and Jenkins, 1989a; 1989b). Triphenylphosphine **156** and diethyl azodicarboxylate (DEAD) (or diisopropyl azodicarboxylate DIAD **155**) quickly form a betaine intermediate that is able to deprotonate the nucleophile (a carboxylic acid, formic acid in Scheme 6). The generated carboxylate anion deprotonates the alcohol, forming an alkoxide which can then attack the betaine at phosphorus, eventually forming phosphorane **A** and oxyphosphonium ion **B** in a ratio that is highly dependant on the pKa of the acid and solvent polarity. The carboxylate anion participates in a bimolecular nucleophilic displacement of triphenylphosphine oxide which proceeds with inversion. It is generally accepted that the oxyphosphonium ion **B** is the active intermediate which undergoes S_N2 displacement.

assigned to the C-3 (Table 11, entry 3). These suggest that the configuration of OH in C-3 was inverted.

Table 11. Structural data for 3-epioleanolic acid **157**.

Compounds	$[\alpha]_D^{20}$ (MeOH, c 0.4)	HPLC R_t (min)	^{13}C NMR (δ C-3, ppm, CDCl ₃ , 500 MHz)
oleanolic acid 5	+106.01 °	3.6	79.4
3-epioleanolic acid 157 /literature	+57.25 °/ nf	5.1 / nf	74.5 / 76.1

nf = data not found in literature

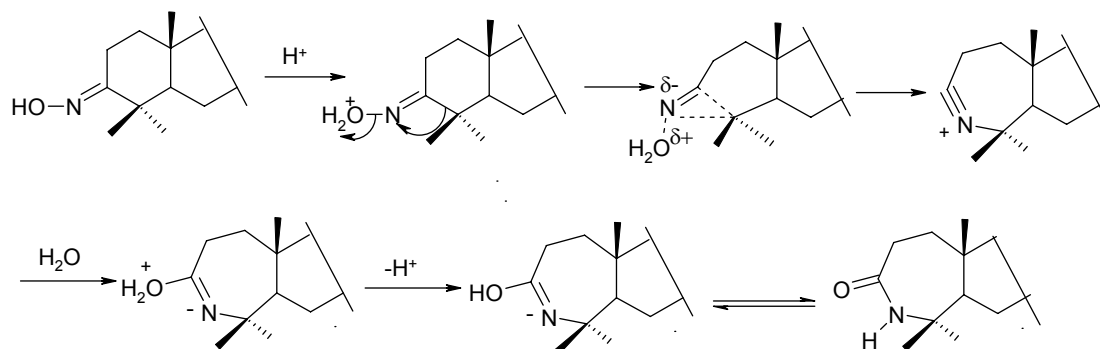
IV.2.1.4 Beckmann rearrangement (Cycle A expansion)

The mechanism of the Beckmann rearrangement establishes that acid converts the oxime OH into a leaving group, and an alkyl group migrates on to the nitrogen as water departs. Then, ionization and migration occur as a concerted process. The migration results in a nitrilium ion formation which captures a nucleophile. Eventually, hydrolysis leads to the amide. In the Beckmann rearrangement of unsymmetrical ketones there are two groups that could migrate. There are also two possible geometrical isomers (*cis* and *trans*) of an unsymmetrical oxime C=N.

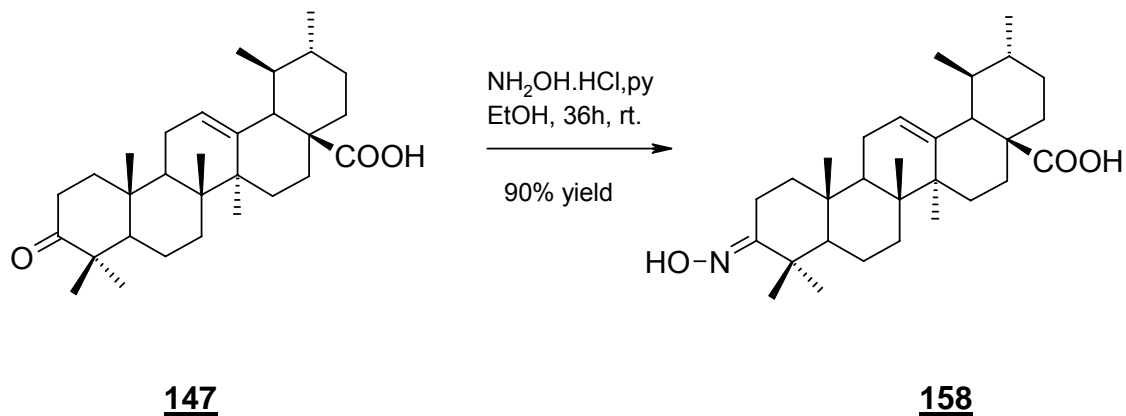
When mixtures of geometrical isomers of oximes are rearranged, it results on mixtures of products which have exactly the ratio of the geometrical isomers in the starting materials. The group that has migrated is in each case the group *trans* to the OH in the starting material (Untherhalt, 1986; Chandrasckahar and Gopalaiah, 2003). To occur migration, a migrating group has to be able to interact with the σ^* of the leaving group, and this is the reason for the specificity of Beckmann rearrangement. If one of the alkyl chains is branched, more of the oxime with the OH group *anti* to that chain will be formed

and, correspondingly, more of the branched group will migrate (Carey and Sundberg, 2001) (Scheme 7).

Scheme 7 (Carey and Sundberg, 2001).



The 3-oxo-ursolic acid **147** was successfully converted to its oxime **158** under mild conditions (hydroxylamine hydrochloride, in absolute ethanol and pyridine at room temperature for 36 hours) (Koutsourea *et al.*, 2003).



The oxime **158** was the only product (in 90% yield) observed in HPLC analysis, isolated and identified by HRMS, IR and NMR spectroscopy.

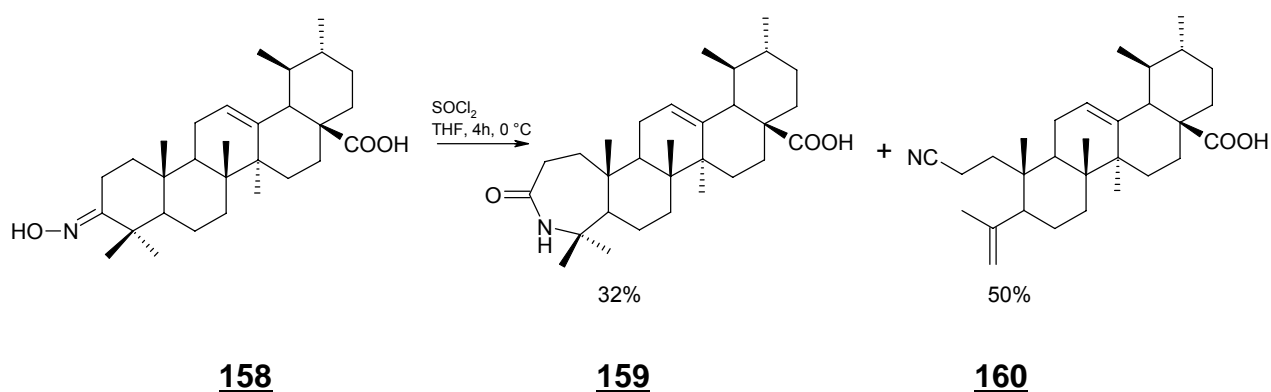
The IR spectrum of **158** showed a band at 1657 cm^{-1} characteristic of the C-N vibration of oxime.

The ^1H NMR spectrum of **158** revealed the presence of characteristic signals of triterpene skeleton previously described for **1**. This spectrum also showed a singlet signal at δ 3.42 attributed to the OH proton of oxime and a

multiplet integrating for two protons attributed to the CH₂-2. The signals corresponding to the four methyl groups (H-23, H-24, H-25 and H-26) were observed in higher field in relation to the ¹H NMR spectrum of the parent compound **147**.

The ¹³C NMR spectrum revealed the presence of signals at δ 168.0 assigned to the quaternary C-3 and, at δ 181.4 attributed to the carbonyl group at C-28. In comparison to the starting material **147**, the signals attributed to C-23, C-24 and C-26 were observed in higher field, while the signal attributed to C-2 was observed in lower field of ¹³C NMR spectrum (δ 23.4). By HMQC analysis the compound was characterized as *anti* oxime.

The crucial step, in this procedure, was the rearrangement of oxime **158** to the lactam derivative. We used the conditions described in literature (Koutsourea *et al.*, 2003) using dropwise addition of freshly distilled SOCl₂ in THF at 0 °C over the oxime. However, as shown below, Beckmann reaction of compound **158** resulted in **160** as the main product (50%) and **159** as a second product (32%). The compound **160** was identified as the product of Beckmann fragmentation and the compound **159** as the product of Beckmann rearrangement.

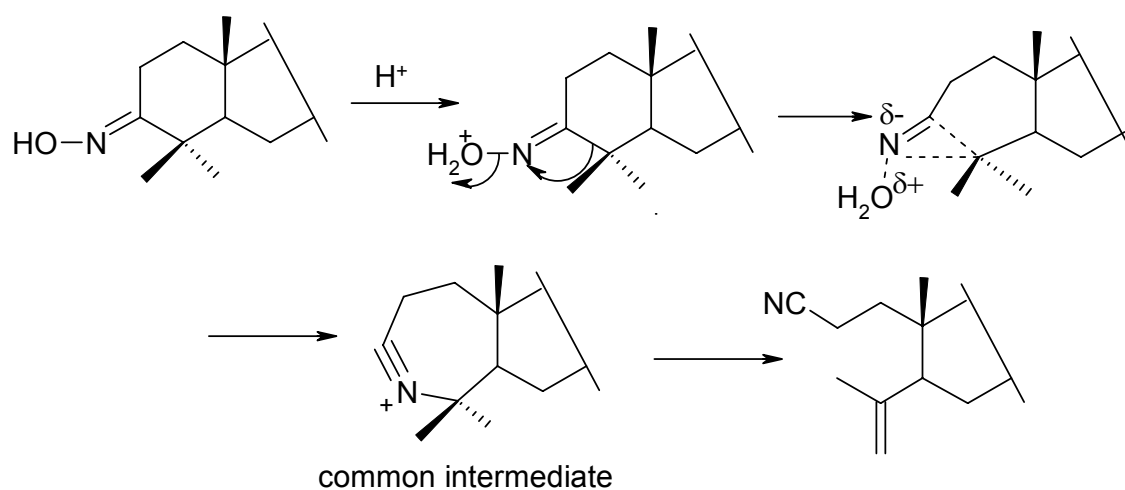


The HRMS of the Beckmann rearrangement product **159** gave a peak at *m/z* 492.3466 [M+Na]⁺ consistent with the molecular formula C₃₀H₄₇NO₃Na. The IR spectrum of **159** showed characteristic absorption bands at 1694 cm⁻¹ and 1680 cm⁻¹ attributed to the carboxylic acid and to the lactam, respectively. The

^1H NMR spectrum of **159** showed three singlet signals at δ 1.48, 1.37 and 1.19 attributed to the methyl groups H-23, H-24 and H-25, respectively. Also, at δ 2.58 (2H) a triplet doublet was attributed to CH_2 -2, as well as, at δ 8.70 a broad singlet was attributed to the lactam NH proton. Considering the ^{13}C NMR spectrum, signals of the cycle A carbons were observed at δ 30.1 (C-2); at δ 41.3 (C-1); at δ 59.4 (C-4) and at δ 179.4 (C-3).

A fragmentation reaction occurs if one of the oxime substituents can give rise to a relatively stable carbocation as happened in this case (Scheme 8). The HRMS of compound **160** gave a peak at m/z 474.3352 $[\text{M}+\text{Na}]^+$ consistent with the molecular formula $\text{C}_{30}\text{H}_{45}\text{NO}_2\text{Na}$. The IR spectrum of **160** showed characteristic absorption bands from a nitrile at 2246 cm^{-1} and, at 1692 cm^{-1} from a carboxylic acid.

Scheme 8 (Carey and Sundberg, 2001).



Compound **160** was elucidated by ^1H and ^{13}C NMR, HMQC and HMBC spectra. The ^1H NMR spectrum of **160** showed two doublets signals at δ 4.69 (1H) and 4.95 (1H) which were attributed to the methylene bond between C-4 and C-24. Also, at δ 2.39 (2H) a multiplet was attributed to CH_2 -2, and, at δ 1.78 (3H) a singlet was attributed to the methyl group 23. In ^{13}C NMR spectrum, the signal at δ 12.0 was attributed to C-2; at δ 41.5 to C-1; at δ 114.6 to C-24; at δ

120.6 to the quaternary carbon of nitrile (CN), and at δ 147.2 to the C-4 quaternary carbon.

All above mentioned data led us to the conclusion that only one of the oxime isomers was obtained or was stable. In addition, the crucial step of the Beckmann rearrangement of the triterpene cycle A was the formation of the lactam ring.

At last, through the applied strategies, it was possible to obtain three derivatives to study the importance of the hydroxyl at C-3 and that of the cycle A of the triterpene skeleton. It was synthesized 3-oxo-ursolic acid **147**, 3-acetylursolic acid **154**, and, using Mitsunobu reaction, 3-epioleanolic acid **157**. It was also obtained the product of the Beckmann reaction, 3 α -azo-3-oxo-ursolic acid **159**.

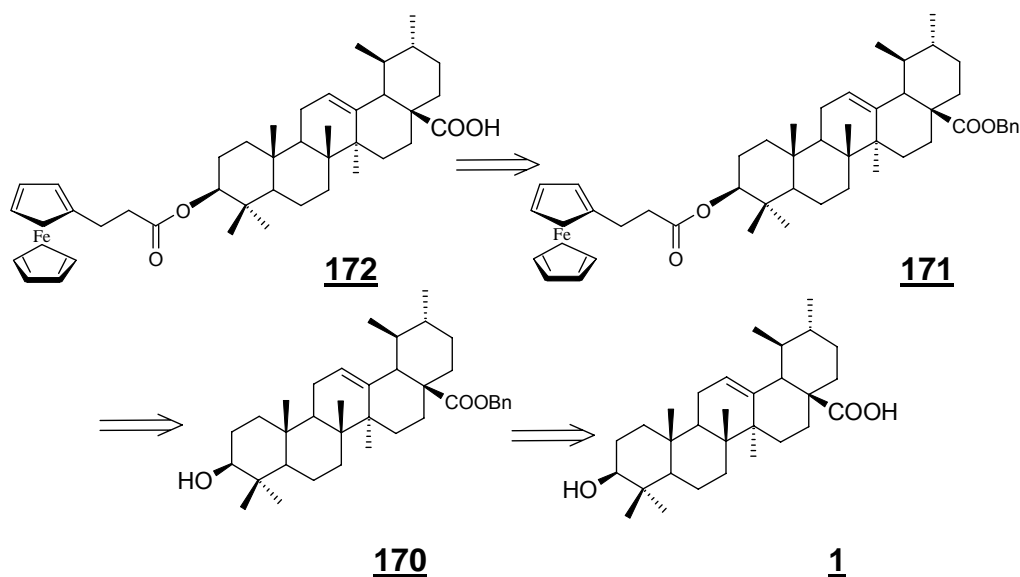
IV.2.2 Synthesis of ferrocenic derivatives from ursolic acid

Research using ferrocenic derivatives in order to obtain antiparasitodal compounds began at 90's decade by Professeur's Brocard team from *Université des Sciences et Technologies de Lille*, France. At that time, this group proposed compounds possessing a ferrocenic moiety considering that the *Plasmodium* would use these compounds in substitution of the human hemoglobin. The mechanism of action of ferrocenic derivatives possessing antimalarial activity is still unknown.

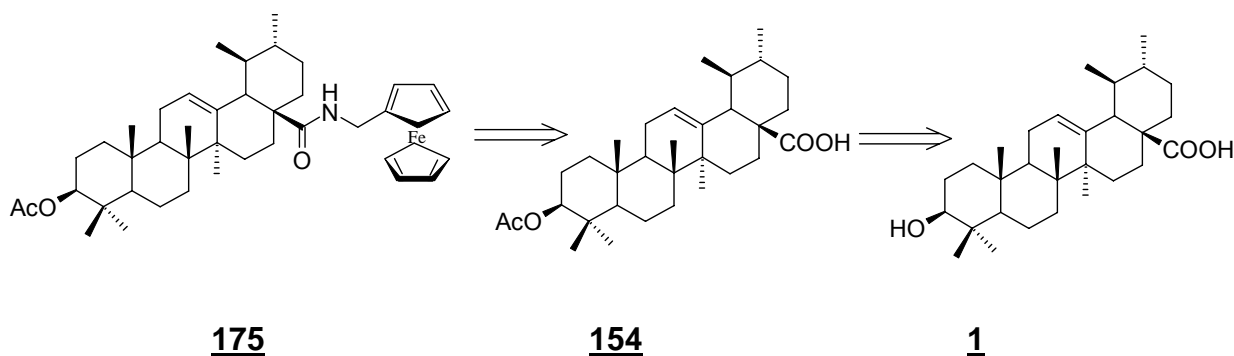
Considering the antimalarial activity of ursolic acid and ferrocenic derivatives, we decided to add the ferrocenic moiety to this aglycon in order to study their structural activity relationship in relation to its effect as substituent at C-3 and C-28.

Compounds **172** and **175** were synthesized (Scheme 9 and 10):

Scheme 9.



Scheme 10.



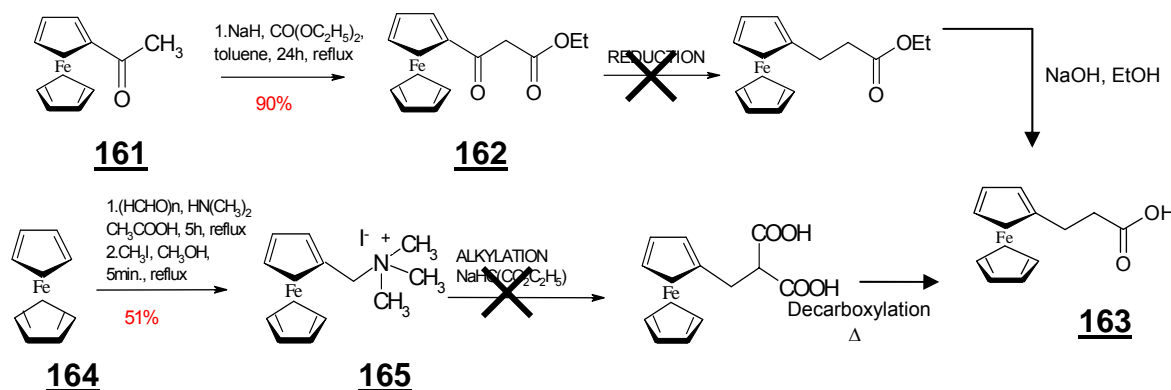
IV.2.2.1 Ferrocene coupling at C-3

The synthesis of the ester 172 began with the preparation of the 3-ferrocenylpropanoic acid 163. Initially, two strategies were developed to the 3-ferrocenylpropanoic acid synthesis.

The first strategy was based in the work of the Rinehart and co-workers (1962). The authors used sodium hydride suspended in toluene for the carboxylation of acetylferrocene 161 with diethylcarbonate. The resulting keto ester 162 was hydrogenolyzed over platinum oxide in acetic acid to give,

after hydrolysis, the 3-ferrocenylpropanoic acid **163** in 70-78% yield (Scheme 11).

Scheme 11.

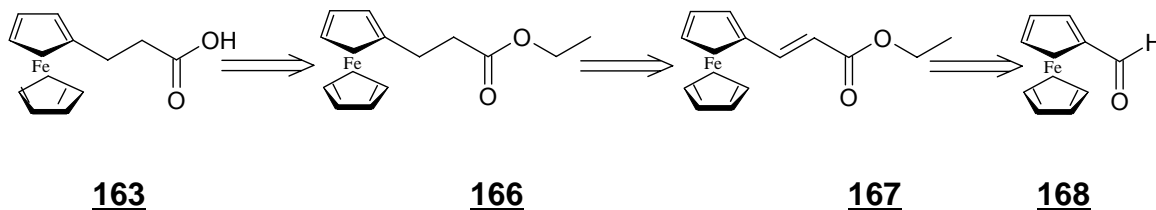


In the present study, we employed 2 equiv. of the sodium hydride (mineral oil dispersion) in toluene. The keto ester **162** was obtained in 90% yield. However, in the second step, two methods were investigated for the reductive deoxygenation of the keto ester: 1. the Wolf Kishner reaction using hydrazine and potassium hydroxide in ethyleneglycol; and 2. the Clemmensen reduction carried out in hot concentrated acetic acid or using acetic acid and toluene with co-solvent. We had no success.

In the second strategy used by us, ferrocene **164** was aminomethylated with paraformaldehyde and dimethylamine in glacial acetic acid to form *N,N*-dimethylaminomethylferrocene. The methylation of this compound by methyl iodide in absolute methanol gives the quaternary ion **165** (Lindsay and Hauser, 1957). The critical and unsuccessful step in this strategy was the alkylation of malonic ester with methiodide of *N,N*-dimethylaminomethylferrocene (Hauser and Lindsay, 1957). This reaction was assayed using: 1. sodium ethoxide powder and diethylmalonate; 2. a solution of the sodium ethoxide at 21% and diethylmalonate; and 3. sodium metallic in ethanol and diethylcarbonate. All reactions did not work.

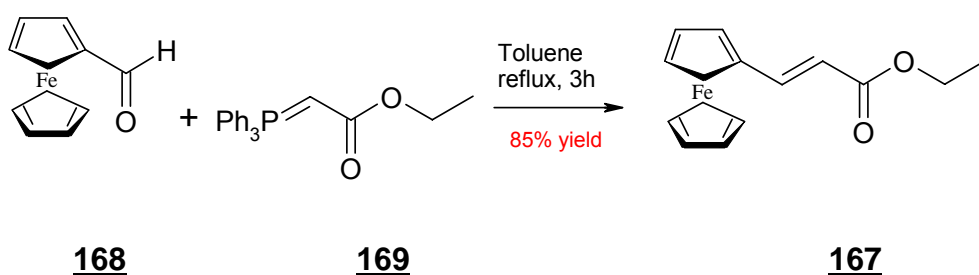
Finally, the successful strategy was based in the recent work of Debroy and co-workers (2006) (Scheme 12).

Scheme 12.



Ethyl 3-ferrocenylpropenoate **167** was prepared by the Wittig reaction of formylferrocene **168** with ethoxycarbonylmethylene-triphenylphosphorane **169** in dry toluene, in 85% yield. The stereoselectivity of the Wittig reaction depends strongly on both the structure of the ylide and the reaction conditions. The broadest generalization is that non stabilized ylides give predominantly the *Z*-alkenes, whereas stabilized ylides give mainly the *E*-alkene.

We found that β -ketophosphonium salt results in ylides stabilized by the carbonyl group and, consequently, the *E/Z* ratio was 94/6 (*E*-isomer was predominant). It was also possible to separate the two isomers by silica gel column chromatography. The ^1H NMR analysis showed for the *E*-isomers two doublet signals at δ 6.04 and 7.57 ($^3J = 15.7$ Hz) attributed to the protons of the double bond; while signals at δ 5.72 and 6.69 were attributed to the *Z*-isomer protons ($^3J = 12.4$ Hz).

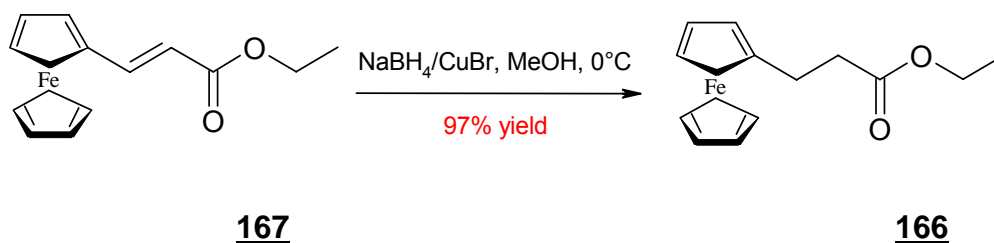


HPLC : *E* = 94%, *Z* = 06%

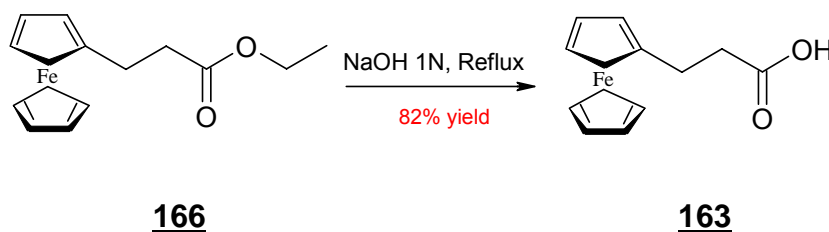
E ^1H -RMN: δ 6.04 (*d*, 1H, $^3J = 15.7$ Hz); δ 7.57 (*d*, 1H, $^3J = 15.7$ Hz)

Z ^1H -RMN: δ 5.72 (*d*, 1H, $^3J = 12.4$ Hz); δ 6.69 (*d*, 1H, $^3J = 12.4$ Hz)

Ethyl 3-ferrocenylpropanoate **166** was prepared by the selective reduction of the corresponding unsaturated analogue **167** using CuBr and NaBH₄ in methanol, in 97% yield.



Then, a saponification of the **166** with NaOH 1 N afforded the 3-ferrocenylpropanoic acid **163** in 82% yield.



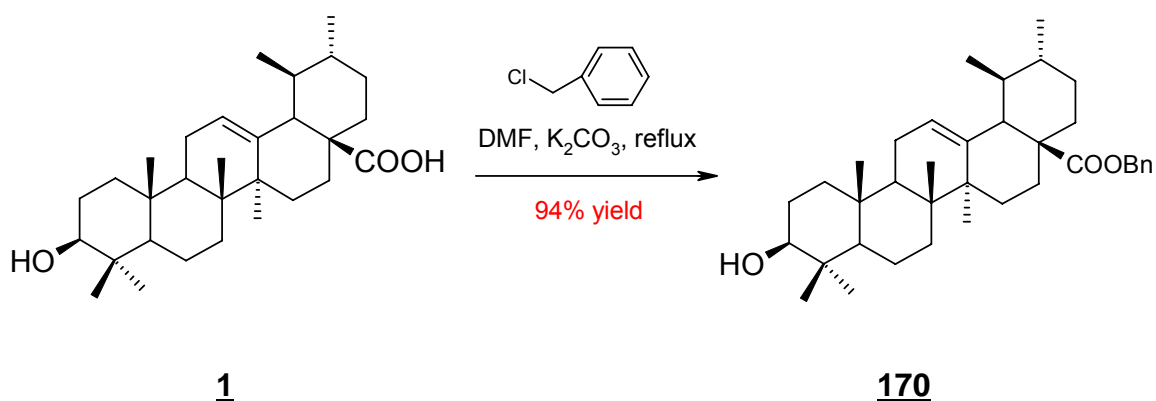
Considering the four steps, 3-ferrocenylpropanoic acid **163** was obtained in a overall 68% yield.

The structure elucidation of all ferrocenyl intermediates were based on their HRMS, IR, ¹H and ¹³C NMR spectra.

Especially to ferrocenylpropanoic acid **163**, evidence for the exact structure of this compound was obtained by mass spectrometry. The HRMS analysis showed a molecular peak at *m/z* 281.0237 [M+Na]⁺ corresponding to the molecular formula C₁₃H₁₄FeO₂Na. Ferrocenyl hydrogen's appeared at δ 4.34 (singlet, 9H) and, at δ 2.64 as a broad singlet, integrating for four protons attributed to the exocyclic CH₂.

IV.2.2.1.1 Benzylation of ursolic acid

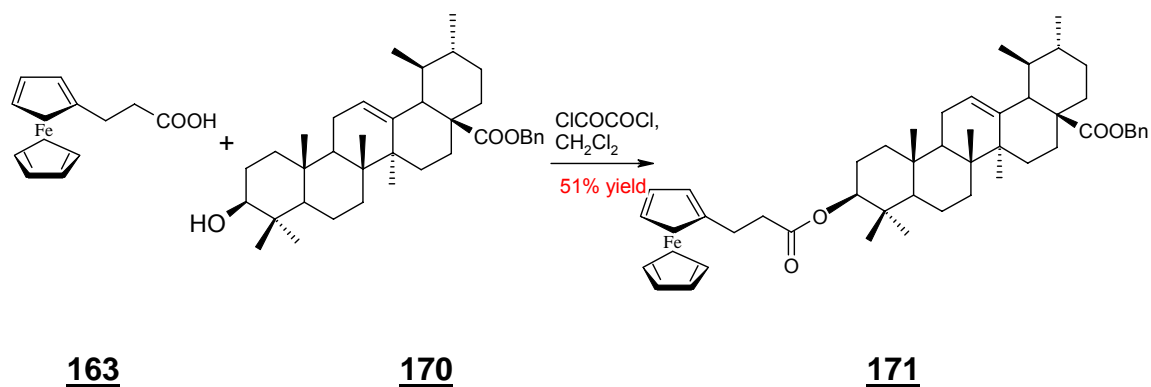
In order to accomplish the coupling between ursolic acid and the 3-ferrocenylpropanoic acid, it was necessary to protect the carboxylic group. The ursolic acid was then alkylated with benzyl chloride to afford the ester **170** in 94% yields. The structural elucidation of the benzyl product was based on spectroscopic data.



The IR spectrum of compound **170** showed a band at 1722 cm^{-1} characteristic to the absorption of the carbonyl of the carboxylic ester.

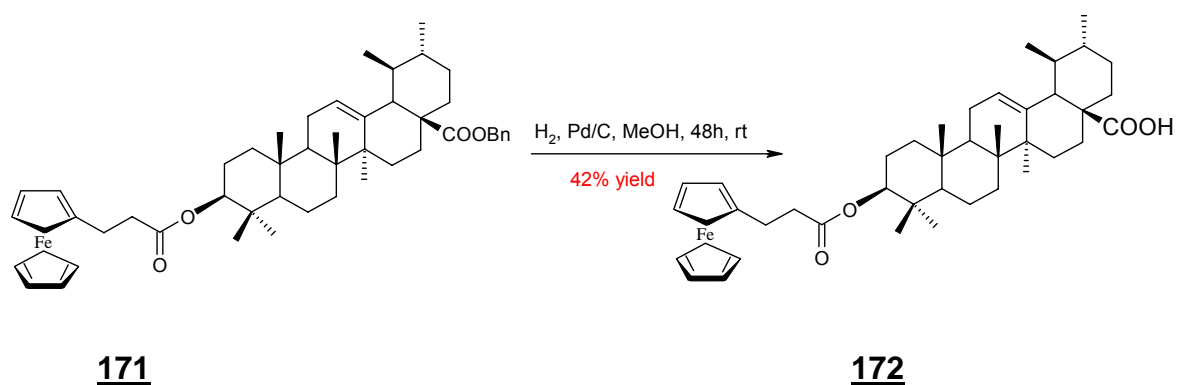
The ^1H NMR of **170** showed two doublets at δ 5.03 and 5.16 ($^2J = 12.5$ Hz) attributed to benzylic CH_2 . The presence of a multiplet resonating at δ 7.39 was attributed to the benzylic protons. Evidence for the benzylation was also observed in the ^{13}C NMR spectrum. The signal at δ 66.4 was attributed to benzylic CH_2 , and signals at δ 128.3, 128.5, 128.8 and 136.8 were attributed to the aromatic carbons *meta*, *ortho*, *para* and *ipso*, respectively. Also, the quaternary C-28 was observed at δ 177.7.

The coupling reaction between the 3-ferrocenylpropanoic acid **163** and the ester **170** afforded the compound **171** in 51% yield using oxalyl chloride in dichloromethane, at $0\text{ }^\circ\text{C}$ to room temperature, 24 hours.



The structure elucidation of **171** was based on its HRMS, IR, ^1H and ^{13}C NMR spectra. It was presented the characteristic signals from the triterpene skeleton, the ferrocenyl and benzyl atoms together with a new ester carbonyl signal.

Hydrogenolysis of the benzyl ester with black palladium afforded the compound **172** in 42% yields after 48 hours of reaction.



The structure elucidation of compound **172** was based on their HRMS, IR, ^1H and ^{13}C NMR spectra. These were similar to the compound **171** data, except for the benzyl signals.

The synthesis of compound **172** had overall yields of 21%.

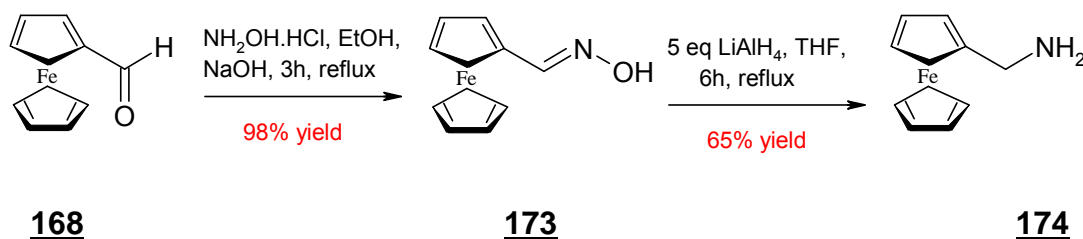
IV.2.2.2 Ferrocene coupling at C-28

The synthesis of the amide **175** possessing a ferrocene moiety at C-28 began with the preparation of the ferrocenylmethylamine **174** (Baramée *et al.*, 2006).

Initially, the oxime **173** was synthesized from formylferrocene **168** by condensation of hydroxylamine at the aldehyde function in 98% yield. The oxime **173** was analyzed by IR, ^1H NMR spectroscopy and HRMS. The IR spectrum of **173** showed a band at 1648 cm^{-1} characteristic of the C-N vibration of oxime.

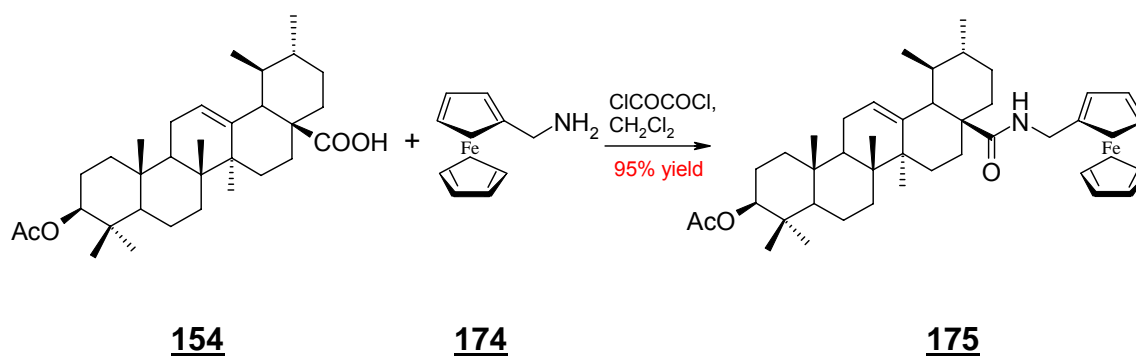
The ^1H NMR spectrum revealed the presence of the ferrocenyl hydrogen's signals at δ 4.28, 4.39 and 4.60, and at δ 8.06 a singlet attributed to the hydrogen attached to the tertiary carbon of the oxime.

Following, a reduction with LiAlH_4 afforded the amine **174** in 65% yields.



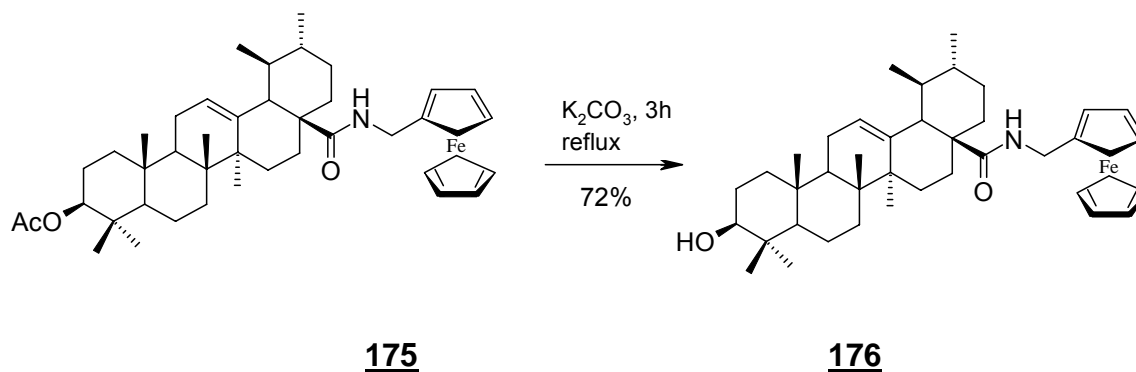
Ferrocenylmethylamine **174** was analyzed by IR and ^1H NMR spectra. The IR spectrum showed the disappearance of the absorption band at 1648 cm^{-1} attributed to the C-N of the oxime. The ^1H NMR spectrum of **174** showed a broad singlet at δ 1.58 which was attributed to the primary amine and, at δ 3.60 (2H) it was observed a singlet attributed to the CH_2 attached to the amine. Also, it was observed two signals at δ 4.20 and 4.22 attributed to the ferrocenyl hydrogens.

Finally, a coupling reaction between 3-acetylursolic acid **154** and ferrocenylmethylamine **174**, using the reaction conditions previously described to **171**, gave the compound **175** in 95% yield.



The compound **175** was obtained in an overall 60% yield. It was identified by IR, ^1H and ^{13}C NMR spectroscopy and HRMS. The HRMS analysis of **175** showed a molecular peak at m/z 695.4020 corresponding to the molecular formula $\text{C}_{43}\text{H}_{61}\text{NO}_3\text{Fe}$. The IR spectrum showed characteristic absorption bands of the amide carbonyl (C-28) at 1648 cm^{-1} and the acetyl carbonyl (C-3) at 1731 cm^{-1} . Also, it was possible to observe the disappearance of the band at 1697 cm^{-1} attributed to the carboxylic acid (C-28). The ^1H NMR spectrum of **175** showed five singlet signals at δ 1.03 (C-23), 1.00 (C-24), 0.97 (C-25), 1.05 (C-26) and 1.13 (C-27), and two doublets at δ 0.83 and 0.91 which were attributed to the methyl groups 30 and 29, respectively. Also, the doublet at δ 1.91 (1H) characteristic of the ursane skeleton was attributed to CH-18 ($^3J = 10.3\text{ Hz}$), as well as, the broad triplet at δ 5.31 was attributed to CH-12. At δ 2.04 (3H), it was observed the presence of a singlet attributed to the acetyl group. Evidence for the ferrocenyl group was observed at δ 3.92 (1H, d, $^3J = 13.4\text{ Hz}$), attributed to the CH_2 attached to the ferrocene group; at δ 4.23 was observed the overlap of the signal of ferrocenyl hydrogens and the CH_2 attached to the ferrocene, and H-3. Finally, at δ 6.10 it was observed a singlet attributed to the amide $N\text{-H}$. Another evidence for the exact structure of compound **175** was obtained by ^{13}C NMR spectrum. The signals attributed to the methyl groups resonated at δ 28.4 (C-23), 17.4 (C-24), 16.2 (C-25), 17.1 (C-26), 23.9 (C-27), 17.9 (C-29), 21.6 (C-30) and at δ 21.7 (acetyl methyl group). Ferrocenyl carbons signals were observed at δ 69.1, 69.6 and 70.0 and, carbonyl carbons signals were observed at δ 171.8 (acetyl) and δ 178.2 (amide).

In order to investigate the importance of acetyl group at C-3 for the antiplasmodial activity of this series, the compound **175** were submit to the reaction of deacetylation. **176** were obtained with 72% yield and their structure elucidation was based on IR, ^1H and ^{13}C NMR, and HRMS spectra. These were similar to the compound **175** data, excepting the acetyl signals.



The strategies employed in this chapter allowed obtaining three ferrocenic derivatives from ursolic acid (compounds **172**, **175**, **176**) that were submitted to antiplasmodial assays.

IV.2.3 Synthesis of piperazine derivatives from ursolic acid

The importance of *N*-1,4-bis(3-aminopropyl)piperazine moiety to the antimalarial activity was described in studies about bisquinoline derivatives and their activity towards *P. falciparum* strains. The authors proposed that this moiety improve the accumulation of such derivative compounds in the acidic vacuole. It was also proposed that *N*-1,4-bis(3-aminopropyl)piperazine moiety interfere in the haemozoin formation (Vennerstrom *et al.*, 1992; Raynes *et al.*, 1995). Other studies demonstrated that this moiety improve the antimalarial activity of quinolinic derivatives (Ryckebusch *et al.*, 2003, 2005; Guillon *et al.*, 2004).

By taking this into account, compound **180** possessing the *N*-1,4-bis(3-aminopropyl)piperazine moiety and its derivatives (series **181** to **200**), with

different substituents at the terminal amine, were designed to evaluate the influence of the introduction of new basic nitrogen on the antimalarial activity.

The construction of the desired *N*-[1,4-bis(3-aminopropyl)piperazinyl]-3-*O*-acetylursolamide **180** is shown in Scheme 13.

IV.2.3.1 Synthesis of *N*-[1,4-bis(3-aminopropyl)piperazinyl]-3-*O*-acetylursolamide **180**

Initially, the commercially available bis(3-aminopropyl)piperazine **177** was protected to afford its *N*-Boc derivative **178**. Five different reaction conditions were evaluated in order to obtain **178** with improve yield (Table 12).

Table 12. Results of *N*-Boc protection of **177** under various conditions.

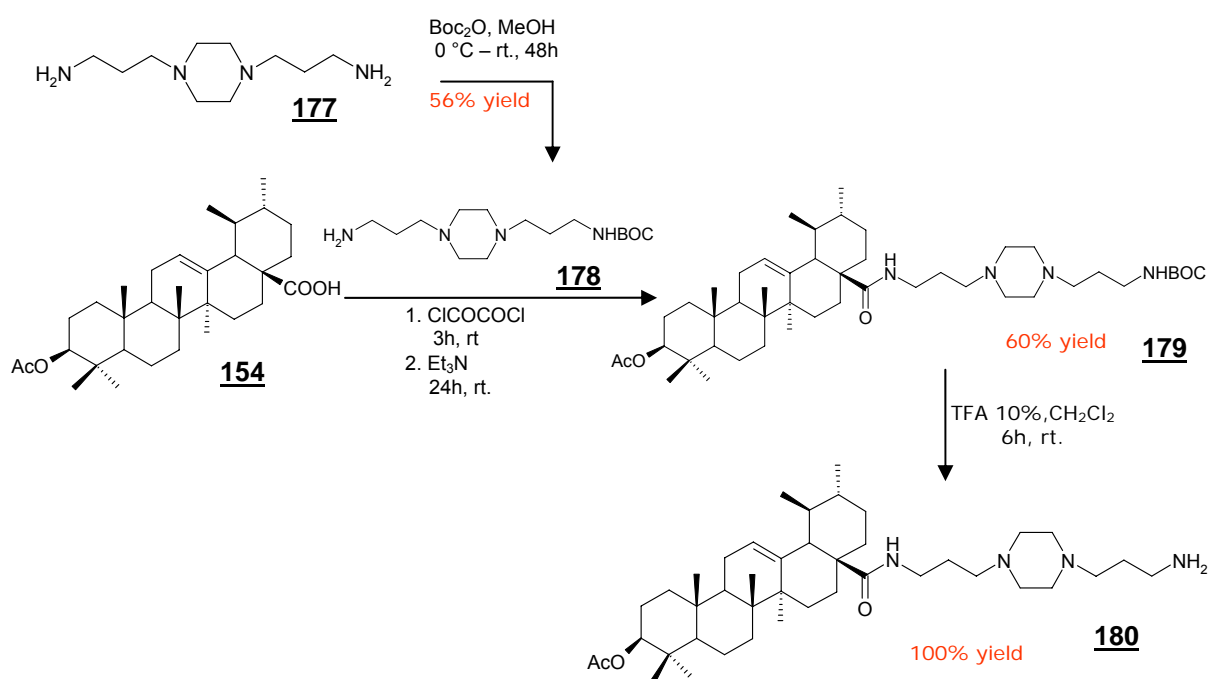
Entry	conditions			Yield (%) mono-protected
	Solvent	<i>N</i> -1,4-bis(3-aminopropyl)piperazine	di- <i>tert</i> -butyl dicarbonate	
1	dioxane	1.0	1.0	0
2	dioxane	1.0	0.5	10
3	dichloromethane	1.0	1.0	0
4	dichloromethane	1.0	0.5	10
5	methanol	1.0	0.5	28

When di-*tert*-butyl dicarbonate was used in equimolar concentration to *N*-1,4-bis(3-aminopropyl)piperazine, the compound bi-protected was the only obtained product (Table 12, Entries 1 and 3).

We found that conditions similar to those reported by Zheng *et al.* (2005) gave the best selectivity in the *N*-protection, furnishing the desired monoprocted-*N*-1,4-bis(3-aminopropyl)piperazine **178** in 28% yield (Table 12, Entry 5). The reaction conditions were as follows: a solution of di-*tert*-butyl dicarbonate (0.5 equiv) in MeOH was slowly added to a stirring solution of *N*-1,4-bis(3-aminopropyl)piperazine (1 equiv) in MeOH at 0 °C. The mixture was then stirred for 2 days at room temperature, and the solvent removed in

vacuum. The crude solid was dissolved in diethyl ether with gentle warming, and the resulted white precipitate was filtered off. The crucial in this procedure was the extraction step. The product was extracted from the mother liquor with 5% citric acid solution, and the aqueous layer was washed with AcOEt, basified with Na_2CO_3 and extracted with AcOEt. The organic layer gave the compound **178** as yellow oil.

Scheme 13.



The high-resolution mass spectra (HRMS) of the compound **178** presented m/z 301.2622 $[\text{M}+\text{H}]^+$ consistent with the molecular formula $\text{C}_{15}\text{H}_{33}\text{N}_4\text{O}_2$. The IR analysis presented N-H absorption at 3365 cm^{-1} and an amide (C=O) characteristic absorption at 1685 cm^{-1} .

The ^1H NMR spectrum of **178** showed a singlet at δ 1.48 (9H) attributed to the methyl protons of the boc group. At δ 1.72 (4H), it was observed a multiplet which was assigned to the CH_2 -c and c' to the lateral chain to the piperazine. At δ 2.50 (12 H), a broad multiplet was attributed to the piperazine hydrogens and the CH_2 -b and b'. Finally, at δ 2.81 and 3.12 it was observed two triplet attributed to CH_2 -d and d', respectively.

Within the second step of the synthetic pathway (Scheme 13), a coupling reaction was employed between the previously mentioned compound **178** and **154**, leading to the compound **179**. This compound was obtained in an overall 60% yield. For this purpose, 3-*O*-acetyl-ursolic acid was first treated with oxalyl chloride in CH₂Cl₂, leading the formation of the 3-*O*-acetyl-ursolic acid chloride. This reaction was monitored by IR because, in general, acyl chloride groups display characteristic carboxylic acid absorption at about 1770 cm⁻¹. The reaction was terminated when the peak at 1697 cm⁻¹ completely disappeared, in turn the peak at 1770 cm⁻¹ had its bigger intensity. Subsequently, coupling reaction was performed by addition of triethylamine and piperazine **178**.

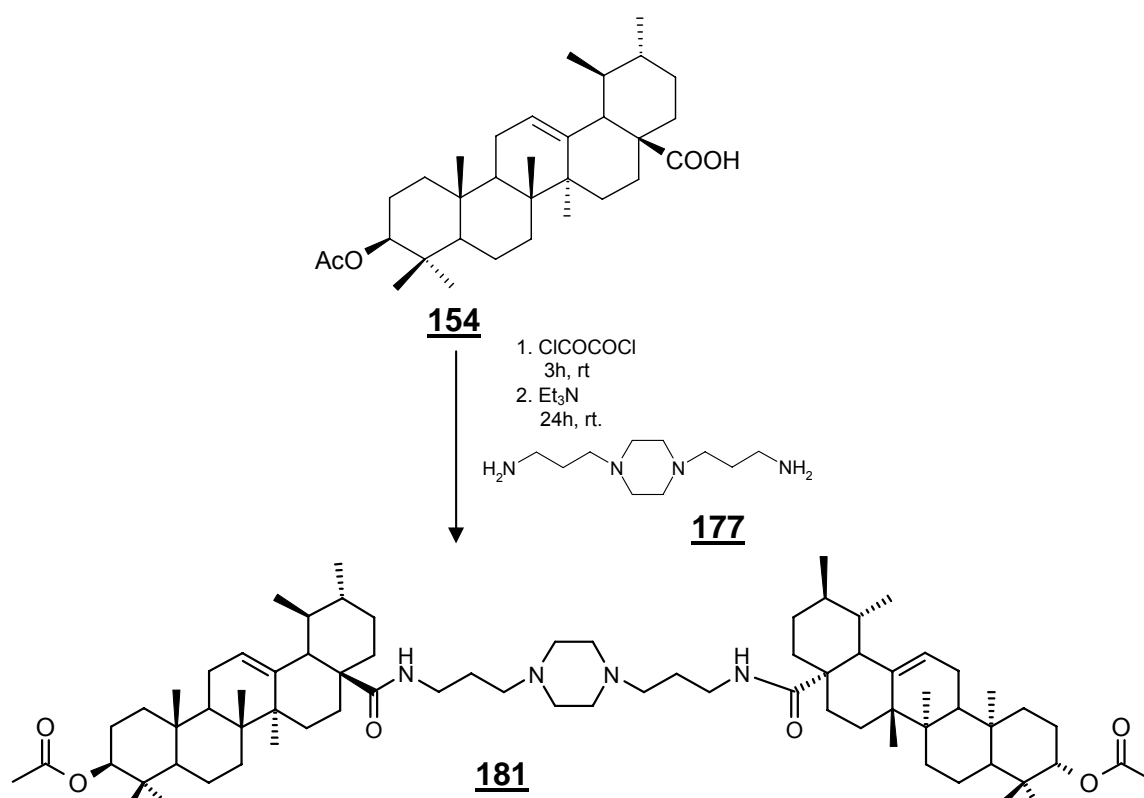
Deprotection of **179** using trifluoroacetic acid yielded the *N*-1,4-bis(3-aminopropyl)piperazinyl-ursolamine **180**. This compound was obtained as a white solid in 60% overall yield. It was analyzed by IR, ¹H and ¹³C NMR spectroscopy and HRMS.

The HRMS gave a peak at *m/z* 681.5667 [M+Na]⁺ consistent with the molecular formula C₄₂H₇₃N₄O₃. The IR spectrum of **180** showed characteristic absorption bands of the amide carbonyl (C-28) at 1683 cm⁻¹ and of an acetyl carbonyl (C-3) at 1731 cm⁻¹. The ¹H NMR spectrum showed the presence of six singlet (3H each) signals at δ 2.10 (acetyl), 1.17 (C-27), 1.01 (C-26), 1.00 (C-23), 0.99 (C-24), and 0.94 (C-25), and two doublets (3H each) at δ 0.81 (C-30) (³*J* = 6.9 Hz) and 0.91 (C-29) (³*J* = 6.6 Hz). Also, it was observed at δ 4.54 (dd, ³*J* = 13.8 and 6.4 Hz) attributed to H-3. Evidence of bis-aminopropylpiperazine group was observed at δ 1.70 by a multiplet signal attributed to the CH₂-c and c'; at δ 2.51, it was observed a broad multiplet (13H) attributed to the piperazine hydrogens, CH₂-b and b' and, H-18; and at δ 2.93 and 3.49 it was observed two multiplet attributed to CH₂-d and d'. Finally, at δ 6.46 it was observed a broad singlet attributed to the NH of the amide at C-28. The ¹³C NMR spectrum of the compound **180** showed the signals attributed to methyl groups at δ 15.9 (C-25), 17.1 (C-26), 17.3 (C-24), 17.6 (C-29), 21.7 (C-30 overlapped to methyl of the acetyl group), 23.9 (C-30) and at δ 28.2 (C-27). The signal attributed to the CH₂ of the piperazine groups resonated at δ 54.7 with overlapping. It was observed

the presence of the quaternary carbons of the amide and acetyl groups at δ 179.4 and 171.4, respectively.

The dimer **181** was obtained by coupling reaction of commercially available bis(3-aminopropyl)piperazine **177** with 3-acetylursolic acid **154** in a 1:2 ratio under similar conditions previously described to **180**, using dichloromethane as solvent (Scheme 14.).

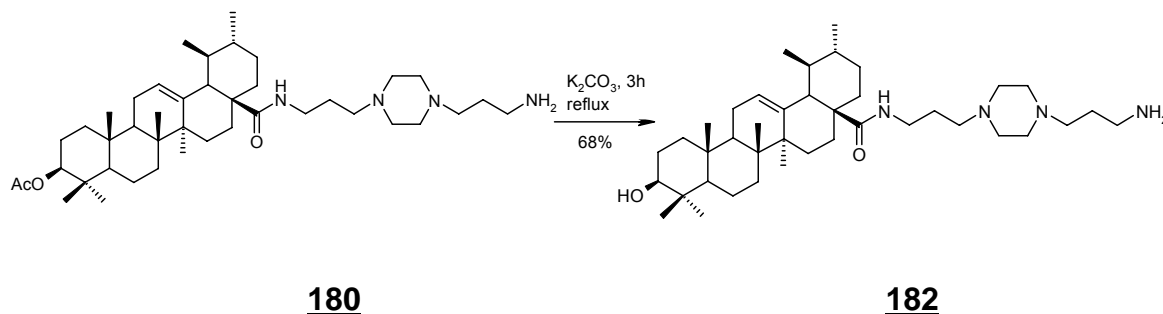
Scheme 14.



The structure elucidation of **181** was based on its MS, IR, ¹H and ¹³C NMR spectra. Considering that the signals of the triterpene skeleton in the ¹H NMR spectrum were very similar of compound **180**, the mass value and the different hydrogen integrations were very important to elucidate this compound.

In order to investigate the importance of the acetyl group at C-3 for the antiplasmodial activity of this series, the compound **180** was submitted to the deacetylation reaction to obtain compound **182**. Compound **182** was obtained

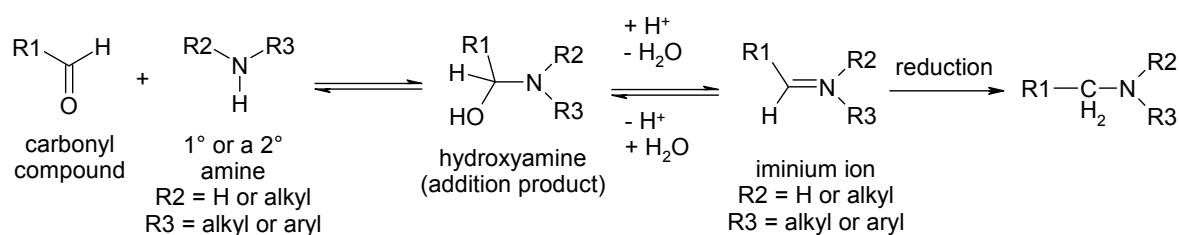
with 50% yield and its structure elucidation was based on IR, ^1H and ^{13}C NMR, and HRMS spectra. These data were similar to the compound **180**, excepting the acetyl signals.



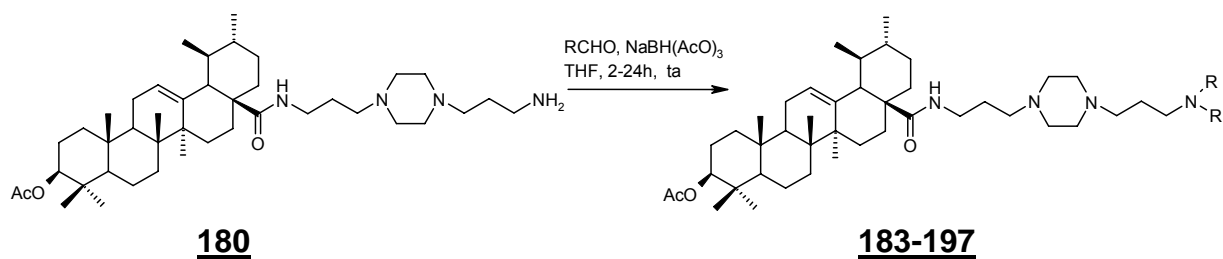
IV.2.3.2 Reductive amination reactions to obtain tertiary amines

The synthesis of *N*-[1,4-bis(3-aminopropyl)piperazinyl]-3-*O*-acetylyrsolamide **180** led us to design new compounds with additional chains or cycles at the terminal primary amine of the piperazine. These new derivatives were accomplished through reductive amination reactions (Scheme 15).

Scheme 15.



The reductive amination reactions were carried out using compound **180** and several aldehydes in tetrahydrofuran. The standard reaction conditions were as follows: a mixture of the carbonyl compound (3 equiv) and the amine **180** was stirred with 3.0 equiv of sodium triacetoxyborohydride under nitrogen atmosphere, at room temperature, to give the dialkylated compounds (Abdel-Magid *et al.*, 1996; Ryckebusch *et al.*, 2003).



After literature review, we selected sodium triacetoxyborohydride considering its low toxicity in relation to sodium cyanoborohydride. This borohydride reagent is mild and exhibits remarkable selectivity as a reducing agent. Our selection was also based on the results of reductive amination reported by Abdel-Magid and co-workers (1996).

The obtained compounds from reductive amination reactions using compound **180** and aldehydes are listed in Table 13, 14 and 15.

Table 13 present the synthesized compounds using aromatic aldehydes.

Table 13. Compounds **183-190** obtained by reductive amination reactions from **180**.

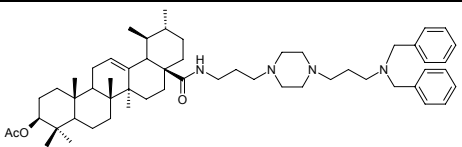
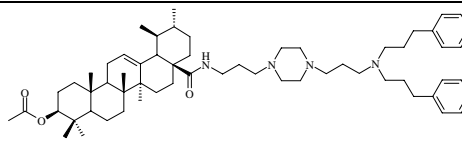
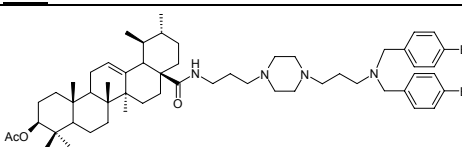
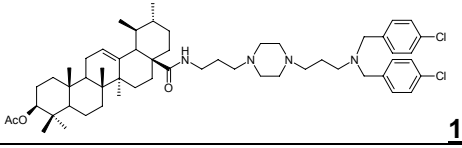
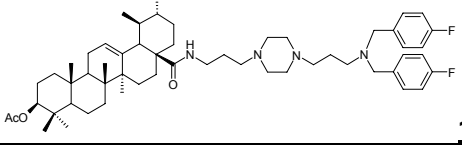
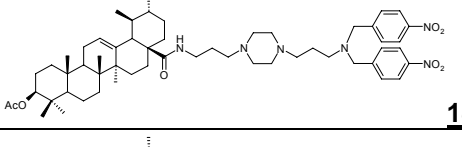
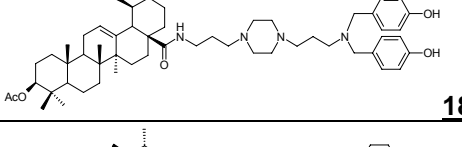
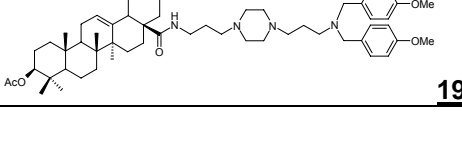
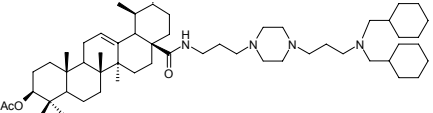
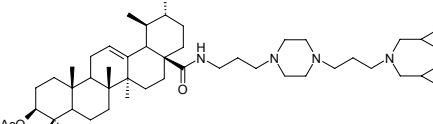
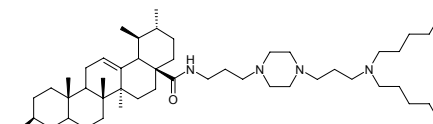
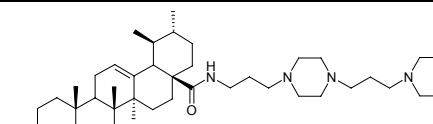
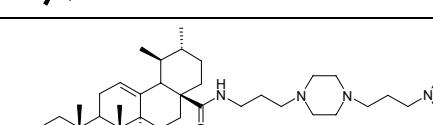
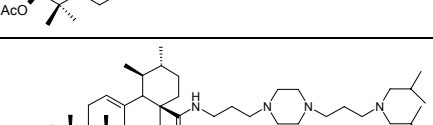
Aldehyde	product / yield
$C_6H_5CH_2CHO$	 183 / 76%
$C_6H_5(CH_2)_2CHO$	 184 / 27%
$C_6H_5BrCH_2CHO$	 185 / 56%
$C_6H_5ClCH_2CHO$	 186 / 53%
$C_6H_5FCH_2CHO$	 187 / 70%
$C_6H_5NO_2CH_2CHO$	 188 / 40%
$C_6H_5OHCH_2CHO$	 189 / 30%
$C_6H_5MeOCH_2CHO$	 190 / 25%

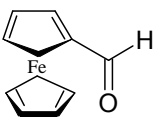
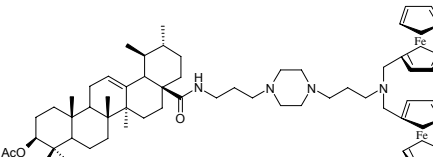
Table 14 present the synthesized compounds using aliphatic aldehydes.

Table 14. Compounds **191-196** obtained by reductive amination reactions from **180**.

Aldehyde	product / yield
C₆H₁₁CHO	 191/50%
C₃H₅CHO	 192/30%
C₅H₁₁CHO	 193/30%
C₃H₇CHO	 194/30%
C₂H₅CHO	 195/45%
C₃H₇CHO	 196/39%

Finally, Table 15 presents the synthesized compound using ferrocenecarboxaldehyde.

Table 15. Compound **197** obtained by reductive amination reactions from **180**.

Aldehyde	product / yield
	 197/60%

Under the described reaction conditions, compound **180** was successfully employed in the reductive amination of a variety of aldehydes with yields ranging from 25% to 76%.

We may point some explanations to these large yields range. It is important to emphasize that the conditions of these reactions were not optimized. Also, the reactivity of these aldehydes is different. It is known that aldehydes can be reduced with sodium triacetoxyborohydride, thus, it would be possible that the reduction of the aldehyde competed with the reductive amination process. On the other hand, it was obtained by us one monoalkylated compound as byproducts.

Eight derivatives were synthesized with aromatic (**183-190**) and aliphatic (**191-196**) aldehydes and ferrocenecarboxaldehyde (**197**).

In the aromatic series, substitution on the phenyl ring at *para* position was evaluated. The presence of electron-donating groups, as OH (**189**) or OMe (**190**); or electron-withdrawing group as NO₂ (**188**); and halogens as F (**187**), Cl (**186**) or Br (**185**) were studied.

In the aliphatic series, the effect of the elongation of the chain was studied in compounds **193-195**. Also, two cyclic derivatives **191** and **192** were synthesized, together with one compound **196** with branched chain.

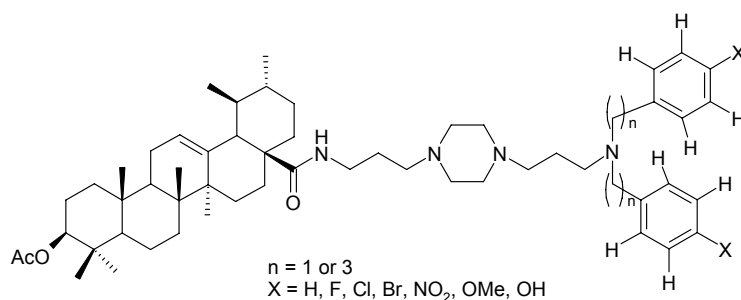
Finally, a ferrocenyl derivative **197** was also synthesized in order to compare to the ursolic acid-ferrocenyl derivatives themselves.

All compounds were elucidated by IR, ¹H and ¹³C NMR spectroscopy and HRMS.

IV.2.3.2.1 Identification of aromatic compounds

The aromatic proton and carbon signals of compounds **183** to **190** were summarized in the Table 16.

Table 16. ^1H and ^{13}C NMR spectral data of the aromatic groups of compounds **183** to **190**. (CDCl_3 , 500 MHz).



compound	δ H-ortho/ δ C-ortho (ppm)	δ H-meta/ δ C-meta (ppm)	δ H-para/ δ C-para (ppm)	δ C-ipso (ppm)
183 n=1, X=H	7.50, <i>d</i> , $^3J=7.5$ Hz/ 129.2	7.34, <i>dd</i> , $^3J=7.5$ Hz/ 128.6	7.27, <i>dd</i> , $^3J=7.1$ Hz/ 127.3	145.3
184 n=3, X=H	7.32, <i>d</i> , $^3J=6.2$ Hz/ 129.2	7.24, <i>dd</i> , $^3J=7.3$ Hz/ 128.7	7.21, <i>dd</i> , $^3J=7.1$ Hz/ 126.3	134.3
185 n=1, X=Br	7.25, <i>d</i> , $^3J=8.1$ Hz/ 121.1	7.47, <i>d</i> , $^3J=8.2$ Hz/ 130.8	-/ 139.0	131.7
186 n=1, X=Cl	7.30, <i>d</i> , $^3J=8.8$ Hz/ 138.5	7.32, <i>d</i> , $^3J=8.5$ Hz/ 128.8	-/ 133.0	130.4
187 n=1, X=F	7.32, <i>dd</i> , $^3J_{\text{HH}}=8.2$ Hz; $^3J_{\text{HF}}=5.7$ Hz/ 130.6	7.03, <i>dd</i> , $^3J_{\text{HH}}=8.5$ Hz; $^3J_{\text{HF}}=8.6$ Hz/ 115.5	-/ 161.1	125.6
188 n=1, X=NO ₂	7.58, <i>d</i> , $^3J=8.2$ Hz/ 124.1	8.24, <i>d</i> , $^3J=8.3$ Hz/ 129.6	-/ 148.1	143.0
189 n=1, X=OH	6.77, <i>d</i> , $^3J=8.1$ Hz/ 130.6	7.16, <i>d</i> , $^3J=8.2$ Hz/ 115.8	-/ 156.0	130.9
190 n=1, X=OMe	6.89, <i>d</i> , $^3J=8.4$ Hz/ 130.6	7.29, <i>d</i> , $^3J=8.4$ Hz/ 113.9	-/ 158.9	125.6

(-)= quaternary carbon

All aryl substituted compounds showed in the ^1H NMR spectrum a singlet at about δ 3.60 (4H) attributed to the $\text{N}(\text{CH}_2)_2$ hydrogens. The ^1H NMR spectrum of compound **190** showed a singlet at δ 3.85 attributed to the methoxyl group, and in the ^{13}C NMR spectrum this signal was observed at δ 56.6.

IV.2.3.2.2 Identification of aliphatic compounds

In the ^1H and ^{13}C NMR spectra of the aliphatic compound, it was observed the overlap of the CH_2 signals of the ursane skeleton and the CH_2 of the chain attached to *N*. In these cases the HMQC and HMBC, and the HRMS were very important to the structural elucidation.

The ^1H NMR spectrum of compounds **191** and **192** showed at δ 2.13 and 2.09 respectively, integrating to four protons, a doublet signal ascribed to the $\text{N}(\text{CH}_2)_2$ hydrogens. The HRMS of **191** gave a peak at m/z 873.7553 $[\text{M}+\text{H}]^+$ consistent with the molecular formula $\text{C}_{56}\text{H}_{97}\text{N}_4\text{O}_3$, and the HRMS of **192** gave $m/z = 789.6609$ $[\text{M}+\text{H}]^+$ consistent with $\text{C}_{50}\text{H}_{85}\text{N}_4\text{O}_3$.

The structure elucidation of compound **193** was primarily based on their mass spectrometry. The HRMS gave a peak at m/z 877.7901 $[\text{M}+\text{H}]^+$ consistent with the molecular formula $\text{C}_{56}\text{H}_{101}\text{N}_4\text{O}_3$. The ^1H NMR spectrum of **193** revealed the signal at δ 0.94 attributed to the methyl group of the heptyl chain. The signal at δ 1.32 was attributed to the five methylene groups of the heptyl chain overlapped with the ursane hydrogens. At δ 2.46, it was observed a broad multiplet attributed to the piperazine hydrogens overlapped to the H-18. Evidence for the presence of the heptyl chain was observed in the ^{13}C NMR spectrum. It was observed the signal at δ 14.4 assigned to the two methyl groups of the heptyl chain, a signal at δ 23.0 assigned to $-\text{CH}_2\text{CH}_3$, and successively, at δ 30.1 a signal assigned to $-\text{CH}_2\text{CH}_2\text{CH}_3$, at δ 28.7 a signal assigned to $-\text{CH}_2(\text{CH}_2)_2\text{CH}_3$, at δ 27.9 a signal assigned to $-\text{CH}_2(\text{CH}_2)_3\text{CH}_3$, and at δ 29.7 a signal assigned to $-\text{CH}_2(\text{CH}_2)_4\text{CH}_3$. Finally, at δ 57.8 it was observed a signal assigned to the $-\text{N}(\text{CH}_2(\text{CH}_2)_5\text{CH}_3)_2$.

The HRMS of compound **194** gave a peak at m/z 793.6981 $[M+H]^+$ consistent with the molecular formula $C_{50}H_{89}N_4O_3$. The 1H NMR spectrum of compound **194** showed the presence of methyl protons from the butyl chain at δ 0.93. Also, at δ 1.35 (11H) a multiplet attributed to the methylene groups of the butyl chain $-N(\underline{CH_2CH_2CH_2}CH_3)_2$, as well as, at δ 2.51 a broad multiplet attributed to the overlapping of the piperazine hydrogens, H-18 and the methylene of the butyl chain ($-N(\underline{CH_2}CH_2CH_2CH_3)_2$). Evidence for the presence of the butyl chain was observed in the ^{13}C NMR spectrum. It was observed the presence of a signal assigned to the two methyl groups of the butyl chain at δ 14.0, a signal assigned to $-\underline{CH_2}CH_3$ at δ 20.6, and at δ 25.4 a signal assigned to $-\underline{CH_2}CH_2CH_3$. Finally, a signal at δ 54.8 assigned to the $-N(\underline{CH_2}(CH_2)_2CH_3)_2$.

For the compound **195**, the HRMS gave a peak at m/z 765.6000 $[M+H]^+$ consistent with the molecular formula $C_{48}H_{85}N_4O_3$. The 1H NMR spectrum of **195** revealed the signal at δ 0.93 attributed to the methyl group of the propyl chain. The signal at δ 1.32 was attributed to the methylene group of the propyl chain overlapped with the ursane hydrogens. At δ 2.56 was observed a broad multiplet attributed to the piperazine hydrogens overlapped to H-18, and the methylene groups of the propyl chain. Evidence for the presence of the propyl chain was observed in the ^{13}C NMR spectrum. It was observed the signal δ 12.3 assigned to the two methyl groups of the propyl chain, a signal at δ 20.5 assigned to $-\underline{CH_2}CH_3$, and a signal at δ 57.8 assigned to the $-N(\underline{CH_2}CH_2CH_3)_2$.

The HRMS of compound **196** gave a peak at m/z 793.6942 $[M+H]^+$ consistent with the molecular formula $C_{50}H_{89}N_4O_3$. The 1H NMR spectrum of **196** revealed a signal at δ 0.91 attributed to the methyl group of the isobutyl chain overlapped to the methyl 29 of the ursane skeleton. The signal at δ 1.31 was attributed to CH groups of the isobutyl chain overlapped with the ursane hydrogens. Also, at δ 2.41 it was observed a broad multiplet attributed to the piperazine hydrogens overlapped to H-18 and the methylene protons of the isobutyl chain. In the ^{13}C NMR spectrum of **196**, it was observed the signal δ 21.3 assigned to the four methyl groups, a signal at δ 27.0 assigned to $-\underline{CH}(CH_3)_2$, and a signal at δ 57.7 assigned to the $-N(\underline{CH_2}CH(CH_3)_2)_2$.

IV.2.3.2.3 Identification of **197**

The ferrocenyl derivative **197** was obtained as a red amorphous solid and the HRMS gave a peak at m/z 1077.5945 $[M+H]^+$ consistent with the molecular formula $C_{64}H_{93}N_4O_3$.

The IR spectrum showed characteristic absorption bands of the amide carbonyl (C-28) at 1646 cm^{-1} and an ester carbonyl of the acetyl group (C-3) at 1733 cm^{-1} . The absorption bands at 1105 and 1002 cm^{-1} were attributed to the C-H vibration of the ferrocenyl groups.

The ^1H NMR spectrum of **197** showed the presence of the characteristic signals of the ursane skeleton. Also, the presence of three methyl singlet protons at δ 2.11 was attributed to the acetyl protons. The characteristic signals of the piperazine group resonated at δ 2.34 (8H) as a multiplet. A singlet signal was observed at δ 3.53 and it was attributed to the methylene between nitrogen and ferrocenyl group. Evidence for the ferrocenyl groups was observed at δ 4.17 (a singlet integrating for 10H) and 4.26 (a multiplet integrating for 8H).

In the ^{13}C NMR spectrum of **197**, it was observed the presence of the characteristic signals assigned to the ursane skeleton. The spectrum revealed, also, the signal at δ 21.7 assigned to the methyl group of acetyl. The characteristic signals of the piperazine group were observed at δ 53.1, 26.1, 29.7, 39.0, 53.4, 54.0, 55.7 and 70.9. The ferrocenic carbons resonated at δ 69.1, 69.7 and 70.0. Also, at δ 179.2 it was observed a signal attributed to the quaternary carbon of the amide (C-28) and at δ 171.4 a signal was attributed to the quaternary carbon of the acetyl group (C-3).

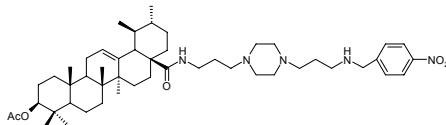
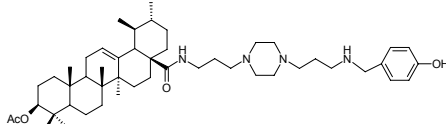
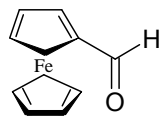
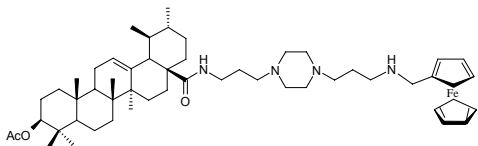
IV.2.3.3 Reductive amination reactions to obtain secondary amines

In order to investigate the importance of the secondary amine in the piperazinyl chain for the antiplasmodial activity of this series, the compounds **198** to **200** was synthesized by reductive amination. The reaction condition was

similar to those of compounds **188**, **189** and **197**, but using 1.5 equiv to both aldehyde and reducing agent.

The obtained compounds from this method are listed in Table 17.

Table 17. Compounds **198-200** obtained by reductive amination from **180**

Aldehyde (1.5 equiv)	product / yield
C₆H₅NO₂CH₂CHO	 198/20%
C₆H₅OHCH₂CHO	 199/62%
	 200/52%

In the ¹H NMR spectrum, the new aryl monoalkylated compounds showed a signal at about δ 3.75 (2H) attributed to the NHCH₂ hydrogens.

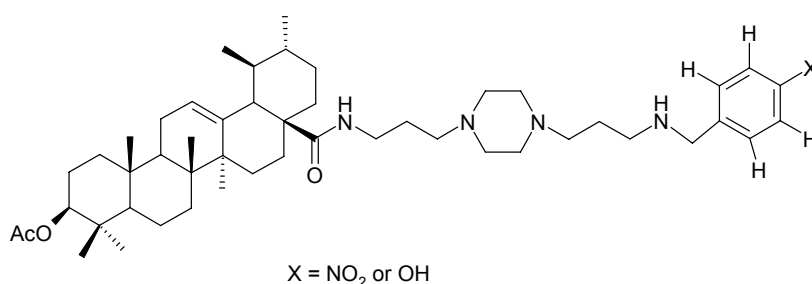
The aromatic proton and carbon signals of compound **198** and **199** were summarized in Table 18.

The ferrocenyl monoalkylated derivative **200** was obtained as a red amorphous solid and the IR spectrum showed characteristic absorption bands of the carbonyl of amide in C-28 at 1639 cm⁻¹ and a carbonyl of ester of the acetyl group in C-3 at 1731 cm⁻¹. The absorption bands at 1105 and 1003 cm⁻¹ was ascribed to the C-H vibration of the ferrocenyl groups.

The ¹H NMR spectrum of **200** showed the presence of the characteristic signals of the ursane skeleton. Also, the singlet signal at δ 2.10 was attributed to the three methyl protons from acetyl group. The characteristic signals of the piperazine group give resonance at δ 2.36 as a multiplet integrating for 13H. A singlet signal was observed at δ 3.78 ascribed to the methylene between nitrogen and ferrocenyl group. Evidence for the ferrocenyl groups was observed

at δ 4.21 (s, 5H) and 4.28 (m, 4H). In the ^{13}C NMR spectrum of **200** was observed the presence of the characteristic signals assigned to the ursane skeleton, to the methyl group of acetyl at δ 21.6 and to the presence of piperazine at δ 53.4, 26.2, 30.1, 39.0, 48.6, 53.6, 57.3 and 58.1. The ferrocenic carbons give resonance at δ 68.5, 69.2 and 69.6.

Table 18. ^1H and ^{13}C NMR spectral data of the aromatic groups of compounds **198** and **199**. (CDCl_3 , 500 MHz).



Compound	δ H-ortho/ δ C-ortho (ppm)	δ H-meta/ δ C-meta (ppm)	δ H-para/ δ C-para (ppm)	δ C-ipso (ppm)
198 X=NO ₂	7.58, d, $^3J=8.2$ Hz 124.1	8.22, d, $^3J=8.3$ Hz 129.6	-/ 148.0	143.0
199 X=OH	6.78, d, $^3J=8.1$ Hz 130.3	7.20, d, $^3J=8.2$ Hz 115.7	-/ 156.0	130.3

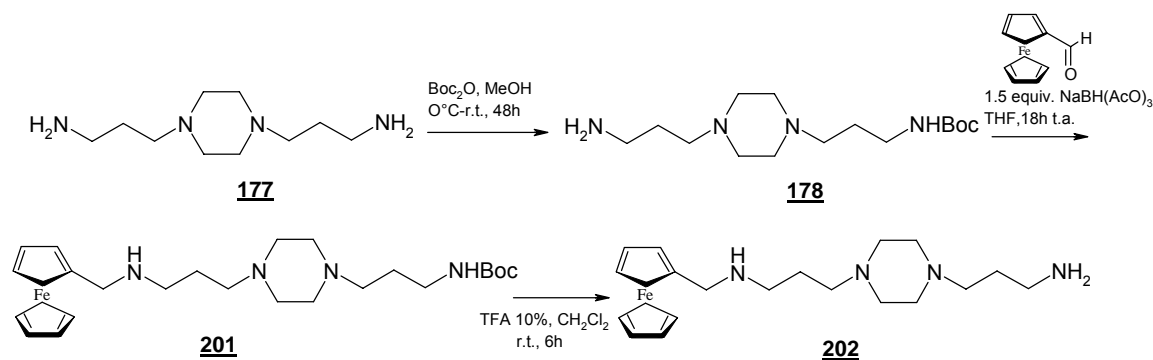
(-)= quaternary carbon

In conclusion to this series, using *N*-[1-(4-(3-aminopropyl)piperazinyl)-propyl]-3-*O*-acetylursolamide **180**, it was possible to synthesized twenty-one compounds, being one of them a dimer compound **181**. Relating to monomer compounds, beyond *N*-[1,4-bis(3-aminopropyl)piperazinyl]-3-*O*-acetylursolamide **180** and its deacetylated derivative **182**, it was obtained two ferrocenyl derivatives, ten aromatic and six aliphatic derivatives.

These derivatives were designed in order to study the electronic effects and steric hindrance in this series in relation to antiplasmodial activity. As

examples, it is cited the presence of electron-donating group (OH, OMe), electron-withdrawing group (NO₂), halogens (F, Cl, Br) and the *para* substitution on the phenyl ring. It was, also, possible to study the effect of the elongation of the aliphatic chain, the effect of terminal cyclic derivatives, and the effect of terminal branched chain together with a ferrocenyl derivative. It is important to emphasize that, from these compounds, two derivatives have terminal primary amines, three derivatives have terminal secondary amines and fifteen derivatives have terminal tertiary amines.

In order to evaluate the significance of the piperazine and the ferrocene groups for the antimalarial activity of these series, the compound **202** was synthesized. The ferrocenylpiperazine derivative **202** was obtained as orange oil. Its ¹H NMR spectrum showed the presence of the characteristic signals of the piperazine at δ 2.52 as a multiplet integrating for 13H. Also, a singlet signal was observed at δ 3.58 ascribed to the methylene between nitrogen and ferrocenyl group. Evidence for the ferrocenyl groups was observed at δ 4.17 (s, 5H) and 4.21 (m, 2H).



All ursolic acid derivatives obtained by organic synthesis and presented in this thesis were tested *in vitro* upon the *P. falciparum* chloroquine-resistant FcB1 strain in order to evaluate its antimalarial activity. Some compounds characterized by good *in vitro* antimalarial activity were then studied in an assay *in vitro* on inhibition of β -haematin.

IV. 3. Biological Results

In this part, the results obtained on the *in vitro* antimalarial activity will be presented together with cytotoxicity and β -hematin inhibition test.

IV.3.1 Antimalarial activity assay

Fractionation of plant extracts is a standard method for bioactive natural products identification. Especially in the area of antiparasitic agents, natural products have played a pivotal role in the past, and there is a continued interest in antimalarial activity of plant and plant isolates.

Hydroalcoholic extracts of *I. paraguariensis* and *I. dumosa* led to the isolation of the pentacyclic triterpenes **1** and **5**, respectively; the saponins **2**, **3** and the peracetylated compounds **151**, **152** and **153** were also obtained by *I. paraguariensis* extraction. Using ursolic and oleanolic acids, three series of their derivatives were synthesized.

These compounds were tested for their antimalarial activity *in vitro* upon the *P. falciparum* chloroquine-resistant strain FcB1 (IC_{50} (chloroquine) = 110 nM). The most active compounds were also tested against the *P. falciparum* chloroquine-sensitive strain Thai (IC_{50} (chloroquine) = 0.01 μ M). In parallel, these compounds were tested for cytotoxicity upon a human diploid embryonic lung cell line (MRC-5 cell).

These biological assays were performed by Pr. Grellier group from *Museum National d'Histoire Naturelle, Laboratoire de Biologie Parasitaire, Protistologie, Helminthologie, ERS CNRS 156*, at Paris, France.

IV.3.1.1 *In vitro* *P. falciparum* Culture and Drug Assays

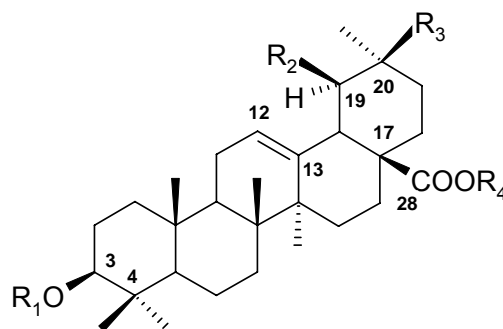
P. falciparum strains were maintained continuously in culture on human erythrocytes as described by Trager and Jensen (1976). *In vitro* antiplasmodial activity was determined using a modification of the semi-automated microdilution technique of Desjardins *et al.* (1979). *P. falciparum* CQ-sensitive (Thai) and CQ-resistant (FcB1) strains were used in sensitivity testing. Stock solutions of chloroquine diphosphate and test compounds were prepared in

sterile distilled water and DMSO, respectively. Drug solutions were serially diluted with culture medium and added to asynchronous parasite cultures (1% parasitemia and 1% final hematocrite) in 96-well plates for 24 h, at 37°C, prior to the addition of 0.5 µCi of [³H]hypoxanthine (1 to 5 Ci/mmol; Amersham, Les Ulis, France) *per* well, for 24 h. The growth inhibition for each drug concentration was determined by comparison of the radioactivity incorporated into the treated culture with that in the control culture (without drug) maintained on the same plate. The concentration causing 50% inhibition (IC₅₀) was obtained from the drug concentration-response curve and the results were expressed as the mean ± the standard deviations determined from several independent experiments. The DMSO concentration never exceeded 0.1% and did not inhibit the parasite growth.

The biological results obtained for the natural products, **1**, **2**, **3**, peracetylated **151**, **152**, **153** and **5** (Figure 10) are shown in Table 19.

Ursolic **1** and oleanolic **5** acids exhibited similar potency presenting IC₅₀ values of 52.93 µM and 44.36 µM, respectively. *In vitro* antiplasmodial activities of **1** and **5** were reported previously by Steele and co-workers (1999) against *P. falciparum* K1 strain with IC₅₀ inferiors to those found in the present work.

For the saponins and peracetylated ones isolated from *I. paraguariensis*, this is the first report relating to antimalarial activity. The compound **2** showed an IC₅₀ of 20.05 µM and compound **3** an IC₅₀ of 93.6 µM. Their peracetylated analogues resulted being more active (20.05 µM versus 9.23 µM for peracetylated **151**, 93.6 µM versus 2.40 µM for peracetylated **153**).



1 ursolic acid R₁= H, R₂ = CH₃, R₃ = R₄ = H

2 R₁= β-D-Glc-(1→3)-α-L-ara, R₂ = CH₃, R₃ = H, R₄ = β-D-Glc

3 R₁= β-D-Glc-(1→3)-α-L-ara, R₂ = CH₃, R₃ = H, R₄ = β-D-Glc-(1→6)-β-D-Glc

151 peracetylated R₁= β-D-Glc-(1→3)-α-L-ara, R₂ = CH₃, R₃ = H, R₄ = β-D-Glc

152 peracetylated R₁= β-D-Glc-(1→3)-α-L-ara, R₂ = CH₃, R₃ = H, R₄ = β-D-Glc

153 peracetylated R₁= β-D-Glc-(1→3)-α-L-rha-(1→2)-α-L-ara, R₂ = CH₃, R₃ = H, R₄ = β-D- (1→6)-β-D-Glc

5 oleanolic acid R₁ = R₂ = H, R₃ = CH₃, R₄ = H

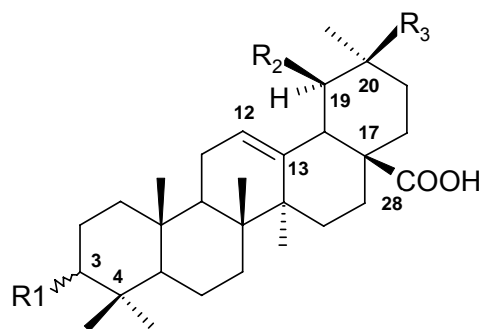
Figure 10. Natural products obtained from *Ilex*.

Table 19. *In vitro* Sensitivity of *P. falciparum* FcB1 to ursolic **1** and oleanolic **5** acids, saponins **2** and **3**, and peracetylated saponins **151-153**.

Compound	IC ₅₀ (μM)
chloroquine	0.13 ± 0.04
<u>1</u>	52.93 ± 5.71
<u>5</u>	44.36 ± 15.15
<u>2</u>	20.05 ± 3.50
<u>3</u>	93.6
<u>151</u>	9.23 ± 3.00
<u>152</u>	2.40 ± 0.60
<u>153</u>	4.86 ± 0.89

IV.3.1.2 Compounds with modifications in the cycle A

The analogues of **1** and **5** obtained by modifications in the cycle A (Figure 11) were tested to their antiplasmodial activity *in vitro* against *P. falciparum* FcB1 strain, as previously described. The results are shown in Table 20.



<u>147</u>	R ₁ = = O	R ₂ = CH ₃	R ₃ = H
<u>154</u>	R ₁ = β-acetyl	R ₂ = CH ₃	R ₃ = H
<u>157</u>	R ₁ = α-OH	R ₂ = H	R ₃ = CH ₃
<u>158</u>	R ₁ = =NOH	R ₂ = CH ₃	R ₃ = H

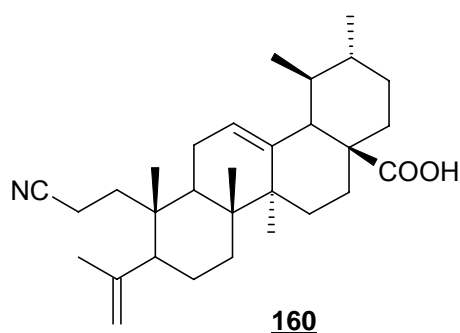
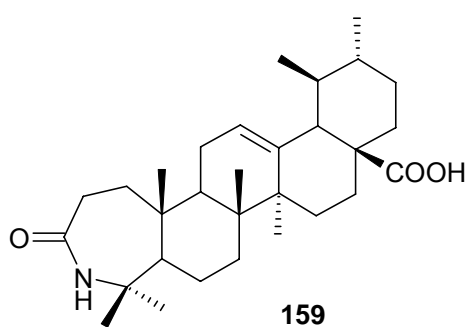


Figure 11. Derivatives with pharmacomodulations at cycle A.

Table 20. *In vitro* Sensitivity of *P. falciparum* FcB1 to Compounds **147**, **154**, **157-160**.

Compound	IC ₅₀ (μM)
<u>147</u>	41.47 ± 2.65
<u>154</u>	24.93 ± 7.44
<u>157</u>	61.49 ± 10.54
<u>158</u>	34.54 ± 3.60
<u>159</u>	54.54 ± 9.59
<u>160</u>	27.69 ± 5.98

The 3-oxo-ursolic acid **147**, the 3-epioleanolic acid **157** obtained by Mitsunobu reaction and the lactam **159** (3α-azo-3-oxo-ursolic acid) were active in the same concentration than ursolic acid. While the nitrile **160**, the oxime **158** and **154** presented the same activity with an IC₅₀ 2.0 times lower than ursolic acid (Table 20).

IV.3.1.3 Compounds with ferrocene moiety

We reported the incorporation of ferrocenyl moieties to ursolic acid focusing attention on amide and ester at C-28 and C-3 positions, respectively, hoping to enhance the antimalarial effect. So, these compounds (Figure 12) were assayed against the *P. falciparum* strain FcB1 and the results are summarized in Table 21.

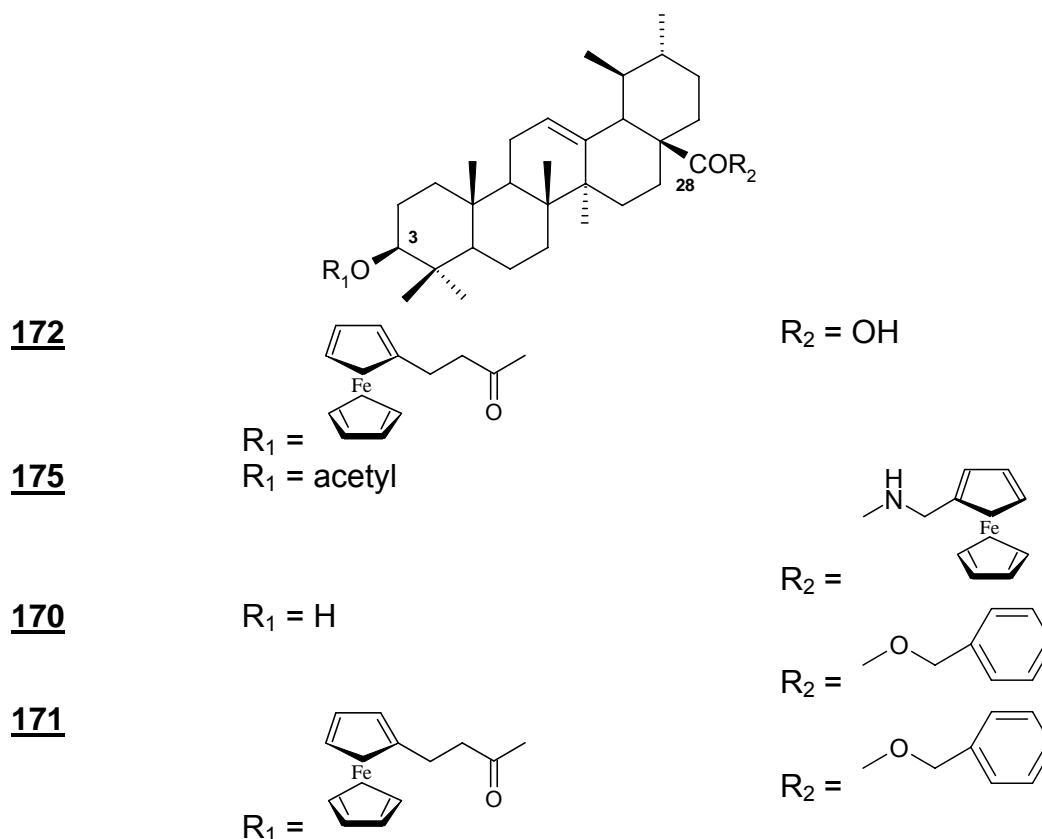


Figure 12. Ferrocenyl derivatives of ursolic acid.

Table 21. *In vitro* Sensitivity of *P. falciparum* FcB1 to Compounds **170-172** and **175**.

Compound	IC ₅₀ (μM)
172	81.80 ± 17.65
175	7.91 ± 2.01
170	60.71 ± 15.36
171	34.33 ± 18.58

Nevertheless these organometallic compounds did not present improvement in the antimalarial activity (Table 21). Compared to the parent

compound, ursolic acid ($IC_{50} = 52.93 \mu M$), compound **175** stood out as the most active *in vitro* against *P. falciparum*, with a lower activity, but this activity was very inferior to chloroquine ($IC_{50} = 110 \text{ nM}$). Notably, this compound has an acetyl group at C-3 and it was the only compound possessing the amide group at C-28.

IV.3.1.4 Compounds with piperazine moiety

The antimalarial profiles of the new piperazinyl derivatives obtained from ursolic acid (**180-200**), its dimer **181**, its deacetylated analogue **182**, and its structurally simplified analogue **183-200** are summarized in Table 22.

As shown in Table 22, piperazinyl derivatives from ursolic acid were all more active than their parent compound (ursolic acid $IC_{50} (\text{FcB1 strain}) = 52.93 \mu M$). The analysis of the biological results allowed us to evidence that the most active antimalarial compounds were the piperazinyl derivatives possessing a primary amine **180** and its corresponding monosubstituted analogue **199** and, their respective dimer **189**. These characteristics allowed us to determine that the introduction of a polar group in the terminal moiety of the piperazinyl derivatives from ursolic acid produced strong beneficial effects over its antimalarial activity.

The antimalarial activity of the non-substituted compound **183**, the nitrated compound **188** and the methoxylated compound **190** were also assayed in the same biological protocol presenting only activity at μM concentration. Their activities varied from $3.57 \mu M$ (**188**) to $21.12 \mu M$ (**183**).

Next, It was investigated the eventual importance of the distance between the *N* and the aromatic ring by evaluating the antimalarial activity of the more flexible conformational analogue **184** which presents a C-3 spacer unit. The introduction of the ethylene spacer did not produce a significantly increase in the antimalarial activity ($IC_{50} = 8.06 \mu M$).

Additionally, in order to investigate the relevance of the halogen substitution in the phenyl ring to the antimalarial activity, the compounds **185**, **186** and **187** were assayed. The compound **187** presented an IC_{50} of $20.27 \mu M$,

compound **186** presented an IC_{50} of 46.04 μ M and compound **185** presented an IC_{50} of 98.98 μ M.

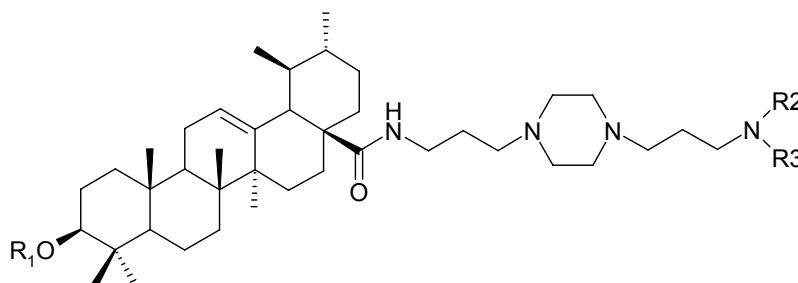


Table 22. *In vitro* Sensitivity of *P. falciparum* FcB1 Strain to Compounds **180-200**.

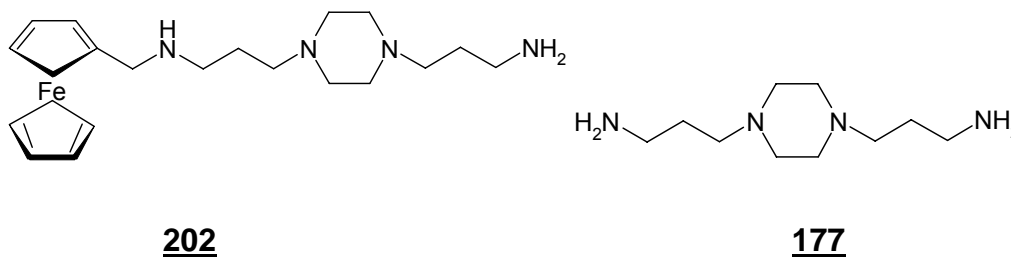
compound	R ₁	R ₂	R ₃	IC ₅₀ FcB1 (μ M)
180	R ₁ = acetyl	R ₂ = R ₃ = H		0.167 \pm 0.07
181	R ₁ = acetyl	R ₂ = H	R ₃ = ursolic acid residue	> 86
183	R ₁ = acetyl	R ₂ = R ₃ =	benzyl	21.12 \pm 2.90
184	R ₁ = acetyl	R ₂ = R ₃ =	benzylethyl	8.06 \pm 0.65
185	R ₁ = acetyl	R ₂ = R ₃ =	4-bromobenzyl	> 98
186	R ₁ = acetyl	R ₂ = R ₃ =	4-chlorobenzyl	46.04 \pm 10.76
187	R ₁ = acetyl	R ₂ = R ₃ =	4-fluorobenzyl	20.27 \pm 5.46
188	R ₁ = acetyl	R ₂ = R ₃ =	4-nitrobenzyl	3.57 \pm 1.47
189	R ₁ = acetyl	R ₂ = R ₃ =	4-hydroxybenzyl	0.161 \pm 0.02
190	R ₁ = acetyl	R ₂ = R ₃ =	4-methoxybenzyl	6.50 \pm 1.74
191	R ₁ = acetyl	R ₂ = R ₃ =	methylcyclohexyl	114.44
192	R ₁ = acetyl	R ₂ = R ₃ =	methylcyclopropyl	0.492 \pm 0.21
193	R ₁ = acetyl	R ₂ = R ₃ =	heptyl	41.81 \pm 6.72
194	R ₁ = acetyl	R ₂ = R ₃ =	butyl	1.00 \pm 0.12
195	R ₁ = acetyl	R ₂ = R ₃ =	propyl	0.795 \pm 0.13
196	R ₁ = acetyl	R ₂ = R ₃ =	<i>tert</i> -butyl	18.77 \pm 1.14
197	R ₁ = acetyl	R ₂ = R ₃ =	methylferrocenyl	1.21 \pm 0.46
182	R ₁ = H	R ₂ = R ₃ =	H	0.322 \pm 0.18
198	R ₁ = acetyl	R ₂ = H	R ₃ =4-nitrobenzyl	1.04 \pm 0.33
199	R ₁ = acetyl	R ₂ = H	R ₃ = 4-hydroxybenzyl	0.078 \pm 0.04
200	R ₁ = acetyl	R ₂ = H	R ₃ = methylferrocenyl	0.768 \pm 0.09
chloroquine				0.13 \pm 0.04

On the aliphatic series, the compound was **195** showed an IC_{50} of 795 nM. Elongation of the chain (compounds **194** and **193**) decreases the activity of the compounds. The branched derivative **196** had an IC_{50} of 18.77 μ M. Introducing a constraint via cyclization of the butyl group (compound **194** IC_{50} =

1.0 μM) into a methylcyclopropyl (compound **192** IC_{50} = 493 nM) increases the activity, but it was not verify to compounds **193** (heptyl group) and **191** (methylcyclohexyl group).

Continuing our studies with the ferrocene derivatives two new compounds were synthesized and assayed. Relating compounds **197** and **200** it was also possible to observe the importance of the secondary amine to the antimalarial activity *in vitro*. The activity is not dependent to the ferrocenyl group but to the amine secondary donor of the hydrogen.

Two other compounds were also tested in order to evaluate the importance of the triterpenic skeleton at the activity of the piperazinyll series. The commercially available **177** and the synthesized **202** presented, respectively, the following activity: IC_{50} >100 μM and IC_{50} = 0.2 μM . Thus, it is reasonable to think that the attachment of a piperazine to ursolic acid brings a significant antimalarial activity.



IV.3.1.5 Assays using *P. falciparum* chloroquine-sensitive strain Thai and MRC-5 cells

The most active compounds were assayed against the *P. falciparum* chloroquine-sensitive strain Thai (IC_{50} (chloroquine) = 0.01 μM) and upon a human diploid embryonic lung cell line (MRC-5 cell) with the objective to evaluate their cytotoxicity. The resistance index FcB1/Thai and the selectivity index FcB1/MRC-5 were also calculated. The results for the compounds **180**, **182**, **188**, **189**, **192**, **195**, **197** to **200** are shown in Table 23.

As seen in Table 23, the majority of compounds presented higher IC₅₀ values to inhibition of growth of chloroquine sensitive strain Thai than for chloroquine resistant strain FcB1. A comparison of the IC₅₀ values relating the inhibition of growth of the resistance and sensitive strains of *P. falciparum* suggested low levels of cross-resistance to chloroquine. The resistance index values calculated from the comparison of the IC₅₀ values of the resistant and sensitive strains of *P. falciparum* were in the range of 0.37 to 1.17, lower than those for chloroquine (RI = 11).

All tested compounds showed cytotoxicity upon MRC-5 cells in the μM range, and IC₅₀ values varied from 1.57 to 18.28 μM . The selectivity index was defined as the ratio of the IC₅₀ value on the MRC-5 cells to the IC₅₀ value on the chloroquine resistant strain FcB1. The compound **199** presented high selectivity with a SI = 27.

Table 23. *In vitro* Sensitivity of *P. falciparum* Thai Strain and MRC-5.

Compound	IC ₅₀ (μM)		Resistance Index FcB1	Selectivity Index
	Thai	MRC-5		
180	0.455 \pm 0.04	1.61 \pm 0.14	0.37	9.6
188	3.05 \pm 0.27	18.28 \pm 0.10	1.17	5.1
189	0.347 \pm 0.03	1.57 \pm 0.67	0.46	9.7
192	0.949 \pm 0.01	2.53 \pm 0.51	0.51	5.1
195	1.00 \pm 0.55	1.96 \pm 0.78	0.79	2.5
197	1.48 \pm 0	4.08 \pm 0.09	0.81	3.5
182	0.50 \pm 0.09	6.57 \pm 0.15	0.64	20.4
198	0.98 \pm 0.21	5.39 \pm 0.10	1.06	5.2
199	0.18 \pm 0.03	2.10 \pm 0.20	0.43	27
200	1.13 \pm 0.12	2.00 \pm 0.20	0.68	2.6
Chloroquine	0.01 \pm 0.005	NA	11	NA

NA = Non available

IV.3.2 Inhibition of β -hematin formation test

Aiming at understanding the mechanism of action of the active antimalarial compounds synthesized in this thesis, the *in vitro* inhibition of β -haematin formation was only performed on those compounds having enough

quantity. These compounds were compared to chloroquine ability to inhibit β -haematin formation. These tests were performed under the responsibility of Dr. Demailly Catherine from *Laboratoire de Chimie Organique et Thérapeutique*, DMAG-EA3901, *Université de Picardie Jules Verne*, Amiens. The methodology was the same as protocol 2 published by Baelmans and co-workers (2000). The results were summarized in Table 24.

Ursolic acid **1** at the range of 1 to 20 mM concentration, showed low inhibition of β -haematin formation, while compounds oleanolic acid **5** and acetyl-ursolic acid **154** did not exhibit any inhibitory activity. These observations are in agreement with the very small antimalarial activity obtained for them.

Table 24. Inhibition of β -hematin formation

compound	Concentration (mM)	Inhibition (%)	IC ₅₀ (mM)	CQ Index**
chloroquine phosphate	5	36.9 ± 8.6	5.9 ± 1.15	1
	10	97.4 ± 0.2		
deferoxamine mesylate	1 to 20	0		
189	4.2	39.6 ± 25.5	5.25 ± 2.82	0.89
	8.4	82.2 ± 14.2		
188	1.14	5.8 ± 17.06	>>20	>>3.4
	5.7	3.6 ± 4.86		
	11.4	18.6 ± 5.84		
180	5	12.9 ± 3.1	> 20	> 3.4
	10	24.6 ± 3.1		
	20	46.7 ± 18.2		
5	1 to 20	0		
1	5	17.9 ± 8.6	>> 20	>> 3.4
	10 to 20	0		
154	1 to 20	0		
202	1 to 20	0		

*mean ± standard deviation from three independent experiments.

** IC₅₀ compound/IC₅₀ chloroquine

On the other hand, the compound **189** and **180** inhibit respectively 82% β -haematin formation at 8.4 mM and 46% β -haematin formation at 20 mM. At the similar concentration, 97% of inhibition was obtained for chloroquine. These observations are in accordance to the *in vitro* tests against *P. falciparum*, and demonstrated that the mechanism of action of their antimalarial activity could be due the inhibition of β -haematin formation.

IV.4 The antimalarial activity of ursolic acid derivatives and their structure-activity relationships (SAR)

In order to support the rational design of new ursolic acid derivatives showing improved antimalarial activity it is necessary to establish the mechanism of action, at the molecular level, for this class of compounds. This is not a simple task, since even for time honored drugs as quinine and chloroquine their mechanism of action is still a matter of debate (Moreau *et al.*, 1985; Constantinidis and Satterlee, 1988; Egan *et al.*, 2000; Leed *et al.*, 2002; Portela *et al.*, 2003; Egan, 2003; 2006; Kumar *et al.*, 2007). Considering that the most broadly accepted mechanism for these compounds is the inhibition of haemozoin formation (Egan, 2003; 2006), we considered that the ursolic acid and its derivatives share such mechanism.

There are many assumptions about the molecular mechanisms involved in the malaria disease which were previously shown in the Literature Review of this thesis (Chapter III).

Oxidation of membrane components induced by free haeme (Fe(III)) promotes cell lysis and ultimately death of the parasite. To overcome free haeme (Fe(III)) toxicity, malaria parasite is equipped with unique haeme detoxification system. Among these, haemozoin formation is considered to be the main system and this inhibition leads to parasite death (Aikawa *et al.*, 1966; Krugliak *et al.*, 2002; Egan *et al.*, 2002). Thus, the detoxification through haemozoin formation is supposed to be the target of several antimalarial known drugs and others that can be designed.

IV.4.1 Design

Our previously studies (presented in the introduction of this manuscript) showed that ursolic acid has antimalarial activity *in vitro* tests. It is possible that the triterpenic skeleton mimics the quinoline aromatic rings. In the approach developed herein, the π interaction would be substituted by hydrophobic interactions, due to the aliphatic chain and low dielectric constants. In view of

this, we performed the topological exploration¹ of the compound (Wermuth, 2004) that led us to make the following molecule modifications (see Scheme 16).

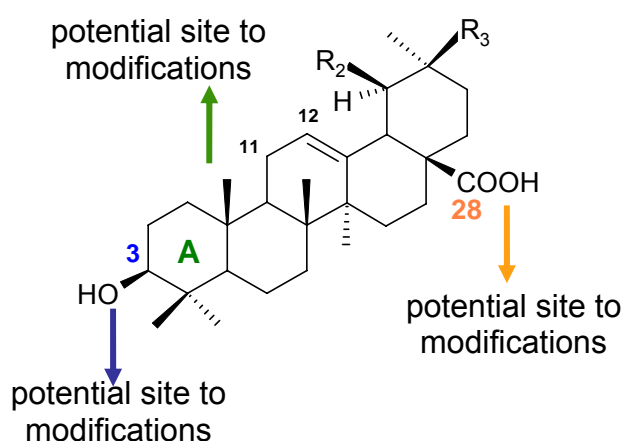
IV.4.1.1 Modifications at cycle A

We expected that enhancing lipophilicity should give us derivatives more actives. In order to verify it, we did: *i.* the 3-OH acetylation, and *ii.* its oxidation to ketone. Aiming to check the influence of the 3-OH configuration to the antimalarial activity, *iii.* it was proceeded to the inversion of the β -configuration. We also performed *iv.* the expansion of the cycle A, in order to evaluate the size and surface area importance to this activity.

IV.4.1.2 Modifications at C-28

Considering the high electron density at C-28 position of ursolic acid, and the presence of one carboxylate group at haeme structure, we may postulate that replacing the C-28 carboxyle for positively charged moiety (or low electron density moiety) leads to favorable electrostatic interactions, and, thereby, to the highest resulting compounds activity. Thus, a series of *N*-[1,4-bis(3-aminopropyl)piperazinyl]-3-*O*-acetylsolamide derivatives were synthesized.

Scheme 16.

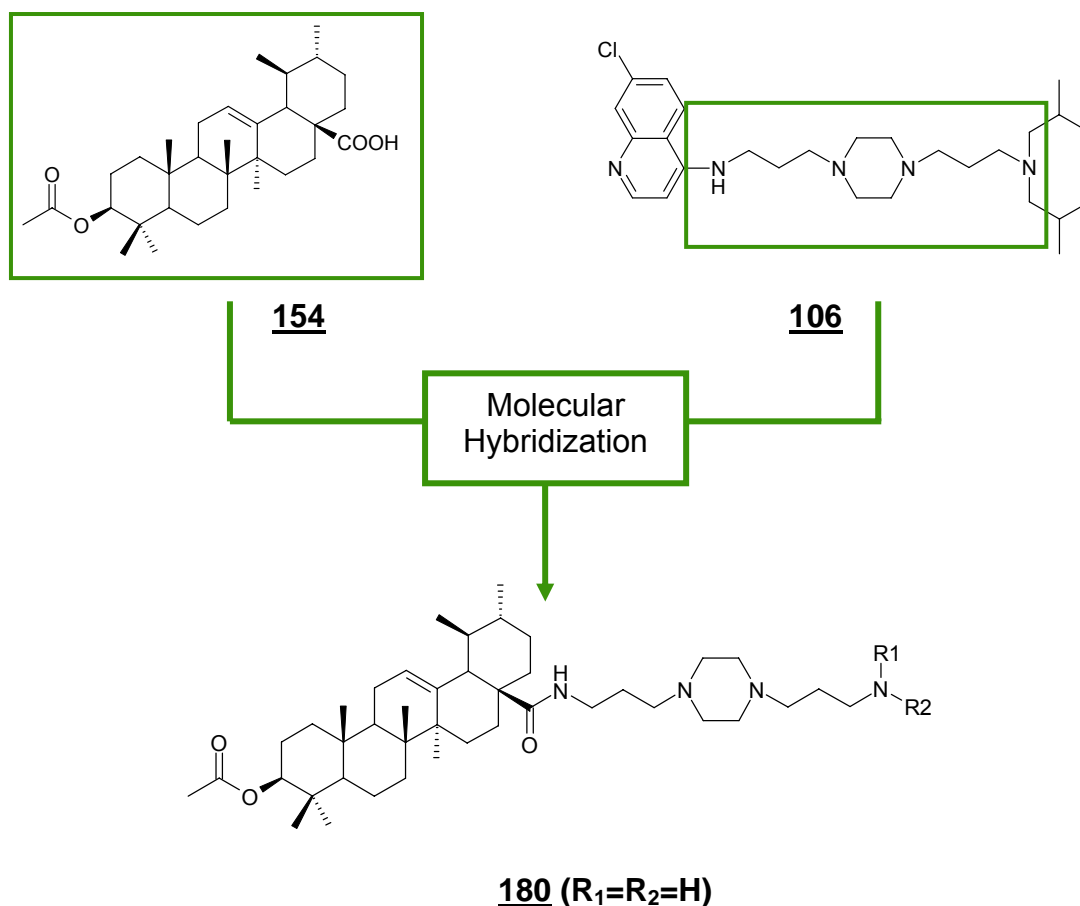


¹ *Topological exploration of the lead compound* is one of the most fruitful strategies revealing the features associated with activity. In this approach, the possible modifications of the molecule are considered from the four cardinal points: the south, the north, the west or the east, or from the centre of the molecule (Wermuth, 2004).

In literature, the antimalarial activity of quinoline-piperazinyl series was characterized (Girauld *et al*, 2001; Rychebusch *et al*, 2002; 2003) and the pharmacophoric characteristics of this group were indicated. For instance, the most active compound of this family, that is, **106**, showed an IC_{50} of 0.9 nM (FcB1 strain), what is superior to the inhibitory concentration of chloroquine (IC_{50} = 126 nM) (Rychebusch *et al*, 2003).

Compound **180** was structurally designed through molecular hybridization between the *N*-1,4-bis(3-aminopropyl)piperazine group of *N*-(7-chloro-4-quinoly)-1,4-bis(3-aminopropyl)piperazine series and the acetylursolic acid, in order to evaluate any eventual influence of this conjunctive approach in the antimalarial activity (Schema 17).

Schema 17.



The substituents of the terminal chain, attached at the amine function of *N*-[1-(4-(3-aminopropyl)piperazinyl)-propyl]-3-*O*-acetylursolamide derivatives (**183-200**) were rationally elected in order to acquire information about the influence of the polarity and accessibility parameters of these groups on the electrostatic interactions with haeme structure (Wermuth, 2004, Kubinyi, 1995).

A similar approach was used for the design of ferrocenyl derivatives: the pharmacophoric ferrocenyl framework was attached to ursolic acid in order to study its influence at the antimalarial activity.

IV.4.2 Structure-Activity Relationships

In relation to the modifications at the cycle A, acetylation at 3-OH gives the best results. The acetylated compounds were more active compounds than their parent ones. As example, it was obtained an $IC_{50} = 24.93 \mu\text{M}$ to acetyl-ursolic acid versus $IC_{50} = 52.93 \mu\text{M}$ to the ursolic acid. It was possible to identify the acetyl moiety as a pharmacophoric group in the triterpene series, due to an expected increase of lipophilicity in that site. The increases in the surface area by the cycle A expansion, the oxidation at C-3 and the inversion of C-3-OH configuration did not improve the antimalarial activity.

About the modifications at C-28, the new piperazinyl analogues of ursolic acid **1** obtained by molecular hybridization showed good antimalarial activity (see Tables 22 and 23, Chapter IV).

The expressive increasing of the *in vitro* activity in the piperazinyl derivative **180** ($IC_{50} = 0.167 \mu\text{M}$) indicated to us the pharmacophoric character of the piperazine framework to the antimalarial profile of the new ursolic acid derivatives. This profile is in agreement with that observed for the *N*-(7-chloro-4-quinolyl)-1,4-bis(3-aminopropyl)piperazine derivatives and the bispyrrolo[1,2-*a*]quinoxalines described previously by Ryckebusch and co-workers (2003; 2005) and Guillon and co-workers (2004), respectively. It is possible to suppose an interaction of the protonated piperazine *N* atoms with the carboxylate moiety of haematin. Guillon and co-workers (2004) demonstrated these interactions

through salt bridge using molecular modeling. In this same way, our studies show that the commercially available 1,4-bis(3-aminopropyl)piperazine assayed in the same test did not presented antimalarial activity ($IC_{50} > 100 \mu M$) showing that the presence of a quinoline or triterpenic nucleus in this series is important to the activity.

In addition, there are evidences that compounds possessing tertiary amines were less active than their monosubstituted counterparts, which suggest that the basicity of the amine may play a role in the activity of this series. Probably the stronger basicity of the molecule increases the antimalarial activity due to a better uptake in the vacuole owing to the pH gradient between the cytosol and the acidic vacuole. In both cases, it is to believe that the secondary amine of the compound **198** ($IC_{50} = 1.04 \mu M$) and the compound **199** ($IC_{50} = 0.078 \mu M$) can interact with the carboxylate moiety in the haematin. The importance of the primary amine for these interactions was characterized for the compound **180**. Concluding, the antimalarial activity decreases in the order – $NHR > -NR_2 \approx -NH_2$.

The results from our study did not give any indication that the presence of ferrocene in the triterpene series can improve its antimalarial activity, in view that compounds **172** ($IC_{50} = 81.80 \mu M$) and **175** ($IC_{50} = 7.91 \mu M$) presented activity at the μM concentration. However, for the compounds **197** disubstituted ($IC_{50} = 1.21 \mu M$) and **200** monosubstituted ($IC_{50} = 0.769 \mu M$) in the piperazinyl series, it was possible to observe also the importance of the secondary amine for antimalarial activity *in vitro*. It seems that the activity is not dependent of ferrocenyl group but of the amine secondary donor of the hydrogen.

IV.4.3 Quantitative Structure-Activity Relationships to the piperazinyl analogues of ursolic acid– Preliminary studies

A preliminary Quantitative Structure-Activity Relationship (QSAR) study, using regression and correlation coefficients between the biological and chemical data, was developed in order to rationalize a structure-activity

relationship to the *N*-substituted series. This preliminary QSAR model was possible considering that this series presented a good number of compounds having a great diversity of substituents that resulted in a great range of antimalarial activity. Initially, thirteen *N* substituted derivatives were used (training set), namely 180, 183, 184, 186, 187, 189 to 191, 193 to 195, 198, 199. Compounds 196, 185, 188 and 192 were used as the test set for the validation procedures shown below.

The IC₅₀ obtained from FcB1 strain of *P. falciparum* were used as the biological activity (Table 22, Chapter IV). log₁₀1/IC₅₀ was used as the dependent variable in the linearization procedure (Table 25).

The descriptor named lipophilic constant (π) was used as an independent variable. A large set of parameters or also called chemical descriptors of molecular structure and fragments has been reported in the literature. These parameters are needed to describe the intermolecular forces of the molecule-target interaction (Wermuth, 2004, Kubinyi, 1995). Lipophilicity parameter π were defined by Hansch, in the same manner that Hammett σ constants are defined and these values were tabled (Kubinyi, 1995, 1997a, 1997b).

The lipophilic constants π of the substituent groups were calculated from the previously tabulated logP using the Equation 1 (Hansch *et al.*, 1995).

Equation 1.

$$\pi = \log P_{X-H} - \log P_{H-H} \text{ (compound 180)}$$

Regression Analysis of the generated model (Equation 2) used π descriptor as an independent variable. When *N* is disubstituted, the sum of the individual π values was used for lipophilic descriptor ($\Sigma\pi$). This descriptor was able to explain 64% of variance to the antimalarial activity.

Equation 2.

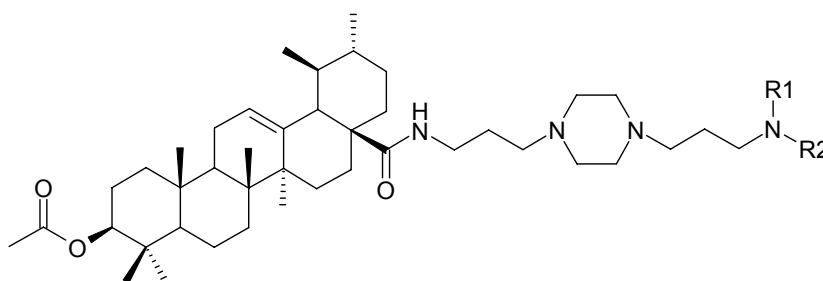
$$\log 1/IC_{50} = + 7.03 + (- 0.376) \pi$$

$$(n = 13; R^2 = 0,638; s = 0.664; F = 19.44)$$

In this equation, n represents the number of data points, R^2 is the correlation coefficient, s is the standard deviation of the regression equation, F value is related to the F -statistic analysis (Fischer test).

The calculated $\log 1/IC_{50}$ values for the compounds are listed in Table 25. The linear plots of experimental and calculated $\log 1/IC_{50}$ (according to the QSAR model) are presented in Table 25 and Figure 13.

Table 25. Experimental values of IC_{50} calculated by the Equation 2, according to model, and the π values calculated for R.



Compound	R ₁	R ₂	IC ₅₀ (μM)	log1/IC ₅₀		
				experimental	π ^a calculated	
180	H	H	0.167	6.78	0	7.03
183	CH ₂ C ₆ H ₅	CH ₂ C ₆ H ₅	21.12	4.67	2.28	5.31
184	(CH ₂) ₃ C ₆ H ₅	(CH ₂) ₃ C ₆ H ₅	8.063	5.09	3.27	4.57
186	CH ₂ C ₆ H ₄ Cl	CH ₂ C ₆ H ₄ Cl	46.04	4.34	2.88	4.86
187	CH ₂ C ₆ H ₄ F	CH ₂ C ₆ H ₄ F	20.27	4.69	2.28	5.31
189	CH ₂ C ₆ H ₄ OH	CH ₂ C ₆ H ₄ OH	0.161	6.79	1.55	5.86
190	CH ₂ C ₆ H ₅ OCH ₃	CH ₂ C ₆ H ₅ OCH ₃	6.509	5.19	1.47	5.92
191	CH ₂ C ₆ H ₁₁	CH ₂ C ₆ H ₁₁	114.44	3.94	3.16	4.65
193	C ₇ H ₁₄	C ₇ H ₁₄	41.81	4.38	4.025	4.00
194	C ₄ H ₉	C ₄ H ₉	1.008	5.97	2.44	5.19
195	C ₃ H ₇	C ₃ H ₇	0.795	6.10	1.91	5.59
198	CH ₂ C ₆ H ₄ OH	H	1.04	6.07	1.92	6.31
199	CH ₂ C ₆ H ₄ NO ₂	H	0.078	7.11	1.55	6.46

^a For N -disubstituted, the sum of the individual parameters was used for lipophilic descriptor ($\Sigma\pi$).

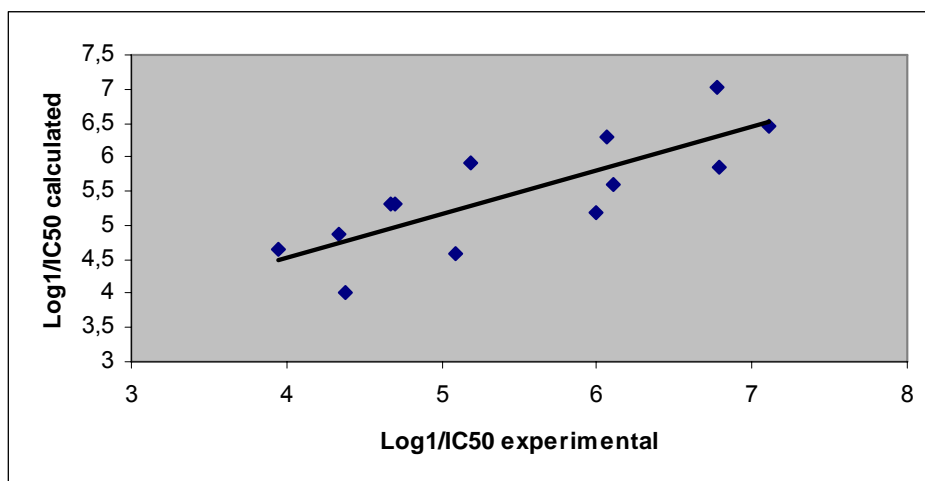


Figure 13. Graphic of experimental activity values (\log_1/IC_{50}) versus calculated activity values for the model.

Through the analysis of the errors (according Table 26), it was possible to see a tendency of distribution of the points excepting three outliers: compounds **189**, **190** and **194**.

Table 26. Experimental values of \log_1/IC_{50} calculated by Equation 1, according to the model, and the respective errors.

Compound	\log_1/IC_{50} experimental	\log_1/IC_{50} calculated	Errors (calculated – experimental)
180	6.78	7.03	0.253
183	4.67	5.31	0.640
184	5.09	4.57	-0.522
186	4.34	4.86	0.527
187	4.69	5.31	0.622
189	6.79	5.86	-0.929
190	5.19	5.92	0.738
191	3.94	4.65	0.712
193	4.38	4.00	-0.375
194	5.97	5.19	-0.801
195	6.10	5.59	-0.506
198	6.07	6.31	0.237
199	7.11	6.46	-0.661

The outliers were excluded of the model and the equation was recalculated. The new equation obtained by linear regression is shown below (Equation 3):

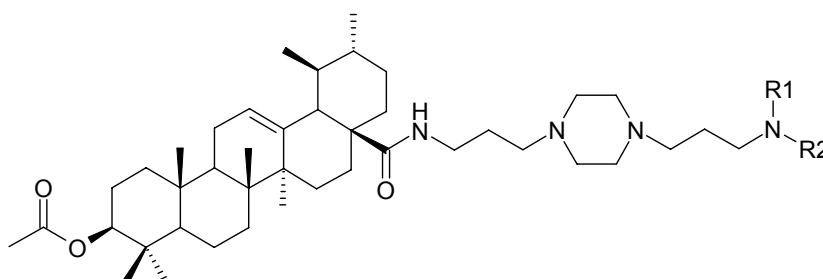
Equation 3

$$\log 1/IC_{50} = + 6.96 + (- 0.382) \pi$$

$$(n = 10; R^2 = 0,755; s = 0.583; F = 24.64)$$

The calculated $\log 1/IC_{50}$ values for the compounds according to Equation 3 are listed in Table 27. The linear plots of experimental and calculated $\log 1/IC_{50}$ (according to the QSAR model) are presented in Table 27 and Figure 14.

Table 27. Experimental values of IC_{50} calculated by the Equation 3, according to model, and the π values calculated for R.



Compound	R ₁	R ₂	$\log 1/IC_{50}$ experimental	π^a	$\log 1/IC_{50}$ calculated	Errors (calculated- experimental)
180	H	H	6.78	0	6.96	0.183
183	CH ₂ C ₆ H ₅	CH ₂ C ₆ H ₅	4.67	2.28	5.22	0.528
184	(CH ₂) ₃ C ₆ H ₅	(CH ₂) ₃ C ₆ H ₅	5.09	3.27	4.46	-0.632
186	CH ₂ C ₆ H ₄ Cl	CH ₂ C ₆ H ₄ Cl	4.34	2.88	4.76	0.423
187	CH ₂ C ₆ H ₄ F	CH ₂ C ₆ H ₄ F	4.69	2.28	5.22	0.525
191	CH ₂ C ₆ H ₁₁	CH ₂ C ₆ H ₁₁	3.94	3.16	4.55	0.604
193	C ₇ H ₁₄	C ₇ H ₁₄	4.38	4.025	3.88	-0.494
195	C ₃ H ₇	C ₃ H ₇	6.10	1.91	5.50	-0.599
198	CH ₂ C ₆ H ₄ OH	H	6.07	1.92	6.23	0.156
199	CH ₂ C ₆ H ₄ NO ₂	H	7.11	1.55	6.37	-0.740

^a For *N*-disubstituted, the sum of the individual parameters was used for lipophilic descriptor ($\Sigma\pi$).

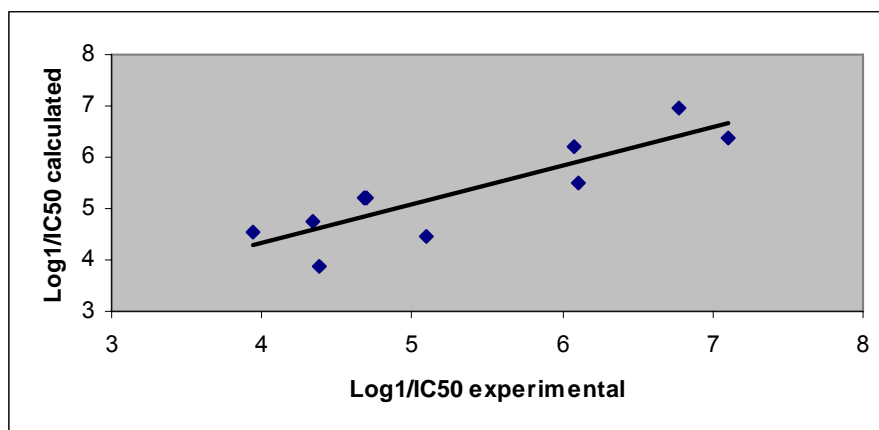


Figure 14. Graphic of experimental activity values ($\log 1/IC_{50}$) versus calculated activity values for the model.

For this new series of the compounds, the descriptor π was able to explain 75% of variance to the antimalarial activity.

Analyzing Table 27 and Figure 14, it can be noticed the clear structure-activity dependence. The calculated ranges of the biological activity, according to the developed QSAR model, are in good agreement with the experimental data. The calculated range for the model in Table 27 is 3.88 to 6.96 compared with the experimental range of 3.94 to 7.11.

It is important to notice that it was used one descriptor to rationalize the antimalarial activity for the studied molecule set. Thus, more lipophilic substituents results in less active compounds (π possesses larger values for the less active compounds compared with the active ones).

The lipophilicity has a direct relationship to solubility in aqueous phases, to membrane permeation, and to entropic contribution to binding. Lipophilicity is defined by the partitioning of a compound between an aqueous and a non aqueous phase. Moreover, the parameter lipophilicity π depends on solute bulk, polar and hydrogen bonding effects (Kubinyi, 1995, 1997a, 1997b). In our model it is possible to suppose that most polar substituents at the terminal *N* could perform more interactions with the haeme, probably by electrostatic interaction with the carboxylate groups.

IV.4.3.1 Validation of the test set

As already stated, compounds **185**, **188**, **192**, and **196** were used as the test set for the validation procedures shown below. Table 28 and Figure 15 showed a significant validation of the test set. There is a significant linear adjustment and the model obtained from equation 3 was able to predict and differentiate the activity of the compounds ($R^2 = 0.91$).

Table 28. Experimental values of IC_{50} predicted by Equation 3, for the test set, and the respective errors.

Compound	\log_1/IC_{50} experimental	\log_1/IC_{50} calculated	Errors (predicted-experimental)
185	4.01	4.67	0.659
188	5.46	5.49	0.046
192	6.31	5.63	-0.673
196	4.73	5.20	0.469

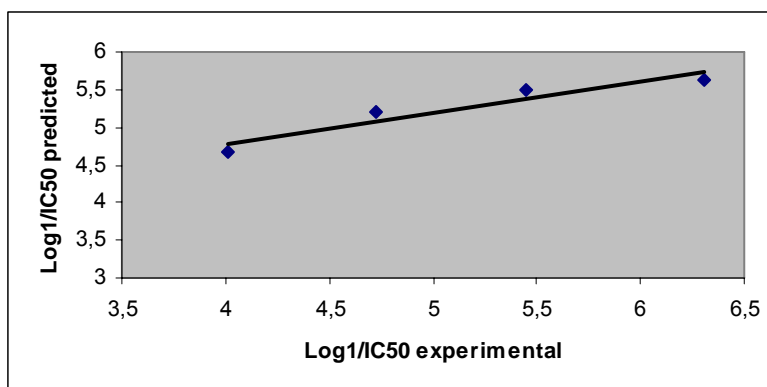


Figure 15. Graphic of experimental activity values versus predicted activity values for the test set.

Finally, a second model using bi-variable (π and MR) regressions between the compound activities and descriptors was also studied. Unfortunately, these two variables were highly inter-correlated ($R = 0.68$) and, in general, if two or more variables, having high inter-correlation, are used simultaneously in the multiple regression analysis they may suffer from the defect due to collinearity (Zandonale and Gaudio, 2001; Gaudio *et al.*, 2002).

IV.4.4 Molecular Modeling

Considering the SAR above mentioned for the synthesized compounds, the evidence for polar interactions between basic nitrogen atoms from ursolic acid derivatives and haematin was explored through molecular dynamics simulations (MD) in explicit aqueous solutions.

These simulations were performed in collaboration with Prof. Dr. Hugo Verli, Structural Bioinformatics Group, Center of Biotechnology and Faculty of Pharmacy, UFRGS, Porto Alegre, Brazil. The calculations employed methodology previously described by the group (Verli and Guimarães, 2004; Becker *et al.*, 2005; Verli and Guimarães, 2005). Briefly, the compounds were constructed and geometry optimized at the HF/3-21G level using GAMESS (Schmidt *et al.*, 1993). The so obtained geometries were submitted to a single-point calculation at the HF/6-31G** level in order to obtain atomic charges suitable for MD simulations. These charges were included in PRODRG derived topologies (van Aalten *et al.*, 1996) for each compound, allowing the description of the molecules through MD. All simulations were performed under GROMACS simulation suite (van der Spoel *et al.*, 2005) and GROMOS96 force field for 10.0 ns using explicit water molecules and counter-ions to neutralize the system.

While such methodology does not include π - π interactions, it is indeed capable to describe the effect of solvent over the solvated compounds conformation, diffusion and complexation in a high level of accuracy.

In fact, MD has been recently employed to study the interaction of two Fe(III)PPIX molecules in both vacuum and aqueous solutions (Egan *et al.*, 2006). However, this work uses as a π - π packed starting orientation for the simulations. So in order to complement such observations, we decided for the use of randomly placed haeme molecules as the initial configuration for the simulated system. As doing so, we were capable to observe a spontaneously haematin formation in water. To our knowledge, such observation is one of the first descriptions, at the atomic level, of a non-enzymatic and spontaneously formation of haematin in solution. Additionally, the so obtained conformational ensemble confirmed previous descriptions of an $\sim 180^\circ$ orientation between

carboxylate groups (Figure 16a) (Villiers *et al.*, 2007), strongly supporting the proposal that aqueous Fe(III)PPIX dimers consist of coplanar back-to-back complexes between two porphyrins (Dorn *et al.*, 1998). Additionally, the distance between two haeme molecules is in agreement with previous data (Figure 16b) (Dorn *et al.*, 1998).

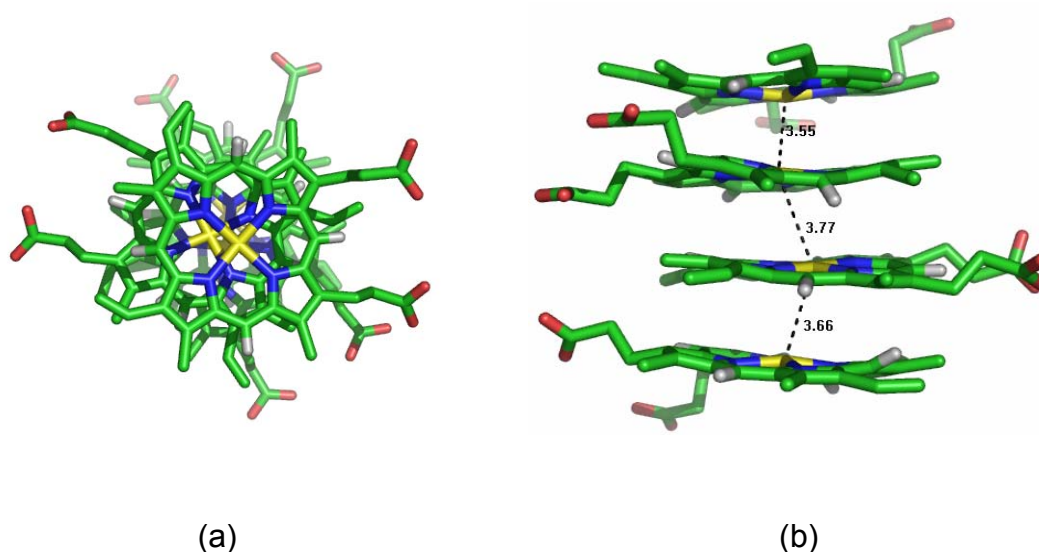


Figure 16. Orientation of haeme molecules observed to occur in solution from a 10.0 ns MD simulation, starting from random orientations. (a) Top view, showing that the angle between two consecutive haeme molecules is around 180°; (b) side view, presenting the distances between Fe(III) atoms.

Since the nanosecond time scale simulations of haeme molecules were capable to adequately describe the formation of haematin, we used the same approach to evaluate the complexation of the synthesized compounds with such biopolymer. Based on such approach, the compounds **182**, **195**, **185**, chloroquine and a bispyrrolo[1,2- α]quinoxaline (Guillon *et al.*, 2004) were observed to spontaneously interact with haeme molecules by diffusion, forming stable complexes during the 10.0 ns trajectories (Figure 17). Furthermore, it is important to note that the geometry observed for the complex between chloroquine and haeme is in agreement with interatomic distances previously described to occur in such complex by NMR methods (Leed *et al.*, 2002).

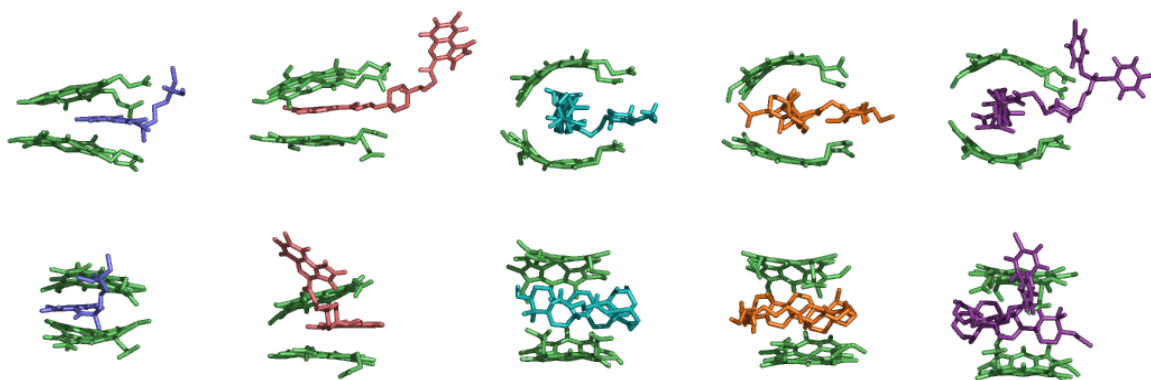


Figure 17. Side and front views of complexes between haematin and chloroquine (blue), bispyrrolo[1,2- α]quinoxaline derivative (Guillon *et al.*, 2004) (red), **182** (cyan), **195** (orange) and **185** (purple).

Related to the ursolic acid derivatives complexation to haeme molecules, important details could be obtained from the performed simulations, confirming and expanding, at the atomic level, the SAR established for this class of compounds, as follows:

1. The inverse relation between the hydrophobicity of the substituent attached to the terminal nitrogen atom of the *N*-[1,4-bis(3-aminopropyl)piperazinyl] pharmacophoric group and the antimalarial activity could be explained in the basis of its capability to perform strong electrostatic interactions with carboxylate groups of haeme molecules, *i.e.* more hydrophobic and steric imposing groups would abolish or reduce such interaction and so reduce the activity of the compounds;

2. The molecular basis for the *N*-[1,4-bis(3-aminopropyl)piperazinyl] pharmacophoric group can be rationalized in terms of its interaction with the carboxylate groups of haeme: while in systems composed only by haeme molecules the carboxylate groups are in opposite orientations, when the haeme molecules are packed to anti-malarial agents, the negatively charged groups show a re-orientation and point to the same side, where the positively charged amino groups are placed. As a result, several salt bridges can be performed simultaneously in solution between ligands and haematin (Figure 18). A similar

scheme of interactions was recently proposed to occur with diethyl-amino-alkoxyxanthenes (Solomov *et al.*, 2007), supporting these observations;

3. One of the main interactions expected to occur in most of anti-malarial agents evolves a π - π packing between the flat and aromatic rings from compounds and haeme. However, in molecules as artemisinin and the ursolic acid derivatives such interaction is not possible. At least for this last class of molecules, we observed that the substitution of an aromatic heterocyclic group by a triterpene skeleton is accompanied by the creation of a wide hydrophobic surface interacting with haeme molecules. Additionally, such group shows a perpendicular orientation related to the aromatic ring in compounds as chloroquine and the bispyrrolo[1,2- α]quinoxaline derivative (Figure 17). Such orientation can still be related to similar hydrophobic nucleus in complex with haeme proteins (Podust *et al.*, 2004). If confirmed, such new orientation may represent a completely novel lead for future optimizations, exploring original interactions with haeme and, mainly, the iron atom.

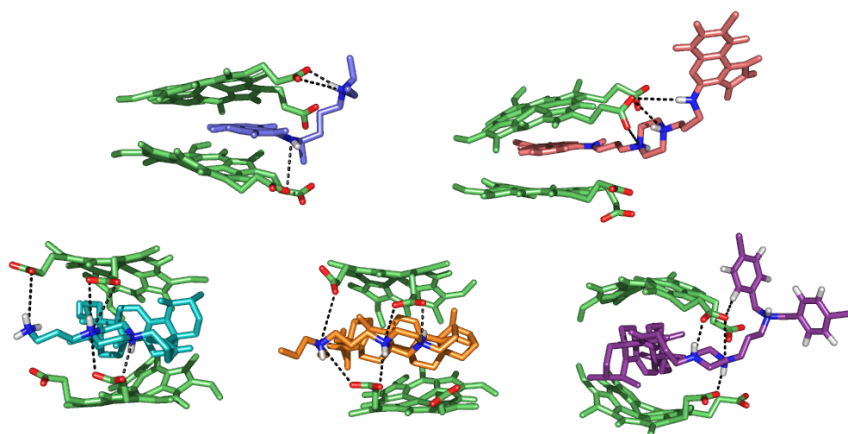


Figure 18. Interactions (black dashes) between haematin and chloroquine (blue), the bispyrrolo[1,2- α]quinoxaline derivative (Guillon *et al.*, 2004) (red), **182** (cyan), **195** (orange) and **185** (purple).

V CONCLUDING REMARKS

In this thesis seven natural products were obtained from South American *Ilex* species, namely the triterpenes ursolic and oleanolic acids, and **matesaponins 1 and 3**, and the **peracetylated matesaponins 1, 2 and 3**.

Through a rational design, based on the known molecular mechanism, of the malaria disease, a series of new derivatives of ursolic and oleanolic acids were successfully synthesized. These compounds could be divided in three series: ursolic and oleanolic acids with modifications at cycle A, ferrocene derivatives from ursolic acid and piperazine derivatives from ursolic acid.

These compounds were tested for their antimalarial activity *in vitro* upon the *P. falciparum* Chloroquine-resistant strain FcB1 (IC_{50} (chloroquine) = 0.13 μ M) and for the most active compounds against the *P. falciparum* chloroquine-sensitive strain Thai (IC_{50} (chloroquine) = 0.01 μ M).

In relation to the modifications at the cycle A, acetylation at 3-OH gives the best results. The acetylated compounds were more active compounds than their parent ones, due to an expected increase of lipophilicity. But in contrast, the increases in the surface area by the cycle A expansion, the oxidation at C-3 and the inversion of C-3-OH configuration did not improve the antimalarial activity.

Whatever the nature of the substituents on the triterpene ring, the presence of a piperazine in the linker seems to increase the antimalarial activity. Indeed, seven new piperazinyl analogues of ursolic acid **1** showed significant activity in the order of nano molar range including compounds **199** IC_{50} 78 nM, **189** IC_{50} 161 nM and **180** IC_{50} 167 nM, while chloroquine presented IC_{50} 130 nM.

A comparison of the IC_{50} values relating the inhibition of growth of the resistance and sensitive strains of *P. falciparum* suggested low levels of cross-resistance to chloroquine. All tested compounds showed cytotoxicity upon the human diploid embryonic lung cell line (MRC-5 cells) in the micromolar range, IC_{50} values varied from 1.57 to 18.28 μ M.

This study had also contributed to provide better knowledge on structure-activity relationships (SAR) of these piperazine derivatives from ursolic acid. In this way, it was demonstrated the importance of the triterpene skeleton and the acetyl group at C-3 for antimalarial activity; piperazine was identified as a pharmacophore in this series. The importance of the hydrophilic framework attached at *N* terminal of the bis-(3-aminopropyl)piperazine joined to the triterpene ring was also characterized by QSAR approaches.

The most active compounds showed an *in vitro* inhibition of β -haematin formation, suggesting an effect on this target. These results suggest that they may share some similarities in their mechanism of action with chloroquine, but this should be more deeply investigated.

We additionally propose a preliminary molecular modeling to understand the mechanism of action of these new ursolic acid derivatives with implication on the binding of triterpene to β -hematin crystal surface. The more active compounds could constitute suitable candidates for further physicochemical and biological studies in order to use these molecules to improve our knowledge about the molecular mechanism involved in the malaria. This means to understand their mechanism of action as antimalarial compounds and/or their capacity to interfere in the parasite mechanism of resistance.

Finally, we believe that these results could provide suitable information for the development of new antimalarial compounds.

VI EXPERIMENTAL PART

VI.1. Généralités

VI.1.1. Réactifs et Solvants

Pour les réactions organiques qui nécessitent des solvants anhydres :

- le dichlorométhane est séché sur chlorure de calcium, puis distillé;
- le tétrahydrofurane, l'éther diéthylique et le toluène sont distillés sur sodium en présence de benzophénone ;
- la pyridine est séchée sur KOH, puis distillée.
- le méthanol et l'éthanol sont distillés sur magnésium en présence d'iode.
- le *N,N*-diméthylformamide et le chlorure de thionyle sont purifiés par distillation fractionnée.

Le Réactif de Jones a été préparé en milieu fortement acide (H_2SO_4) à partir du sel $\text{K}_2\text{Cr}_2\text{O}_7$.

Les autres solvants et réactifs sont utilisés sans purification additionnelle.

VI.1.2. Chromatographies

Les CCM ont été effectuées sur plaques d'aluminium recouvertes de silice 60 F₂₅₄, observées dans l'ultraviolet ($\lambda = 254 \text{ nm}$) avant d'être révélées par l'anisaldehyde sulfurique pour les composés naturels or l'acide phosphomolybdique (Stahl, 1988) dans du méthanol à 95% pour les composés synthétisés, après chauffage.

Les chromatographies préparatives en phase liquide sur colonne ont été effectuées sur gel de silice 60 (35-70 μm).

Les analyses CLHP ont été réalisées sur un chromatographe Shimadzu® équipé d'un détecteur UV (254 nm) et d'une colonne RP-18 et un système gradient d'acétonitrile et l'eau.

VI.1.3. Instrumentation

Les spectres de RMN ont été réalisés sur un spectromètre Bruker AC 500. Les déplacements chimiques (δ) sont exprimés en partie par million (ppm) par rapport au résidu non deutérié du solvant pris comme référence interne. L'analyse des spectres RMN est donnée en spécifiant le déplacement chimique, la multiplicité, l'intégration, la constante de couplage (s'il y a lieu) et l'assignation.

Les abréviations suivantes sont utilisées pour préciser la multiplicité des signaux :

s : singulet	dd : doublet de doublet	d : doublet
t : triplet	ddd : doublet de doublet de doublet	q : quadruplet
m : multiplet	sl : singulet large	tl : triplet large

Les spectres RMN ^1H et RMN ^{13}C ont été réalisés dans le CDCl_3 ou dans $\text{CD}_3\text{OH}-d_4$.

Les spectres infrarouges (IR) ont été enregistrés sur un spectromètre Jasco FT/IR-4200 muni d'un système ATR Goldengate permettant une analyse « en directe » sans préparation préalable des solides et des liquides.

Les spectres de masse (SM) ont été obtenus sur un appareil haute résolution Micromass-Waters Q-TOF Ultima, en mode d'ionisation électrospray.

Les pouvoirs rotatoires ont été mesurés sur un polarimètre Perkin Elmer 241.

Les points de fusion (pF) ont été déterminés sur un banc Köffler.

VI.2 Plant material

Aerial parts of *Ilex paraguariensis* A. St. Hilaire, Aquifoliaceae, were collected in Mato Leitão, RS, Brazil, and they were authenticated by Marcos Sobral (*Programa de Pós-Graduação em Ciências Farmacêuticas/UFRGS*). A herbarium specimen is on deposit in the Botany Department Herbarium of Universidade Federal do Rio Grande do Sul, Porto Alegre, Brazil.

Aerial parts of *Ilex dumosa* Reissek, Aquifoliaceae, were collected in Viamão, RS, Brazil, and were authenticated by Prof. Dr Sérgio Bordignon (*Universidade Luterana do Brasil (ULBRA), Canoas, RS*). A herbarium specimen is on deposit in the Botany Department Herbarium of Universidade Federal do Rio Grande do Sul, Porto Alegre, Brazil

VI.2.1 Extraction

Air-dried powdered leaves of *I. paraguariensis* and *I. dumosa* (3 kg) were extracted, separately, by maceration with 70% EtOH (15% plant:solvent) at room temperature during 7 days. Each extract was filtrated, then evaporated *in vacuum*, and each aqueous residue (6 L) was extracted, separately, with cyclohexane (3 x 2 L). The resulting aqueous solutions were submitted, separately, to acid hydrolysis and to chromatographic isolation.

VI.2.2 Acid Hydrolysis of aqueous extracts

To each *Ilex* aqueous extract, separately, it was added enough sulfuric acid in order to obtain an acid concentration of 10%. The mixture was refluxed for 1 h and most part of aglycones precipitate. The sapogenins left in the aqueous solution were extracted, separately, from the acid solution with chloroform (three times). The chloroform fractions were evaporated, separately, to dryness under vacuum. This residue was fractionated, separately, by column chromatography (Si, CH₂Cl₂:MeOH 95:05). The precipitates and the aglycones from the column chromatography were submitted, separately, to crystallization

using AcOEt:MeOH 70:30). Ursolic acid (8 g) was obtained from *I. paraguariensis* extract and oleanolic acid (5 g) was obtained from *I. dumosa* extract (Gnoatto *et al.*, 2005a).

VI.2.3 Isolation of matesaponins

The aqueous extract of *I. paraguariensis* (1 L) was extracted with *n*-BuOH (3 x 350 mL). The residue (36.6 g) obtained after evaporation of the *n*-BuOH fraction was repeatedly chromatographed over silica gel and eluting with a gradient system of CHCl₃:MeOH:H₂O (80:40:05 to 40:40:05). Fractions were collected and pooled together according TLC. Fraction 1 was column chromatographed over silica gel using a gradient system of CHCl₃:MeOH:H₂O (60:40:05 to 40:40:05) to give a white amorphous solid of matesaponin 1 **2** (15 mg) and matesaponin 3 **4** (10 mg). Fraction 2 was acetylated in the usual manner, using pyridine and Ac₂O at room temperature overnight. The acetyl derivatives were chromatographed over silica gel using a gradient system of CHCl₃:MeOH (98:02 to 90:10) to give peracetylated matesaponin 1 **2** (10 mg), peracetylated matesaponin 2 **3** (10 mg) and peracetylated matesaponin 3 **4** (10 mg).

VI.2.4 Identification of aglycons and saponins

Ursolic and oleanolic acid were subjected to MS, ¹H, ¹³C NMR and IR spectroscopic analysis. It was also measured the melting point and the optical rotation. The purity of ursolic acid was determined through HPLC using a reverse phase column C-18 and acetonitrile:water in gradient sistem (Gnoatto *et al.*, 2005).

The identification of the purified saponins was performed by co-TLC using reference substances from our laboratory and, ¹H and ¹³C NMR by comparison with previously published data (Gosmann *et al.*, 1989; 1995).

VI.3. Méthodes Générales

VI.3.1. Réactions d'amination réductrice

VI.3.1.1. Méthode A

A une solution de **180** (34 mg, 0,05 mmol, 1 éq) dans du THF distillé (1 mL), ajouter de l'aldéhyde (0,15 mmol, 3 éq) et du NaBH(OAc)₃ (16,4 mg, 0,075 mmol, 1,5 éq). Après 3 heures de réaction sous atmosphère d'azote, additionner de nouveau 1,5 éq de NaBH(OAc)₃. Laisser le milieu réactionnel sous agitation pendant 18 heures. Ajouter une solution aqueuse de NaOH 1N (0,5 mL) et agiter le mélange pendant 1 heure. Extraire la phase aqueuse par du CH₂Cl₂ (3 x 1 mL). Réunir les phases organiques, sécher sur Na₂SO₄ et évaporer sous vide. Purifier le produit par chromatographie sur colonne de silice (éluant CH₂Cl₂ : MeOH gradient 98 : 02).

VI.3.1.2. Méthode B

A une solution de **180** (34 mg, 0,05 mmol, 1 éq) dans du THF distillé (1 mL) ajouter de l'aldéhyde (0,075 mmol, 1,5 éq) et du NaBH(OAc)₃ (16,4 mg, 0,075 mmol, 1,5 éq). Laisser agiter le milieu réactionnel pendant 18 heures sous atmosphère d'azote. Ajouter une solution aqueuse de NaOH 1N (0,5 mL) et agiter le mélange pendant 1 heure. Extraire la phase aqueuse par du CH₂Cl₂ (3 x 1 mL). Réunir les phases organiques, sécher sur Na₂SO₄ et évaporer sous vide. Purifier le produit par chromatographie sur colonne de silice (éluant CH₂Cl₂ : MeOH gradient 98 : 02).

VI.3.1.3. Méthode C

A une solution de **178** (60 mg, 0,2 mmol, 1 éq) dans du THF distillé (2 mL) ajouter l'aldéhyde (0,22 mmol, 1,1 éq) et le NaBH(OAc)₃ (65,6 mg, 0,3 mmol, 1,5 éq). Puis agiter le milieu réactionnel pendant 18 heures sous atmosphère d'azote. Ensuite ajouter une solution aqueuse de NaOH 1N (1 mL)

et agiter le mélange pendant 1 heure. Extraire la phase aqueuse par du CH_2Cl_2 (3 x 2 mL). Réunir les phases organiques, sécher sur Na_2SO_4 et évaporer sous vide. Le produit est purifié par chromatographie sur colonne de silice (éluant CH_2Cl_2 : MeOH gradient 98 : 02).

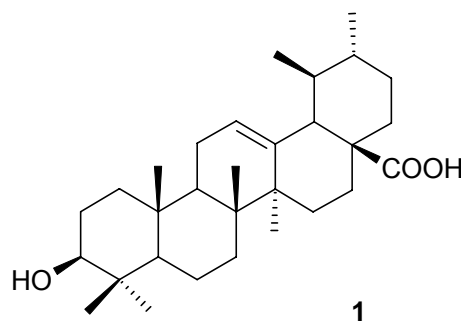
VI.3.2. Réaction de déprotection d'une fonction amine protégée par un groupement Boc

A une amine protégée par un groupement Boc (0,1 mmol, 1 éq), ajouter une solution d'acide trifluoracétique (TFA) à 10% dans du CH_2Cl_2 (5 mL). Agiter le mélange à température ambiante pendant 3 heures. Laver avec une solution aqueuse saturée de K_2CO_3 , sécher sur Na_2SO_4 et évaporer sous pression réduite.

VI.3.3. Réaction de déprotection d'une fonction alcool protégée par un groupement acétyle

Dissoudre l'alcool protégé par un groupement acétyle (0,1 mmol, 1 éq) dans de l'EtOH (2 mL) et ajouter 1 mL d'une solution aqueuse de NaOH 1N. Porter à reflux pendant 2 heures. Evaporer le solvant organique et extraire la phase aqueuse par du CH_2Cl_2 (3 x 1 mL). Réunir les phases organiques, sécher sur Na_2SO_4 et évaporer sous pression réduite.

VI.4. Obtention de l'acide ursolique **1** par extraction d'*Ilex paraguariensis*



Poudre blanche

$C_{30}H_{46}O_3$

$MM = 454 \text{ g/mol}$

IR (ATR, cm^{-1}): 3562 (OH alcool); 2947 (OH acide); 2866 (C-H); 1697 (C=O); 1460 (C-O); 1385 (C-H); 1306 (C-O); 1030 (C-O-H).

RMN 1H (500 MHz, $CDCl_3$: CD_3OD , 9:1), δ (ppm), J en Hz: 0,68 (d, $^3J=11,4$, 1H, CH-5); 0,73 (s, 3H, CH_3 -25); 0,76 (s, 4H, CH_3 -24 et $CH_{2(H\alpha)}$ -1 superposé); 0,81 (d, $^3J = 6,4$, 3H, CH_3 -30); 0,87 (s, 3H, CH_3 -26); 0,90 (d, $^3J = 6,0$, 3H, CH_3 -29); 0,93 (sl, 4H, CH_3 -23 et CH_2 -11 superposé); 0,90 (1H, CH-20); 1,04 (s, 3H, CH_3 -27); 1,21 (m, 1H, $CH_{2(H\alpha)}$ -7); 1,33 (m, 3H, CH_2 -2, CH-19); 1,47 (m, 4H, $CH_{2(H\beta)}$ -6, $CH_{2(H\beta)}$ -7, $CH_{2(H\alpha)}$ -9, $CH_{2(H\alpha)}$ -21); 1,58 (m, 4H, $CH_{2(H\beta)}$ -1, $CH_{2(H\alpha)}$ -15, $CH_{2(H\beta)}$ -16, $CH_{2(H\beta)}$ -21); 1,67 (td, $^3J=13,9$ et 6,8, 1H, $CH_{2(H\alpha)}$ -6); 1,81 (td, $^3J=13,6$ et 7,2, 1H, $CH_{2(H\alpha)}$ -16); 1,86 (dd, $^3J=12,6$ et 7,3, 2H, CH_2 -22); 1,96 (td, $^3J=13,4$ et 4,9, 1H, $CH_{2(H\beta)}$ -15); 2,13 (d, $^3J = 11,3$, 1H, CH-18); 3,20 (dd, $^3J = 11,7$ et 4,5, 1H, CH-3); 5,40 (tl, 1H, CH-12).

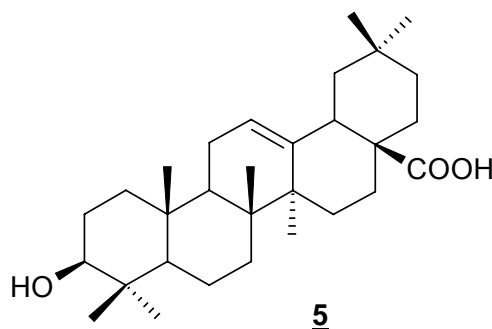
RMN ^{13}C (125 MHz, $CDCl_3$: CD_3OH-d_4 , 9:1), δ (ppm): 15,7 (C-25); 15,9 (C-26); 17,1 (C-24); 17,3 (C-29); 18,6 (C-6); 21,5 (C-30); 23,6 (C-11); 23,8 (C-27); 24,5 (C-16); 27,0 (C-15); 28,3 (C-2); 28,3 (C-23); 30,9 (C-21); 33,3 (C-7); 37,1 (C-10); 37,2 (C-22); 38,9 (C-8); 39,0 (C-1); 39,2 (C-4); 39,4 (C-19); 39,7 (C-20); 42,3 (C-14); 47,8 (C-9); 48,1 (C-17); 53,1 (C-18); 55,5 (C-5); 79,1 (C-3); 125,8 (C-12); 138,5 (C-13); 181,1 (C-28).

SMHR: calculé pour $C_{30}H_{47}O_3$: 455,3525. Trouvé: 455,3522 (100%).

$[\alpha]_D^{20} = +72,5$ (MeOH, c 0,4)

pF: 237-240 °C

VI.5. Obtention de l'acide oléanolique 5 par extraction d'*Ilex dumosa*



Poudre blanche

$C_{30}H_{46}O_3$

$MM = 454 \text{ g/mol}$

IR (ATR, cm^{-1}): 3565 (OH alcool); 2950 (OH acide); 2870 (C-H); 1698 (C=O); 1460 (C-O); 1388 (C-H); 1310 (C-O); 1240 (CH_3); 1025 (C-O-H).

RMN ^1H (500 MHz, CDCl_3), δ (ppm), J en Hz: 0,80 (d, $^3J = 11,1$, 1H, CH-5); 0,82 (s, 3H, CH_3 -25); 0,83 (sl, 4H, CH_3 -24 et $\text{CH}_{2(\text{H}\alpha)}$ -1 superposé); 0,96 (s, 3H, CH_3 -26); 0,97 (s, 3H, CH_3 -30); 0,99 (s, 3H, CH_3 -23); 1,05 (s, 3H, CH_3 -27); 1,19 (s, 3H, CH_3 -29); 1,22 (m, 1H, $\text{CH}_{2(\text{H}\alpha)}$ -7); 1,33 (m, 3H, CH_2 -2, CH-19); 1,47 (m, 4H, $\text{CH}_{2(\text{H}\beta)}$ -6, $\text{CH}_{2(\text{H}\beta)}$ -7, CH-9, $\text{CH}_{2(\text{H}\alpha)}$ -21); 1,58 (m, 4H, $\text{CH}_{2(\text{H}\beta)}$ -1, $\text{CH}_{2(\text{H}\alpha)}$ -15, $\text{CH}_{2(\text{H}\beta)}$ -16, $\text{CH}_{2(\text{H}\beta)}$ -21); 1,67 (td, $^3J = 13,9$ et 6,8, 1H, $\text{CH}_{2(\text{H}\alpha)}$ -6); 1,81 (td, $^3J = 13,6$ et 7,0, 1H, $\text{CH}_{2(\text{H}\alpha)}$ -16); 1,86 (dd, $^3J = 12,5$ et 7,3, 2H, CH_2 -22); 1,96 (td, $^3J = 13,4$ et 4,9, 1H, $\text{CH}_{2(\text{H}\beta)}$ -15); 2,88 (dd, $^3J = 13,8$ et 4,2, 1H, CH-18); 3,27 (dd, $^3J = 11,7$ et 4,7, 1H, CH-3); 5,34 (tl, $^3J = 16,6$, 1H, CH-12).

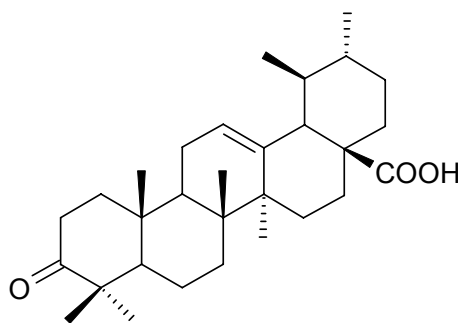
RMN ^{13}C (125 MHz, CDCl_3), δ (ppm): 15,7 (C-25); 15,9 (C-26); 17,5 (C-24); 18,7 (C-6); 23,4 (C-11); 23,8 (C-30); 23,9 (C-27); 26,3 (C-16); 27,6 (C-15); 28,1 (C-2); 28,5 (C-23); 31,0 (C-21); 32,8 (C-29); 33,1 (C-19); 33,4 (C-7); 34,2 (C-22); 37,5 (C-10); 38,8 (C-8); 39,2 (C-1); 39,7 (C-4); 41,4 (C-20); 42,1 (C-14); 46,3 (C-9); 46,9 (C-17); 48,1 (C-18); 55,6 (C-5); 79,4 (C-3); 123,1 (C-12); 143,9 (C-13); 182,6 (C-28).

SMHR: calculé pour $C_{30}H_{47}O_3$: 455,3525. Trouvé: 455,3522 (100%).

$[\alpha]_D^{20} = +106$ (MeOH, c 0,4)

pF: >250 °C.

VI.6. Oxydation de 1 par le Réactif de Jones

**147**

Poudre blanche

 $C_{30}H_{44}O_3$ $MM = 453 \text{ g/mol}$

Ce composé est synthétisé par une réaction d'oxydation, au moyen du Réactif de Jones, à partir du acide ursolique 1. Additionner le Réactif de Jones (1,5 mL) à une solution de 1 (455 mg, 1,0 mmol) dans l'acétone (5,0 mL) à 0 °C. Agiter la solution pendant 1 heure à température ambiante et refroidir à 0 °C pour additionner le propanol (20 mL). Après 30 minutes supplémentaire à la température ambiante, filtrer le précipité et évaporer le filtrat sous pression réduite. Purifier sur colonne de silice (éluant: CH_2Cl_2). L'acide 3-oxo-ursolique 147, est obtenu avec un **rendement de 80%**.

IR (ATR, cm^{-1}): 3562 (OH alcool); 2948 (OH acide); 2866 (C-H); 1705 (C=O, de cétone); 1697 (C=O d'acide); 1460 (C-O-H); 1385 (C-H); 1306 (C-O); 1030 (C-O-H).

RMN 1H (500 MHz, $CDCl_3$), δ (ppm), J en Hz: 0,87 (s, 3H, CH_3 -25 et 1H, CH-5); 0,91 (d, $^3J = 6,3$, 3H, CH_3 -30); 0,89 (m, 2H, CH_2 -11 et CH-20); 0,99 (d, $^3J = 6,0$, 3H, CH_3 -29); 1,07 (s, 3H, CH_3 -26); 1,11 (s, 3H, CH_3 -24); 1,13 (s, 6H, CH_3 -23 et CH_3 -27); 1,36 (m, 5H, CH_2 -2, CH_2 -7 et CH-19); 1,52 (m, 5H, CH_2 -1, $CH_{2(H\alpha)}$ -15, $CH_{2(H\beta)}$ -16, $CH_{2(H\beta)}$ -21); 1,64 (td, 1H, $^3J = 14,3$ et 7,0, $CH_{2(H\alpha)}$ -6); 1,76 (dd, $^3J = 13,6$ et 7,0, 1H, $CH_{2(H\alpha)}$ -16); 1,94 (m, 2H, $CH_{2(H\beta)}$ -15 et CH_2 -22); 2,24 (d, $^3J = 11,2$, 1H, CH-18); 5,31 (tl, 1H, CH-12).

RMN ^{13}C (125 MHz, $CDCl_3$), δ (ppm): 15,6 (C-25); 15,9 (C-26); 17,3 (C-29); 19,6 (C-6); 19,9 ou 34,5 (C-2); 21,6 (C-30); 21,8 (C-24); 23,8 (C-11 et C-27); 24,5 (C-16); 26,9 (C-15); 28,4 (C-23); 31,0 (C-21); 33,7 (C-7); 37,1 (C-10 et C-

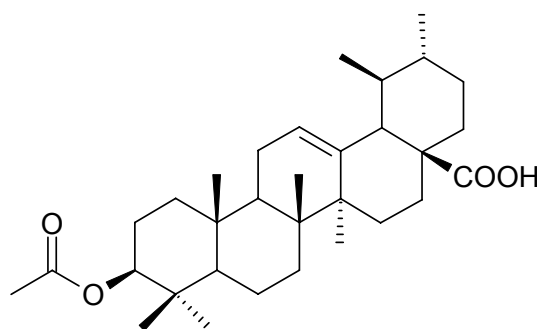
22); 39,2 (C-1); 39,4 (C-4); 39,7 (C-19); 39,8 (C-20); 40,6 (C-8) ; 42,7 (C-14); 47,8 (C-9); 48,4 (C-17); 52,9 (C-18); 55,6 (C-5); 125,9 (C-12); 138,5 (C-13); 184,1 (C-28), 217,7 (C-3).

SMHR: calculé pour $C_{30}H_{45}O_3Na$: 477,3345. Trouvé: 477,3339 (100%).

$[\alpha]_D^{20} = +83,4$ ($CHCl_3$, c 0,1)

pF: 172 °C.

VI.7. Préparation de l'acide 3-acétylursolique **154**



154

Poudre blanche

$C_{32}H_{48}O_4$

MM = 496 g/mol

A une solution d'acide ursolique **1** (91mg, 0,2 mmol) dans de la pyridine distillée (2,5 mL) ajouter de l'anhydride acétique (2,5 mL). Agiter le milieu réactionnel à la température ambiante pendant 24 heures. Verser le mélange réactionnel dans de l'eau glacée, filtrer et sécher sous vide. Le produit est obtenu avec un **rendement quantitatif**.

IR (ATR, cm^{-1}): 3562 (OH alcool); 2947 (OH acide); 2866 (C-H); 1732 (C=O acétyle); 1697 (C=O d'acide); 1460 (C-O); 1385 (C-H); 1306 (C-O); 1248 (C-O-C); 1030 (C-O-H).

RMN 1H (500 MHz, $CDCl_3$), δ (ppm), J en Hz: 0,83 (s, 3H, CH_3 -25); 0,87 (m, 1H, CH-5); 0,90 (s, 3H, CH_3 -24); 0,91 (s, 3H, CH_3 -23); 0,92 (d, $^3J = 5,2$, 3H, CH_3 -30); 0,93 (m, 1H, CH_2 -1); 1,00 (d, $^3J = 6,8$, 3H, CH_3 -29, 1H, CH_2 -20); 1,01 (s, 3H, CH_3 -26); 1,13 (s, 3H, CH_3 -27); 1,32 (m, 1H, CH-19); 1,39 (m, 4H, CH_2 -2, $CH_{2(H\beta)}$ -6, $CH_{2(H\alpha)}$ -21); 1,56 (m, 6H, $CH_{2(H\beta)}$ -1, CH_2 -7, CH_{α} -9, $CH_{2(H\alpha)}$ -15,

CH_{2(Hβ)}-16, CH_{2(Hβ)}-21); 1,67 (td, ³J=13,9 et 6,8, 1H, CH_{2(Hα)}-6); 1,84 (m, 1H, H_{2(Hα)}-16); 1,96 (m, 2H, CH₂-22); 2,07 (td, ³J=13,5 et 5,0, 1H, CH_{2(Hβ)}-15); 2,10 (s, 3H, H₃CCOO); 2,13 (d, ³J = 11,3, 1H, CH-18); 4,55 (dd, ³J=13,3 et 7,5, 1H, CH-3); 5,30 (tl, 1H, CH-12).

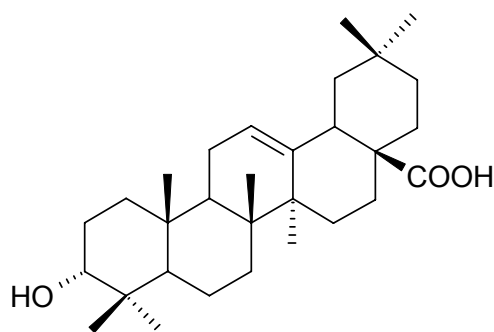
RMN ¹³C (125 MHz, CDCl₃), δ (ppm): 15,7 (C-25); 17,5 (C-26); 17,7 (C-29); 18,7 (C-6); 21,4 (C-24); 21,6 (C-30 et H₃CCOO); 23,4 (C-2); 23,9 (C-11); 23,9 (C-27); 25,1 (C-16); 28,2 (C-23); 28,5 (C-15); 31,3 (C-21); 33,4 (C-7); 37,3 (C-10); 37,8 (C-22); 38,1 (C-4); 38,8 (C-1); 39,2 (C-19); 39,8 (C-20); 40,9 (C-8); 42,2 (C-14); 46,3 (C-9); 47,9 (C-17); 54,0 (C-18); 55,7 (C-5); 80,3 (C-3); 124,9 (C-12); 140,1 (C-13); 171,7 (H₃CCOO-); 182,1 (C-28).

SMHR: calculé pour C₃₂H₄₉O₄: 497,3631. Trouvé: 497,3635 (100%).

[α]_D²⁰ = + 99,3 (CHCl₃, c 0,1)

pF: 170 °C

VI.8. Epimerisation de 5 par la triphenylphosphine



157

Poudre blanche

C₃₀H₄₆O₃

MM = 454 g/mol

A une solution de triphenylphosphine (28,8 mg, 0,11 mmol) dans le THF distillé (5 mL) ajouter du DIAD (22,2 mg, 0,11 mmol) et agiter pendant 1 heure sous atmosphère d'azote à température ambiante. Ajouter de l'acide oleanolique 5 (45,5 mg, 0,1 mmol) et de l'acide formique (46,0 mg, 0,11 mmol). Agiter pendant 24 heures à température ambiante et sous atmosphère d'azote. Evaporer le solvant et hydrolyser le résidu par une solution aqueuse de H₂SO₄ 10% pendant 1 heure sous reflux. Filtrer le précipité formé et purifier par

chromatographie sur colonne de silice (éluant CH₂Cl₂ : MeOH gradient 98 : 02). Une poudre blanche-jaunâtre d'acide *epi*-oléanolique **157** est obtenue avec un rendement de 37%.

IR (ATR, cm⁻¹): 3561 (OH alcool); 2947 (OH acide); 2865 (C-H); 1696 (C=O); 1463 (C-O); 1385 (C-H); 1306 (C-O); 1028 (C-O-H).

RMN ¹H (500 MHz, CDCl₃), δ (ppm), *J* en Hz: 0,79 (d, ³*J*= 12,8, 1H, CH-5); 0,82 (s, 8H, CH₃-25); 0,84 (sl, 4H, CH₃-24 et CH_{2(Hα)}-1 superposé); 0,96 (s, 3H, CH₃-26); 0,97 (s, 3H, CH₃-30); 0,99 (s, 3H, CH₃-23); 1,05 (s, 3H, CH₃-27); 1,20 (s, 3H, CH₃-29); 1,22 (m, 1H, CH_{2(Hα)}-7); 1,33 (m, 3H, CH₂-2, CH-19); 1,47 (m, 4H, CH_{2(Hβ)}-6, CH_{2(Hβ)}-7, CH-9, CH_{2(Hα)}-21); 1,58 (m, 4H, CH_{2(Hβ)}-1, CH_{2(Hα)}-15, CH_{2(Hβ)}-16, CH_{2(Hβ)}-21); 1,67 (td, ³*J*=13,9 et 6,8, 1H, CH_{2(Hα)}-6); 1,81 (td, ³*J*=13,6 et 6,8, 1H, CH_{2(Hα)}-16); 1,86 (dd, ³*J*=12,6 et 7,3, 2H, CH₂-22); 1,96 (td, ³*J*=13,4 et 4,9, 1H, CH_{2(Hβ)}-15); 2,87 (dd, ³*J*= 13,7 et 4,0, 1H, CH-18); 3,51 (dd, ³*J*= 11,7 et 4,8, 1H, CH-3); 5,35 (tl, 1H, CH-12).

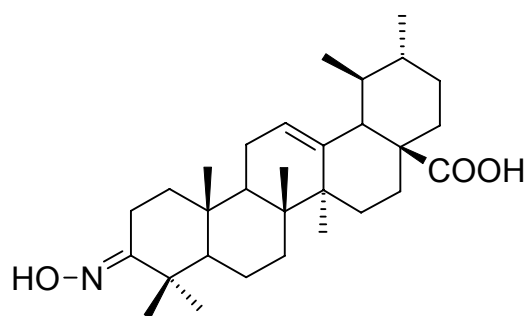
RMN ¹³C (125 MHz, CDCl₃), δ (ppm): 15,7 (C-25); 15,9 (C-26); 17,5 (C-24); 18,7 (C-6); 23,4 (C-11); 23,8 (C-29); 23,9 (C-27); 26,3 (C-16); 27,6 (C-15); 28,5 (C-23); 30,4 (C-2); 31,0 (C-21); 32,8 (C-30); 33,1 (C-19); 33,4 (C-7); 34,2 (C-22); 37,5 (C-10); 38,8 (C-8); 39,2 (C-1); 39,7 (C-4); 41,5 (C-20); 42,1 (C-14); 46,3 (C-9); 46,9 (C-17); 48,0 (C-18); 55,6 (C-5); 74,5 (C-3); 123,1 (C-12); 143,9 (C-13); 182,6(C-28).

SMHR: calculé pour C₃₀H₄₇O₃: 455,3525. Trouvé: 455,3524 (100%).

[α]_D²⁰ = +57,25 (MeOH, c 0,4)

pF: >250 °C.

VI.9. Préparation de l'oxime de l'acide 3-oxo-ursolique **158**

**158**

Poudre blanche

 $C_{30}H_{47}NO_3$ $MM = 469$ g/mol

A une solution de l'acide 3-oxo-ursolique **147** (77 mg, 0,17 mmol) dans de l'éthanol absolu (1 mL) et de la pyridine (0,6 mL), ajouter le chlorhydrate d'hydroxylamine (28 mg, 0,4 mmol). Agiter le milieu réactionnel à température ambiante et sous atmosphère d'azote pendant 36 heures. Verser sur de l'eau glacée et filtrer. Une poudre blanche est obtenue avec un **rendement de 89%**.

IR (ATR, cm^{-1}) : 2943 (OH acide) ; 1685 (C=O); 1657 (C=N); 1460 (C-O); 1385 (C-H); 1277 (C-N); 1045 (C-O-H).

RMN 1H (500 MHz, $CDCl_3$ et CD_3OH-d_4), δ (ppm), J en Hz: 0,78 (1H, CH-5); 0,73 (s, 3H, CH_3 -25); 0,83 (s, 3H, CH_3 -24); 0,92 (d, $^3J = 6,4$, 3H, CH_3 -30); 0,94 (s, 3H, CH_3 -26); 1,02 (d, $^3J = 6,0$, 3H, CH_3 -29); 1,06 (sl, 4H, CH_3 -23 et CH_2 -11 superposé); 1,05 (1H, CH-20 superposé); 1,14 (s, 3H, CH_3 -27); 1,21 (m, 1H, $CH_{2(H\alpha)}$ -7); 1,32 (m, 2H, $CH_{2(H\alpha)}$ -1, CH-19); 1,46 (m, 4H, $CH_{2(H\beta)}$ -6, $CH_{2(H\beta)}$ -7, CH-9, $CH_{2(H\alpha)}$ -21); 1,60 (m, 4H, $CH_{2(H\beta)}$ -1, $CH_{2(H\alpha)}$ -15, $CH_{2(H\beta)}$ -16, $CH_{2(H\beta)}$ -21); 1,72 (m, 2H, $CH_{2(H\alpha)}$ -6, $CH_{2(H\alpha)}$ -16); 1,87-2,01 (m, 3H, $CH_{2(H\beta)}$ -15, CH_2 -22); 2,07 (d, $^3J = 11,0$, 1H, CH-18); 2,17 (m, 2H, CH_2 -2); 3,42 (s, 1H, OH); 5,31 (tl, 1H, H-12).

RMN ^{13}C (125 MHz, $CDCl_3$ et CD_3OH-d_4), δ (ppm): 14,3 (C-24); 15,3 (C-25); 17,1 (C-26); 17,5 (C-29); 19,4 (C-6); 21,5 (C-30); 23,4 (C-2); 23,6 (C-11); 23,8 (C-27); 24,5 (C-16); 27,0 (C-15); 27,9 (C-23); 31,0 (C-21); 32,9 (C-7); 34,2 (C-10); 37,4 (C-22); 38,7 (C-8); 39,6 (C-19); 39,7 (C-20); 40,5 (C-1); 41,5 (C-4);

42,2 (C-14); 47,8 (C-9); 48,1 (C-17); 53,1 (C-18); 55,5 (C-5); 125,8 (C-12);
138,5 (C-13); 168,0 (C-3); 181,4 (C-28).

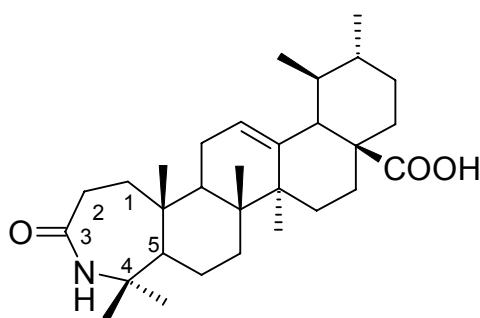
$[\alpha]_D^{20} = +48$ (CHCl₃, c 0,2)

pF: 188 °C.

VI.10. Réaction de Beckmann

A une solution de l'oxime de l'acide 3-oxo-ursolique **147** (68 mg, 1,12 mmol) dans du THF distillé (0,5 mL) à 0 °C sous atmosphère d'azote, ajouter goutte-à-goutte une solution de chlorure de thionyle distillé (72 µL) dans du THF distillé (0,25 mL). Agiter le milieu réactionnel à 0 °C pendant 4 heures. Puis, verser sur de l'eau glacée. Neutraliser à l'aide d'une solution aqueuse de NH₄OH à et extraire par du CH₂Cl₂ (3 x 2 mL). Réunir les phases organiques, sécher sur Na₂SO₄ et évaporer sous vide. Purifier le résidu par chromatographie sur colonne de silice (éluant CH₂Cl₂:MeOH, gradient 98:02). Deux produits sont obtenus : **159** avec un rendement de 32% et **160** avec un rendement de 50%.

VI.10.1. Acide 4-aza A-homo-3-oxo-ursolique **159**



159

Cristaux blancs

C₃₀H₄₇NO₃

MM = 469 g/mol

IR (ATR, cm⁻¹): 3027 (NH); 2931 (OH acide); 2855 (C-H); 1694 (C=O acide);
1680 (C=O lactame); 1457 (C-O).

RMN ¹H (500 MHz, CDCl₃), δ (ppm), J en Hz: 0,87 (1H, CH-5); 0,89 (s, 3H,
CH₃-26); 0,90 (d, ³J = 6,4, 3H, CH₃-30); 0,92 (m, 3H, CH₂-11 et CH-20

superposés); 1,00 (d, $^3J = 6,0$, 3H, CH₃-29); 1,14 (s, 3H, CH₃-27); 1,18 (m, 1H, CH₂(H_α)-7); 1,19 (s, 3H, CH₃-25); 1,34 (m, 1H, CH-19); 1,37 (s, 3H, CH₃-24); 1,48 (s, 4H, CH₃-23); 1,50 (m, 4H, CH₂(H_β)-6, CH₂(H_β)-7, CH-9, CH₂(H_α)-21); 1,60 (m, 5H, CH₂-1, CH₂(H_α)-15, CH₂(H_β)-16, CH₂(H_β)-21); 1,67 (td, $^3J = 13,9$ et $6,8$, 1H, CH₂(H_α)-6); 1,74 (td, $^3J = 13,6$ et $7,0$, 1H, CH₂(H_α)-16); 1,90 (dd, $^3J = 12,0$ et $7,3$, 2H, CH₂-22); 2,03 (td, $^3J = 13,8$ et $4,8$, 1H, CH₂(H_β)-15); 2,27 (d, $^3J = 11,3$, 1H, CH-18); 2,58 (td, $^3J = 14,0$ et $6,4$, 2H, CH₂-2); 5,35 (tl, 1H, CH-12); 8,70 (sl, 1H, NH).

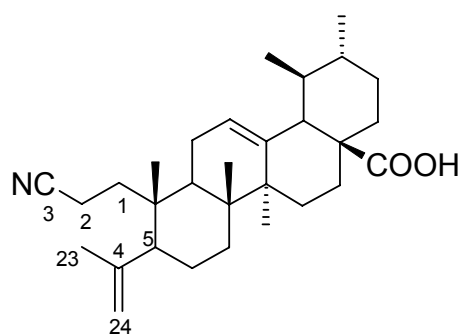
RMN ¹³C (125 MHz, CDCl₃), δ (ppm): 17,0 (C-25); 17,4 (C-26); 17,5 (C-29); 21,5 (C-30); 21,9 (C-6); 23,8 (C-11); 23,9 (C-27); 24,5 (C-24); 26,0 (C-16); 28,3 (C-15); 30,1 (C-2); 30,9 (C-21); 33,0 (C-7); 34,7 (C-23); 37,0 (C-22 et 10); 39,2 (C-19); 39,4 (C-20); 40,0 (C-8); 41,3 (C-1); 42,7 (C-14); 47,4 (C-17); 48,3 (C-9); 52,9 (C-18); 55,3 (C-5); 59,4 (C-4); 125,7 (C-12); 138,5 (C-13); 179,4 (C-3); 182,1 (C-28).

SMHR: calculé pour C₃₀H₄₇NO₃Na: 492,3454. Trouvé: 492,3466 (100%).

$[\alpha]_D^{20} = +33,2$ (CHCl₃, c 0,2)

pF: 180 °C .

VI.10.2. Composé 160



160

Cristaux blancs

C₃₀H₄₅NO₂

MM = 451 g/mol

IR (ATR, cm⁻¹): 2924 (OH acide); 2867 (C-H); 2246 (-CN); 1692 (C=O acide); 1635 (H₂C=C); 1454 (C-O).

RMN ^1H (500 MHz, CD_3OD), δ (ppm), J en Hz: 0,89 (s, 3H, CH_3 -26); 0,89-0,98 (m, 3H, CH_2 -11 et CH -20 superposé); 0,93 (d, $^3J = 6,3$, 3H, CH_3 -30); 0,99 (d, $^3J = 6,4$, 3H, CH_3 -29); 1,00 (s, 3H, CH_3 -25); 1,16 (s, 3H, CH_3 -27); 1,20 (m, 1H, $\text{CH}_{2(\text{H}\alpha)}$ -7); 1,35 (m, 1H, CH -19); 1,52 (m, 4H, $\text{CH}_{2(\text{H}\beta)}$ -6, $\text{CH}_{2(\text{H}\beta)}$ -7, CH -9, $\text{CH}_{2(\text{H}\alpha)}$ -21); 1,71 (m, 5H, $\text{CH}_{2(\text{H}\alpha)}$ -6, $\text{CH}_{2(\text{H}\alpha)}$ -15, CH_2 -16, $\text{CH}_{2(\text{H}\beta)}$ -21); 1,78 (s, 3H, CH_3 -23); 1,94 (dd, $^3J = 12,5$ et $7,3$, 2H, CH_2 -22); 2,07 (m, 2H, $\text{CH}_{2(\text{H}\beta)}$ -15, CH -18); 2,29 (m, 3H, CH_2 -1 et CH -5); 2,39 (m, 2H, CH_2 -2); 4,69 (d, $^2J = 0,8$, 1H, CH_2 -24); 4,95 (d, $^2J = 0,8$, 1H, CH_2 -24); 5,35 (tl, 1H, H-12).

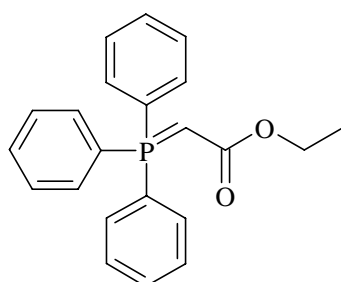
RMN ^{13}C (125 MHz, $\text{CD}_3\text{OH}-d_4$), δ (ppm): 12,0 (C-2); 17,4 (C-25); 17,5 (C-26 et C-29); 19,5 (C-6); 21,6 (C-30); 23,8 (C-11); 23,9 (C-27); 24,4 (C-16); 28,3 (C-15); 30,9 (C-21); 32,8 (C-7); 37,0 (C-22); 38,1(C-10); 39,2 (C-19); 39,6 (C-20); 39,8 (C-8); 41,5 (C-1); 42,9 (C-14); 46,9 (C-17); 48,4 (C-9); 51,1 (C-18); 53,1 (C-5); 114,6 (C-24) ; 120,6 (C-3); 125,9 (C-12); 138,7 (C-13); 147,2 (C-4); 183,2 (C-28).

SMHR: calculé pour $\text{C}_{30}\text{H}_{45}\text{NO}_2\text{Na}$: 474,3348. Trouvé: 474,3352 (100%).

$[\alpha]_{\text{D}}^{20} = +37,3$ (CHCl_3 , c 0,15)

pF : 130 °C

VI.11. Préparation de l'ylure d'éthoxycarbonylméthylène-triphenylphosphonium 169 (selon Seibum *et al.*, 2003)



169

Cristaux incolores

$\text{C}_{22}\text{H}_{21}\text{O}_2\text{P}$

$MM = 348$ g/mol

Ajouter, goutte-à-goutte une solution de bromoacétate d'éthyle (1,53 g, 10 mmol) dans de l'acétate d'éthyle distillé (10 mL) à une solution du triphenylphosphine (2,75 g, 10,5 mmol) dans de l'acétate d'éthyle (50 mL).

Agiter le mélange réactionnel pendant 12 heures à température ambiante. Filtrer le précipité formé, laver avec 10 mL d'acétate d'éthyle et sécher sur vide. Sécher la phase organique sur Na₂SO₄, filtrer et évaporer sur vide. Des cristaux incolores sont obtenus avec un **rendement de 80%**.

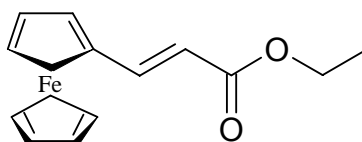
IR (ATR, cm⁻¹): 2976 et 2924 (C-H); 1603 (C=O); 1482 (C-O); 1370 (C-H); 1328 (C-O); 1024 (CH=C); 996 (CH=C).

RMN ¹H (500 MHz, CDCl₃), δ (ppm), *J* en Hz: 1,10 (t, ³*J*_{H,H} = 7,1, 3H, CH₃); 4,08 (q, ³*J*_{H,H} = 7,1, -OCH₂), 5,61 (d, ²*J*_{P,H} = 13,7, 1H, CH), 7,72 (*m*, 15H).

SMHR : calculé pour C₂₂H₂₂O₂P: 349,1357. Trouvé: 349,1370 (100%).

pF: 125 °C

VI.12. Préparation du 3-ferrocénylpropén-2-oate d'éthyle **167** (selon Debroy *et al.*, 2006)



167

Solide rouge

C₁₅H₁₆FeO₂

MM = 284 g/mol

Porter à reflux pendant 3 heures une solution du ferrocénecarboxaldéhyde (1,5 g, 7 mmol) et d'ethoxycarbonylméthylène-triphenylphosphorane **169** (3,15 g, 9 mmol) dans du toluène distillé (20 mL). Evaporer le solvant sous pression réduite. Dissoudre le résidu obtenu dans du dichlorométhane puis laver successivement avec de l'eau et avec une solution saturée du NaCl. Sécher la phase organique sur Na₂SO₄ et évaporer sur vide. Purifier le produit par chromatographie sur colonne de silice (éluant cyclohexane/AcOEt gradient 90 : 10). Un solide rouge est obtenu avec un **rendement de 51%**.

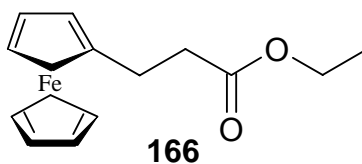
IR (ATR, cm^{-1}): 1701 (C=O), 1633 (C=C), 1438 (C-O); 1366 (C-H); 1313 (C-O); 1104 et 998 (Cp-ferrocène).

RMN ^1H (500 MHz, CDCl_3), δ (ppm), J en Hz: 1,34 (t, $^3J = 7,0$, 3H, CH_3); 4,17 (s, 5H, Cp'), 4,23 (q, $^3J = 7,0$, 2H, $-\text{OCH}_2$), 4,41 (sl, 2H, Cp), 4,49 (sl, 2H, Cp), 6,69 (d, $^3J_{trans} = 16,0$, 1H, $\underline{\text{CH}}=\text{CH}$), 7,57 (d, $^3J_{trans} = 16,0$, 1H, $\text{CH}=\underline{\text{CH}}$).

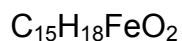
SMHR : calculé pour $\text{C}_{15}\text{H}_{16}\text{FeO}_2\text{Na}$: 307,0397. Trouvé: 307,0387 (100%).

pF : 76 °C.

VI.13. Préparation de 3-ferrocénylpropanoate d'éthyle **166** (selon Debroy *et al.*, 2006)



Huile orange



$MM = 286 \text{ g/mol}$

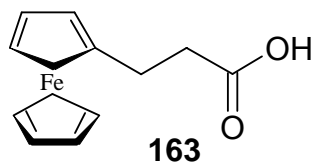
A une solution de 3-ferrocénylpropén-2-oate d'éthyle **167** (284 mg, 1 mmol) et de CuBr (215 mg, 1,5 mmol) dans du MeOH distillé (20 mL) à 0 °C, ajouter, petit à petit, pendant 30 minutes du NaBH_4 (378 mg, 10 mmol). Agiter le mélange réactionnel pendant 1 heure. La couleur passe du rouge au jaune et un précipité noir est observé. Oter le précipité par filtration, laver la phase organique avec une solution aqueuse d'acide chlorhydrique 5% et extraire par de l'éther éthylique (3 x 10 mL). Réunir les phases organiques, laver successivement par une solution aqueuse saturée de NaHCO_3 (3 x 10 mL) puis par de l'eau (3 x 10 mL). Sécher la phase organique sur Na_2SO_4 et évaporer sous vide. Une huile orange est obtenue avec un **rendement de 97%**.

IR (ATR, cm^{-1}): 1726 (C=O); 1632 (C=C), 1443 (C-O); 1103 et 999 (Cp-ferrocène).

RMN ^1H (500 MHz, CDCl_3), δ (ppm), J en Hz: 1,31 (t, 3H, $^3J = 7,1$ Hz, CH_3); 2,60 (sl, 4H, 2 x CH_2); 4,34 (s, 9H, Cp et Cp'); 4,39 (q, 2H, $^3J = 7,0$ Hz, $-\text{OCH}_2$).

SMHR : calculé pour $\text{C}_{15}\text{H}_{18}\text{FeO}_2$: 286,0656. Trouvé: 286,0648 (100%).

VI.14. Préparation de l'acide 3-ferrocénylpropanoïque 163 (selon Debroy *et al.*, 2006)



Solide jaune

$\text{C}_{13}\text{H}_{14}\text{FeO}_2$

$MM = 258$ g/mol

Dissoudre l'ester 3-ferrocénylpropanoate d'éthyle 166 (0,97 mmol, 277 mg) dans de l'éthanol absolu (2 mL) et ajouter 1,0 mL d'une solution aqueuse de NaOH 1N. Porter à reflux pendant 2 heures. Après évaporation du solvant organique, acidifier le milieu par une solution de l'acide chlorhydrique 6N. Filtrer le précipité formé, laver avec de l'eau et sécher sous vide. On obtient un solide jaune avec un **rendement de 82%**.

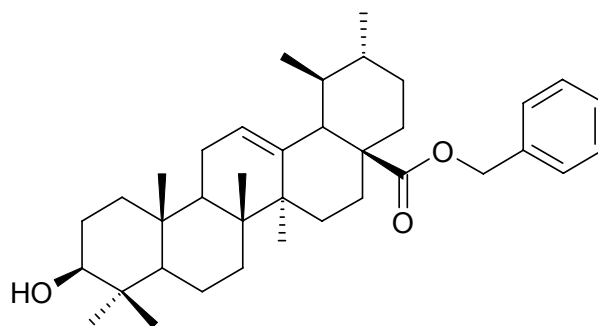
IR (ATR, cm^{-1}): 3929 (OH); 2851(C-H); 1704 (C=O), 1428 (C-O); 1343 (C-H); 1028 (C-O-H); 1104 et 1007 (Cp-ferrocène).

RMN ^1H (500 MHz, CDCl_3), δ (ppm), J en Hz: 2,64 (tl, 4H, 2 x CH_2); 4,34 (s, 9H, Cp et Cp').

SMHR : calculé pour $\text{C}_{13}\text{H}_{14}\text{FeO}_2\text{Na}$: 281,0241. Trouvé: 281,0237 (100%).

pF : 125 °C.

VI.15. Préparation de l'ursolate de benzyle 170

**170**

Solide blanc

 $C_{37}H_{54}O_3$ $MM = 546 \text{ g/mol}$

A une solution d'acide ursolique 1 (90 mg, 0,2 mmol) et de K_2CO_3 (25,2 mg, 0,2 mmol) dans du DMF distillé (2 mL), ajouter le chlorure de benzyle (22,9 μL , 0,2 mmol). Porter à reflux pendant 3 heures sous agitation et sous atmosphère d'azote. Filtrer, évaporer sous pression réduite et verser le résidu dans 2 mL d'une solution aqueuse du NaOH 1N. Extraire par de l'éther diéthylique (3 x 2 mL), sécher sur Na_2SO_4 et évaporer sous vide. Une poudre blanche est obtenue avec un **rendement de 94%**.

IR (ATR, cm^{-1}): 3599 (OH); 2866 (C-H); 1722 (C=O); 1457 (C-O); 1387 (C-H); 1260 (C-O-C); 1030 (C-O-H); 1011 (CH=C); 996 (CH=C).

RMN ^1H (500 MHz, CDCl_3), δ (ppm), J en Hz: 0,70 (s, 3H, CH_3 -25); 0,78 (1H, CH-5); 0,83 (sl, 4H, CH_3 -24 et $\text{CH}_{2(\text{H}\alpha)}$ -1 superposé); 0,90 (d, $^3J = 6,4$, 3H, CH_3 -30); 0,95 (s, 3H, CH_3 -26); 0,99 (d, $^3J = 6,3$, 3H, CH_3 -29); 1,04 (sl, 4H, CH_3 -23 et CH_2 -11 superposé); 1,11 (1H, CH-20); 1,13 (s, 3H, CH_3 -27); 1,33 (1H, $\text{CH}_{2(\text{H}\alpha)}$ -7); 1,36 (m, 3H, CH_2 -2, CH-19); 1,53 (m, 4H, $\text{CH}_{2(\text{H}\beta)}$ -6, $\text{CH}_{2(\text{H}\beta)}$ -7, CH-9, $\text{CH}_{2(\text{H}\alpha)}$ -21); 1,67 (m, 4H, $\text{CH}_{2(\text{H}\beta)}$ -1, $\text{CH}_{2(\text{H}\alpha)}$ -15, $\text{CH}_{2(\text{H}\beta)}$ -16, $\text{CH}_{2(\text{H}\beta)}$ -21); 1,75 (td, $^3J = 13,9$ et $6,8$, 1H, $\text{CH}_{2(\text{H}\alpha)}$ -6); 1,88 (td, $^3J = 13,6$ et $7,2$, 1H, $\text{CH}_{2(\text{H}\alpha)}$ -16); 1,93 (dd, $^3J = 16,7$ et $7,3$, 2H, CH_2 -22); 2,06 (td, $^3J = 13,2$ et $4,4$, 1H, $\text{CH}_{2(\text{H}\beta)}$ -15); 2,32 (d, $^3J = 11,3$, 1H, CH-18); 3,26 (dd, $^3J = 11,1$ et $4,7$, 1H, CH-3); 5,03 (d, $^2J = 12,4$, 1H, $-\text{CH}_2\text{-Bn}$); 5,16 (d, $^2J = 12,5$, 1H, $-\text{CH}_2\text{-Bn}$); 5,29 (tl, $^3J = 6,4$, 1H, CH-12); 7,39 (m, 5H, Bn).

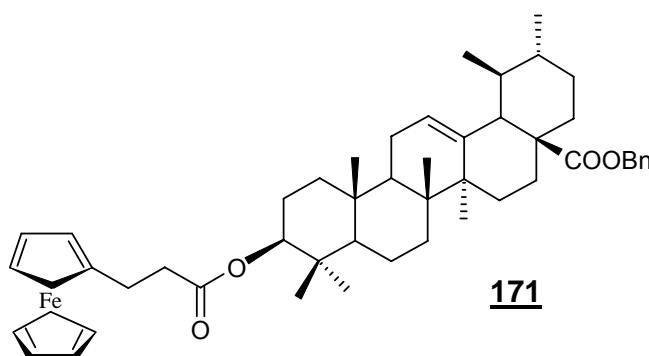
RMN ^{13}C (125 MHz, CDCl_3), δ (ppm): 15,8 (C-25); 16,0 (C-26); 16,9 (C-24); 17,4 (C-29); 18,7 (C-6); 21,6 (C-30); 23,7 (C-11); 23,9 (C-27); 24,7 (C-16); 27,6 (C-15); 28,4 (C-2); 28,5 (C-23); 31,1 (C-21); 33,4 (C-7); 37,0 (C-10); 37,4 (C-22); 39,0 (C-8); 39,2 (C-1); 39,3 (C-4); 39,5 (C-19); 39,9 (C-20); 42,5 (C-14); 47,9 (C-9); 48,5 (C-17); 53,3 (C-18); 55,6 (C-5); 66,4 ($-\text{CH}_2\text{-Bn}$); 79,5 (C-3); 126,1 (C-12); 128,3 (C-*mé*ta); 128,5 (C-*ortho*); 128,8 (C-*para*); 136,8 (C-*ipso*); 138,5 (C-13); 177,7 (C-28).

SMHR : calculé pour $\text{C}_{37}\text{H}_{54}\text{O}_3\text{Na}$: 569,3971. Trouvé: 569,3954 (100%).

$[\alpha]_{\text{D}}^{20} = +37,21$ (CHCl_3 , c 0,1)

pF: 62 °C.

VI.16. Préparation du 3-O- β -(3-ferrocénylpropanoyle)ursolate de benzyle 171



Solide rouge

$\text{C}_{50}\text{H}_{66}\text{FeO}_4$

$MM = 786$ g/mol

A une solution de l'acide 3-ferrocénylpropanoïque **163** (25,8 mg, 0,1 mmol) dans du CH_2Cl_2 distillé (1 mL) à 0°C ajouter, goutte-à-goutte, du chlorure d'oxalyle (17,3 μL , 0,2 mmol). Agiter le mélange réactionnel pendant 3 heures. Ajouter, goutte-à-goutte, une solution d'ursolate de benzyle **170** (81,15 mg, 0,15 mmol) dans du CH_2Cl_2 distillé (1 mL). Agiter le mélange réactionnel pendant 24 heures. Evaporer le solvant sous pression réduite. Une huile verte est obtenue. Purifier le produit par chromatographie sur colonne de silice (éluant CH_2Cl_2). Le produit est obtenu avec un **rendement de 51%**.

IR (ATR, cm^{-1}): 1726 (C=O); 1457 (C-O); 1363 (C-H); 1028 (C-O-H); 1106 et 1011 (Cp-ferrocène).

RMN ^1H (500 MHz, CDCl_3), δ (ppm), J en Hz: 0,67 (s, 3H, CH_3 -25); 0,87 (1H, CH-5); 0,90 (s, 6H, CH_3 -24 et CH_3 -26); 0,96 (m, 6H, CH_3 -29 et CH_3 -30); 0,98 (s, 3H, CH_3 -23); 1,10 (m, 2H, CH_2 -11 et CH-20 superposé); 1,18 (s, 3H, CH_3 -27); 1,23 (1H, $\text{CH}_{2(\text{H}\alpha)}$ -7); 1,27 (dd, $^3J = 11,8$ et $6,0$, 1H, CH-19); 1,31 (m, 2H, CH_2 -2); 1,43 (m, 4H, $\text{CH}_{2(\text{H}\beta)}$ -6, $\text{CH}_{2(\text{H}\beta)}$ -7, $\text{CH}_{2(\text{H}\alpha)}$ -9, $\text{CH}_{2(\text{H}\alpha)}$ -21); 1,60 (m, 4H, $\text{CH}_{2(\text{H}\beta)}$ -1, $\text{CH}_{2(\text{H}\alpha)}$ -15, $\text{CH}_{2(\text{H}\beta)}$ -16, $\text{CH}_{2(\text{H}\beta)}$ -21); 1,75 (m, 2H, CH_2 -6, $\text{CH}_{2(\text{H}\alpha)}$ -16); 1,90 (dd, $^3J = 12,8$ et $8,0$, 2H, CH_2 -22); 2,03 (td, $^3J = 13,6$ et $4,5$, $\text{CH}_{2(\text{H}\beta)}$ -15); 2,13 (d, $^3J = 11,3$, 1H, CH-18); 2,59 (t, $^3J = 7,5$, 2H, $-\text{CH}_2\text{CH}_2-$); 2,70 (t, $^3J = 7,0$, 2H, $-\text{CH}_2\text{CH}_2-$); 4,12 (d, $^3J = 10,4$, 4H, Cp'); 4,17 (s, 5H, Cp); 4,56 (dd, $^3J = 15,9$ et $4,6$, 1H, CH-3); 5,09 (d, $^3J = 12,6$, 1H, CH_2 -Bn); 5,12 (d, $^3J = 12,6$, 1H, CH_2 -Bn); 5,34 (tl, 1H, CH-12); 7,39 (m, 4H, Bn).

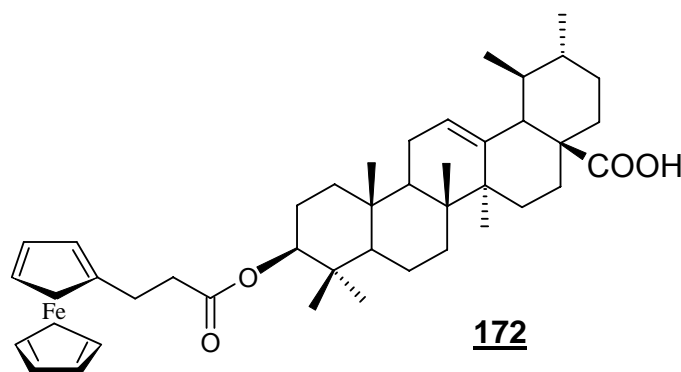
RMN ^{13}C (125 MHz, CDCl_3), δ (ppm): 15,9 (C-25); 17,3 (C-26); 17,4 (C-29); 18,6 (C-6); 21,6 (C-30); 23,7 (C-11); 23,9 (C-27); 24,1 (C-16); 24,6 (C-2); 25,5 (C-24); 27,3 (C-15); 28,4 (C-23); 31,1 (C-21); 33,4 (C-7); 37,0 (C-22); 37,3 (C-10); 38,2 (C-4); 38,7 (C-1); 39,2 (C-8); 39,5 (C-19); 39,9 (C-20); 42,4 (C-14); 47,9 (C-9); 48,5 (C-17); 53,3 (C-18); 55,7 (C-5); 66,3 ($-\text{CH}_2$ -Bn); 67,7 (2 x CH_2); 68,3 (Cp); 68,4 (Cp); 68,9 (Cp); 81,3 (C-3); 126,8 (C-12); 128,3 (C-*mé*ta); 128,4 (C-*ortho*); 128,8 (C-*para*); 136,9 (C-*ipso*); 138,5 (C-13); 173,3 (C=O); 177,8 (C-28).

SMHR : calculé pour $\text{C}_{50}\text{H}_{66}\text{FeO}_4$: 786,4311. Trouvé: 786,4282 (100%).

$[\alpha]_{\text{D}}^{20} = +48,6$ (CHCl_3 , c 0,2)

pF: 94 °C

VI.17. Préparation de l'acide 3-O-β-(3-ferrocénylpropanoyle)ursolique 172



Solide rouge



$MM = 696 \text{ g/mol}$

Mélanger dans un ballon du 3-O-β-(3-ferrocénylpropanoyle)ursolate de benzyle 171 (86 mg, 0,11 mmol) et du Pd/C 10% (quantité ??) dans 2 mL de MeOH distillé. Laisser sous agitation et atmosphère d'hydrogène pendant 4 jours. Filtrer (sur célite) et évaporer le filtrat. Un solide rouge est obtenu avec un **rendement de 42%**.

IR (ATR, cm^{-1}): 2924 (OH acide); 2857 (C-H); 1729 (C=O); 1688 (C=O); 1457 (C-O); 1368 (C-H); 1315 (C-O); 1031 (C-O-H); 1101 et 1000 (Cp-ferrocène).

RMN ^1H (500 MHz, CDCl_3), δ (ppm), J en Hz: 0,81 (1H, CH-5); 0,84 (s, 3H, CH_3 -25); 0,91 (s, 6H, CH_3 -24 et CH_3 -26); 0,93 (d, $^3J = 6,3$, 3H, CH_3 -30); 0,98 (d, $^3J = 6,3$, 3H, CH_3 -29); 1,00 (s, 3H, CH_3 -23); 1,10 (m, 2H, CH_2 -11 et CH-20 superposé); 1,14 (s, 3H, CH_3 -27); 1,19 (m, 1H, CH_2 -7); 1,31 (m, 2H, CH_2 -2); 1,36 (m, 1H, CH-19); 1,43 (m, 4H, $\text{CH}_2(\text{H}\beta)$ -6, CH_2 -7, CH-9, $\text{CH}_2(\text{H}\alpha)$ -21); 1,59 (m, 4H, $\text{CH}_2(\text{H}\beta)$ -1, $\text{CH}_2(\text{H}\alpha)$ -15, $\text{CH}_2(\text{H}\beta)$ -16, $\text{CH}_2(\text{H}\beta)$ -21); 1,73 (m, 2H, CH_2 -6, $\text{CH}_2(\text{H}\alpha)$ -16); 1,97 (dd, $^3J = 12,6$ et $6,6$, 2H, CH_2 -22); 2,05 (td, $^3J = 14,6$ et $4,5$, $\text{CH}_2(\text{H}\beta)$ -15); 2,23 (d, $^3J = 11,3$, 1H, CH-18); 2,59 (t, $^3J = 7,5$, 2H, $-\text{CH}_2\text{CH}_2$); 2,72 (t, $^3J = 7,0$, 2H, $-\text{CH}_2\text{CH}_2$); 4,12 (d, $^3J = 10,4$, 4H, Cp); 4,17 (s, 5H, Cp); 4,56 (dd, $^3J = 15,9$ et $5,6$, 1H, CH-3); 5,34 (tl, 1H, H-12).

RMN ^{13}C (125 MHz, CDCl_3), δ (ppm): 15,9 (C-25); 17,2 (C-26); 17,4 (C-29); 18,6 (C-6); 21,6 (C-30); 23,7 (C-11); 23,8 (C-27); 24,0 (C-16); 25,4 (C-24) 27,3 (C-15); 24,5 (C-2); 28,4 (C-23); 31,0 (C-21); 33,3 (C-7); 37,1 (C-22); 37,3 (C-

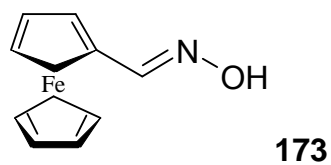
10); 39,2 (C-8); 38,2 (C-4); 38,7 (C-1); 39,4 (C-19); 39,9 (C-20); 42,4 (C-14); 47,9 (C-9); 48,3 (C-17); 53,0 (C-18); 55,7 (C-5); 67,7 (2 x CH₂); 68,3 (Cp); 68,4 (Cp); 68,9 (Cp); 81,3 (C-3); 126,2 (C-12); 138,4 (C-13); 173,4 (C=O); 182,8 (C-28).

SMHR : calculé pour C₄₃H₆₀FeO₄: 696,3841. Trouvé: 696,3810 (100%).

[α]_D²⁰ = +56,3 (CHCl₃, c 0,1)

pF: 110 °C

VI.18. Préparation de l'oxime du ferrocénylcarboxaldéhyde 173 (selon Baramee *et al.*, 2006)



Poudre orange

C₁₁H₁₁ONFe

MM = 229 g/mol

Chauffer à reflux, pendant 3 heures, une solution de ferrocèncarboxaldéhyde (500 mg, 2,3 mmol), de NaOH (550 mg, 14,7 mmol) et de chlorhydrate d'hydroxylamine (650 mg, 9,3 mmol) dans de l'éthanol distillé (25 mL). Ajouter de l'eau (25 mL), agiter pendant 1 heure trente puis extraire par du CH₂Cl₂ (3 x 10 mL). Réunir les phases organiques, sécher sur Na₂SO₄ et évaporer sous vide. Une poudre orange est obtenue avec un **rendement de 98,5%**.

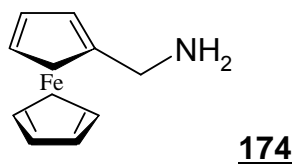
IR (ATR, cm⁻¹): 3209 (OH); 2926 (C-H); 2856 (C-H); 1648 (C=N); 1565 (C=C); 1106 et 1001 (Cp-ferrocène).

RMN ¹H (500 MHz, CDCl₃), δ (ppm), J en Hz: 4,28 (s, 5H, Cp'-ferrocène); 4,39 (m, 2H, Cp-ferrocène); 4,60 (m, 2H, Cp-ferrocène); 8,06 (s, 1H, CH=N).

SMHR: calculé pour C₁₁H₁₂ONFe: 230,01245. Trouvé: 230,0141 (100%).

pF: 105 °C

VI.19. Préparation de la Ferrocénylméthylamine 174 (selon Baramée *et al.*, 2006)



Poudre orange

$C_{11}H_{13}NFe$

$MM = 215 \text{ g/mol}$

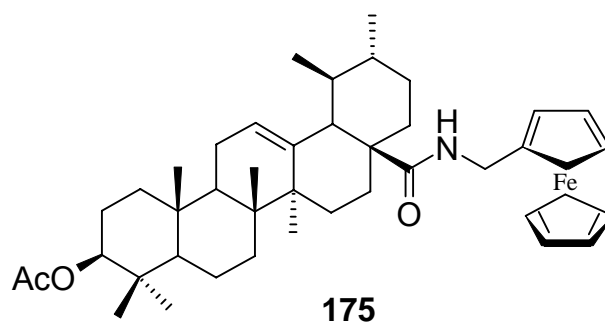
A une solution de l'oxime du ferrocénylcarboxaldéhyde 173 (400 mg, 1,75 mmol) dans du THF distillé (10 mL) à 0 °C, sous atmosphère d'azote, ajouter, petit à petit, du $LiAlH_4$ (351 mg, 9,24 mmol). Chauffer à reflux pendant 6 heures. Ajouter 0,7 mL d'une solution aqueuse du NaOH 1N et de l'eau (1,05 mL). Agiter pendant 1 heure trente et extraire par de l'éther diéthylique (3 x 10 mL). Réunir les phases organiques, sécher sur Na_2SO_4 et évaporer sous vide. Une huile orange est obtenue avec un **rendement de 65%**.

IR (ATR, cm^{-1}): 3085 (NH_2); 2925 (C-H); 2853 (C-H); 1565 (C=C); 1105 et 1001 (Cp-ferrocène).

RMN 1H (500 MHz, $CDCl_3$), δ (ppm), J en Hz: 1,58 (sl, 2H, NH_2); 3,60 (s, 2H, CH_2), 4,17 (s, 5H, Cp'-ferrocène); 4,20 (m, 2H, Cp-ferrocène); 4,22 (m, 2H, Cp-ferrocène).

pF: 80 °C.

VI.20. Préparation du *N*-ferrocénylméthyle-3-*O*-acétylursolamide **175**



Huile jaune

 $C_{43}H_{60}NO_3Fe$ $MM = 694 \text{ g/mol}$

A une solution d'acide 3-acétylursolique **154** (49,6 mg, 0,1 mmol) dans du CH_2Cl_2 distillé (1mL) sous atmosphère d'azote et à 0°C, ajouter, goutte-à-goutte, du chlorure d'oxalyle (26 μ L, 0,3 mmol). Agiter le milieu réactionnel pendant 3 heures à température ambiante. Porter à 0°C et ajouter la TEA (84 μ L, 0,6 mmol) et l'amine **174** (64,5 mg, 0,3 mmol). Agiter le milieu réactionnel pendant 24 heures à température ambiante. Ajouter 1 mL d'eau et extraire par du CH_2Cl_2 (3 x 3mL). Réunir les phases organiques, sécher sur Na_2SO_4 et évaporer sous vide. Purifier l'huile jaune obtenue par chromatographie sur colonne de silice (éluant CH_2Cl_2 : MeOH, gradient 95 : 05). Le produit est obtenu avec un **rendement de 100%**.

IR (ATR, cm^{-1}): 3096 (NH); 2870 (C-H); 1731 (C=O acétyle); 1648 (C=O amide); 1508 (C=C); 1457 (C-O); 1368 (C-H); 1243 (C-N); 1106 et 1001 (Cp-ferrocène); 1025 (C-O-H).

RMN 1H (500 MHz, $CDCl_3$), δ (ppm), J en Hz: 0,76 (1H, CH-5); 0,83 (d, $^3J = 6,5$, 3H, CH_3 -30); 0,91 (d, $^3J = 6,3$, 3H, CH_3 -29); 0,93 (1H, CH_2 -1); 0,97 (s, 3H, CH_3 -25); 0,95 (1H, CH_2 -11); 1,00 (sl, 4H, CH_3 -24, CH-20); 1,03 (s, 3H, CH_3 -23); 1,05 (s, 3H, CH_3 -26); 1,13 (s, 3H, CH_3 -27); 1,21 (m, 1H, $CH_{2(H\alpha)}$ -7); 1,38 (m, 3H, CH-19 et CH_2 -2); 1,48 (m, 4H, $CH_{2(H\beta)}$ -6, $CH_{2(H\beta)}$ -7, CH-9, $CH_{2(H\alpha)}$ -21); 1,60 (m, 4H, $CH_{2(H\beta)}$ -1, $CH_{2(H\alpha)}$ -15, $CH_{2(H\beta)}$ -16, $CH_{2(H\beta)}$ -21); 1,69 (m, 1H, $CH_{2(H\alpha)}$ -6); 1,78 (td, $^3J = 14,0$ et 7,2, 1H, $CH_{2(H\alpha)}$ -16); 1,91 (d, $^3J = 10,3$, 1H, CH-18); 1,99 (m, 3H, $CH_{2(H\beta)}$ -15, CH_2 -22); 2,04 (s, 3H, H_3C COO); 3,92 (d, $^2J = 13,4$, 1H, CH_2 -

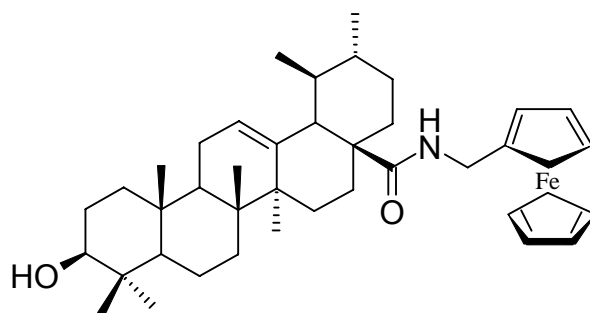
ferrocène); 4,23 (m, 11H, Cp-ferrocène, CH₂-ferrocène, CH-3); 5,31 (tl, 1H, CH-12); 6,10 (s, 1H, NH).

RMN ¹³C (125 MHz, CDCl₃), δ (ppm): 16,2 (C-25); 17,1 (C-26); 17,4 (C-24); 17,9 (C-29); 18,6 (C-6); 21,6 (C-30); 21,7 (H₃CCOO); 23,7 (C-11); 23,9 (C-27); 24,2 (C-2); 25,4 (C-16); 28,4 (C-23); 28,5 (C-15); 31,3 (C-21); 33,2 (C-7); 37,3 (C-10); 37,7 (C-22); 38,1 (C-4); 38,7 (C-1); 39,8 (C-19); 39,9 (C-20); 40,1 (C-8); 43,0 (C-14); 47,9 (C-9 et C-17); 53,4 (C-18); 55,7 (C-5); 69,1 (Cp); 69,6 (Cp'); 70,0 (Cp et CH₂-ferrocène); 81,3 (C-3); 125,9 (C-12); 139,0 (C-13); 171,8 (H₃CCOO); 178,2 (C-28).

SMHR: calculé pour C₄₃H₆₁NO₃Fe: 695,4001. Trouvé: 695,4020 (100%).

[α]_D²⁰ = +53,6 (CHCl₃, c 0,2).

VI.21. Préparation de *N*-ferrocénylmethylursolamide **176**



176

Poudre jaune

C₄₁H₅₈NO₂Fe

MM = 652 g/mol

Ce composé a été synthétisé selon la **Méthode Générale VI.3.3. Réaction de déprotection d'une fonction alcool protégée par un groupement acétyle**, à partir du *N*-ferrocénylméthyle-3-*O*-acétylursolamide **175**. Le produit est obtenu avec un **rendement de 72%**.

IR (ATR, cm⁻¹): 3096 (NH et OH); 2868 (C-H); 1638 (C=O amide); 1518 (C=C); 1457 (C-O); 1377 (C-H); 1271 (C-N); 1106 et 999 (Cp-ferrocène).

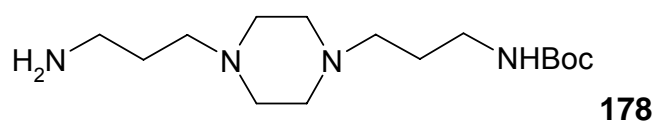
RMN ^1H (500 MHz, CDCl_3), δ (ppm), J en Hz: 0,77 (1H, CH-5); 0,83 (d, $^3J = 6,5$, 3H, CH_3 -30); 0,91 (d, $^3J = 6,3$, 3H, CH_3 -29); 0,93 (m, 1H, CH_2 -1); 0,97 (s, 3H, CH_3 -25); 0,95 (m, 1H, CH_2 -11); 1,00 (sl, 4H, CH_3 -24, CH-20); 1,04 (s, 3H, CH_3 -23); 1,05 (s, 3H, CH_3 -26); 1,14 (s, 3H, CH_3 -27); 1,21 (m, 1H, $\text{CH}_2(\text{H}\alpha)$ -7); 1,38 (m, 3H, CH-19 et CH_2 -2); 1,48 (m, 4H, $\text{CH}_2(\text{H}\beta)$ -6, $\text{CH}_2(\text{H}\beta)$ -7, CH-9, $\text{CH}_2(\text{H}\alpha)$ -21); 1,59 (m, 4H, $\text{CH}_2(\text{H}\beta)$ -1, $\text{CH}_2(\text{H}\alpha)$ -15, $\text{CH}_2(\text{H}\beta)$ -16, $\text{CH}_2(\text{H}\beta)$ -21); 1,69 (m, 1H, $\text{CH}_2(\text{H}\alpha)$ -6); 1,78 (td, $^3J = 14,0$ et $6,0$, 1H, $\text{CH}_2(\text{H}\alpha)$ -16); 1,91 (d, $^3J = 10,3$, 1H, CH-18); 2,00 (m, 3H, $\text{CH}_2(\text{H}\beta)$ -15, CH_2 -22); 3,26 (dd, $^3J = 12,0$ et $5,5$, 1H, CH-3); 3,92 (d, $^2J = 13,4$, 1H, CH_2 -ferrocène); 4,23 (m, 10H, Cp-ferrocène, CH_2 -ferrocène); 5,35 (tl, 1H, CH-12); 6,10 (sl, 1H, NH).

RMN ^{13}C (125 MHz, CDCl_3), δ (ppm): 16,0 (C-25 et C-26); 17,5 (C-24); 17,8 (C-29); 18,7 (C-6); 21,7 (C-30); 23,7 (C-11); 23,8 (C-27); 25,3 (C-16); 27,5 (C-2); 28,2 (C-23); 28,5 (C-15); 31,3 (C-21); 33,1 (C-7); 37,3 (C-10); 37,7 (C-22); 38,9 (C-1); 39,3 (C-4); 39,6 (C-19); 39,9 (C-20); 40,1 (C-8); 42,9 (C-14); 47,9 (C-9) 48,0 (C-17); 54,5 (C-18); 55,5 (C-5); 68,2 (Cp); 68,5 (Cp'); 69,2 (Cp et CH_2 -ferrocène); 79,3 (C-3); 126,0 (C-12); 140,4 (C-13); 177,7 (C-28).

$[\alpha]_{\text{D}}^{20} = +50,1$ (CHCl_3 , c 0,3).

pF : 148 °C

VI.22. Préparation de la 3-[4-(3-aminopropyl)piperaziny]propyl]carbamate de terbutyle 178



Huile jaune transparente

$\text{C}_{15}\text{H}_{32}\text{N}_4\text{O}_2$

MM= 300 g/mol

Ajouter, goutte-à-goutte, une solution de Boc_2O (293 mg, 1,3 mmol) dans du MeOH distillé (2,5 mL) à une solution de 1,4-bis(3-aminopropyl)piperazine (444 mg, 2,2 mmol) dans du MeOH distillé (5 mL) à 0°C. Agiter le milieu réactionnel pendant 48 heures à température ambiante. Après l'évaporation du solvant, dissoudre le solide blanc obtenu dans l'éther diéthylique. Extraire la phase

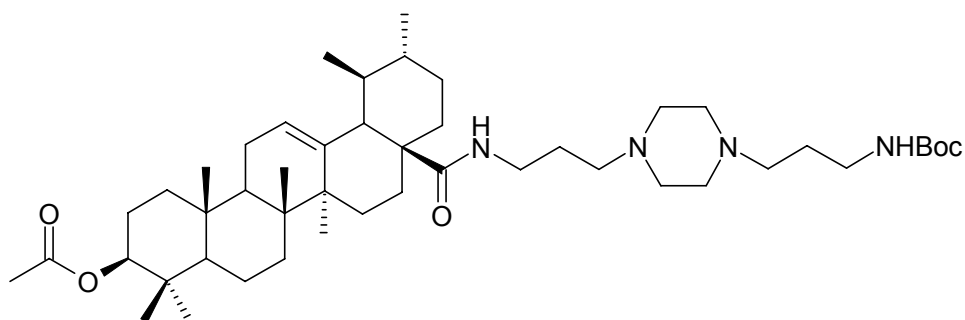
organique par une solution aqueuse d'acide citrique 5% (3 x 5 mL) et laver la phase aqueuse par de l'acétate d'éthyle. Alcaliniser la phase aqueuse par une solution aqueuse saturée de Na₂CO₃ jusqu'à pH = 11 et extraire de nouveau par de l'acétate d'éthyle (3 x 5 mL). Réduire le volume de la phase aqueuse jusqu'à 2 mL et réaliser une nouvelle extraction par de l'acétate d'éthyle (3 x 5 mL). Sécher cette dernière phase organique sur Na₂SO₄ et évaporer sous vide. Le produit est obtenu avec un **rendement de 28%**.

IR (ATR, cm⁻¹): 3365 (NH₂); 2940 (C-H); 2813 (C-H); 1685 (C=O); 1390 (C-H); 1250 (C-O-C).

RMN ¹H (500 MHz, CDCl₃), δ (ppm), *J* en Hz: 1,48 (s, 9H, CH₃-Boc); 1,72 (m, 4H, CH₂-c et CH₂-c'); 2,50 (m, 12H, CH₂-a1, CH₂-a1', CH₂-a2, CH₂-a2', CH₂-b et CH₂-b'); 2,80 (t, ³*J* = 6,9, 2H, CH₂-d); 3,12 (t, ³*J* = 6,7, 2H, CH₂-d').

SMHR: calculé pour C₁₅H₃₃N₄O₂: 301,2604. Trouvé: 301,2622 (100%).

VI.23. Préparation du *N*-{3-[4-(3-aminopropyl)piperazino]propyl}carbamate de *tert*-butyle-3-*O*-acétylursolamide 179



179

Poudre blanche

C₄₇H₈₀N₄O₅

MM = 780 g/mol

À une solution d'acide 3-*O*-acétylursolique 154 (1,48 g, 3 mmol) dans du CH₂Cl₂ distillé (30 mL) à 0°C, ajouter, goutte-à-goutte, du chlorure d'oxalyle (7,8 mL, 9 mmol). Agiter le milieu réactionnel pendant 3 heures à température ambiante. Ajouter de la TEA (25 mL, 18 mmol) et du *N*-*t*-butoxycarbonyl-1,4-bis(3-aminopropyl)piperazine 178 (2,7 g, 9 mmol). Agiter le milieu réactionnel pendant 24 heures à température ambiante. Puis, ajouter de l'eau (10 mL) et extraire la phase aqueuse par du CH₂Cl₂ (3 x 30 mL). Réunir les phases

organiques, sécher sur Na₂SO₄ et évaporer sous vide. Le produit est obtenu avec un **rendement de 80%**.

IR (ATR, cm⁻¹): 3325 (NH); 2873 (C-H); 2807 (C-H); 1731 (C=O acétyle); 1683 (C=O amides); 1640 (C=C); 1460 (C-O); 1365 (C-H); 1310 (C-O-C); 1245 (C-N); 1010 (CH=C).

RMN ¹H (500 MHz, CDCl₃), δ (ppm), *J* en Hz: 0,79 (d, ³*J* = 6,9 3H, CH₃-30); 0,86 (1H, CH-5); 0,89 (d, ³*J* = 5,2, 3H, CH₃-29); 0,93 (m, 1H, CH₂(H_α)-1); 0,94 (s, 3H, CH₃-25); 0,96 (1H, CH₂-20); 0,98 (s, 3H, CH₃-24); 1,00 (s, 6H, CH₃-26 et CH₃-23); 1,12 (s, 3H, CH₃-27); 1,19 (m, 1H, CH₂(H_α)-7); 1,33 (m, 3H, CH₂-2, CH-19); 1,48 (s, 9H, CH₃-Boc); 1,56 (m, 4H, CH₂(H_β)-6, CH₂(H_β)-7, CH-9, CH₂(H_α)-21); 1,66 (m, 10H, CH₂(H_β)-1, CH₂(H_α)-6, CH₂(H_α)-15, CH₂-16, CH₂(H_β)-21, CH₂-c, CH₂-c'); 1,83 (m, 2H, CH₂-22); 1,99 (m, 1H, CH₂(H_β)-15); 2,10 (s, 3H, H₃C₃COO); 2,56 (m, 13H, CH₂-a1, CH₂-a1', CH₂-a2, CH₂-a2'; CH₂-b, CH₂-b', CH-18); 3,23 (m, 2H, CH₂-d'); 3,49 (m, 2H, CH₂-d); 4,54 (dd, ³*J* = 11,6 et 6,5, 1H, CH-3); 5,35 (tl, 1H, CH-12); 6,56 (1H, NH).

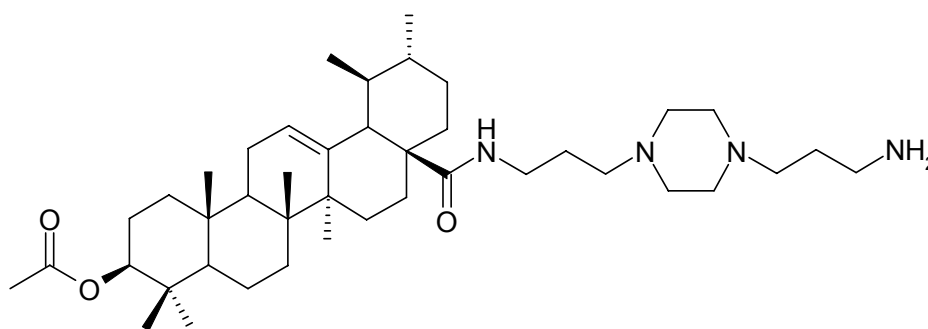
RMN ¹³C (125 MHz, CDCl₃), δ (ppm): 15,9 (C-25), 17,2 (C-26); 17,3 (C-26); 17,8 (C-29); 18,5 (C-6); 21,7 (C-30); 21,8 (H₃C₃COO); 23,8 (C-11); 23,9 (C-27); 24,1 (C-2); 25,1 (C-16); 26,0 (C-c); 28,2 (C-23); 28,5 (C-15), 28,9 (3 x CH₃-Boc); 31,2 (C-21); 33,0 (C-7); 34,4 (C-c'); 37,2 (C-10); 37,8 (C-22); 38,1 (C-4); 38,6 (C-1); 39,2 (C-d); 39,4 (C-19); 39,9 (C-20); 40,0 (C-8); 42,7 (C-14); 47,8 (C-9); 47,9 (C-17); 53,4 (C-a1, C-a1', C-a2, C-a2'); 53,7 (C-d'); 53,9 (C-18); 55,6 (C-5); 57,1 (C-b); 57,6 (C-b'); 79,3 (Cq-Boc); 81,2 (C-3); 125,7 (C-12); 140,0 (C-13); 156,5 (C=O-Boc); 171,6 (H₃C₃COO); 178,3 (C-28).

SMHR: calculé pour C₄₇H₈₁N₄O₅: 781,6207. Trouvé: 781,6224 (100%).

[α]_D²⁰ = +60,5 (CHCl₃, c 0,1)

pF: 152 °C

VI.24. Préparation du *N*-{3-[4-(3-aminopropyl)piperazinyl]propyl}-3-*O*-acétylursolamide **179**

**179**

Poudre blanche

 $C_{42}H_{73}N_4O_3$ $MM = 680 \text{ g/mol}$

Ce composé a été synthétisé selon la **Méthode Générale VI.3.2. Réactions de déprotection d'une fonction amine protégée par un groupement Boc**, à partir du *N*-[*N*-*t*-butoxycarbonyl-1,4-bis(3-aminopropyl)piperazinyl]-3-*O*-acétylursolamide **178**. Le produit est obtenu avec un **rendement de 72%**.

IR (ATR, cm^{-1}): 3325 (NH_2); 2873 (C-H); 2807 (C-H); 1731 (C=O acétyle); 1683 (C=O amide); 1637 (C=C); 1462 (C-O); 1367 (C-H); 1308 (C-O-C); 1245 (C-N); 1008 (CH=C).

RMN ^1H (500 MHz, CDCl_3), δ (ppm), J en Hz: 0,81 (d, $^3J = 6,9$, 3H, CH_3 -30); 0,87 (1H, CH-5); 0,91 (d, $^3J = 6,6$, 3H, CH_3 -29); 0,93 (m, 1H, $\text{CH}_{2(\text{H}\alpha)}$ -1); 0,94 (s, 3H, CH_3 -25); 0,96 (1H, CH_2 -20); 0,94 (m, 1H, CH-11); 0,99 (s, 3H, CH_3 -24); 1,00 (s, 3H, CH_3 -23) 1,01 (s, 3H, CH_3 -26); 1,14 (s, 3H, CH_3 -27); 1,21 (m, 1H, $\text{CH}_{2(\text{H}\alpha)}$ -7); 1,33 (m, 1H, CH-19); 1,41 (m, 2H, CH_2 -2); 1,55 (m, 4H, $\text{CH}_{2(\text{H}\beta)}$ -6, $\text{CH}_{2(\text{H}\beta)}$ -7, CH-9, $\text{CH}_{2(\text{H}\alpha)}$ -21); 1,62 (m, 4H, $\text{CH}_{2(\text{H}\beta)}$ -1, $\text{CH}_{2(\text{H}\alpha)}$ -15, $\text{CH}_{2(\text{H}\beta)}$ -16, $\text{CH}_{2(\text{H}\beta)}$ -21); 1,70 (m, 5H, CH_2 -c, CH_2 -c' et $\text{CH}_{2(\text{H}\alpha)}$ -6); 1,77 (td, $^3J = 14,0$ et 6,6, 1H, $\text{CH}_{2(\text{H}\alpha)}$ -16); 1,83 (m, 2H, CH_2 -22); 2,00 (m, 1H, $\text{CH}_{2(\text{H}\beta)}$ -15); 2,10 (s, 3H, H_3CCOO); 2,51 (m, 13H, CH_2 -a1, CH_2 -a1', CH_2 -a2, CH_2 -a2'; CH_2 -b, CH_2 -b' et CH-18); 3,03 (m, 2H, CH_2 -d'); 3,49 (m, 2H, CH_2 -d); 4,54 (dd, $^3J = 13,8$ et 6,4, 1H, CH-3); 5,34 (tl, 1H, CH-12); 6,46 (sl, 1H, NH).

RMN ^{13}C (125 MHz, CDCl_3), δ (ppm): 15,9 (C-25), 17,1 (C-26); 17,3 (C-24); 17,6 (C-29); 18,6 (C-6); 21,7 (C-30; H_3CCOO); 23,8 (C-11); 23,9 (C-27); 24,1

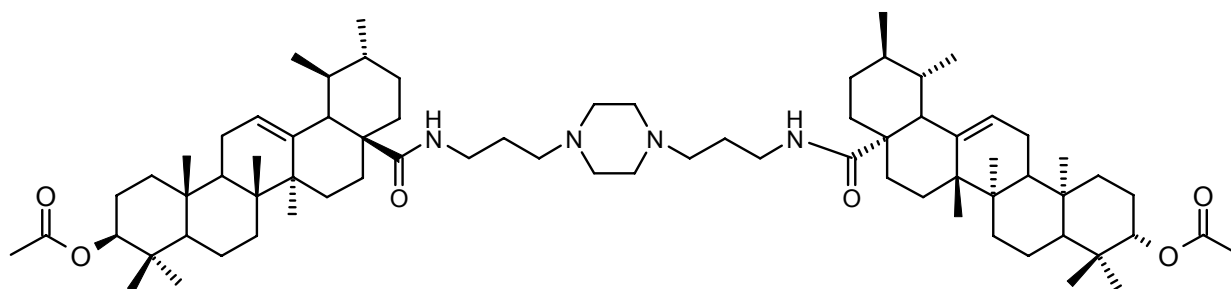
(C-2); 25,1 (C-16); 26,2 (C-c); 28,2 (C-23); 28,5 (C-15); 31,2 (C-21); 31,8 (C-c'); 33,1 (C-7); 37,2 (C-10); 37,8 (C-22); 38,1 (C-4) ; 38,5 (C-1); 39,2 (C-d); 39,4 (C-19); 39,9 (C-20); 40,0 (C-8); 40,2 (C-d'); 42,6 (C-14); 47,8 (C-9); 47,9 (C-17); 53,4 (C-18); 54,7 (C-a1, C-a1', C-a2, C-a2'); 55,6 (C-b et C-b'); 55,7 (C-5); 81,2 (C-3); 123,1 (C-12); 139,5 (C-13); 171,4 (H₃CCOO); 179,5 (C-28).

SMHR: calculé pour C₄₂H₇₃N₄O₃: 681,5683. Trouvé: 681,5667 (100%).

$[\alpha]_D^{20} = +54,5$ (CHCl₃, c 0,1)

pF: 138 °C

VI.25. Préparation du 4-[[3-(4-{3-[(3-O-acétylursolamide)amino]propyl}-piperazinyl)propyl]-3-O-acétylursolamide 181



181

Huile transparente

C₇₄H₁₂₀N₄O₆

MM = 1160 g/mol

À une solution d'acide 3-O-acétylursolique 154 (99,2 g, 0,2 mmol) dans du CH₂Cl₂ distillé (1 mL) ajouter, goutte-à-goutte, du chlorure d'oxalyle (26 µL, 0,3 mmol). Agiter le milieu réactionnel pendant 3 heures à température ambiante. Puis ajouter du TEA (84 µL, 0,6 mmol) et du 1,4-bis(3-aminopropyl)piperazine (120 mg, 0,6 mmol). Agiter le milieu réactionnel pendant 24 heures à température ambiante. Ajouter de l'eau (1 mL) et extraire la phase aqueuse par du CH₂Cl₂ (3 x 3 mL). Réunir les phases organiques, sécher sur Na₂SO₄ et évaporer sous vide. Le produit est obtenu avec un **rendement de 18%**.

IR (ATR, cm⁻¹): 3032 (N-H); 2880 (C-H); 2803 (C-H); 1732 (C=O acétyle); 1682 (C=O amide); 1637 (C=C); 1462 (C-O); 1366 (C-H); 1305 (C-O-C); 1245 (C-N); 1006 (CH=C).

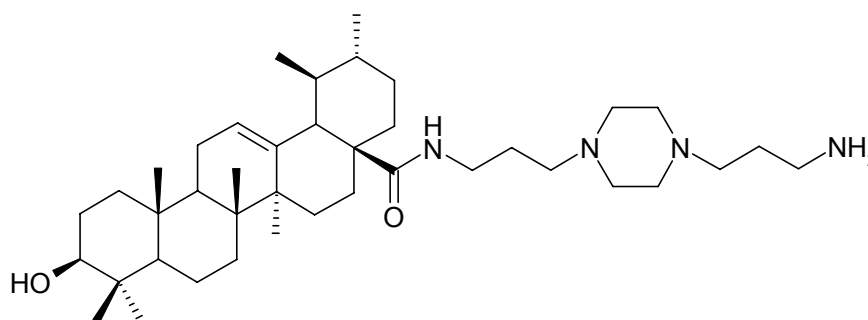
RMN ^1H (500 MHz, CDCl_3), δ (ppm), J en Hz: 0,81(m, 6H, 2 x CH_3 -30 et 2H, 2 x CH -5); 0,91 (d, $^3J = 6,0$, 6H, 2 x CH_3 -29); 0,93 (m, 2H, 2 x CH_2 -1); 0,95 (s, 6H, 2 x CH_3 -25); 0,96 (m, 2H, 2 x CH -20); 0,94 (m, 2H, 2 x CH -11); 0,99 (s, 6H, 2 x CH_3 -24); 1,00 (s, 6H, 2 x CH_3 -23) 1,01 (s, 6H, 2 x CH_3 -26); 1,14 (s, 6H, 2 x CH_3 -27); 1,20 (m, 2H, 2 x CH_{α} -7); 1,32 (m, 2H, 2 x CH -19); 1,43 (m, 4H, 2 x CH_2 -2); 1,54 (m, 8H, 2 x $\text{CH}_{2(\text{H}\beta)}$ -6, 2 x $\text{CH}_{2(\text{H}\beta)}$ -7, 2 x CH -9, 2 x $\text{CH}_{2(\text{H}\alpha)}$ -21); 1,63 (m, 8H, 2 x $\text{CH}_{2(\text{H}\beta)}$ -21, 2 x $\text{CH}_{2(\text{H}\beta)}$ -16, 2 x $\text{CH}_{2(\text{H}\beta)}$ -1, 2 x $\text{CH}_{2(\text{H}\alpha)}$ -15); 1,70 (m, 6H, CH_2 -c, CH_2 -c' et 2 x $\text{CH}_{2(\text{H}\alpha)}$ -6); 1,77 (m, 2H, 2 x $\text{CH}_{2(\text{H}\alpha)}$ -16); 1,85 (m, 4H, 2 x CH_2 -22); 2,00 (m, 2H, 2 x $\text{CH}_{2(\text{H}\beta)}$ -15); 2,10 (s, 6H, 2 x H_3CCOO); 2,51 (m, 14H, CH_2 -a1, CH_2 -a1', CH_2 -a2, CH_2 -a2', CH_2 -b, CH_2 -b' et 2 x CH -18); 3,09 (m, 4H, CH_2 -d', CH_2 -d); 4,54 (m, 2H, 2 x CH -3); 5,34 (tl, 2H, 2 x CH -12); 6,46 (sl, 2H, 2 x NH).

RMN ^{13}C (125 MHz, CDCl_3), δ (ppm): 15,9 (C-25), 17,1 (C-26); 17,5 (C-24); 17,7 (C-29); 18,6 (C-6); 21,6 (C-30; H_3CCOO); 23,7 (C-11); 23,9 (C-27); 24,1 (C-2); 25,3 (C-16); 26,0 (C-c et C-c'); 28,1 (C-23); 28,5 (C-15); 31,2 (C-21); 33,1 (C-7); 37,4 (C-10); 37,7 (C-22); 37,8 (C-4); 38,5 (C-1); 39,1 (C-d et C-d'); 39,5 (C-19); 39,7 (C-20); 39,8 (C-8); 42,6 (C-14); 47,8 (C-9); 48,2 (C-17); 53,0 (C-18); 54,7 (C-a1, C-a1', C-a2, C-a2'); 55,6 (C-5); 57,5 (C-b et C-b'); 81,2 (C-3); 123,1 (C-12); 140,1 (C-13); 171,3 (H_3CCOO); 178,9 (C-28).

SM: 1162,06 trouvé pour $\text{C}_{74}\text{H}_{120}\text{N}_4\text{O}_6$ $[\text{M}+2\text{H}]^+$

$[\alpha]_{\text{D}}^{20} = +26$ (CHCl_3 , c 0,15)

VI.26. Préparation du composé *N*-{3-[4-(3-amino)propyl]piperazinyl}propyl}-ursolamide 182

**182**

Poudre blanche

 $C_{40}H_{71}N_4O_2$ $MM = 639 \text{ g/mol}$

Ce composé a été synthétisé selon la **Méthode Générale VI.3.3. Réaction de déprotection d'une fonction alcool protégée par un groupement acétyle**, à partir du *N*-{3-[4-(3-aminopropyl)piperazin-1-yl]propyl}-3-*O*-acétylursolamide 180. Le produit est obtenu avec un **rendement de 50%**.

IR (ATR, cm^{-1}): 3385 (NH_2 et OH); 2869 (C-H); 1698 (C=O amide); 1636 (C=C); 1454 (C-O); 1385 (C-H); 1306 (C-O); 1254 (C-N); 1029 (C-O-H); 999 (CH=C).

RMN ^1H (500 MHz, CDCl_3), δ (ppm), J en Hz: 0,78 (1H, CH-5); 0,82 (s, 3H, CH_3 -24); 0,83 (d, $^3J = 7,0$, 3H, CH_3 -30); 0,91 (d, $^3J = 6,6$, 3H, CH_3 -29); 0,93 (1H, CH_2 -1); 0,94 (s, 3H, CH_3 -25); 0,96 (m, 1H, CH-20); 0,94 (1H, CH_2 -11); 0,98 (s, 3H, CH_3 -23) 1,02 (s, 3H, CH_3 -26); 1,14 (s, 3H, CH_3 -27); 1,21 (m, 1H, $\text{CH}_{2(\text{H}\alpha)}$ -7); 1,33 (m, 1H, CH-19); 1,41 (m, 2H, CH_2 -2); 1,55 (m, 4H, $\text{CH}_{2(\text{H}\beta)}$ -6, $\text{CH}_{2(\text{H}\beta)}$ -7, CH-9, $\text{CH}_{2(\text{H}\alpha)}$ -21); 1,62 (m, 4H, $\text{CH}_{2(\text{H}\beta)}$ -1, $\text{CH}_{2(\text{H}\alpha)}$ -15, $\text{CH}_{2(\text{H}\beta)}$ -16, $\text{CH}_{2(\text{H}\beta)}$ -21); 1,70 (m, 5H, CH_2 -c, CH_2 -c' et $\text{CH}_{2(\text{H}\alpha)}$ -6); 1,77 (td, $^3J = 14,0$ et 6,0, 1H, $\text{CH}_{2(\text{H}\alpha)}$ -16); 1,83 (m, 2H, CH_2 -22); 2,00 (m, 1H, $\text{CH}_{2(\text{H}\beta)}$ -15); 2,52 (m, 13H, CH_2 -a1, CH_2 -a1', CH_2 -a2, CH_2 -a2', CH_2 -b, CH_2 -b' et CH-18); 3,03 (m, 2H, CH_2 -d'); 3,25 (dd, $^3J = 13,8$ et 6,4, 1H, CH-3); 3,34 (m, 2H, CH_2 -d); 5,35 (tl, 1H, CH-12); 6,46 (sl, 1H, NH).

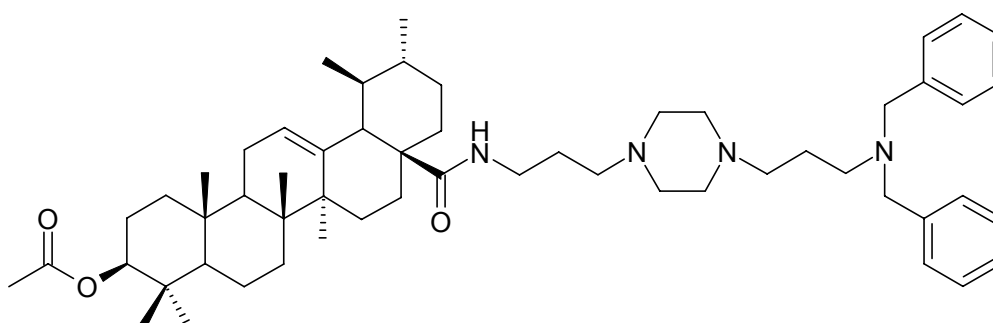
RMN ^{13}C (125 MHz, CDCl_3), δ (ppm): 15,8 (C-25); 15,9 (C-26), 16,8 (C-24); 17,4 (C-29); 18,7 (C-6); 21,7 (C-30); 23,8 (C-11 et C-27); 25,1 (C-16); 27,2 (C-c); 28,3 (C-23); 28,4 (C-2); 28,5 (C-15); 31,3 (C-21); 33,2 (C-7); 31,5 (C-c');

37,4 (C-10); 37,8 (C-22); 38,9 (C-8); 39,0 (C-1); 39,2 (C-d); 39,3 (C-4); 39,5 (C-19); 39,9 (C-20); 40,1 (C-d'); 42,8 (C-14); 47,9 (C-9 et C-17); 53,4 (C-18); 53,7 (C-a1, C-a1', C-a2, C-a2'); 55,6 (C-5); 56,5 (C-b et b'); 79,3 (C-3); 123,0 (C-12); 140,1 (C-13); 178,2 (C-28).

$[\alpha]_D^{20} = +56$ (CHCl₃, c 0,2)

pF: 140 °C.

VI.27. Préparation du composé **183** *N*-{3-[4-(3-(dibenzylamino)propyl)piperazinyl]propyl}-3-*O*-acétylursolamide



183

Huile jaune transparente

C₅₆H₈₄N₄O₃

MM = 860 g/mol

Ce composé est synthétisé selon la **Méthode Générale, VI.3.1.1. Réactions d'amination réductrice**, à partir du benzaldéhyde (15,2 µL, 0,15 mmol). Le produit est obtenu avec un **rendement de 76%**.

IR (ATR, cm⁻¹): 3351 (NH); 2872 (C-H); 1732 (C=O acétyle); 1643 (C=O amide); 1519 (C=C); 1452 (C-O-C); 1367 (C-H); 1244 (C-N); 970, 735, 699 (noyaux aromatiques monosubstitués).

RMN ¹H (500 MHz, CDCl₃), δ (ppm), *J* en Hz: 0,81 (d, ³*J* = 6,9, 3H, CH₃-30); 0,87 (1H, CH-5); 0,91 (d, ³*J* = 5,2, 3H, CH₃-29); 0,93 (m, 1H, CH₂-1); 0,96 (s, 3H, CH₃-25); 0,95 (m, 1H, CH₂-11); 0,99 (sl, 3H, CH₃-24, 1H, CH-20); 1,00 (s, 3H, CH₃-23); 1,01 (s, 3H, CH₃-26); 1,14 (s, 3H, CH₃-27); 1,21 (m, 1H, CH₂(H_α)-7); 1,33 (m, 3H, CH-19 et CH₂-2); 1,48 (m, 4H, CH₂(H_β)-6, CH₂(H_β)-7, CH-9, CH₂(H_α)-21); 1,60 (m, 4H, CH₂(H_β)-1, CH₂(H_α)-15, CH₂(H_β)-16, CH₂(H_β)-21); 1,71 (m, 5H, CH₂-c, CH₂-c' et CH₂(H_α)-6); 1,77 (td, ³*J* = 14,0 et 6,0, 1H, CH₂(H_α)-16); 1,84

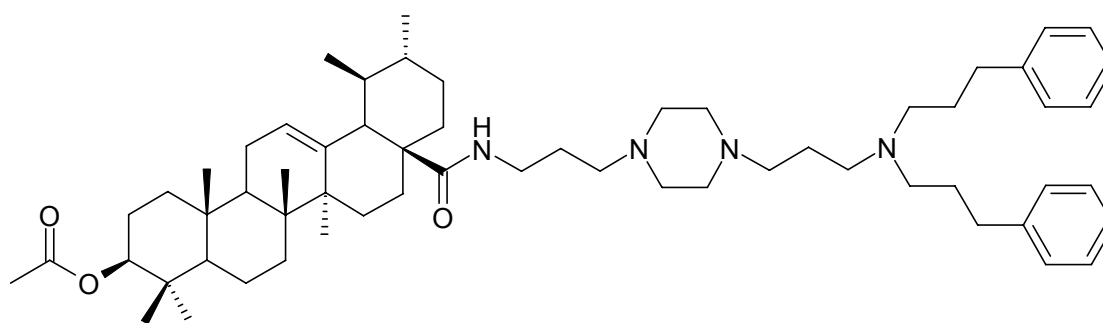
(2H, CH₂-22); 1,99 (m, 1H, CH₂(H β)-15); 2,10 (s, 3H, H₃C_{COO}); 2,49 (m, 13H, CH₂-a1, CH₂-a1', CH₂-a2, CH₂-a2', CH₂-b, CH₂-b' et 1H, CH-18); 3,09 (m, 2H, CH₂-d'); 3,47 (m, 2H, CH₂-d); 3,60 (s, 4H, -N(CH₂)₂); 4,54 (dd, ³J = 11,5 et 5,9, 1H, CH-3); 5,35 (tl, 1H, CH-12); 6,48 (sl, 1H, NH); 7,27 (dd, ³J = 7,1, 2 x 1H, CH-*para*); 7,34 (dd, ³J = 7,3, 2 x 2H, CH-*mé*ta); 7,39 (d, ³J = 7,5, 2 x 2H, CH-*ortho*).

RMN ¹³C (125 MHz, CDCl₃), δ (ppm): 15,8 (C-25); 17,1 (C-26); 17,4 (C-24); 17,7 (C-29); 18,6 (C-6); 21,6 (C-30); 21,7 (H₃C_{COO}); 23,8 (C-11); 23,9 (C-27); 24,1 (C-2); 25,1 (C-16); 26,2 (C-c); 28,2 (C-23); 28,5 (C-15); 31,3 (C-21); 32,8 (C-c'); 33,4 (C-7); 37,3 (C-10); 37,8 (C-22); 38,1 (C-4); 38,5 (C-1); 38,7 (C-d); 39,5 (C-19); 39,8 (C-20); 39,9 (C-8); 42,5 (C-14); 47,9 (C-9 et C-17); 51,7 (C-b'); 52,9 (C-a1, a1', a2, a2'); 53,9 (C-d'); 54,0 (C-18); 55,6 (C-5); 56,6 (C-b); 58,9 (C-e); 81,3 (C-3); 123,9 (C-12); 127,3 (C-*para*); 128,6 (C-*mé*ta); 129,2 (C-*ortho*); 140,1 (C-13); 145,3 (C-*ipso*); 171,4 (H₃C_{COO}); 178,1 (C-28).

SMHR: calculé pour C₅₆H₈₅N₄O₃: 861,6622. Trouvé: 861,6649 (100%).

$[\alpha]_D^{20} = +33,6$ (CHCl₃, c 0,1).

VI.28. Préparation du composé **184** *N*-{3-[4-(3-(di(3-phenylpropyl)amino)propyl)piperazinyl]propyl}-3-*O*-acétylursolamide



184

Huile jaune

C₆₀H₉₂N₄O₃

MM = 916 g/mol

Ce composé est synthétisé selon la **Méthode Générale, VI.3.1.1. Réactions d'amination réductrice**, à partir du 3-phenylpropionaldéhyde (26,5 μL , 0,15 mmol). Le produit est obtenu avec un **rendement de 27%**.

IR (ATR, cm^{-1}): 3318 (NH); 2854 (C-H); 2811 (N-H); 1731 (C=O acétyle); 1648 (C=O amide); 1455 (C-O-C); 1370 (C-H); 1245 (C-N); 904, 749, 701 (noyaux aromatiques monosubstitués).

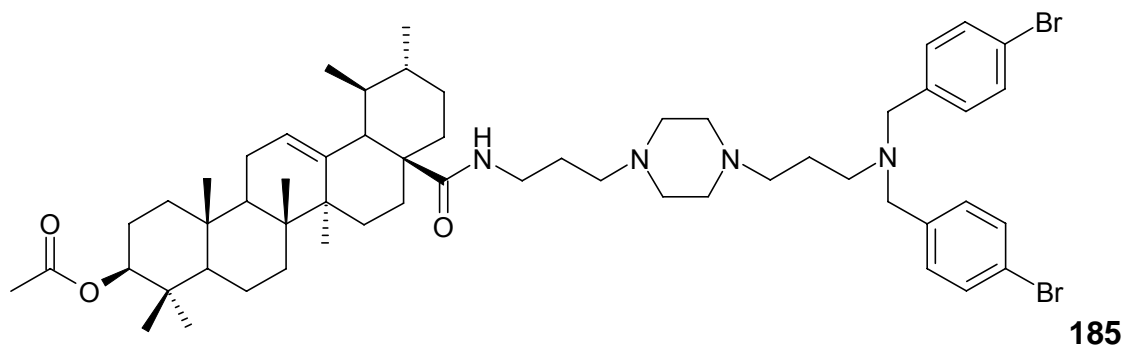
RMN ^1H (500 MHz, CDCl_3), δ (ppm), J en Hz: 0,81 (d, $^3J = 7,0$, 3H, CH_3 -30); 0,87 (1H, CH-5); 0,91 (d, $^3J = 5,0$, 3H, CH_3 -29); 0,93 (m, 1H, CH_2 -1); 0,94 (m, 1H, CH_2 -11); 0,98 (s, 3H, CH_3 -25); 0,99 (sl, 7H, CH_3 -24, CH_3 -26 et CH-20); 1,00 (s, 3H, CH_3 -23); 1,14 (s, 3H, CH_3 -27); 1,21 (m, 1H, $\text{CH}_{2(\text{H}\alpha)}$ -7); 1,33 (m, 1H, CH-19); 1,42 (2H, CH_2 -2); 1,53 (m, 4H, $\text{CH}_{2(\text{H}\beta)}$ -6, $\text{CH}_{2(\text{H}\beta)}$ -7, CH-9, $\text{CH}_{2(\text{H}\alpha)}$ -21); 1,63 (m, 4H, $\text{CH}_{2(\text{H}\beta)}$ -1, $\text{CH}_{2(\text{H}\alpha)}$ -15, $\text{CH}_{2(\text{H}\beta)}$ -16, $\text{CH}_{2(\text{H}\beta)}$ -21); 1,74 (m, 6H, CH_2 -c, CH_2 -c', $\text{CH}_{2(\text{H}\alpha)}$ -6, $\text{CH}_{2(\text{H}\alpha)}$ -16); 1,97 (2H, CH_2 -22); 2,02 (m, 5H, $\text{CH}_{2(\text{H}\beta)}$ -15, 2 x $-\text{CH}_2\text{CH}_2\text{Ar}$); 2,10 (s, 3H, H_3CCOO); 2,54 (m, 21H, CH_2 -a1, CH_2 -a1', CH_2 -a2, CH_2 -a2', CH_2 -b, CH_2 -b', CH-18, $-\text{N}(\text{CH}_2)_2$, 2 x $-\text{CH}_2\text{Ar}$); 3,10 (m, 2H, CH_2 -d'); 3,48 (m, 2H, CH_2 -d); 4,27 (dd, $^3J = 11,2$ et $6,2$, 1H, CH-3); 5,34 (tl, 1H, CH-12); 6,51 (sl, 1H, NH); 7,21 (d, $^3J = 7,1$, 2 x 2H, CH-*para*); 7,24 (d, $^3J = 7,3$, 2 x 2H, CH-*mé*ta); 7,32 (d, $^3J = 6,2$, 2 x 2H, CH-*ortho*).

RMN ^{13}C (125 MHz, CDCl_3), δ (ppm): 15,9 (C-25); 17,1 (C-26); 17,4 (C-24); 17,7 (C-29); 18,6 (C-6); 21,6 (C-30); 21,7 (H_3CCOO); 23,8 (C-11); 23,9 (C-27); 24,2 (C-2); 25,1 (C-16); 26,1 (C-c); 28,2 (C-23); 28,5 (C-15); 30,1 (2 x $-\text{CH}_2\text{CH}_2\text{Ar}$); 31,3 (C-21); 33,2 (C-c'); 33,9 (C-7); 37,3 (C-10); 37,8 (C-22); 38,1 (C-4); 38,7 (C-1); 39,2 (C-d); 39,5 (C-19); 39,9 (C-20); 40,1 (C-8); 42,7 (C-14); 47,9 (C-9 et C-17); 52,0 (C-b'); 53,3 (C-a1, C-a1', C-a2, C-a2'); 53,5 (C-d'); 54,1 (C-18); 55,7 (C-5); 56,6 (C-b); 57,4 (C-e); 68,6 (2 x $-\text{CH}_2\text{Ar}$); 81,3 (C-3); 125,8 (C-12); 126,3 (C-*para*); 128,7 (C-*mé*ta); 129,2 (C-*ortho*); 134,3 (C-*ipso*); 140,1 (C-13); 171,4 (H_3CCOO); 178,2 (C-28).

SMHR: calculé pour $\text{C}_{60}\text{H}_{93}\text{N}_4\text{O}_3$: 917,7248. Trouvé: 917,7242 (100%).

$[\alpha]_{\text{D}}^{20} = +18,8$ (CHCl_3 , c 0,4).

VI.29. Préparation du composé 185 N-{3-[4-(3-(di(4-bromobenzyl)amino)propyl)piperazinyl]propyl}-3-O-acétylursolamide



Huile jaune

$C_{56}H_{82}N_4O_3Br_2$

$MM = 1016 \text{ g/mol}$

Ce composé a été synthétisé selon la **Méthode Générale, VI.3.1.1. Réactions d'amination réductrice**, à partir du *para*-bromobenzaldéhyde (27,5 mg, 0,15 mmol). Le produit est obtenu avec un **rendement de 56%**.

IR (ATR, cm^{-1}): 3325 (NH); 2872 (C-H); 2810 (N-H); 1730 (C=O acétyle); 1644 (C=O amide); 1519 (C=C); 1368 (C-H); 1245 (C-N); 1069 ($C_{aromatique}-Br$); 804 (noyaux aromatiques *p*-substitués).

RMN 1H (500 MHz, $CDCl_3$), δ (ppm), J en Hz: 0,79 (d, $^3J = 7,8$, 3H, CH_3 -30); 0,86 (1H, CH-5); 0,90 (d, $^3J = 6,2$, 3H, CH_3 -29); 0,93 (m, 1H, CH_2 -1); 0,93 (m, 1H, CH_2 -11); 0,98 (sl, 7H, CH_3 -25, CH_3 -24 et CH-20); 0,99 (s, 6H, CH_3 -26 et CH_3 -23); 1,13 (s, 3H, CH_3 -27); 1,19 (m, 1H, $CH_{2(H\alpha)}$ -7); 1,31 (m, 1H, CH-19); 1,41 (m, 2H, CH_2 -2); 1,51 (m, 4H, $CH_{2(H\beta)}$ -6, $CH_{2(H\beta)}$ -7, CH-9, $CH_{2(H\alpha)}$ -21); 1,59 (m, 4H, $CH_{2(H\beta)}$ -1, $CH_{2(H\alpha)}$ -15, $CH_{2(H\beta)}$ -16, $CH_{2(H\beta)}$ -21); 1,72 (m, 6H, CH_2 -c, CH_2 -c', $CH_{2(H\alpha)}$ -6, $CH_{2(H\alpha)}$ -16); 1,84 (m, 2H, CH_2 -22); 2,11 (s, 3H, H_3C COO); 2,41 (m, 13H, CH_2 -a1, CH_2 -a1', CH_2 -a2, CH_2 -a2', CH_2 -b, CH_2 -b', CH-18); 3,07 (m, 2H, CH_2 -d'); 3,48 (m, 2H, CH_2 -d); 3,50 (s, 4H, $-N(CH_2)_2$); 4,53 (dd, $^3J = 11,7$ et 5,8, 1H, CH-3); 5,33 (tl, 1H, CH-12); 6,56 (sl, 1H, NH); 7,25 (d, $^3J = 8,1$, 2 x 2H, CH-ortho); 7,47 (d, $^3J = 8,2$, 2 x 2H, CH-méta).

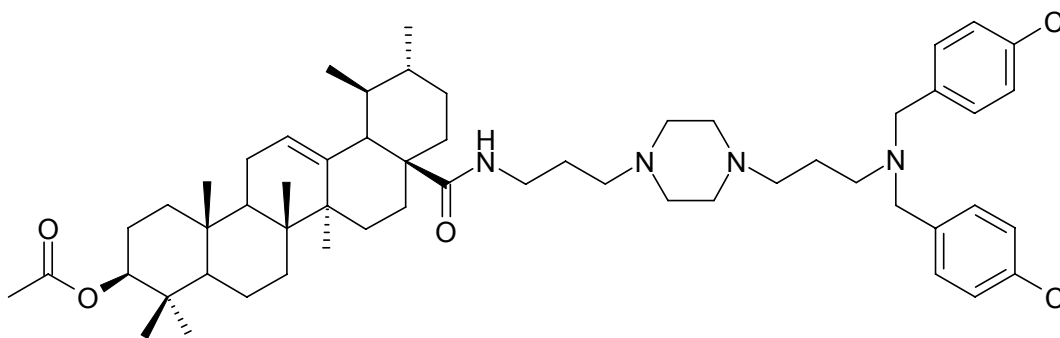
RMN ^{13}C (125 MHz, $CDCl_3$), δ (ppm): 15,9 (C-25); 17,1 (C-26); 17,4 (C-24); 17,7 (C-29); 18,6 (C-6); 21,6 (C-30); 21,7 (H_3C COO); 23,8 (C-11); 23,9 (C-27); 24,1 (C-2); 25,1 (C-16); 26,2 (C-c); 28,2 (C-23); 28,5 (C-15); 31,3 (C-21); 33,1

(C-7 et C-c'); 37,3 (C-10); 37,8 (C-22); 38,1 (C-4); 38,7 (C-1); 39,2 (C-d); 39,5 (C-19); 39,9 (C-20); 40,1 (C-8); 42,8 (C-14); 47,9 (C-9 et C-17); 51,8 (C-b'); 53,4 (C-a1, C-a1', C-a2, C-a2'); 53,6 (C-d'); 54,1 (C-18); 55,7 (C-5); 56,6 (C-b); 58,2 (C-e); 81,3 (C-3); 121,1 (C-ortho); 125,8 (C-12); 130,8 (C-méta); 131,7 (C-*ipso*); 139,0 (C-*para*); 140,2 (C-13); 171,4 (H₃CCOO); 178,2 (C-28).

SMHR: calculé pour C₅₆H₈₃N₄O₃Br₂: 1017,4832. Trouvé: 1017,4812 (100%).

$[\alpha]_D^{20} = +31,2$ (CHCl₃, c 0,1).

VI.30. Préparation du composé **186** *N*-{3-[4-(3-(di(4-chlorobenzyl)amino)propyl)piperazinyl]propyl}-3-*O*-acétylursolamide



186

Huile jaune-verte

C₅₆H₈₂N₄O₃Cl₂

MM = 928 g/mol

Ce composé est synthétisé selon la **Méthode Générale, VI.3.1.1. Réactions d'amination réductrice**, à partir du *para*-chlorobenzaldéhyde (21,9 mg, 0,15 mmol). Le produit est obtenu avec un **rendement de 53%**.

IR (ATR, cm⁻¹): 3374 (NH); 2874 (C-H); 1731 (C=O acétyle); 1645 (C=O amide); 1490 (C=C); 1367 (C-H); 1246 (C-N); 809 (noyaux aromatiques *p*-substitués).

RMN ¹H (500 MHz, CDCl₃), δ (ppm), *J* en Hz: 0,82 (d, ³*J* = 6,9, 3H, CH₃-30); 0,88 (1H, CH-5); 0,91 (d, ³*J* = 5,6, 3H, CH₃-29); 0,93 (m, 1H, CH₂-1); 0,96 (s, 3H, CH₃-25); 0,94 (m, 1H, CH₂-11); 0,99 (sl, 4H, CH₃-24 et CH-20); 1,00 (s, 3H,

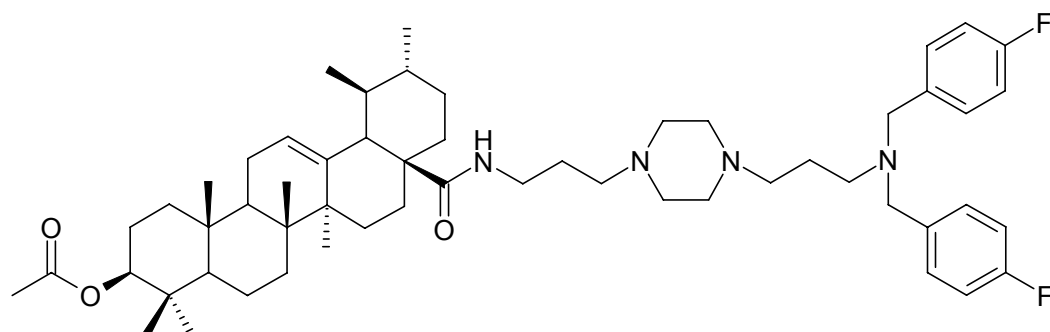
CH₃-23); 1,01 (s, 3H, CH₃-26); 1,14 (s, 3H, CH₃-27); 1,21 (m, 1H, CH_{2(Hα)}-7); 1,34 (m, 1H, CH-19); 1,42 (2H, CH₂-2); 1,53 (m, 4H, CH_{2(Hβ)}-6, CH_{2(Hβ)}-7, CH-9, CH_{2(Hα)}-21); 1,63 (m, 4H, CH_{2(Hβ)}-1, CH_{2(Hα)}-15, CH_{2(Hβ)}-16, CH_{2(Hβ)}-21); 1,72 (m, 6H, CH₂-c, CH₂-c', CH_{2(Hα)}-6, CH_{2(Hα)}-16); 1,97 (m, 2H, CH₂-22); 2,02 (m, 1H, CH_{2(Hβ)}-15); 2,10 (s, 3H, H₃CCOO); 2,49 (m, 13H, CH₂-a1, CH₂-a1', CH₂-a2, CH₂-a2', CH₂-b, CH₂-b' et CH-18); 3,09 (m, 2H, CH₂-d'); 3,47 (m, 2H, CH₂-d); 3,54 (s, 4H, -N(CH₂)₂)); 4,55 (dd, ³J = 11,3 et 5,3, 1H, CH-3); 5,34 (tl, 1H, CH-12); 6,46 (sl, 1H, NH); 7,30 (d, ³J = 8,8, 2 x 2H, CH-ortho); 7,32 (d, ³J = 8,5, 2 x 2H, CH-méta).

RMN ¹³C (125 MHz, CDCl₃), δ (ppm): 15,9 (C-25); 17,1 (C-26); 17,4 (C-24); 17,7 (C-29); 18,6 (C-6); 21,6 (C-30); 21,8 (H₃CCOO); 23,8 (C-11); 23,9 (C-27); 24,1 (C-2); 25,1 (C-16); 26,2 (C-c); 28,3 (C-23); 28,5 (C-15); 31,3 (C-21); 33,2 (C-c'); 33,4 (C-7); 37,3 (C-10); 37,8 (C-22); 38,1 (C-4); 38,7 (C-1); 39,1 (C-d); 39,5 (C-19); 39,8 (C-20); 40,0 (C-8); 42,5 (C-14); 47,9 (C-9); 47,9 (C-17); 51,8 (C-b'); 53,3 (C-a1, C-a1', C-a2, C-a2'); 53,5 (C-d'); 54,1 (C-18); 55,7 (C-5); 56,6 (C-b); 58,1 (C-e); 81,3 (C-3); 122,9 (C-12); 128,8 (C-méta); 130,4 (C-ipso); 133,0 (C-para); 138,5 (C-ortho); 140,2 (C-13); 171,3 (H₃CCOO); 178,2 (C-28).

SMHR: calculé pour C₅₆H₈₃N₄O₃Cl₂: 929,5842. Trouvé: 929,5825 (100%).

[α]_D²⁰ = +18,2 (CHCl₃, c 0,5).

VI.31. Préparation du composé **187** N-{3-[4-(3-(di(4-fluorobenzyl)amino)propyl)piperazinyl]propyl}-3-O-acétylursolamide



Huile vert

C₅₆H₇₉N₄O₃F₂

MM = 896 g/mol

Ce composé est synthétisé selon la **Méthode Générale, VI.3.1.1. Réactions d'amination réductrice**, à partir du *p*-fluorobenzaldéhyde (16,2 μ L, 0,15 mmol). Le produit est obtenu avec un **rendement de 70%**.

IR (ATR, cm^{-1}): 3361 (NH); 2874 (C-H); 1731 (C=O acétyle); 1644 (C=O amide); 1507 (C=C), 1454 (C-O); 1368 (C-H); 1245 (C-N); 1219 ($\text{C}_{\text{aromatique}}\text{-F}$); 826 (noyaux aromatiques *p*-substitués).

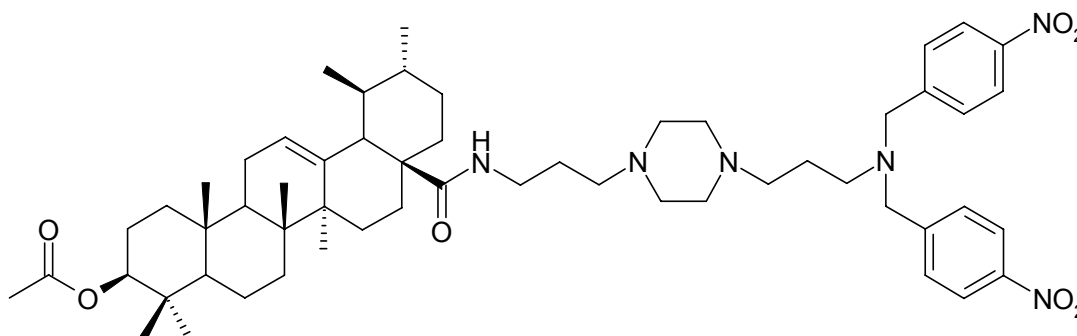
RMN ^1H (500 MHz, CDCl_3), δ (ppm), J en Hz: 0,81 (d, $^3J = 7,0$, 3H, $\text{CH}_3\text{-30}$); 0,87 (1H, CH-5); 0,91 (d, $^3J = 5,8$, 3H, $\text{CH}_3\text{-29}$); 0,94 (m, 1H, $\text{CH}_2\text{-1}$); 0,95 (s, 3H, $\text{CH}_3\text{-25}$); 0,94 (m, 1H, $\text{CH}_2\text{-11}$); 0,98 (sl, 4H, $\text{CH}_3\text{-24}$ et CH-20); 0,99 (s, 3H, $\text{CH}_3\text{-23}$); 1,00 (s, 3H, $\text{CH}_3\text{-26}$); 1,14 (s, 3H, $\text{CH}_3\text{-27}$); 1,20 (m, 1H, $\text{CH}_{2(\text{H}\alpha)}\text{-7}$); 1,33 (m, 1H, CH-19); 1,41 (m, 2H, $\text{CH}_2\text{-2}$); 1,54 (m, 4H, $\text{CH}_{2(\text{H}\beta)}\text{-6}$, $\text{CH}_{2(\text{H}\beta)}\text{-7}$, CH-9, $\text{CH}_{2(\text{H}\alpha)}\text{-21}$); 1,62 (m, 4H, $\text{CH}_{2(\text{H}\beta)}\text{-1}$, $\text{CH}_{2(\text{H}\alpha)}\text{-15}$, $\text{CH}_{2(\text{H}\beta)}\text{-16}$, $\text{CH}_{2(\text{H}\beta)}\text{-21}$); 1,70 (m, 5H, $\text{CH}_2\text{-c}$, $\text{CH}_2\text{-c'}$ et $\text{CH}_{2(\text{H}\alpha)}\text{-6}$); 1,77 (td, $^3J = 13,6$ et 4,9, 1H, $\text{CH}_{2(\text{H}\alpha)}\text{-16}$); 1,84 (m, 2H, $\text{CH}_2\text{-22}$); 1,97 (m, 1H, $\text{CH}_{2(\text{H}\beta)}\text{-15}$); 2,10 (s, 3H, H_3CCOO); 2,45 (m, 13H, $\text{CH}_2\text{-a1}$, $\text{CH}_2\text{-a1'}$, $\text{CH}_2\text{-a2}$, $\text{CH}_2\text{-a2'}$, $\text{CH}_2\text{-b}$, $\text{CH}_2\text{-b'}$ et CH-18); 3,10 (m, 2H, $\text{CH}_2\text{-d'}$); 3,47 (m, 2H, $\text{CH}_2\text{-d}$); 3,54 (s, 4H, $\text{-N}(\text{CH}_2)_2$); 4,54 (dd, $^3J = 11,3$ et 5,5, 1H, CH-3); 5,33 (tl, 1H, CH-12); 6,49 (sl, 1H, NH); 7,03 (dd, $^3J_{\text{HH}} = 8,5$, $^3J_{\text{HF}} = 8,6$, 2 x 2H, CH-*mé*ta); 7,32 (dd, $^3J_{\text{HH}} = 8,2$, $^3J_{\text{HF}} = 5,7$, 2 x 2H, CH-*ortho*).

RMN ^{13}C (125 MHz, CDCl_3), δ (ppm): 15,9 (C-25); 17,1 (C-26); 17,4 (C-24); 17,7 (C-29); 18,9 (C-6); 21,6 (C-30); 21,7 (H_3CCOO); 23,8 (C-11); 23,9 (C-27); 24,1 (C-2); 25,1 (C-16); 26,1 (C-c); 28,2 (C-23); 28,5 (C-15); 31,3 (C-21); 33,1 (C-c'); 33,4 (C-7); 37,3 (C-10); 37,8 (C-22); 38,1 (C-4); 38,7 (C-1); 39,2 (C-d); 39,5 (C-19); 39,8 (C-20); 40,1 (C-8); 42,8 (C-14); 47,9 (C-9 et C-17); 51,7 (C-b'); 53,5 (C-a1, C-a1', C-a2, C-a2'); 53,6 (C-d'); 53,8 (C-18); 55,6 (C-5); 56,8 (C-b); 57,9 (C-e); 81,3 (C-3); 115,5 (C-*mé*ta); 122,9 (C-12); 125,6 (C-*ipso*); 130,6 (C-*ortho*); 140,2 (C-13); 161,3 (C-*para*); 171,4 (H_3CCOO); 178,2 (C-28).

SMHR: calculé pour $\text{C}_{56}\text{H}_{83}\text{N}_4\text{O}_3\text{F}_2$: 897,6433. Trouvé: 897,6407 (100%).

$[\alpha]_{\text{D}}^{20} = +23,2$ (CHCl_3 , c 0,2).

VI.32. Préparation du composé 188 *N*-{3-[4-(3-(di(4-nitrobenzyl)amino)propyl)piperazinyl]propyl}-3-*O*-acétylursolamide



188

Huile jaune foncée

$C_{56}H_{83}N_6O_7$

$MM = 950$ g/Mol

Ce composé est synthétisé selon la **Méthode Générale, VI.3.1.1. Réactions d'amination réductrice**, à partir du *p*-nitrobenzaldéhyde (22,6 mg, 0,15 mmol). Le produit est obtenu avec un rendement de 40%.

IR (ATR, cm^{-1}): 3325 (NH); 2854 (C-H); 1729 (C=O acétyle); 1644 (C=O amide); 1597 (C=C); 1518 ($C_{aromatique}-NO_2$); 1454 (C-O); 1368 (C-H); 1245 (C-N); 854 (noyaux aromatiques *p*-substitués).

RMN 1H (500 MHz, $CDCl_3$), δ (ppm), J en Hz: 0,80 (d, $^3J = 6,9$, 3H, CH_3-30); 0,89 (1H, CH-5); 0,90 (d, $^3J = 5,7$, 3H, CH_3-29); 0,93 (m, 1H, CH_2-1); 0,96 (s, 3H, CH_3-25); 0,94 (m, 1H, CH_2-11); 0,97 (sl, 4H, CH_3-24 et CH-20); 0,99 (s, 6H, CH_3-23 , CH_3-26); 1,12 (s, 3H, CH_3-27); 1,19 (m, 1H, $CH_{2(H\alpha)}-7$); 1,31 (m, 1H, CH-19); 1,40 (m, 2H, CH_2-2); 1,57 (m, 8H, $CH_{2(H\beta)}-1$, $CH_{2(H\beta)}-6$, $CH_{2(H\beta)}-7$, CH-9, $CH_{2(H\alpha)}-15$, $CH_{2(H\beta)}-16$, CH_2-21); 1,72 (m, 6H, CH_2-c , CH_2-c' , $CH_{2(H\alpha)}-6$, $CH_{2(H\alpha)}-16$); 1,97 (m, 2H, CH_2-22); 2,02 (m, 1H, $CH_{2(H\beta)}-15$); 2,11 (s, 3H, H_3C-COO); 2,48 (m, 13H, CH_2-a1 , CH_2-a1' , CH_2-a2 , CH_2-a2' , CH_2-b , CH_2-b' et CH-18); 3,09 (m, 2H, CH_2-d'); 3,51 (m, 2H, CH_2-d); 3,70 (s, 4H, $-N(CH_2)_2$); 4,53 (dd, $^3J = 11,7$ et 4,5, 1H, CH-3); 5,34 (tl, 1H, CH-12); 6,46 (sl, 1H, NH); 7,58 (d, $^3J = 8,2$, 2 x 2H, CH-ortho); 8,24 (d, $^3J = 8,3$, 2 x 2H, CH-méta).

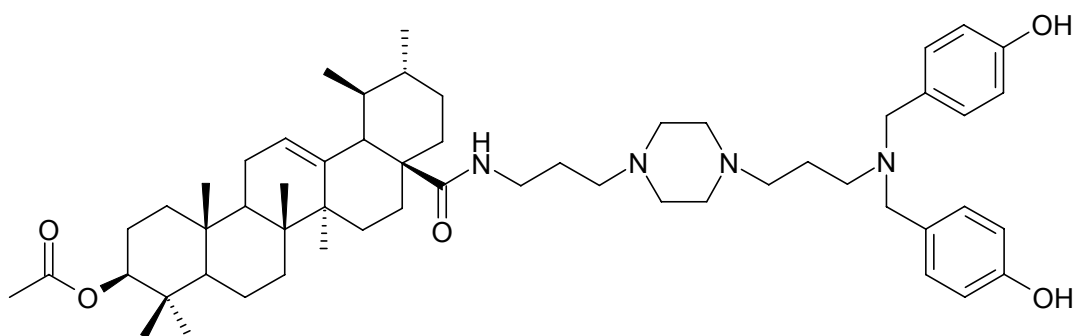
RMN ^{13}C (125 MHz, $CDCl_3$), δ (ppm), J en Hz: 15,9 (C-25); 17,1 (C-26); 17,4 (C-24); 17,7 (C-29); 18,6 (C-6); 21,6 (C-30); 21,7 (H_3C-COO); 23,8 (C-11); 23,9

(C-27); 24,1 (C-2); 25,1 (C-16); 26,1 (C-c); 28,2 (C-23); 28,5 (C-15); 31,3 (C-21); 33,1 (C-c'); 33,4 (C-7); 37,2 (C-10); 37,8 (C-22); 38,1 (C-4); 38,7 (C-1); 39,2 (C-d); 39,5 (C-19); 39,9 (C-20); 40,1 (C-8); 42,8 (C-14); 47,9 (C-9 et C-17); 51,8 (C-b); 53,3 (C-a1, C- a1', C-a2, C-a2'); 53,5 (C-d'); 54,1 (C-18); 55,6 (C-5); 56,4 (C-b'); 58,4 (C-e); 81,3 (C-3); 124,1 (C-ortho); 125,8 (C-12); 129,6 (C-méta); 139,1 (C-13); 143,0 (C-*ipso*); 148,1 (C-*para*); 171,4 (H₃CCOO); 178,1 (C-28).

SMHR: calculé pour C₅₆H₈₃N₆O₇: 951,6323. Trouvé: 951,6326 (100%).

$[\alpha]_D^{20} = +19,6$ (CHCl₃, c 0,3).

VI.33. Préparation du composé **189** *N*-{3-[4-(3-(di(4-hydroxybenzyl)amino)propyl)piperazinyl]propyl}-3-*O*-acétylursolamide



189

Huile jaune

C₅₆H₈₄N₄O₅

MM = 892 g/mol

Ce composé est synthétisé selon la **Méthode Générale, VI.3.1.1. Réactions d'amination réductrice**, à partir du *p*-hydroxybenzaldéhyde (18,3 mg, 0,15 mmol). Le produit est obtenu avec un **rendement de 30%**.

IR (ATR, cm⁻¹): 3309 (NH); 2872 (C-H); 1728 (C=O acétyle); 1629 (C=O amide); 1514 (C=C); 1453 (C-O); 1367 (C-H); 1246 (C-N, C_{aromatique}-OH); 827 (noyaux aromatiques *p*-substitués).

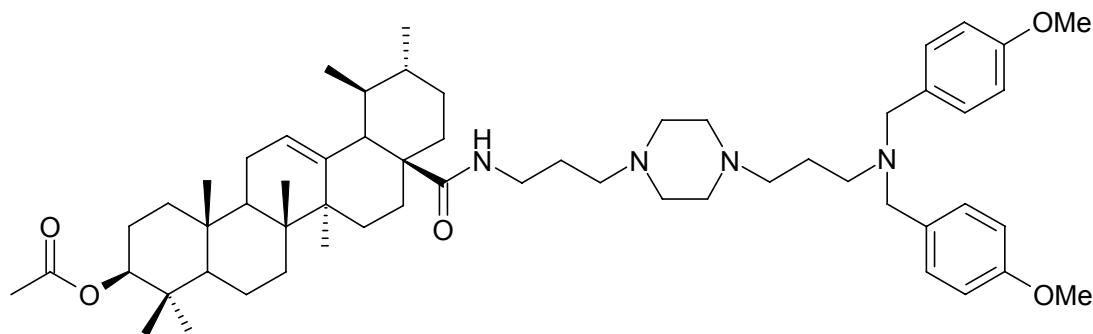
RMN ^1H (500 MHz, CDCl_3), δ (ppm), J en Hz: 0,79 (d, $^3J = 7,0$, 3H, CH_3 -30); 0,87 (m, 1H, CH-5); 0,91 (d, $^3J = 5,8$, 3H, CH_3 -29); 0,93 (m, 1H, CH_2 -1); 0,96 (s, 3H, CH_3 -25); 0,94 (1H, CH_2 -11); 0,96 (sl, 4H, CH_3 -24 et CH-20); 0,97 (s, 3H, CH_3 -23); 1,00 (s, 3H, CH_3 -26); 1,13 (s, 3H, CH_3 -27); 1,21 (m, 1H, $\text{CH}_{2(\text{H}\alpha)}$ -7); 1,38 (m, 3H, CH-19 et CH_2 -2); 1,53 (m, 4H, $\text{CH}_{2(\text{H}\beta)}$ -6, $\text{CH}_{2(\text{H}\beta)}$ -7, CH-9, $\text{CH}_{2(\text{H}\alpha)}$ -21); 1,62 (m, 4H, $\text{CH}_{2(\text{H}\beta)}$ -1, $\text{CH}_{2(\text{H}\alpha)}$ -15, $\text{CH}_{2(\text{H}\beta)}$ -16, $\text{CH}_{2(\text{H}\beta)}$ -21); 1,69 (m, 6H, CH_2 -c, CH_2 -c', $\text{CH}_{2(\text{H}\alpha)}$ -6, $\text{CH}_{2(\text{H}\alpha)}$ -16); 1,95 (m, 2H, CH_2 -22); 1,98 (m, 1H, $\text{CH}_{2(\text{H}\beta)}$ -15); 2,11 (s, 3H, H_3CCOO); 2,48 (m, 13H, CH_2 -a1, CH_2 -a1', CH_2 -a2, CH_2 -a2', CH_2 -b, CH_2 -b' et CH-18); 3,06 (m, 2H, CH_2 -d'); 3,45 (m, 2H, CH_2 -d); 3,54 (s, 4H, $-\text{N}(\text{CH}_2)_2$); 4,54 (dd, $^3J = 11,3$ et $5,5$, 1H, CH-3); 5,33 (tl, 1H, CH-12); 6,39 (sl, 1H, NH); 6,77 (d, $^3J = 8,1$, 2 x 2H, CH-ortho); 7,16 (d, $^3J = 8,2$, 2 x 2H, CH-méta).

RMN ^{13}C (125 MHz, CDCl_3), δ (ppm): 15,9 (C-25); 17,1 (C-26); 17,3 (C-24); 17,7 (C-29); 18,5 (C-6); 21,6 (C-30); 21,7 (H_3CCOO); 23,8 (C-11); 23,9 (C-27); 24,1 (C-2); 25,2 (C-16); 26,2 (C-c); 28,2 (C-23); 28,5 (C-15); 31,2 (C-21); 33,0 (C-c'); 33,4 (C-7); 37,2 (C-10); 37,7 (C-22); 38,1 (C-4); 38,7 (C-1); 39,1 (C-d); 39,5 (C-19); 39,9 (C-20); 40,1 (C-8); 42,6 (C-14); 47,8 (C-17); 48,1 (C-9); 51,3 (C-b); 52,7 (C-a1, C-a1', C-a2, C-a2'); 53,8 (C-18); 54,2 (C-d'); 55,6 (C-5); 56,4 (C-b'); 58,3 (C-e); 81,3 (C-3); 115,8 (C-méta); 125,9 (C-12); 130,6 (C-ortho); 130,9 (C-*ipso*); 140,2 (C-13); 156,0 (C-*para*); 171,6 (H_3CCOO); 179,0 (C-28).

SMHR: calculé pour $\text{C}_{56}\text{H}_{85}\text{N}_4\text{O}_5$: 893,6493. Trouvé: 893,6498 (100%).

$[\alpha]_{\text{D}}^{20} = +19,9$ (CHCl_3 , c 0,1).

VI.34. Préparation du composé 190 *N*-{3-[4-(3-(di(4-methoxybenzyl)amino)propyl)piperazinyl]propyl}-3-*O*-acétylursolamide



190

Huile jaune claire

$C_{58}H_{88}N_4O_5$

MM = 920 g/mol

Ce composé est synthétisé selon la **Méthode Générale, VI.3.1.1. Réactions d'amination réductrice**, à partir du *p*-methoxybenzaldéhyde (18,2 μ L, 0,15 mmol). Le produit est obtenu avec un **rendement de 25%**.

IR (ATR, cm^{-1}): 3363 (NH); 2873 (C-H); 1731 (C=O acétyle); 1645 (C=O amide); 1510 (C=C), 1456 (C-O); 1367 (C-H) 1244 (C-N, C-O-C); 984 (CH=C); 822 (noyaux aromatiques *p*-substitués).

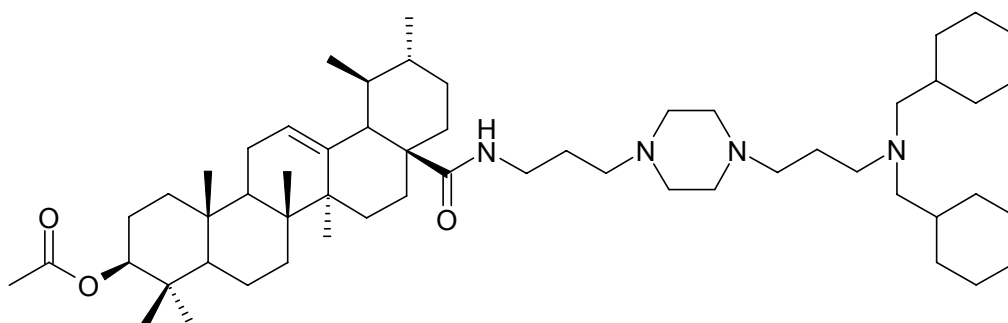
RMN 1H (500 MHz, $CDCl_3$), δ (ppm), *J* en Hz: 0,81 (d, $^3J=6,9$, 3H, CH_3 -30); 0,87 (m, 1H, CH-5); 0,91 (d, $^3J=5,3$, 3H, CH_3 -29); 0,93 (m, 1H, CH_2 -1); 0,96 (s, 3H, CH_3 -25); 0,94 (m, 1H, CH_2 -11); 0,99 (sl, 4H, CH_3 -24, CH-20); 1,00 (s, 3H, CH_3 -23); 1,01 (s, 3H, CH_3 -26); 1,14 (s, 3H, CH_3 -27); 1,23 (m, 1H, $CH_{2(H\alpha)}$ -7); 1,33 (m, 1H, CH-19); 1,41 (m, 2H, CH_2 -2); 1,52 (m, 4H, $CH_{2(H\beta)}$ -6, $CH_{2(H\beta)}$ -7, CH-9, $CH_{2(H\alpha)}$ -21); 1,62 (m, 4H, $CH_{2(H\beta)}$ -1, $CH_{2(H\alpha)}$ -15, $CH_{2(H\beta)}$ -16, $CH_{2(H\beta)}$ -21); 1,73 (m, 6H, CH_2 -c, CH_2 -c', $CH_{2(H\alpha)}$ -6 et $CH_{2(H\alpha)}$ -16); 1,87 (m, 2H, CH_2 -22); 2,00 (m, 1H, $CH_{2(H\beta)}$ -15); 2,10 (s, 3H, H_3C COO); 2,50 (m, 13H, CH_2 -a1, CH_2 -a1', CH_2 -a2, CH_2 -a2', CH_2 -b, CH_2 -b', CH-18); 3,10 (m, 2H, CH_2 -d'); 3,47 (m, 2H, CH_2 -d); 3,52 (s, 4H, $-N(CH_2)_2$); 3,85 (s, 6H, CH_3O -); 4,54 (dd, $^3J = 11,5$ et 5,9, 1H, CH-3); 5,35 (tl, 1H, CH-12); 6,50 (sl, 1H, NH); 6,89 (d, $^3J = 8,4$, 2 x 2H, CH-ortho); 7,29 (d, $^3J = 8,4$, 2 x 2H, CH-méta).

RMN ^{13}C (125 MHz, CDCl_3), δ (ppm): 15,9 (C-25); 17,1 (C-26); 17,4 (C-24); 17,7 (C-29); 18,6 (C-6); 21,6 (C-30); 21,7 (H_3CCOO); 23,8 (C-11); 23,9 (C-27); 24,1 (C-2); 25,1 (C-16); 26,2 (C-c); 28,2 (C-23); 28,5 (C-15); 31,3 (C-21); 33,1 (C-7 et C-c'); 37,2 (C-10); 37,8 (C-22); 38,1 (C-4); 38,7 (C-1); 39,1 (C-d); 39,5 (C-19); 39,8 (C-20); 40,1 (C-8); 42,5 (C-14); 47,9 (C-9 et C-17); 51,7 (C-b'); 52,9 (C-d'); 53,1 (C-a1, C-a1', C-a2, C-a2'); 54,0 (C-18); 55,6 (C-5 et C-b); 56,6 (CH_3O); 57,9 (C-e); 81,3 (C-3); 113,9 (C-méta); 123,9 (C-12); 125,8 (C-*ipso*); 130,3 (C-*ortho*); 140,1 (C-13); 158,9 (C-*para*); 171,4 (H_3CCOO); 178,1 (C-28).

SMHR: calculé pour $\text{C}_{58}\text{H}_{89}\text{N}_4\text{O}_5$: 921,6833. Trouvé: 921,6792 (100%).

$[\alpha]_{\text{D}}^{20} = +23,5$ (CHCl_3 , c 0,3).

VI.35. Préparation du composé 191 *N*-{3-[4-(3-(di(cyclohexylmethyl)amino)propyl)piperazinyl]propyl}-3-*O*-acétylursolamide



191

Huile jaune claire

$\text{C}_{56}\text{H}_{96}\text{N}_4\text{O}_3$

$MM = 872$ g/mol

Ce composé est synthétisé selon la **Méthode Générale, VI.3.1.1. Réactions d'amination réductrice**, à partir du cyclohexanecarboxaldéhyde (18,14 μL , 0,15 mmol). Le produit est obtenu avec un **rendement de 50%**.

IR (ATR, cm^{-1}): 3310 (NH); 2849 (C-H); 2805 (N-H); 1733 (C=O acétyle); 1643 (C=O amide); 1520 (C=C); 1448 (C-O); 1368 (C-H); 1242 (C-N).

RMN ^1H (500 MHz, CDCl_3), δ (ppm), J en Hz: 0,83 (d, $^3J = 6,7$, 3H, CH_3 -30); 0,87 (m, 1H, CH-5); 0,92 (d, $^3J = 6,4$, 3H, CH_3 -29); 0,93 (m, 1H, CH_2 -1); 0,94 (m, 1H, CH_2 -11); 0,96 (s, 3H, CH_3 -25); 0,97 (sl, 4H, CH_3 -24 et CH-20); 0,99 (s,

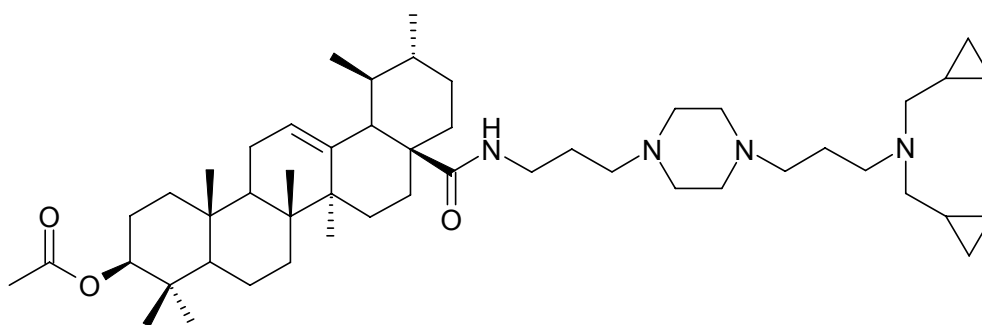
3H, CH₃-23); 1,01 (s, 3H, CH₃-26); 1,15 (s, 3H, CH₃-27); 1,20 (m, 1H, CH₂(H_α)-7); 1,25 (m, 12H, 6 x CH₂-cyclohexyle); 1,33 (m, 13H, CH-19, CH₂-2, 4 x CH₂-cyclohexyle); 1,54 (m, 6H, CH₂(H_β)-6, CH₂(H_β)-7, CH-9, CH₂(H_α)-21 et 2 x CH-cyclohexyle); 1,74 (m, 10H, CH₂(H_β)-1, CH₂(H_α)-15, CH₂(H_β)-16, CH₂(H_β)-21, CH₂-c, CH₂-c', CH₂(H_α)-6, CH₂(H_α)-16); 1,99 (m, 3H, CH₂(H_β)-15, CH₂-22); 2,10 (s, 3H, H₃C₃COO); 2,13 (d, ³J = 6,3, 4H, N(CH₂)₂); 2,48 (m, 13H, CH₂-a1, CH₂-a1', CH₂-a2, CH₂-a2', CH₂-b, CH₂-b', CH-18); 3,10 (m, 2H, CH₂-d'); 3,49 (m, 2H, CH₂-d); 4,55 (dd, ³J = 11,3 et 5,5, 1H, CH-3); 5,35 (tl, 1H, CH-12); 6,53 (sl, 1H, NH).

RMN ¹³C (125 MHz, CDCl₃), δ (ppm): 15,9 (C-25); 17,1 (C-26); 17,4 (C-24); 17,7 (C-29); 18,6 (C-6); 21,6 (C-30 et H₃C₃COO); 23,8 (C-11); 23,9 (C-27); 24,1 (C-2); 25,1 (C-16); 26,1 (C-c); 26,6 (6 x CH₂-cyclohexyle); 27,4 (4 x CH₂-cyclohexyle); 28,3 (C-23); 28,5 (C-15); 31,3 (C-21); 32,3 (C-c'); 33,2 (C-7); 36,7 (2 x CH-cyclohexyle); 37,3 (C-10); 37,9 (C-22); 38,1 (C-4); 38,7 (C-1); 39,3 (C-d); 39,5 (C-19); 40,0 (C-20); 40,1 (C-8); 42,9 (C-14); 47,9 (C-9 et C-17); 53,0 (C-b'); 53,5 (C-a1, C-a2, C-a1', C-a2'); 53,6 (C-d'); 54,1 (C-18); 55,7 (C-5); 57,0 (C-b); 57,7 (C-e); 81,3 (C-3); 125,8 (C-12); 140,1 (C-13); 171,3 (H₃C₃COO); 178,1 (C-28).

SMHR: calculé pour C₅₆H₉₇N₄O₃: 873,7561. Trouvé: 873,7553 (100%).

[α]_D²⁰ = +19,0 (CHCl₃, c 0,2).

VI.36. Préparation du composé 192 *N*-{3-[4-(3-(di(cypropylmethyl)amino)propyl)piperazinyl]propyl}-3-*O*-acétylursolamide

**192**

Huile jaune claire

 $C_{50}H_{84}N_4O_3$ $MM = 788 \text{ g/mol}$

Ce composé est synthétisé selon la **Méthode Générale, VI.3.1.1. Réactions d'amination réductrice**, à partir du cyclopropanecarboxaldéhyde (11,4 μL , 0,15 mmol). Le produit est obtenu avec un **rendement de 30%**.

IR (ATR, cm^{-1}): 3322 (NH); 2852 (C-H); 2809 (N-H); 1733 (C=O acétyle); 1646 (C=O amide); 1524 (C=C); 1457 (C-O); 1369 (C-H); 1244 (C-N).

RMN ^1H (500 MHz, CDCl_3), δ (ppm), J en Hz: 0,82 (d, $^3J = 6,7$, 3H, CH_3 -30); 0,87 (m, 1H, CH-5); 0,92 (d, $^3J = 5,5$, 3H, CH_3 -29); 0,94 (m, 1H, CH_2 -1); 0,95 (s, 3H, CH_3 -25); 0,93 (m, 1H, CH_2 -11); 1,00 (sl, 4H, CH_3 -24 et CH-20); 1,01 (s, 6H, CH_3 -26 et CH_3 -23); 1,14 (s, 3H, CH_3 -27); 1,21 (1H, $\text{CH}_2(\text{H}\alpha)$ -7); 1,32 (m, 11H, CH-19, CH_2 -2, 4 x CH_2 -cyclopropyle); 1,55 (m, 6H, $\text{CH}_2(\text{H}\beta)$ -6, $\text{CH}_2(\text{H}\beta)$ -7, CH-9, $\text{CH}_2(\text{H}\alpha)$ -21 et 2 x CH-cyclopropyle); 1,72 (m, 10H, $\text{CH}_2(\text{H}\beta)$ -1, $\text{CH}_2(\text{H}\alpha)$ -6, $\text{CH}_2(\text{H}\alpha)$ -15, CH_2 -16, $\text{CH}_2(\text{H}\beta)$ -21, CH_2 -c, CH_2 -c'); 2,01 (m, 3H, $\text{CH}_2(\text{H}\beta)$ -15, CH_2 -22); 2,09 (d, $^3J = 6,0$, 4H, $\text{N}(\underline{\text{CH}_2})_2$); 2,10 (s, 3H, $\underline{\text{H}_3\text{C}}\text{COO}$); 2,55 (m, 13H, CH_2 -a1, CH_2 -a1', CH_2 -a2, CH_2 -a2', CH_2 -b, CH_2 -b', CH-18); 3,10 (m, 2H, CH_2 -d'); 3,51 (m, 2H, CH_2 -d); 4,55 (dd, $^3J = 11,2$ et 5,5, 1H, CH-3); 5,35 (tl, 1H, CH-12); 6,55 (sl, 1H, NH).

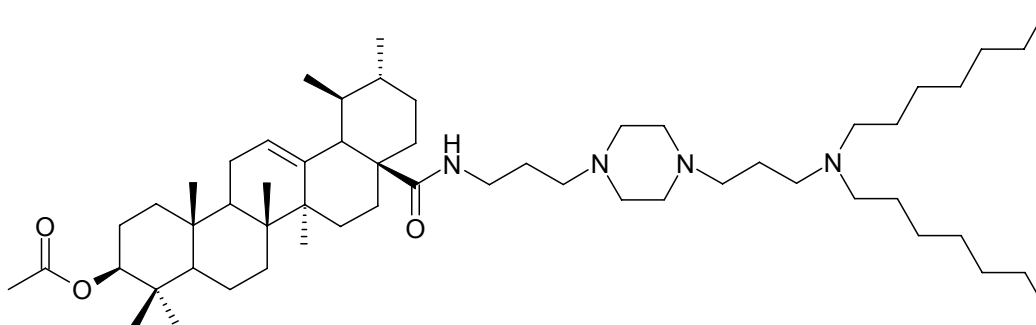
RMN ^{13}C (125 MHz, CDCl_3), δ (ppm): 15,9 (C-25); 17,1 (C-26); 17,4 (C-24); 17,7 (C-29); 18,6 (C-6); 21,6 (C-30 et $\underline{\text{H}_3\text{C}}\text{COO}$); 23,8 (C-11); 23,9 (C-27); 24,1 (C-2); 25,1 (C-16); 26,1 (C-c); 28,3 (C-23); 28,5 (C-15); 29,7 (4 x CH_2 -cyclopropyle); 30,1 (2 x CH-cyclopropyle); 31,9 (C-21); 32,3 (C-c'); 33,2 (C-7);

37,3 (C-10); 37,8 (C-22); 38,1 (C-4); 38,7 (C-1); 39,3 (C-d); 39,5 (C-19); 39,9 (C-20); 40,1 (C-8); 42,8 (C-14); 47,9 (C-9 et C-17); 51,9 (C-b'); 53,6 (C-a1, C-a1', C-a2, C-a2'); 53,8 (C-d'); 54,1 (C-18); 55,7 (C-5); 57,7 (C-b); 59,2 (C-e); 81,3 (C-3); 125,8 (C-12); 140,1 (C-13); 171,4 (H₃CCOO); 178,1 (C-28).

SMHR: calculé pour C₅₀H₈₅N₄O₃: 789,6622. Trouvé: 789,6609 (100%).

$[\alpha]_D^{20} = +18,9$ (CHCl₃, c 0,1).

VI.37. Préparation du composé 193 *N*-{3-[4-(3-(diheptylamino)propyl)piperazinyl]propyl}-3-*O*-acétylursolamide



193

Huile vert jaunée

C₅₆H₁₀₀N₄O₃

MM = 876 g/mol

Ce composé est synthétisé selon la **Méthode Générale, VI.3.1.1. Réactions d'amination réductrice**, à partir de l'heptaldéhyde (22 µL, 0,15 mmol). Le produit est obtenu avec un **rendement de 30%**.

IR (ATR, cm⁻¹): 3318 (NH); 2854 (C-H); 2809 (N-H); 1735 (C=O acétyle); 1640 (C=O amide); 1519 (C=C); 1456 (C-O); 1366 (C-H); 1244 (C-N).

RMN ¹H (500 MHz, CDCl₃), δ (ppm), *J* en Hz: 0,82 (d, ³*J* = 6,8, 3H, CH₃-30); 0,87 (m, 1H, CH-5); 0,91 (d, ³*J* = 6,7, 3H, CH₃-29); 0,93 (m, 1H, CH₂-1); 0,94 (8H, CH₂-11 et 2 x CH₃-heptyle); 0,95 (s, 3H, CH₃-25); 0,97 (sl, 4H, CH₃-24 et CH-20); 0,99 (s, 3H, CH₃-23); 1,01 (s, 3H, CH₃-26); 1,14 (s, 3H, CH₃-27); 1,21 (1H, CH₂(H_α)-7); 1,32 (m, 23H, CH-19, CH₂-2, 10 x CH₂-heptyle); 1,53 (m, 4H,

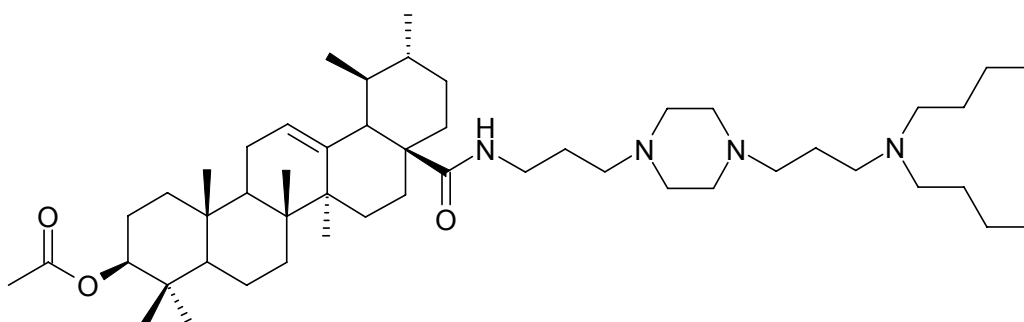
CH_{2(Hβ)}-6, CH_{2(Hβ)}-7, CH-9, CH_{2(Hα)}-21); 1,74 (m, 10H, CH_{2(Hβ)}-1, CH_{2(Hα)}-6, CH_{2(Hα)}-15, CH₂-16, CH_{2(Hβ)}-21, CH₂-c, CH₂-c'); 1,99 (m, 3H, CH_{2(Hβ)}-15, CH₂-22); 2,10 (s, 3H, H₃C_{COO}); 2,46 (m, 17H, CH₂-a1, CH₂-a1', CH₂-a2, CH₂-a2', CH₂-b, CH₂-b', CH-18 et -N(CH₂)₂); 3,09 (m, 2H, CH₂-d'); 3,48 (m, 2H, CH₂-d); 4,56 (dd, ³J = 11,3 et 5,5, 1H, CH-3); 5,35 (tl, 1H, CH-12); 6,53 (sl, 1H, NH).

RMN ¹³C (125 MHz, CDCl₃), δ (ppm): 14,4 (2 x CH₃-heptyle); 15,9 (C-25); 17,1 (C-26); 17,4 (C-24); 17,7 (C-29); 18,6 (C-6); 21,6 (C-30 et H₃C_{COO}); 23,0 (2 x -CH₂CH₃-heptyle); 23,8 (C-11); 23,9 (C-27); 24,1 (C-2); 25,1 (C-16); 26,1 (C-c); 27,9 (2 x -CH₂(CH₂)₃CH₃-heptyle); 28,3 (C-23); 28,5 (C-15); 28,7 (2 x -CH₂(CH₂)₂CH₃-heptyle); 29,7 (2 x -CH₂(CH₂)₄CH₃-heptyle); 30,1 (2 x -CH₂CH₂CH₃-heptyle); 31,3 (C-21); 32,3 (C-c'); 33,2 (C-7); 37,3 (C-10); 37,8 (C-22); 38,1 (C-4); 38,7 (C-1); 39,3 (C-d); 39,5 (C-19); 39,9 (C-20); 40,1 (C-8); 42,8 (C-14); 47,9 (C-17); 48,0 (C-9); 52,3 (C-b'); 53,6 (C-a1, C-a1', C-a2, C-a2'); 54,1 (C-18); 54,4 (C-d'); 55,7 (C-5); 57,1 (C-b); 57,8 (C-e); 81,3 (C-3); 125,8 (C-12); 140,1 (C-13); 171,4 (H₃C_{COO}); 178,1 (C-28).

SMHR: calculé pour C₅₆H₁₀₁N₄O₃: 877,7874. Trouvé: 877,7901 (100%).

[α]_D²⁰ = +26,8 (CHCl₃, c 0,1).

VI.38. Préparation du composé **194** N-{3-[4-(3-(dibutylamino)propyl)-piperaziny]propyl}-3-O-acétylursolamide



194

Huile jaune claire

C₅₀H₈₈N₄O₃

MM = 792 g/mol

Ce composé est synthétisé selon la **Méthode Générale, VI.3.1.1. Réactions d'amination réductrice**, à partir du butyraldéhyde (13,2 μL, 0,15 mmol). Le produit est obtenu avec un **rendement de 30%**.

IR (ATR, cm^{-1}): 3320 (NH); 2870 (C-H); 2807 (N-H); 1733 (C=O acétyle); 1640 (C=O amide); 1520 (C=C); 1461 (C-O); 1368 (C-H); 1242 (C-N).

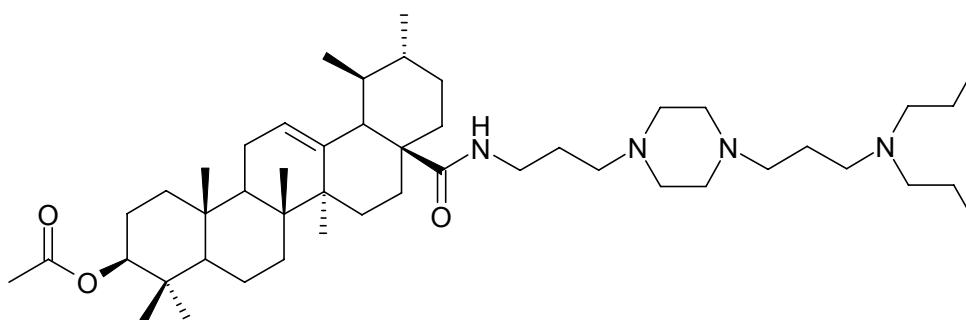
RMN ^1H (500 MHz, CDCl_3), δ (ppm), J en Hz: 0,82 (d, $^3J = 6,9$, 3H, CH_3 -30); 0,88 (m, 1H, CH-5); 0,91 (d, $^3J = 6,7$, 3H, CH_3 -29); 0,94 (m, 1H, CH_2 -1); 0,94 (m, 1H, CH_2 -11); 0,93 (m, 6H, 2 x CH_3 -butyle); 0,95 (s, 3H, CH_3 -25); 0,97 (sl, 3H, CH_3 -24 et 1H, CH-20); 0,98 (s, 3H, CH_3 -23); 1,00 (s, 3H, CH_3 -26); 1,14 (s, 3H, CH_3 -27); 1,21 (1H, $\text{CH}_{2(\text{H}\alpha)}$ -7); 1,35 (m, 11H, CH-19, CH_2 -2, 4 x CH_2 -butyle); 1,53 (m, 4H, $\text{CH}_{2(\text{H}\beta)}$ -6, $\text{CH}_{2(\text{H}\beta)}$ -7, CH-9, $\text{CH}_{2(\text{H}\alpha)}$ -21); 1,73 (m, 10H, $\text{CH}_{2(\text{H}\beta)}$ -1, $\text{CH}_{2(\text{H}\alpha)}$ -6, $\text{CH}_{2(\text{H}\alpha)}$ -15, CH_2 -16, $\text{CH}_{2(\text{H}\beta)}$ -21, CH_2 -c, CH_2 -c'); 1,99 (m, 3H, $\text{CH}_{2(\text{H}\beta)}$ -15, CH_2 -22); 2,10 (s, 3H, H_3CCOO); 2,51 (m, 17H, CH_2 -a1, CH_2 -a1', CH_2 -a2, CH_2 -a2', CH_2 -b, CH_2 -b', CH-18 et $-\text{N}(\text{CH}_2)_2$); 3,10 (m, 2H, CH_2 -d'); 3,47 (m, 2H, CH_2 -d); 4,54 (dd, $^3J = 11,3$ et $5,5$, 1H, CH-3); 5,35 (tl, 1H, CH-12); 6,51 (sl, 1H, NH).

RMN ^{13}C (125 MHz, CDCl_3), δ (ppm): 14,0 (2 x CH_3 -butyle); 15,8 (C-25); 17,1 (C-26); 17,4 (C-24); 17,7 (C-29); 18,6 (C-6); 20,6 (2 x $-\text{CH}_2\text{CH}_3$ -butyle); 21,6 (C-30); 21,7 (H_3CCOO); 23,7 (C-11); 23,9 (C-27); 24,1 (C-2); 25,1 (C-16); 25,4 (2 x $-\text{CH}_2\text{CH}_2\text{CH}_3$ -butyle); 26,2 (C-c); 28,3 (C-23); 28,5 (C-15); 30,1 (C-c'); 31,3 (C-21); 33,1 (C-7); 37,3 (C-10); 37,9 (C-22); 38,1 (C-4); 38,5 (C-1); 39,3 (C-d); 39,5 (C-19); 39,9 (C-20); 40,0 (C-8); 42,7 (C-14); 47,9 (C-17); 48,1 (C-9); 51,2 (C-b'); 52,8 (C-d'); 53,4 (C-a1, C-a1', C-a2, C-a2'); 53,7 (C-18); 54,7 (C-b); 54,8 (C-e); 55,6 (C-5); 81,3 (C-3); 125,8 (C-12); 140,2 (C-13); 171,4 (H_3CCOO); 178,1 (C-28).

SMHR: calculé pour $\text{C}_{50}\text{H}_{89}\text{N}_4\text{O}_3$: 793,6935. Trouvé: 793,6981 (100%).

$[\alpha]_{\text{D}}^{20} = +27,0$ (CHCl_3 , c 0,3).

VI.39. Préparation du composé 195 N-{3-[4-(3-(dipropylamino)propyl)-piperazinyl]propyl}-3-O-acétylursolamide

**195**

Huile jaune claire

 $C_{48}H_{84}N_4O_3$

MM = 764 g/mol

Ce composé est synthétisé selon la **Méthode Générale, VI.3.1.1. Réactions d'amination réductrice**, à partir du propionaldéhyde (11,2 μ L, 0,15 mmol). Le produit est obtenu avec un **rendement de 45%**.

IR (ATR, cm^{-1}): 3325 (NH); 2870 (C-H); 1734 (C=O acétyle); 1639 (C=O amide); 1523 (C=C); 1457 (C-O); 1369 (C-H); 1243 (C-N).

RMN 1H (500 MHz, $CDCl_3$), δ (ppm), J en Hz: 0,80 (d, $^3J = 7,0$, 3H, CH_3 -30); 0,88 (m, 1H, CH-5); 0,91 (d, $^3J = 6,5$, 3H, CH_3 -29); 0,93 (m, 1H, CH_2 -1); 0,94 (m, 1H, CH_2 -11); 0,93 (m, 6H, 2 x CH_3 -propyle); 0,96 (s, 3H, CH_3 -25); 0,99 (sl, 3H, CH_3 -24 et 1H, CH-20); 1,00 (s, 3H, CH_3 -23); 1,01 (s, 3H, CH_3 -26); 1,14 (s, 3H, CH_3 -27); 1,21 (m, 1H, $CH_{2(H\alpha)}$ -7); 1,32 (m, 7H, CH-19, CH_2 -2 et 2 x CH_2 -propyle); 1,53 (m, 4H, $CH_{2(H\beta)}$ -6, $CH_{2(H\beta)}$ -7, CH-9, $CH_{2(H\alpha)}$ -21); 1,62 (m, 4H, $CH_{2(H\beta)}$ -1, $CH_{2(H\alpha)}$ -15, $CH_{2(H\beta)}$ -16, $CH_{2(H\beta)}$ -21); 1,74 (m, 6H, CH_2 -c, CH_2 -c', $CH_{2(H\alpha)}$ -6, $CH_{2(H\alpha)}$ -16); 1,99 (m, 3H, $CH_{2(H\beta)}$ -15, CH_2 -22); 2,10 (s, 3H, CH_3 -COO); 2,56 (m, 17H, CH_2 -a1, CH_2 -a1', CH_2 -a2, CH_2 -a2', CH_2 -b, CH_2 -b', CH-18 et -N(CH_2)₂); 3,08 (m, 2H, CH_2 -d'); 3,49 (m, 2H, CH_2 -d); 4,54 (dd, $^3J = 11,3$ et 5,5, 1H, CH-3); 5,35 (tl, 1H, CH-12); 6,43 (sl, 1H, NH).

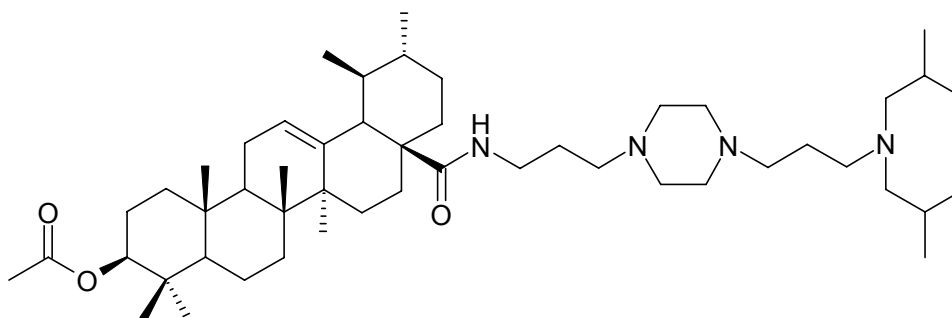
RMN ^{13}C (125 MHz, $CDCl_3$), δ (ppm): 12,3 (2 x CH_3 -propyle); 15,9 (C-25); 17,1 (C-26); 17,4 (C-24); 17,7 (C-29); 18,6 (C-6); 20,5 (CH_2 -propyle); 21,6 (C-30 et H_3C -COO); 23,8 (C-11); 23,9 (C-27); 24,1 (C-2); 25,1 (C-16); 26,1 (C-c); 28,2 (C-23); 28,5 (C-15); 31,3 (C-21); 32,3 (C-c'); 33,2 (C-7); 37,3 (C-10); 37,8 (C-

22); 38,1 (C-4); 38,7 (C-1); 39,3 (C-d); 39,5 (C-19); 39,9 (C-20); 40,1 (C-8); 42,8 (C-14); 47,9 (C-17); 48,1 (C-9); 52,5 (C-b'); 53,7 (C-a1, C-a1', C-a2, C-a2'); 53,9 (C-d'); 54,1 (C-18); 55,7 (C-5); 56,6 (C-b); 57,8 (C-e); 81,3 (C-3); 125,8 (C-12); 140,2 (C-13); 171,6 (H₃CCOO); 179,0 (C-28).

SMHR: calculé pour C₄₈H₈₅N₄O₃: 765,6622. Trouvé: 765,6600 (100%).

$[\alpha]_{\text{D}}^{20} = +26,5$ (CHCl₃, c 0,1).

VI.40. Préparation du composé **196** *N*-{3-[4-(3-(diisobutylamino)propyl)piperazinyl]propyl}-3-*O*-acétylursolamide



196

Huile jaune

C₅₀H₈₈N₄O₃

MM = 792 g/mol

Ce composé est synthétisé selon la **Méthode Générale, VI.3.1.1. Réactions d'amination réductrice**, à partir de l'isobutyraldéhyde (26,4 μL, 0,15 mmol). Le produit est obtenu avec un **rendement de 39%**.

IR (ATR, cm⁻¹): 3335 (NH); 2868 (C-H); 2805 (C-H); 1735 (C=O acétyle); 1637 (C=O amide); 1521 (C=C); 1458 (C-O); 1368 et 1157 (-CH₃ géminaux); 1244 (C-N).

RMN ¹H (500 MHz, CDCl₃), δ (ppm), *J* en Hz: 0,82 (d, ³*J* = 6,5, 3H, CH₃-30); 0,87 (m, 1H, CH-5); 0,91 (m, 15H, CH₃-29, 2 x CH₃-isobutyle); 0,93 (s, 3H, CH₃-25, CH₂-1, CH₂-11); 0,94 (sl, 4H, CH₃-24 et CH-20); 0,97 (s, 6H, CH₃-23, CH₃-26); 1,12 (s, 3H, CH₃-27); 1,20 (m, 1H, CH₂(H_α)-7); 1,31 (m, 5H, CH-19, CH₂-2, 2 x CH-isobutyle); 1,54 (m, 4H, CH₂(H_β)-6, CH₂(H_β)-7, CH-9, CH₂(H_α)-21); 1,73 (m, 10H, CH₂(H_β)-1, CH₂(H_α)-6, CH₂(H_α)-15, CH₂-16, CH₂(H_β)-21, CH₂-c, CH₂-c'); 1,99

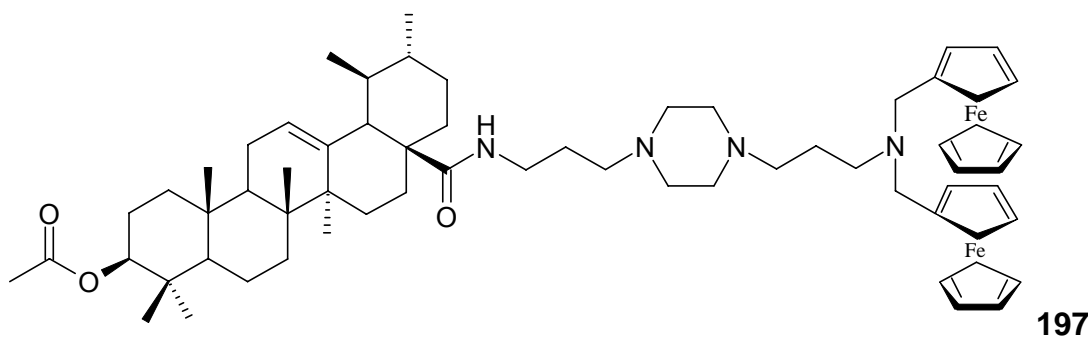
(m, 3H, CH₂(H β)-15, CH₂-22); 2,10 (s, 3H, CH₃-COO); 2,41 (m, 17H, CH₂-a1, CH₂-a1', CH₂-a2, CH₂-a2', CH₂-b, CH₂-b', CH-18 et -N(CH₂)₂); 3,09 (m, 2H, CH₂-d'); 3,50 (m, 2H, CH₂-d); 4,54 (dd, ³J = 11,0 et 5,7, 1H, CH-3); 5,35 (tl, 1H, CH-12); 6,62 (sl, 1H, NH).

RMN ¹³C (125 MHz, CDCl₃), δ (ppm): 15,9 (C-25); 17,1 (C-26); 17,4 (C-24); 17,7 (C-29); 18,6 (C-6); 21,3 (4 x CH₃-isobutyle); 21,6 (C-30); 21,7 (H₃C₂COO); 23,8 (C-11); 23,9 (C-27); 24,1 (C-2); 25,1 (C-16); 26,0 (C-c); 27,0 (2 x CH-isobutyle); 28,3 (C-23); 28,5 (C-15); 30,1 (C-c'); 31,3 (C-21); 33,2 (C-7); 37,3 (C-10); 37,8 (C-22); 38,1 (C-4); 38,7 (C-1); 39,3 (C-d); 39,5 (C-19); 39,9 (C-20); 40,1 (C-8); 42,8 (C-14); 47,9 (C-9 et C-17); 53,0 (C-b'); 53,6 (C-a1, C-a1', C-a2, C-a2'); 54,1 (C-18); 54,5 (C-d'); 55,7 (C-5); 57,2 (C-b); 57,7 (C-e); 81,3 (C-3); 125,8 (C-12); 140,1 (C-13); 171,4 (H₃C₂COO); 178,2 (C-28).

SMHR: calculé pour C₅₀H₈₉N₄O₃: 793,6935. Trouvé: 793,6942 (100%).

$[\alpha]_D^{20} = +29,3$ (CHCl₃, c 0,1).

VI.41. Préparation du composé 197 *N*-{3-[4-(3-(diferrocenyl-amino)propyl)piperazinyl]propyl}-3-*O*-acétylursolamide



Poudre rouge

C₆₄H₉₂N₄O₃Fe₂

MM = 1076 g/mol

Ce composé est synthétisé selon la **Méthode Générale, VI.3.1.1. Réactions d'amination réductrice**, à partir du ferrocénecarboxaldéhyde (65,5 mg, 0,15 mmol). Le composé est obtenu avec un **rendement de 60%**.

IR (ATR, cm^{-1}): 3328 (NH); 2854 (C-H); 2810 (N-H); 1733 (C=O acétyle); 1646 (C=O amide); 1518 (C=C); 1455 (C-O); 1369 (C-H); 1244 (C-N); 1105 et 1002 (Cp-ferrocène).

RMN ^1H (500 MHz, CDCl_3), δ (ppm), J en Hz: 0,81 (d, $^3J = 6,0$, 3H, CH_3 -30); 0,86 (m, 1H, CH-5); 0,90 (d, $^3J = 6,3$, 3H, CH_3 -29); 0,91 (m, 1H, CH_2 -1); 0,94 (m, 1H, CH_2 -11); 0,98 (s, 3H, CH_3 -25); 0,99 (sl, 4H, CH_3 -24, CH-20); 1,00 (s, 6H, CH_3 -26 et CH_3 -23); 1,13 (s, 3H, CH_3 -27); 1,20 (m, 1H, $\text{CH}_{2(\text{H}\alpha)}$ -7); 1,32 (m, 3H, CH-19 et CH_2 -2); 1,53 (m, 4H, $\text{CH}_{2(\text{H}\beta)}$ -6, $\text{CH}_{2(\text{H}\beta)}$ -7, CH-9, $\text{CH}_{2(\text{H}\alpha)}$ -21); 1,62 (m, 4H, $\text{CH}_{2(\text{H}\beta)}$ -1, $\text{CH}_{2(\text{H}\alpha)}$ -15, $\text{CH}_{2(\text{H}\beta)}$ -16, $\text{CH}_{2(\text{H}\beta)}$ -21); 1,72 (m, 6H, CH_2 -c, CH_2 -c', $\text{CH}_{2(\text{H}\alpha)}$ -6, $\text{CH}_{2(\text{H}\alpha)}$ -16); 1,84 (2H, CH_2 -22); 2,02 (m, 1H, $\text{CH}_{2(\text{H}\beta)}$ -15); 2,11 (s, 3H, H_3CCOO); 2,34 (m, 13H, CH_2 -a1, CH_2 -a1', CH_2 -a2, CH_2 -a2', CH_2 -b, CH_2 -b' et CH-18); 3,08 (m, 2H, CH_2 -d'); 3,48 (m, 2H, CH_2 -d); 3,53 (s, 4H, $-\text{N}(\text{CH}_2)_2$); 4,17 (s, 10H, Cp); 4,26 (m, 8H, Cp'); 4,54 (dd, $^3J = 110$ et 5,3, 1H, CH-3); 5,33 (tl, 1H, CH-12); 6,54 (sl, 1H, NH).

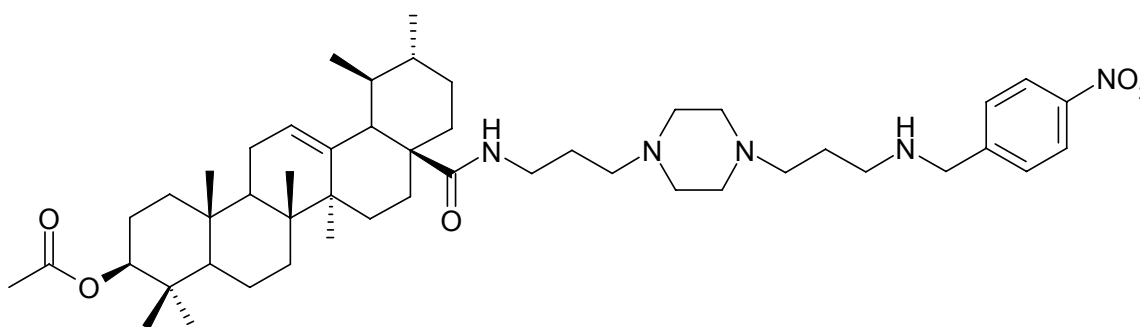
RMN ^{13}C (125 MHz, CDCl_3), δ (ppm): 15,9 (C-25); 17,1 (C-26); 17,4 (C-24); 17,7 (C-29); 18,6 (C-6); 21,6 (C-30); 21,7 (H_3CCOO); 23,8 (C-11); 23,9 (C-27); 24,1 (C-2); 25,1 (C-16); 26,1 (C-c); 28,3 (C-23); 28,5 (C-15); 29,7 (C-c'); 31,3 (C-21); 33,1 (C-7); 37,3 (C-10); 37,8 (C-22); 38,1 (C-4); 38,7 (C-1); 39,0 (C-d); 39,5 (C-19); 39,9 (C-20); 40,1 (C-8); 42,8 (C-14); 47,9 (C-9 et C-17); 53,1 (C-a1, C-a1', C-a2, C-a2'); 53,4 (C-b'); 54,0 (C-d'); 54,1 (C-18); 55,7 (C-5 et C-b); 69,1 (Cp); 69,7 (Cp'); 70,0 (Cp); 70,9 (C-e); 81,3 (C-3); 125,8 (C-12); 140,1 (C-13); 171,4 (H_3CCOO); 179,2 (C-28).

SMHR: calculé pour $\text{C}_{64}\text{H}_{93}\text{N}_4\text{O}_3\text{Fe}_2$: 1077,5946. Trouvé: 1077,5945 (100%).

$[\alpha]_{\text{D}}^{20} = +59$ (CHCl_3 , c 0,1).

pF : 65 °C

VI.42. Préparation du composé 198 N-{3-[4-(3-(4-nitrobenzyl)amino)propyl]piperazinyl}propyl)-3-O-acétylursolamide



198

Huile jaune

C₄₉H₇₇N₅O₅

MM = 815 g/mol

Ce composé a été synthétisé selon la **Méthode Générale VI.3.1.2. Réactions d'amination réductrice**, à partir du *p*-nitrobenzaldéhyde (13,7 mg, 0,075 mmol). Le produit est obtenu avec un **rendement de 20%**.

IR (ATR, cm⁻¹): 3332 (NH); 2854 (C-H); 1729 (C=O acétyle); 1644 (C=O amide); 1597 (C=C); 1518 (aromatique-NO₂); 1454 (C-O); 1368 (C-H); 1245 (C-N); 854 (aromatique *p*-substitué).

RMN ¹H (500 MHz, CDCl₃), δ (ppm), *J* en Hz: 0,81 (d, ³*J* = 7,0, 3H, CH₃-30); 0,89 (1H, CH-5); 0,90 (d, ³*J* = 5,8, 3H, CH₃-29); 0,96 (s, 3H, CH₃-25); 0,95 (m, 2H, CH₂-1, CH₂-11); 0,97 (sl, 4H, CH₃-24 et CH-20); 1,00 (s, 6H, CH₃-23, CH₃-26); 1,13 (s, 3H, CH₃-27); 1,19 (1H, CH₂(H_α)-7); 1,36 (m, 3H, CH₂-2, CH-19); 1,57 (m, 8H, CH₂(H_β)-1, CH₂(H_β)-6, CH₂(H_β)-7, CH-9, CH₂(H_α)-15, CH₂(H_β)-16, CH₂-21); 1,74 (m, 8H, CH₂-c, CH₂H-c', CH₂(H_α)-6, CH₂(H_α)-16, CH₂-22); 2,04 (m, 1H, CH₂(H_β)-15); 2,11 (s, 3H, H₃C₃COO); 2,47 (m, 13H, CH₂-a1, CH₂-a1', CH₂-a2, CH₂-a2', CH₂-b, CH₂-b' et CH-18); 3,04 (m, 2H, CH₂-d'); 3,50 (m, 2H, CH₂-d); 3,75 (s, 2H, -NCH₂); 4,53 (dd, ³*J* = 11,7 et 4,6, 1H, CH-3); 5,34 (tl, 1H, CH-12); 6,57 (sl, 1H, NH); 7,58 (d, ³*J* = 8,2, 2H, H-ortho); 8,22 (d, ³*J* = 8,3, 2H, H-méta).

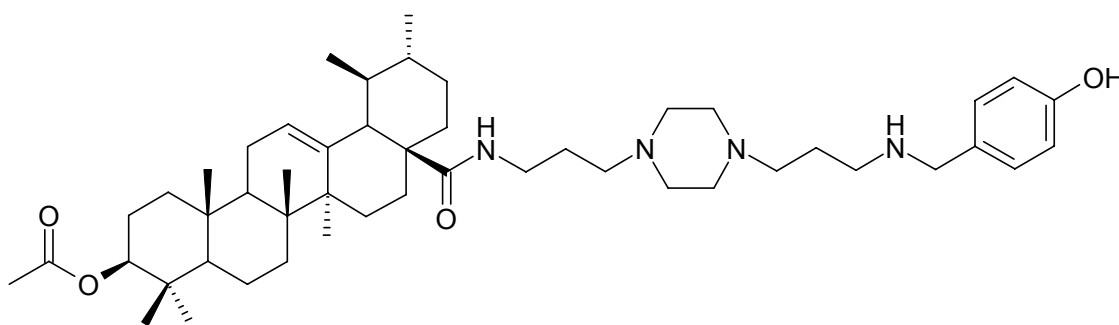
RMN ¹³C (125 MHz, CDCl₃), δ (ppm), *J* en Hz: 15,9 (C-25); 17,1 (C-26); 17,4 (C-24); 17,7 (C-29); 18,6 (C-6); 21,6 (C-30); 21,7 (H₃C₃COO); 23,8 (C-11); 23,9 (C-27); 24,1 (C-2); 25,1 (C-16); 26,0 (C-c); 28,2 (C-23); 28,5 (C-15); 30,2 (C-c'); 31,3 (C-21); 33,1 (C-7); 37,2 (C-10); 37,8 (C-22); 38,1 (C-4); 38,7 (C-1); 39,2

(C-d); 39,5 (C-19); 39,9 (C-20); 40,1 (C-8); 42,8 (C-14); 47,9 (C-17); 48,0 (C-9); 48,8 (C-b); 53,5 (C-a1, C-a1', C-a2, C-a2'); 53,5 (C-d'); 54,1 (C-18); 55,6 (C-5); 57,1 (C-b'); 57,5 (C-e); 81,3 (C-3); 124,1 (C-ortho); 125,8 (C-12); 129,6 (C-méta); 139,2 (C-13); 143,0 (C-*ipso*); 148,0 (C-*para*); 171,5 (H₃CCOO); 178,1 (C-28).

SMHR: calculé pour C₄₉H₇₈N₅O₅: 816,6003. Trouvé: 816,5983 (100%).

$[\alpha]_D^{20} = +29,1$ (CHCl₃, c 0,1).

VI.43. Préparation du composé **199** *N*-{3-[4-(3-(4-hydroxybenzyl)amino)propyl)piperazinyl]propyl}-3-*O*-acétylursolamide



199

Huile jaune

C₄₉H₇₈N₄O₄

MM = 786 g/Mol

Ce composé a été synthétisé selon la **Méthode Générale VI.3.1.2. Réactions d'amination réductrice**, à partir du *p*-hydroxybenzaldéhyde (9,15 mg, 0,075 mmol). Le produit est obtenu avec un **rendement de 62%**.

IR (ATR, cm⁻¹): 3309 (NH); 2853 (C-H); 1732 (C=O acétyle); 1637 (C=O amide); 1518 (C=C); 1457 (C-O); 1369 (C-H); 1246 (C-N); 753 (aromatique *p*-substitué).

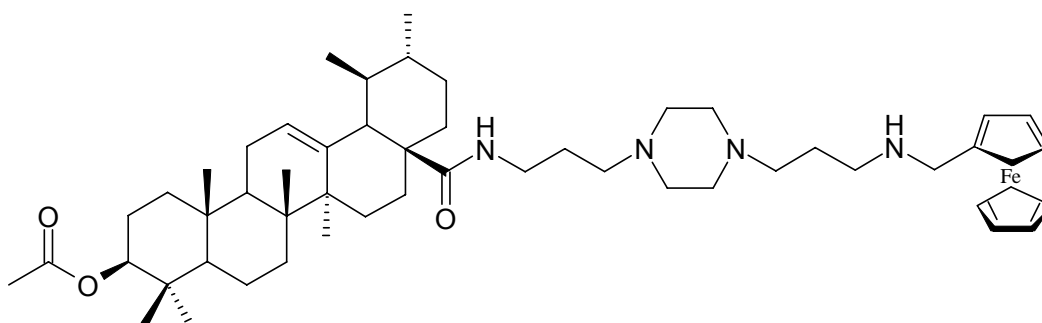
RMN ¹H (500 MHz, CDCl₃), δ (ppm), *J* en Hz: 0,81 (d, ³*J* = 6,9, 3H, CH₃-30); 0,87 (m, 1H, CH-5); 0,91 (d, ³*J* = 5,9, 3H, CH₃-29); 0,96 (s, 3H, CH₃-25); 0,95 (m, 2H, CH₂-1, CH₂-11); 0,96 (sl, 4H, CH₃-24 et CH-20); 0,99 (s, 3H, CH₃-23); 1,01 (s, 3H, CH₃-26); 1,14 (s, 3H, CH₃-27); 1,21 (m, 1H, CH₂(H_α)-7); 1,37 (m, 3H,

CH-19 et CH₂-2); 1,53 (m, 4H, CH₂(H_β)-6, CH₂(H_β)-7, CH-9, CH₂(H_α)-21); 1,62 (m, 4H, CH₂(H_β)-1, CH₂(H_α)-15, CH₂(H_β)-16, CH₂(H_β)-21); 1,75 (m, 8H, CH₂-c, CH₂-c', CH₂(H_α)-6, CH₂(H_α)-16, CH₂-22); 2,01 (m, 1H, CH₂(H_β)-15); 2,11 (s, 3H, H₃C_{COO}); 2,44 (m, 13H, CH₂-a1, CH₂-a1', CH₂-a2, CH₂-a2', CH₂-b, CH₂-b', CH-18); 3,04 (m, 2H, CH₂-d'); 3,45 (m, 2H, CH₂-d); 3,75 (s, 2H, -N(CH₂)); 4,55 (dd, ³J = 11,3 et 5,5, 1H, CH-3); 5,34 (tl, 1H, CH-12); 6,47 (sl, 1H, NH); 6,78 (d, ³J = 8,1, 2H, CH-ortho); 7,20 (d, ³J = 8,2, 2H, CH-méta).

RMN ¹³C (125 MHz, CDCl₃), δ (ppm): 15,9 (C-25); 17,1 (C-26); 17,3 (C-24); 17,7 (C-29); 18,6 (C-6); 21,6 (C-30); 21,7 (H₃C_{COO}); 23,8 (C-11); 23,9 (C-27); 24,1 (C-2); 25,1 (C-16); 26,0 (C-c); 28,2 (C-23); 28,5 (C-15); 30,1 (C-c'); 31,2 (C-21); 33,1 (C-7); 37,2 (C-10); 37,8 (C-22); 38,1 (C-4); 38,7 (C-1); 39,2 (C-d); 39,5 (C-19); 39,9 (C-20); 40,1 (C-8); 42,8 (C-14); 47,9 (C-17); 48,0 (C-9); 48,9 (C-b'); 53,5 (C-a1, C-a1', C-a2, C-a2'); 54,1 (C-18); 54,2 (C-d'); 55,6 (C-5); 57,3 (C-b); 57,7 (C-e); 81,3 (C-3); 115,7 (C-méta); 125,9 (C-12); 130,3 (C-ortho et C-ipso); 140,1 (C-13); 156,0 (C-para); 171,5 (H₃C_{COO}); 178,6 (C-28).

[α]_D²⁰ = +58,3 (CHCl₃, c 0,15).

VI.44. Préparation du composé 200 N-{3-[4-(3-ferrocénylamino)propyl]piperaziny]propyl}-3-O-acétylursolamide



200

Huile orange

C₅₃H₈₂FeN₄O₃

MM = 878 g/mol

Ce composé a été synthétisé selon la **Méthode Générale VI.3.1.2. Réactions d'amination réductrice**, à partir du ferrocène-carboxaldéhyde (16,5 mg, 0,075 mmol). Le produit est obtenu avec un **rendement de 52%**.

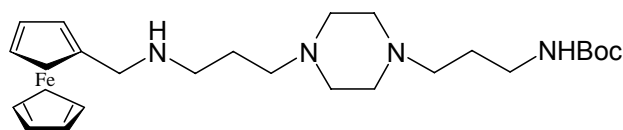
IR (ATR, cm^{-1}): 3328 (NH); 2813 (N-H); 1731 (C=O acétyle); 1639 (C=O amide); 1524 (C=C); 1457 (C-O); 1370 (C-H); 1246 (C-N); 1105 et 10031 (Cp-ferrocène).

RMN ^1H (500 MHz, CDCl_3), δ (ppm), J en Hz: 0,81 (d, $^3J = 6,0$, 3H, CH_3 -30); 0,87 (m, 1H, CH-5); 0,91 (d, $^3J = 6,3$, 3H, CH_3 -29); 0,93 (m, 2H, CH_2 -1, CH_2 -11); 0,96 (m, 7H, CH_3 -25, CH_3 -24, CH-20); 1,00 (s, 6H, CH_3 -26 et CH_3 -23); 1,14 (s, 3H, CH_3 -27); 1,21 (m, 1H, $\text{CH}_{2(\text{H}\alpha)}$ -7); 1,34 (m, 3H, CH-19 et CH_2 -2); 1,52 (m, 4H, $\text{CH}_{2(\text{H}\beta)}$ -6, $\text{CH}_{2(\text{H}\beta)}$ -7, CH-9, $\text{CH}_{2(\text{H}\alpha)}$ -21); 1,61 (m, 4H, $\text{CH}_{2(\text{H}\beta)}$ -1, $\text{CH}_{2(\text{H}\alpha)}$ -15, $\text{CH}_{2(\text{H}\beta)}$ -16, $\text{CH}_{2(\text{H}\beta)}$ -21); 1,73 (m, 6H, CH_2 -c, CH_2 -c', $\text{CH}_{2(\text{H}\alpha)}$ -6, $\text{CH}_{2(\text{H}\alpha)}$ -16); 1,86 (2H, CH_2 -22); 2,01 (m, 1H, $\text{CH}_{2(\text{H}\beta)}$ -15); 2,10 (s, 3H, H_3CCOO); 2,36 (m, 13H, CH_2 -a1, CH_2 -a1', CH_2 -a2, CH_2 -a2', CH_2 -b, CH_2 -b', CH-18); 3,06 (m, 2H, CH_2 -d'); 3,47 (m, 2H, CH_2 -d); 3,78 (s, 2H, $-\text{N}(\underline{\text{CH}_2})_2$); 4,21 (s, 5H, CH-ferrocène); 4,28 (m, 4H, CH-ferrocène); 4,54 (dd, $^3J = 11,3$ et $5,5$, 1H, CH-3); 5,35 (tl, 1H, CH-12); 6,41 (sl, 1H, NH).

RMN ^{13}C (125 MHz, CDCl_3), δ (ppm): 15,9 (C-25); 17,1 (C-26); 17,3 (C-24); 17,7 (C-29); 18,6 (C-6); 21,6 (C-30 et H_3CCOO); 23,8 (C-11); 23,9 (C-27 et C-2); 25,1 (C-16); 26,2 (C-c); 28,2 (C-23); 28,5 (C-15); 30,1 (C-c'); 31,3 (C-21); 33,1 (C-7); 37,3 (C-10); 37,8 (C-22); 38,1 (C-4); 38,7 (C-1); 39,0 (C-d); 39,5 (C-19); 39,9 (C-20); 40,1 (C-8); 42,8 (C-14); 47,9 (C-9); 48,2 (C-17); 48,6 (C-d'); 53,4 (C-a1, C-a1', C-a2, C-a2'); 53,6 (C-b'); 54,1 (C-18); 55,6 (C-5); 57,3 (C-b); 58,1 (C-e); 68,5 (Cp-ferrocène); 69,2 (Cp-ferrocène); 69,6 (Cp-ferrocène); 81,3 (C-3); 125,8 (C-12); 140,2 (C-13); 171,4 (H_3CCOO); 178,5 (C-28).

$[\alpha]_{\text{D}}^{20} = +25,15$ (CHCl_3 , c 0,35).

VI.45. Preparation du 201 3-[4-(3-ferrocenyl-aminopropyl)pipérazinyl]propyl]carbamate de terbutyle

**201**

Huile jaune orangée

 $C_{26}H_{42}FeN_4O_2$

MM = 502 g/mol

Ce composé a été synthétisé selon la **Méthode Générale VI.3.1.3. Réactions d'amination réductrice**, à partir du ferrocène carboxaldéhyde (47,1 mg, 0,22 mmol). Le produit est obtenu avec un **rendement de 58%**.

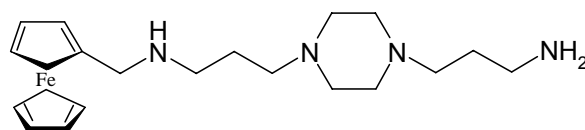
IR (ATR, cm^{-1}): 3088 (NH); 2814 (C-H); 1692 (C=O amide); 1365 (C-H); 1272 (C-O-C); 1105 et 1002 (Cp-ferrocène).

RMN 1H (500 MHz, $CDCl_3$), δ (ppm), J en Hz: 1,48 (s, 9H, $\underline{CH_3}$ -Boc); 1,69 (q, $^3J = 12,8$ et $6,4$, 2H, CH_2 -c); 1,75 (q, $^3J = 14,0$ et $7,0$, 2H, CH_2 -c'); 2,44 (m, 12H, CH_2 -a1, CH_2 -a1', CH_2 -a2, CH_2 -a2', CH_2 -b, CH_2 -b'); 2,74 (tl, 2H, CH_2 -d); 3,23 (tl, 2H, CH_2 -d'); 3,58 (s, 2H, $-NHCH_2$); 4,16 (m, 2H, CH-ferrocène); 4,17 (s, 5H, CH-ferrocène); 4,21 (m, 2H, CH-ferrocène); 5,52 (sl, 1H, NH amide).

RMN ^{13}C (125 MHz, $CDCl_3$), δ (ppm): 26,7 (C-c'); 27,0 (C-c); 28,9 ($\underline{CH_3}$ Boc); 40,4 (C-d); 48,5 (C-b'); 49,3 (C-d'); 53,6 (C-a1, C-a1', C-a2, C-a2'); 57,3 (C-b); 57,4 (C-e); 68,3 (Cp-ferrocène); 68,8 (Cp-ferrocène); 68,9 (Cp-ferrocène); 156,4 (C=O Boc).

$[\alpha]_D^{20} = -2$ ($CHCl_3$, c 0,15).

VI.46. Preparation du **202** *N*-{3-[4-(3-aminopropyl)pipérazinyl]propyl}ferrocène

**202**

Huile jaune orangée

 $C_{21}H_{34}FeN_4$ $MM = 398 \text{ g/mol}$

Ce composé a été synthétisé selon la **Méthode Générale VI.3.2. Réactions de déprotection d'une fonction amine protégée par un groupement Boc**, à partir du **x**. Le produit est obtenu avec un **rendement de 88%**.

IR (ATR, cm^{-1}): 3357 (NH_2); 2812 (C-H); 1396 (C-H); 1105 et 1002 (Cp-ferrocène).

RMN 1H (500 MHz, $CDCl_3$), δ (ppm), J en Hz: 1,69 (q, $^3J = 14,4$ et $7,3$, 2H, CH_2 -c); 1,75 (q, $^3J = 14,0$ et $6,9$, 2H, CH_2 -c'); 2,46 (m, 12H, CH_2 -a1, CH_2 -a1', CH_2 -a2, CH_2 -a2' et CH_2 -b, CH_2 -b'); 2,74 (tl, 2H, CH_2 -d); 2,79 (tl, 2H, CH_2 -d'); 3,58 (s, 2H, $-NHCH_2$); 4,16 (m, 2H, CH-ferrocène); 4,17 (s, 5H, CH-ferrocène); 4,19-4,24 (m, 2H, CH-ferrocène).

RMN ^{13}C (125 MHz, $CDCl_3$), δ (ppm): 27,0 (C-c); 30,9 (C-c'); 41,3 (C-d); 48,5 (C-b'); 49,3 (C-d'); 53,7 (C-a1, C-a1', C-a2, C-a2'); 56,9 (C-b); 57,4 (C-e); 68,3 (Cp-ferrocène); 68,8 (Cp'-ferrocène); 68,9 (Cp-ferrocène).

$[\alpha]_D^{20} = +0,15$ ($CHCl_3$, c 0,3).

VII REFERENCES

- ABDEL-MAGID, A.F.; CARSON, K.G.; HARRIS, B.D.; MARYANOFF, C.A.; SHAH, R.D. Reductive amination of aldehydes and ketones with sodium tracetoxylborohydride. Studies on direct and indirect reductive amination procedures. **Journal of Organic Chemistry**, v. 61, p. 3849-3862, 1996.
- ADAGUT, I.S.; WARHURST, D.C. *Plasmodium falciparum*: linkage disequilibrium between loci in chromosomes 7 and 5 and chloroquine selective pressure in northern Nigeria. **Parasitology**, v. 123, p. 219-224, 2001.
- AIKAWA, M.; HEPLER, P.K.; HUFF, C.G.; SPRINZ, H. Feeding mechanisms of avian malarial parasites. **The Journal of Cell Biology**, v. 28, p. 355-373, 1966.
- ALAKURTTI, S., MAKELA, T., KOSKIMIES, S., YLI-KAUHALUOMA, J. Pharmacological properties of the ubiquitous natural product betulin (Review). **European Journal of Pharmaceutical Sciences**, v. 29, p. 1-13, 2006.
- ALECRIM, M.G.C.; ALECRIM, W.M.; MACEDO, V. *Plasmodium vivax* resistance to chloroquine (R2) and mefloquine (R3) in Brazilian Amazon region. **Revista da Sociedade Brasileira de Medicina Tropical**, v. 32, p. 67-68, 1999.
- ALIKARIDIS, F. Natural constituents of *Ilex* species. **Journal of Ethnopharmacology**, v. 20, p. 121-144, 1987.
- AMUSAN, O.O.G.; ADESOGAN, E.K.; MAKINDE, J.M. Antimalarial active principles of *Spathodea campanulata* stem bark. **Phytotherapy Research**, v. 10, p. 692-693, 1996.
- AUFFRET, G.; LABAIED, M.; FRAPPIER, F.; RASOANAIVO, P.; GRELLIER, P.; LEWIN, G. Synthesis and antimalarial evaluation of a series of piperazinyl flavones. **Bioorganic & Medicinal Chemistry Letters**, v. 17, p. 959-963, 2007.
- AYAD, F.; TILLEY, L.; DEADY, L.W. Synthesis, antimalarial activity and inhibition of Haem detoxification of novel bisquinolines. **Bioorganic & Medicinal Chemistry Letters**, v. 11, p. 2075-2077, 2001.
- BABIKER, H.A.; PRINGLE, S.J.; ABDEL-MUHSIN, A.; MACKINNON, M.; HUNT, P.; WALLIKER, D. High-level chloroquine resistance in Sudanese isolates of *Plasmodium falciparum* is associated with mutations in the chloroquine resistance transporter gene *pfcr1* and the multidrug resistance gene *pfmdr1*. **Journal of Infectious Diseases**, v. 183, p.1535-1538, 2001.
- BAELMANS, R.; DEHARO, E.; MUÑOZ, V.; SAUVAIN, M.; GINSBURG, H. Experimental conditions for testing the inhibitory activity of chloroquine on the formation of β -hematin. **Experimental Parasitology**, v. 96, p. 243-248, 2000.
- BANERJEE, R.; LIU, J.; BEATTY, W.; PELOSOF, L.; KLEMBA, M.; GOLDBERG, D.E. Four plasmepsins are active in the *Plasmodium falciparum* food vacuole, including a protease with an active-site histidine. **Proceedings of the National Academy of Sciences of the United States of America**, v. 99, p. 990-995, 2002.

BARAMÉE, A.; COPPIN, A.; MORTUAIRE, M.; PELINSKI, L.; TOMAVO, S.; BROCARD, J. Synthesis and in vitro activities of ferrocenic aminohydroxynaphthoquinones against *Toxoplasma gondii* and *Plasmodium falciparum*. **Bioorganic & Medicinal Chemistry**, v. 14, p. 1294-1302, 2006.

BASCO, L.K.; RINGWALD, P. *pfmdr1* gene mutation and clinical response to chloroquine in Yaounde, Cameroon. **Transactions of the Royal Society of Tropical Medicine and Hygiene**, v. 91, p. 210-211, 1997.

BASCO, L.K.; RINGWALD, P. Molecular epidemiology of malaria in Yaounde, Cameroon. III. Analysis of chloroquine resistance and point mutations in the multidrug resistance 1 (*pfmdr 1*) gene of *Plasmodium falciparum*. **American Journal of Tropical Medicine and Hygiene**, v. 59, p. 577-581, 1998.

BASCO, L.K.; RINGWALD, P. Molecular epidemiology of malaria in Yaounde, Cameroon. VI. Sequence variations in the *Plasmodium falciparum* dihydrofolate reductase–thymidylate synthase gene and *in vitro* resistance to pyrimethamine and cycloguanil. **American Journal of Tropical Medicine and Hygiene**, v. 62, p. 271-276, 2000.

BASCO, L.K. Molecular epidemiology of malaria in Cameroon. XIII. Analysis of *pfcr1* mutations and in vitro chloroquine resistance. **American Journal of Tropical Medicine and Hygiene**, v. 67, p. 388-391, 2002.

BASCO, L.K.; NDOUNGA, M.; NGANE, V.F.; SOULA, G. Molecular epidemiology of malaria in Cameroon. XIV. *Plasmodium falciparum* chloroquine resistance transporter (*PFCRT*) gene sequences of isolates before and after chloroquine treatment. **American Journal of Tropical Medicine and Hygiene**, v. 67, p. 392-395, 2002.

BASCO, L.K.; RINGWALD, P. Molecular epidemiology of malaria in Cameroon. X. Evaluation of *PFMDR1* mutations as genetic markers for resistance to amino alcohols and artemisinin derivatives. **American Journal of Tropical Medicine and Hygiene**, v. 66, p.667-671, 2002.

BECKER, C.A.; GUIMARÃES, J.A.; VERLI, H. Molecular dynamics and atomic charge calculations in the study of heparin conformation in aqueous solution. **Carbohydrate Research**, v. 340, p. 1499-1507, 2005.

BELL, A. Antimalarial drug synergism and antagonism: Mechanistic and clinical significance. **FEMS Microbiology Letters**. v. 253, p. 171-184, 2005.

BHATTACHARYA, P.R.; BISWAS, S.; KABILAN, L. Alleles of the *Plasmodium falciparum Pfmdr1* gene appear not to be associated with chloroquine resistance in India. **Transactions of the Royal Society of Tropical Medicine and Hygiene**, v. 91, p. 454-455, 1997.

BHATTACHARYA, P.R.; PILLAI, C.R. Strong association, but incomplete correlation, between chloroquine resistance and allelic variation in the *pfmdr-1* gene of *Plasmodium falciparum* isolates from India. **Annals of Tropical Medicine and Parasitology**, v. 93, p. 679-684, 1999.

BIOT, C.; GLORIAN, G.; MACIEJEWSKI, L.A.; BROCARD, J.S. Synthesis and antimalarial activity in vitro and in vivo of a new ferrocene-chloroquine analogue. **Journal of Medicinal Chemistry**, v. 40, p. 3715-3718, 1997.

BIOT, C.; DELHAES, L.; N'DIAYE, C.M.; MACIEJEWSKI, L.; CAMUS, D.; DIVE, D.; BROCARD, J. Synthesis and antimalarial activity in vitro of potential metabolites of ferrochloroquine and related compounds. **Bioorganic & Medicinal Chemistry**, v. 7, p. 2843-2847, 1999.

BIOT, C.; DELHAES, L.; MACIEJEWSKI, L.; MORTUAIRE, M.; CAMUS, D.; DIVE, D.; BROCARD, J. Synthetic ferrocenic mefloquine and quinine analogues as potential antimalarial agents. **European Journal of Medicinal Chemistry**, v. 35, p. 707-714, 2000.

BIOT, C.; DESSOLIN, J.; RICARD, I.; DIVE, D. Easily synthesized antimalarial ferrocene triazacyclononane quinoline conjugates. **Journal of Organometallic Chemistry**, v. 689, p. 4678-4682, 2004.

BIOT, C.; TARAMELLI, D.; FROFAR-BARES, I.; MACIEJEWSKI, L.; BOYCE, M.; NOWOGROCKI, G.; BROCARD, J.; BASILICO, N.; OLLIARO, P.; EGAN, T. Insights into the mechanism of action of ferroquine. Relationship between physicochemical properties and antiplasmodial activity. **Molecular Pharmaceutics**, v. 2, p. 185-193, 2005.

BIOT, C.; CHIBALE, K. Novel approaches to antimalarial drug discovery. **Infectious Disorders- Drug Targets**, v. 6, p. 173-204, 2006.

BRAGA, E.M.; FONTES, C.J.F. *Plasmodium* – Malária. In: NEVES, D.P. **Parasitologia humana**. 11.ed. São Paulo: Atheneu, 2005. p. 143-161.

BREMAN, J.G. The ears of the hippopotamus: manifestations, determinants, and estimates of the malaria burden. **American Journal of Tropical Medicine and Hygiene**. v. 64, p. 1-11, 2001.

BRINGMANN, G.; SAEB, W.; ASSI, L.A.; FRANÇOIS, G.; NARAYANAN, A.S.S.; PETERS, K.; PETERS, E-M. Betulinic Acid: Isolation from *Triphyophyllum peltatum* and *Ancistrocladus heyneanus*, Antimalarial Activity, and Crystal Structure of the Benzyl Ester. **Planta Medica**, v. 63, p. 255-257, 1997.

BULLER, R.; PETERSON, M.L.; ALMARSSON, O.; LEISEROWITZ, L. Quinoline Binding Site on Malaria Pigment Crystal: A Rational Pathway for Antimalarial Drug Design. **Crystal Growth & Design**, v. 2, p. 553-562, 2002.

CAMP, D.; JENKINS, I.D. Mechanism of the Mitsunobu esterification reaction. 1. The involvement of phosphoranes and oxyphosphonium salts. **Journal of Organic Chemistry**, v. 54, p. 3045-3049, 1989a.

CAMP, D.; JENKINS, I.D. Mechanism of the Mitsunobu esterification reaction. 2. The involvement of (acyloxy)alkoxyphosphoranes. **Journal of Organic Chemistry**, v. 54, p. 3049-3054, 1989b.

CANIATO, R.; PURICELLI, L. Review: Natural antimalarial agents (1995-2001). **Critical Reviews in Plant Sciences**, v. 22, p. 79-105, 2003.

CAREY, F.A.; SUNDBERG, R.J. **Advanced Organic Chemistry B Reactions and Synthesis**. 4th ed. New York: Kluwer Academic/Plenum, 2001.

CASEY, G.J.; GINNY, M.; URANOLI, M.; MUELLER, I.; REEDER, J.C.; GENTON, B.; COWMAN, A.F. Molecular analysis of *Plasmodium falciparum* from drug treatment failure patients in Papua New Guinea. **American Journal of Tropical Medicine and Hygiene**, v. 70, p. 251-255, 2004.

CHANDRASCKHAR, S.; GOPALIAH, K. Ketones to amides via a formal Beckmann rearrangement in "one pot": a solvent free reaction promoted by anhydrous oxalic acid. Possible analogy with the Schmidt reaction. **Tetrahedron Letters**, v. 44, p. 7437-7439, 2003.

CHEN, N.; RUSSELL, B.; FOWLER, E.; PETERS, J.; CHENG, Q. Levels of chloroquine resistance in *Plasmodium falciparum* are determined by loci other than *pfcr1* and *pfmdr1*. **Journal of Infectious Diseases**, v. 185, p. 405-407, 2002.

CHOU, A.C.; CHEVLI, R.; FITCH, C.D. Ferriprotoporphyrin IX fulfills the criteria for identification as the chloroquine receptor of malaria parasites. **Biochemistry**, v. 19, p. 1543-1549, 1980.

COHEN, S.N.; PHIFER, K.O.; YIELDING, K.L. Complex formation between chloroquine and ferrihaemic acid in vitro, and its effect on the antimalarial action of chloroquine. **Nature**, v. 202, p. 805-806, 1964.

CONSTANTINIDIS, I.; SATTERLEE, J.D. UV-visible and carbon NMR studies of chloroquine binding to urohemin I chloride and uroporphyrin I in aqueous solution. **Journal of the American Chemical Society**, v. 110, p. 4391-4395, 1988.

DE, D; KROGSTAD, FM; BYERS, LD; KROGSTAD, DJ. Structure-activity relationships for antiplasmodial activity among 7-substituted 4-aminoquinolines. **Journal of Medicinal Chemistry**, v. 41, p. 4918-4926, 1998.

DEBROY, P.; NASKAR, D.; ROY, S. A. Facile Transesterification Route to Ferrocenyl Esters. **Inorganic Chimica Acta**, v. 359, p. 1215-1221, 2006.

DELHAES, L.; BIOT, C.; BERRY, L.; MACIEJEWSKI, L.; CAMUS, D.; BROCARD, J.; DIVE, D. Novel ferrocenic artemisinin derivatives: Synthesis, in vitro antimalarial activity and affinity of binding with ferriprotoporphyrin IX. **Bioorganic & Medicinal Chemistry**, v. 8, p. 2739-2745, 2000.

DELHAES, L.; ABESSOLO, H.; BIOT, C.; BERRY, L.; DELCOURT, P.; MACIEJEWSKI, L.; BROCARD, J.; CAMUS, D.; DIVE, D. In vitro and in vivo antimalarial activity of ferrochloroquine, a ferrocenyl analogue of chloroquine against chloroquine-resistant malaria parasites. **Parasitology Research**, v. 87, p. 239-244, 2001.

- DEJARDINS, R.E.; CANFIELD, C.J.; HAYNES, J.D.; CHULAY, J.D. Quantitative assessment of antimalarial activity in vitro by a semiautomated microdilution technique. **Antimicrobial Agents and Chemotherapy**, v. 16, p. 710-718, 1979.
- DJIMDE, A.; DUOMBO, O.K.; STEKETEE, R.W.; PLOWE, C.V. Application of a molecular marker for surveillance of chloroquine-resistant malaria. **Lancet**, v. 358, p. 890-891, 2001.
- DOMARLE, O.; BLAMPAIN, G.; AGNANIET, H.; NZADIYABI, T.; LEBIBI, J.; BROCARD, J.; MACIEJEWSKI, L.; BIOT, C.; GEORGES, A.J.; MILLET, P. In vitro antimalarial activity of a new organometallic analog, ferrocene-chloroquine. **Antimicrobial Agents and Chemotherapy**, v. 42, p. 540-544, 1998.
- DORN, A.; VIPPAGUNTA, S.R.; MATILE, H.; JAQUET, C.; VANNERSTROM, J.L.; RIDLEY, R.G. An assessment of drug-haematin binding as a mechanism for inhibition of haematin polymerisation by quinoline antimalarials. **Biochemical Pharmacology**, v. 55, p. 727-736, 1998.
- DUKER-ESHUN, G., JAROSZEWSKI, J.W., ASOMANING, W.A., OPPONG-BOACHIE, F., CHRISTENSEN, S.B. Antiplasmodial constituents of *Cajanus cajan*. **Phytotherapy Research**, v. 18, p. 128-130, 2004.
- DURASINGH, M.T.; JONES, P.; SAMBOU, I.; VON SEIDLEIN, L.; PINDER, M.; WARHURST, D.C. The tyrosine-86 allele of the *pfmdr1* gene of *Plasmodium falciparum* is associated with increased sensitivity to the anti-malarials mefloquine and artemisinin. **Molecular and Biochemical Parasitology**, v. 108, p. 13-23, 2000b.
- DURASINGH, M.T.; ROPER, C.; WALLIKER, D.; WARHURST, D.C. Increased sensitivity to the antimalarials mefloquine and artemisinin is conferred by mutations in the *pfmdr1* gene of *Plasmodium falciparum*. **Molecular Microbiology**, v. 36, p. 955-961, 2000a.
- DURRAND, V.; BERRY, A.; SEM, R.; GLAZIOU, P.; BEAUDOU, J.; FANDEUR, T. Variations in the sequence and expression of the *Plasmodium falciparum* chloroquine resistance transporter (*Pfcr1*) and their relationship to chloroquine resistance in vitro. **Molecular and Biochemical Parasitology**, v. 136, p. 273-285, 2004.
- EGAN, T.J.; ROSS, D.C.; ADAMS, P.A. Quinoline anti-malarial drugs inhibit spontaneous formation of β -haematin (malaria pigment). **FEBS Letters**, v. 352, p. 54-57, 1994.
- EGAN, T.J.; MAVUSO, W.W.; ROSS, D.C.; MARQUES, H.M. Thermodynamic Factors Controlling the Interaction of Quinoline Antimalarial Drugs with Ferriprotoporphyrin IX. **Journal of Inorganic Biochemistry**, v. 68, p. 137-145, 1997.

EGAN, T.J.; HEMPELMANN, E.; MAVUSO, W.W. Characterisation of synthetic β -haematin and effects of the antimalarial drugs quinidine, halofantrine, desbutylhalofantrine and mefloquine on its formation. **Journal of Inorganic Biochemistry**, v. 73, p. 101-107, 1999.

EGAN, T.J.; HUNTER, R.; KASCHULA, C.H.; MARQUES, H.M.; MISPLON, A.; WALDEN, J. Structure-function relationships in aminoquinolines: Effects of amino and chloro groups on quinoline-hematin complex formation, inhibition of β -hematin formation, and antiplasmodial activity. **Journal of Medicinal Chemistry**, v. 43, p. 283-291, 2000.

EGAN, T.J.; MAVUSO, W.W.; NCOKAZI, K.K. The mechanism of β -hematin formation in acetate solution. Parallels between hemozoin formation and biomineralization processes. **Biochemistry**, v. 40, p. 204-213, 2001.

EGAN, T.J.; COMBRINCK, J.M.; EGAN, J.; HEARNE, G.R.; MARQUES, H.M.; NIENTENI, S.; SEWELL, B.T.; SMITH, P.J.; TAYLOR, D.; VAN SCHALKWYK, D.A.; WALDEN, J.C. Fate of haem iron in the malaria parasite *Plasmodium falciparum*. **Biochemical Journal**, v. 365, p. 343-347, 2002.

EGAN, T.J. Haemozoin (malarial pigment): a unique crystalline drug target. **Targets**, v. 2, p. 115-124, 2003.

EGAN, T.J.; NCOKAZI, K.K. Effects of solvent composition and ionic strength on the interaction of quinoline antimalarials with ferriprotoporphyrin IX. **Journal of Inorganic Biochemistry**, v. 98, p. 144-152, 2004.

EGAN, T.J. Interactions of quinoline antimalarials with hematin in solution. **Journal of Inorganic Biochemistry**, v. 100, p. 916-926, 2006.

EGAN, T.J.; CHEN, J.Y.-J.; VILLIERS, K.A.; MABOTHA, T.E.; NAIDOO, K.J.; NCOKAZI, K.K.; LANGFORD, S.J.; MCNAUGHTON, D.; PANDIANCHERRI, S.; WOOD, B.R. Haemozoin (β -haematin) biomineralization occurs by self-assembly near the lipid/water interface. **FEBS Letters**, v. 580, p. 5105-5110, 2006.

EGGLESON, K.K.; DUFFIN, K.L.; GOLDBERG, D.E. Identification and characterization of falcilysin, a metallopeptidase involved in haemoglobin catabolism within the malaria parasite *Plasmodium falciparum*. **The Journal of Biological Chemistry**, v. 274, p. 32411-32417, 1999.

FIDOCK, D.A.; NOMURA, T.; TALLEY, A.T.; COOPER, R.A.; DZEKUNOV, S.M.; FERDIG, M.T.; URSOS, L.M.; SIDHU, A.S.; NAUDE, B.; DEITSCH, K.W.; SU, X.Z.; WOOTTON, J.C.; ROEPE, P.D.; WELLEMS, P.D. Mutations in the *P. falciparum* digestive vacuole transmembrane protein *pfcr1* and evidence for their role in chloroquine resistance. **Molecular Cell**, v. 6, p. 861-871, 2000.

FIDOCK, D.A.; ROSENTHAL, P.J.; CROFT, S.L.; BRUN, R.; NWAKA, S. Antimalarial drug discovery: efficacy models for compound screening. **Nature Reviews**, v. 3, p. 509-520, 2004

FINLAY, H.J.; HONDA, T.; GRIBBLE, G.W.; DANIELPOUR, D.; BENOIT, N.E.; SUH, N.; WILLIAMS, C.; SPORN, M.B. Novel A-ring cleaved analogs of oleanolic and ursolic acids which affect growth regulation in NRP.152 prostate cells. **Bioorganic & Medicinal Chemistry Letters**, v. 7, p. 1769-1772, 1997.

FITCH, C.D. Ferriprotoporphyrin IX, phospholipids, and the antimalarial actions of quinoline drugs. **Life Sciences**, v. 74, p. 1957-1972, 2004.

FIVELMAN, Q.L.; BUTCHER, G.A.; ADAGU, I.S.; WARHURST, D.C.; PASVOL, G. Malarone treatment failure and in vitro confirmation of resistance of *Plasmodium falciparum* isolate from Lagos, Nigeria. **Malaria Journal**, v. 1, p. 1, 2002.

FLUECK, T.P.; JELINEK, T.; KILIAN, A.H.; ADAGU, I.S.; KABAGAMBE, G.; SONNENBURG, F.; WARHURST, D.C. Correlation of in vivo-resistance to chloroquine and allelic polymorphisms in *Plasmodium falciparum* isolates from Uganda. **Medicine and International Health**, v. 5, p. 174-178, 2000.

FURNISS, B.S.; HANNAFORD, A.J.; SMITH, P.W.G.; TATCHELL, A.R.; **VOGEL`S Textbook of Practical Organic Chemistry**. 5.ed. Singapura: Longman, 1989.

GAUDIO, A.C.; MONTANARI, C.A.; FERREIRA, M.M.C. Seleção de variáveis em QSAR. **Química Nova**, v. 25, p. 439-448, 2002.

GIL, J.P.; NOGUEIRA, F.; STROMBERG-NORKLIT, J.; LINDBERG, J.; CARROLO, M.; CASIMIRO, C.; LOPES, D.; AREZ, A.P.; CRAVO, P.V.; ROSARIO, V.E. Detection of atovaquone and Malarone resistance conferring mutations in *Plasmodium falciparum* cytochrome *b* gene (*cytb*). **Molecular and Cellular Probes**, v. 17, p. 85-89, 2003.

GIRAULT, S.; GRELLIER, P.; BERECIBAR, A.; MAES, L.; MOURAY, E.; LEMIÈRE, P.; DEBREU, M.; DAVIOUD-CHARVET, E.; SERGHERAERT, C. Antimalarial, antitrypanosomal and antileishmanial activities and cytotoxicity of Bis(9-amino-6-chloro-2-methoxyacridines): Influence of the linker. **Journal of Medicinal Chemistry**, v. 43, p. 2646-2654, 2000.

GIRAULT, S.; GRELLIER, P.; BERECIBAR, A.; MAES, L.; LEMIÈRE, P.; MOURAY, E.; DAVIOUD-CHARVET, E.; SERGHERAERT, C. Antiplasmodial activity and cytotoxicity of Bis-, Tris-, and Tetraquinolines with linear or cyclic amino linkers. **Journal of Medicinal Chemistry**, v. 44, p. 1658-1665, 2001.

GNOATTO, S.C.B.; SCHENKEL, E. P.; BASSANI, V. L. HPLC method to assay total saponins in *Ilex paraguariensis* aqueous extract. **Journal of the Brazilian Chemical Society**, v.16, p.723 - 726, 2005.

GOMEZ-SALADIN, E.; FRYAUFF, D.J.; TAYLOR, W.R.; LAKSANA, B.S.; SUSANTI, A.I.; PURNOMO; SUBIANTO, B.; RICHIE, T.L. . *Plasmodium falciparum* *mdr1* mutations and in vivo chloroquine resistance in Indonesia. **American Journal of Tropical Medicine and Hygiene**, v. 61, p. 240-244, 1999.

GOSMANN, G.; SCHENKEL, E. P.; SELIGMANN, O. A new saponin from Maté, *Ilex paraguariensis*. **Journal of Natural Products**, v. 52, p. 1367-1370, 1989.

GOSMANN, G.; GUILLAUME, D.; TAKETA, A. T. C.; SCHENKEL, E. P. Triterpenoids saponins from *Ilex paraguariensis*. **Journal of Natural Products**, v. 58, p. 438-441, 1995.

GROBUSCH, M.P.; ADAGU, I.S.; KREMSNER, P.G.; WARHURST, D.C. *Plasmodium falciparum*: in vitro chloroquine susceptibility and allele-specific PCR detection of *Pfmdr1* Asn86Tyr polymorphism in Lambarene, Gabon. **Parasitology**, v.116, p. 211-217, 1998.

GUILLOIN, J.; GRELLIER, P.; LABAIED, M.; SONNET, P.; LEGER, J.M.; DEPRESZ-POULAIN, R.; FORFAR-BARES, I.; DALLEMAGNE, P.; LEMAITRE, N.; PEHOURCQ, F.; ROCHETTE, J.; SERGHERAERT, C.; JARRY, C. Synthesis, antimalarial activity, and molecular modeling of new pyrrolo[1,2-a]quinoxalines, bispyrrolo[1,2-a]quinoxalines, bispyrido[3,2-e]pyrrolo[1,2-a]pyrazines, and bispyrrolo[1,2-a]thieno[3,2-e]pyrazines. **Journal of Medicinal Chemistry**, v. 47, p.1997-2009, 2004.

HANKINS, E.G.; WARHURST, D.C.; SIBLEY, C.H. Novel alleles of the *Plasmodium falciparum dhfr* highly resistant to pyrimethamine and chlorocycloguanil, but not WR99210. **Molecular and Biochemical Parasitology**, v. 117, p. 91-102, 2001.

HANSCH, C.; LEO, A.; HOEKMAN, D. **Exploring QSAR, hydrophobic, electronic, and steric constants**. Washington: American Chemical Society, 1995. 348 p.

HAUSER, C.R.; LINDSAY, J.K. Certain Alkylation with the Methiodide of N,N-Dimethylaminomethylferrocene. Synthesis of an α -Amino Acid Having the Ferrocene Group. v. 22, p. 1246-1247, 1957.

HEINZMANN, B. M.; SCHENKEL, E. P. Saponins from *Ilex dumosa*. **Journal of Natural Products**, v. 58, p. 1419-1422, 1995.

HOMEWOOD, C.A.; WARHURST, D.C.; PETERS, W.; BAGGALEY, V.C. Lysosomes, pH and the anti-malarial action of chloroquine. **Nature**, v. 235, p. 50-52, 1972.

HONDA, T.; FINLAY, H.J.; GRIBBLE, G.W. New enone derivatives of oleanolic acid and ursolic acid as inhibitors of nitric oxide production in mouse macrophages. **Bioorganic & Medicinal Chemistry Letters**, v. 7, p. 1623-1628, 1997.

HOSTETTMANN, K.; MARSTON, A. **Saponins**. Cambridge: Cambridge University, 1995.

HOWARD, E.M.; ZHANG, H.; ROEPE, P.D. A novel transporter, *Pfcrt*, confers antimalarial drug resistance. **Journal of Membrane Biology**, v. 190, p. 1-8, 2002.

<http://portal.saude.gov.br/portal/svs>. Access 11.05.07.

http://www.cdc.gov/malaria/biology/life_cycle.htm. Access 03.12.06.

KASCHULA, C.H.; EGAN, T.J.; HUNTER, R.; BASILICO, N.; PARAPINI, S.; TARAMELLI, D.; PASINI, E.; MONTI, D. Structure-activity relationships in 4-aminoquinoline antiplasmodials. The role of the group at the 7-position. **Journal of Medicinal Chemistry**, v. 45, p. 3531-3539, 2002.

KANOKMEDHALKUL, K. KANOKMEDHALKUL, S., PHATCHANA, R. Biological activity of anthraquinones and triterpenoids from *Prismatomeris fragrans*. **Journal of Ethnopharmacology**, v. 100, p. 284-288, 2005.

KASHIWADA, Y.; WANG, H.; NAGAO, T.; KITANAKA, S.; YASUDA, I.; FUJIOKA, T.; YAMAGISHI, T.; COSENTINO, L.M.; KOZUKA, M.; OKABE, H.; IKESHIRO, Y.; HU, C.; YEH, E.; LEE, K. Anti-AIDS agents. 30. Anti-HIV activity of oleanolic, pomolic acid, and structurally related triterpenoids. **Journal of Natural Products**, v. 61, p. 1090-1095, 1998.

KLAN, S.M.; WATERS, A.P. Malaria parasite transmission stages: an update. **Trends in Parasitology**, v. 20, p. 575-580, 2004.

KONOIKE, T.; ARAKI, Y.; KANDA, Y. A novel allylic hydroxylation of sterically hindered olefins by Fe-Porphyrin *m*CPBA oxidation. **Tetrahedron Letters**, v. 40, p. 6971-6974, 1999.

KOUTSOUREA, A.I.; ARSENOU, E.S.; FOUSTERIS, M.A.; NIKOLAROPOULOS, S.S. Synthetic approaches for the synthesis of a cytostatic steroidal B-D bilactam. **Steroids**, v. 68, p. 659-666, 2003.

KRAEMER, K. H.; TAKETA, A. T. C.; SCHENKEL, E. P.; GOSMANN, G.; GUILLAUME, D. Matesaponin 5, a highly polar saponin from *Ilex paraguariensis*. **Phytochemistry**, v. 42, p. 1119-1122, 1996.

KRUDSOOD, S.; IMWONG, M.; WILAIRATANA, P.; PUKRITTAYAKAMEE, S.; NONPRASERT, A.; SNOUNOU, G.; WHITE, N.J.; LOOAREESUWAN, S. Artesunate-dapsone-proguanil treatment of falciparum malaria: genotypic determinants of therapeutic response. **Transactions of the Royal Society of Tropical Medicine and Hygiene**, v. 99, p. 142-149, 2005.

KRUGLIAK, M.; ZHANG, J.; GINSBURG, H. Intraerythrocytic *Plasmodium falciparum* utilizes only a fraction of the amino acids derived from the digestion of host cell cytosol for the biosynthesis of its proteins. **Molecular and Biochemical Parasitology**, v. 119, p. 249-256, 2002.

KUBINYI, H. The quantitative analysis of structure-activity relationships. In WOLFF, M.E. (Ed.). **Burger's Medicinal Chemistry and Drug Discovery**. 5th ed. New York: John Wiley, 1995. v. 1, p. 497-571.

KUBINYI, H. QSAR and 3D QSAR in drug design Part 1. **Drug Design**, v. 2, p. 458-467, 1997a.

- KUBINYI, H. QSAR and 3D QSAR in drug design Part 2: applications and problems. **Drug Design**, v. 2, p. 538-546, 1997b.
- KUMAR, S.; GUHA, M.; CHOUBEY, V.; MAITY, P.; BANDYOPADHYAY, U. Antimalarial drugs inhibiting hemozoin (β -hematin) formation: A mechanistic update. **Life Sciences**, v. 80, p. 813-828, 2007.
- LAMIDI, M.; OLLIVIER, E.; GASQUET, M.; FAURE, R.; NZÉ-EKEKANG, L.; BALANSARD, G. Structural and antimalarial studies of saponins from *Nauclea diderrichii* Bark. In: WALLER, G.R.; YAMASAKI, K. **Saponins Used in Traditional and Modern Medicine** (Advances in experimental medicine and biology, v. 404). New York: Plenum, 1996. p. 383-399.
- LEED, A.; DUBAY, K.; URSOS, K.M.B.; SEARS, D.; DIOS, A.C.; ROEPE, P.D. Solution structures of antimalarial drug-heme complexes. **Biochemistry**, v. 41, p. 10245-10255, 2002.
- LI, Y; HUANG, H; WU, Y-L. Qinghaosu (Artemisinin)- A fantastic antimalarial drug from a traditional Chinese medicine. In: LIANG, X-T; FANG, W-S. (Ed.) **Medicinal Chemistry of Bioactive Natural Products**. New Jersey: John Wiley, 2006.
- LIU, J. Pharmacology of oleanolic acid and ursolic acid. **Journal of Ethnopharmacology**, v. 49, p. 57-68, 1995.
- LIU, J. Oleanolic acid and ursolic acid: research perspectives. **Journal of Ethnopharmacology**, v. 100, p. 92-94, 2005.
- LINDSAY, J.K.; HAUSER, C.R. Aminomethylation of Ferrocene to Form N,N-Dimethylaminomethylferrocene and its Conversion to the Corresponding Alcohol and Aldehyde. **Journal of Organic Chemistry**, v. 22, p. 355-358, 1957.
- LOOAREESUWAN, S. CHULAY, J.D., CANFIELD, C.J.; HUTCHINSON, D.B. Malarone™ (atovaquone and proguanil hydrochloride): a review of its clinical development for treatment of malaria. Malarone Clinical Trials Study Group. **American Journal of Tropical Medicine and Hygiene**, v. 60, p. 533-541, 1999.
- MA, C-M.; CAI, S-Q.; CUI, J-R.; WANG, R-Q.; TU, P-F.; HATTORI, M. ; DANESHTALAB, M. The cytotoxic activity of ursolic acid derivatives. **European Journal of Medicinal Chemistry**, v. 40, p. 582-589, 2005.
- MACREADIE, I.; GINSBURG, W.; SIRAWARAPORN, W.; TILLEY, L. Antimalarial Drug Development and New Targets. **Parasitology Today**, v. 16, p. 438-444, 2000.
- MAGIL, A.J.; ZEGARRA, J.; GARCIA, C.; MARQUINO, W.; RUEBUSH, T.K. Efficacy of sulfadoxine-pyrimethamine and mefloquine for the treatment of uncomplicated *Plasmodium falciparum* malaria in the Amazon basin of Peru. **Revista da Sociedade de Medicina Tropical**, v. 37, p. 279-281, 2004.

MAHATO, S.B.; GARAI, S. Triterpenoid saponins. In: HERZ, W.; KIRBY, G.W.; MOORE, R.E.; STEGLICH, W.; TAMM, Ch. **Progress in the chemistry of organic natural products**. Wien: Springer, 1998. p. 1-196.

MAHATO, S.B.; SARKAR, S.K.; PODDAR, G. Triterpenoid saponins. **Phytochemistry**, v. 27, p. 3037-3067, 1988.

MAHATO, S.; KUNDU, A.P. ¹³C NMR spectra of pentacyclic triterpenoids— A compilation and some salient features. **Phytochemistry**, v. 37, p. 1517-1575, 1994.

MAPPI, T.C.; THOMAS, S.M.; GBOTOSHO, G.O.; FALADE, C.O.; AKINBOYE, D.O.; GERENA, L.; HUDSON, T.; SOWUNMI, A.; KYLE, D.E.; MILHOUS, W.; WIRTH, D.F.; ODUOLA, A.M. Point mutations in the *pfcr* and *pfmdr-1* genes of *Plasmodium falciparum* and clinical response to chloroquine, among malaria patients from Nigeria. **Annals of Tropical Medicine and Parasitology**, v. 97, p. 439-451, 2003.

MARQUES, H.M.; VOSTER, K.; EGAN, T.J. The Interaction of the Heme-Ocatapeptide N-Acetylmicroperoxidase-8 with Animalarial Drugs: Solution Studies and Modeling by Molecular Mechanics Methods. **Journal of Inorganic Biochemistry**, v. 64, p. 7-23, 1996.

MARTIN, A.S.; BYGBJERG, I.C.; BREMANN, J.G. Are Multilateral Malaria Research and Control Programs the Most Successful? Lessons from the Past 100 Years in Africa. **American Journal of Tropical Medicine and Hygiene**, v. 71, p. 268-278, 2004.

MARTINET, A.; NDJOKO, K.; TERREAUX, C.; MARSTON, A.; HOSTETTMANN, K.; SCHUTZ, Y. NMR and LC-MS characterisation of two minor saponins from *Ilex paraguariensis*. **Phytochemical Analysis**, v. 12, p. 48-52, 2001.

MBERU, E.K.; NZILA, A.M.; NDUATI, E.; ROSS, A.; MONKS, S.M.; KOKWARO, G.O.; WATKINS, W.M.; HOPKINS SIBLEY, C. *Plasmodium falciparum*: in vitro activity of sulfadoxine and dapson in field isolates from Kenya: point mutations in dihydropteroate synthase may not be the only determinants in sulfa resistance. **Experimental Parasitology**, v. 101, p. 90-96, 2002.

MENDIVE, J.R. The occurrence of α -amyrin and ursolic acid in the leaves of *Ilex paraguariensis*. **Journal of Organic Chemistry**, v. 5, p. 235-237, 1940.

MITSUNOBU, O. The use of diethyl azodicarboxylate and triphenylphosphine in synthesis and transformation of natural products. **Synthesis**, n. 1, 1981.

MOORE, L.R.; FUJIOKA, H.; WILLIAMS, S.; CHALMERS, J.J.; GRIMBERG, B.; ZIMMERMAN, P.A.; ZBOROWSKI, M. Hemoglobin degradation in malaria-infected erythrocytes determined from live cell magnetophoresis. **The FASEB Journal**, v. 20, p. 747-750, 2006.

MOREAU, S.; PERLY, B.; CHACHATY, C.; DELEUZE, C. A nuclear magnetic resonance study of the interactions of antimalarial drugs with porphyrins. **Biochemical and Biophysical Acta**, v. 840, 107-116, 1985.

NAGESHA, H.S.; DIN-SYAFRUDDIN; CASEY, G.J.; SUSANTI, A.I.; FRYAUFF, D.J.; REEDER, J.C.; COWMAN, A.F. Mutations in the *pfmdr1*, *dhfr* and *dhps* genes of *Plasmodium falciparum* are associated with in vivo drug resistance in West Papua, Indonesia. **Transactions of the Royal Society of Tropical Medicine and Hygiene**, v. 95, p. 43-49, 2001.

NDOUNGA, M.; BASCO, L.K.; RINGWALD, P. Evaluation of a new sulfadoxine sensitivity assay *in vitro* for field isolates of *Plasmodium falciparum*. **Transactions of the Royal Society of Tropical Medicine and Hygiene**, v. 95, p. 55-57, 2001.

NGO, T.; DURAISINGH, M.; REED, M.; HIPGRAVE, D.; BIGGS, B.; COWMAN, A.F. Analysis of *pfcr1*, *pfmdr1*, *dhfr*, and *dhps* mutations and drug sensitivities in *Plasmodium falciparum* isolates from patients in Vietnam before and after treatment with artemisinin. **American Journal of Tropical Medicine and Hygiene**, v. 68, p. 350-356, 2003.

O'NEILL, P.M.; WILLOCK, D.J.; HAWLEY, S.R.; BRAY, P.G.; STORR, R.C.; WARD, S.A.; PARK, B.K. Synthesis, Antimalarial Activity, and Molecular Modeling of Tebuline Analogues. **Journal of Medicinal Chemistry**, v. 40, p. 437-448, 1997.

PAGOLA, S.; STEPHENS, P.W.; BOHLE, D.S.; KOSAR, A.D.; MADSEN, S.K. The structure of malaria pigment β -haematin. **Nature**, v. 404, p. 307-310, 2000.

PATHAK, A.; SINGH, S.K.; BIABANI, M.A.F.; KULSHRESHTHA, D.K.; PURI, S.K.; SRIVASTAVA, S.; KUNDU, B. Synthesis of combinatorial libraries based on triterpenoid scaffolds. **Combinatorial Chemistry & High Throughput Screening**, v. 5, n.3, p. 241-248, 2002.

PILLAI, D.R.; HIJAR, G.; MONTOYA, Y.; MAROUINO, W.; RUEBUSH, T.K.; WONGSRICHANALAI, C.; KAIN, K.C. Lack of prediction of mefloquine and mefloquine-artesunate treatment outcome by mutations in the *Plasmodium falciparum* multidrug resistance 1 (*pfmdr1*) gene for *P. falciparum* malaria in Peru. **American Journal of Tropical Medicine and Hygiene**, v. 68, p. 107-110, 2003.

PIRES, V.S.; GUILLAUME, D.; GOSMANN, G.; SCHENKEL, E.P. Saponins from *Ilex dumosa*, an erva-maté (*Ilex paraguariensis*) adulterating plant. **Journal of Agricultural and Food Chemistry**, v. 45, p. 1027-1031, 1997.

PODUST, L.M.; YERMALITSKAYA, L.V.; LEPESHEVA, G.I.; PODUST, V.N.; DALMASSO, E.A.; WATERMAN, M.R. Estriol bound and ligand-free structures of sterol 14 α -demethylase. **Structure**, v. 12, p. 1937-1945, 2004.

- PORTELA, C.; AFONSO, C.M.; PINTO, M.M.; RAMOS, M.J. Receptor-drug association studies in the inhibition of the hematin aggregation process of malaria. **FEBS Letters**, v. 547, p.217-222, 2003.
- PORTELA, C.; AFONSO, C.M.; PINTO, M.M.; RAMOS, M.J. Definition of an electronic profile of compounds with inhibitory activity against hematin aggregation in malaria parasite. **Bioorganic & Medicinal Chemistry**, v. 12, p. 3313-3321, 2004.
- PRADINES, B.; FUSAI, T.; DARIES, W.; LALOGUE, V.; ROGIER, C.; MILLET, P.; PANCONI, E.; KOMBILA, M.; PARZY, D. Ferrocene-chloroquine analogues as antimalarials agents: *in vitro* activity of ferrochloroquine against 103 Gabonese isolates of *Plasmodium falciparum*. **Journal of Antimicrobial Chemotherapy**, v. 48, p. 179-184, 2001.
- PRICE, K.R., JOHNSON, I.T., FENWICK, G.R. The chemistry and Biological significance of saponins in foods and feedingstuffs. **CRC Critical Review Food Science and Nutrition**, v. 26, p. 27-135, 1987.
- RAYNES, K.; GALATIS, D.; COWMAN, A.F.; TILLEY, L.; DEADY, L.W. Synthesis and activity of some antimalarial bisquinolines. **Journal of Medicinal Chemistry**, v. 6, p. 204-206, 1995.
- REED, M.B.; SALIBA, K.J.; CARUANA, S.R.; KIRK, K.; COWMAN, A.F. *Pgh1* modulates sensitivity and resistance to multiple antimalarials in *Plasmodium falciparum*. **Nature**, v. 403, p. 906-909, 2000.
- RIDLEY, R.G.; HOFHEINZ, W.; MATILE, H.; JAQUET, C.; DORN, A.; MASCIADRI, R.; JOLIDON, S.; RICHTER, W.F.; GUENZI, A.; GIROMETTA, M.A.; URWYLER, H.; HUBER, W.; THAITHONG, S.; PETERS, W. 4-aminoquinoline analogs of chloroquine with shortened side chains retain activity against chloroquine-resistant *Plasmodium falciparum*. **Antimicrobial Agents and Chemotherapy**, v. 40, p. 1846-1854, 1996.
- RINEHART, K.L.; CURBY, R.J.; GUSTAFSON, D.H.; HARRISON, K.G.; BOZAK, R.E.; BUBLITZ, D.E. Organic Chemistry of Ferrocen. V^{1a}. Cyclization of ω -Ferrocenylaliphatic Acids. **Journal of the American Chemical Society**, v. 84, p. 3263-3269, 1962.
- ROSENTHAL, P.J.; SIJWALI, P.S.; SINGH, A.; SHENAI, B.R. Cysteine proteases of malaria parasites: targets for chemotherapy. **Current Pharmaceutical Design**, v. 8, p. 1659-1672, 2002.
- RYCKEBUSCH, A.; DEPRez-POULAIN, R.; DEBREU-FONTAINE, M.A.; VANDAELE, R.; MOURAY, E.; GRELLIER, P.; SERGHERAERT, C. Parallel synthesis and anti-malarial activity of a sulfonamide library. **Bioorganic & Medicinal Chemistry Letters**, v. 12, p. 2595-2598, 2002.

RYCKEBUSCH, A.; DEPREZ-POULAIN, R.; MAES, L.; DEBREU-FONTAINE, M.A.; MOURAY, E.; GRELLIER, P.; SERGHERAERT, C. Synthesis and in vitro and in vivo antimalarial activity of N¹-(7-chloro-4-quinolyl)-1,4-bis(3-aminopropyl)piperazine derivatives. **Journal of Medicinal Chemistry**, v. 46, p. 542-557, 2003.

RYCKEBUSCH, A.; DEBREU-FONTAINE, M.A.; MOURAY, E.; GRELLIER, P.; SERGHERAERT, C.; MELNYK, P. Synthesis and antimalarial evaluation of new N¹-(7-chloro-4-quinolyl)-1,4-bis(3-aminopropyl)piperazine derivatives. **Bioorganic & Medicinal Chemistry Letters**, v. 17, p.297-302, 2005.

SALAS, F.; FICHMANN, J.; LEE, G.K.; SCOTT, M.D.; ROSENTHAL, P.J. Functional Expression of Falcipain, a *Plasmodium falciparum* Cysteine Proteinase, Supports Its Role as a Malarial Hemoglobinase. **Infection and Immunity**, v. 63, p. 2120-2125, 1995.

SCHENKEL, E.P.; MONTANHA, J.A.; GOSMANN, G. Triterpene saponins from mate, *Ilex paraguariensis*. In: WALLER, G.R.; YAMASAKI, K. **Saponins Used in Food and Agriculture** (Advances in experimental medicine and biology, v. 405). New York: Plenum, p. 47-56, 1996.

SCHENKEL, E. P.; GOSMANN, G.; MONTANHA, J. A.; HEINZMANN, B. M.; ATHAYDE, M. L.; TAKETA, A. T. C.; PIRES, V. S.; GUILLAUME, D. Saponins from maté (*Ilex paraguariensis*) and other South American *Ilex* species: ten years of research on *Ilex* saponins. **Ciência e Cultura** (São Paulo), v. 49, p. 359-363, 1997.

SCHMIDT, M.W.; BALDRIDGE, K.K.; BOATZ, J.A.; ELBERT, S.T.; GORDON, M.S.; JENSEN, J.H.; KOSEKI, S.; MATSUNAGA, N.; NGUYEN, K.A.; SU, S.; WINDUS, T.L.; DUPUIS, M.; MONTGOMERY JR, J.A. General atomic and molecular electronic structure system. **Journal of Computational Chemistry**, v. 14, p. 1347-1363, 1993.

SEIBUM, A.H.G.; WOO, W.S.; LUGTENBURG, J. Preparation and Characterization of [5-¹³C]-(2S, 4R)-Leucine and [4-¹³C]-(2S, 3S)-Valine – Establishing Synthetic Schemes to Prepare Any Site-Directed Isotopomer of L-Leucine, L-Isoleucine and L-Valine. **European Journal of Organic Chemistry**, p. 4664-4678, 2003.

SHENAI, B.R.; SIJWALI, P.S.; SINGH, A.; ROSENTHAL, P.J. Characterization of Native and Recombinant Falcipain-2, a Principal Trophozoite Cysteine Protease and Essential Hemoglobinase of *Plasmodium falciparum*. **The Journal of Biological Chemistry**, v. 275, p. 29000-29010, 2000.

SIJWALI, P.S.; SHENAI, B.R.; GUT, J.; SINGH, A.; ROSENTHAL, P.J. Expression and characterization of the *Plasmodium falciparum* haemoglobinase falcipain-3; **Biochemistry Journal**, v. 360, p. 481-489, 2001.

SOLOMONOV, I.; OSIPOVA, M.; FELDMAN, Y.; BAEHTZ, C.; KJAER, K.; ROBINSON, I.K.; WEBSTER, G.T.; MCNAUGHTON, D.; WOOD, B.R.; WEISSBUCH, I.; LEISEROWITZ, L. CRYSTAL Nucleation, growth, and morphology of the synthetic malaria pigment β -hematin and the effect thereon by quinoline additives: The malaria pigment as a target of various antimalarial drugs. **Journal of the American Chemical Society**, v. 129, p. 2615-2627, 2007.

SRINIVASAN, T.; SRIVASTAVA, G.K.; PATHAK, A.; BATRA, S.; RAJ, K.; KSHIPRA, S.; PURI, S.K.; KUNDU, B. Solid-phase synthesis and bioevaluation of lupeol-based libraries as antimalarial agents. **Bioorganic & Medicinal Chemistry Letters**, v. 12, p. 2803-2806, 2002.

STAHL, E. (Ed.) **Thin-Layer Chromatography. A Laboratory Handbook**. 2. ed. Berlin: Springer, 1988. p. 857, 887.

STEELE J.C.P.; WARHHURST, D.C.; KIRBY, G.C.; SIMMONDS, M.S.J. *In vitro* and *in vivo* evaluation of betulinic acid as an antimalarial. **Phytotherapy Research**, v. 13, p. 115-119, 1999.

SU, X.; KIRKMAN, L.A.; FUJIOKA, H.; WELLEMS, T.E. Complex polymorphisms in an approximately 330 kDa protein are linked to chloroquine-resistant *P. falciparum* in Southeast Asia and Africa. **Cell**, v. 91, p. 593-603, 1997.

SULLIVAN, D.J.Jr; GLUZMANN, I.Y.; GOLDBERG, D.E. *Plasmodium* hemozoin formation mediated by histidine-rich proteins. **Science**, v. 271, p. 219-222, 1996.

THOMAS, S.M.; NDIR, O.; DIENG, T.; MBOUP, S.; WYPIJ, D.; MAGUIRE, J.H.; WIRTH, D.F. *In vitro* chloroquine susceptibility and PCR analysis of *pfcr* and *pfmdr1* polymorphisms in *Plasmodium falciparum* isolates from Senegal. **American Journal of Tropical Medicine and Hygiene**, v. 66, p. 474-480, 2002.

TINTO, H.; OUEDRAOGO, J.B.; ERHART, A.; VAN OVERMEIR, C.; DUJARDIN, J.C.; VAN MARCK, E.; GUIGUEMDE, T.R.; D'ALESSANDRO, U. Relationship between the *Pfcr* T76 and the *Pfmdr-1* Y86 mutations in *Plasmodium falciparum* and *in vitro/in vivo* chloroquine resistance in Burkina Faso, West Africa. **Infection, Genetics and Evolution**, v. 3, p. 287-292, 2003.

TKACHEV, A.V.; DENISON, A.Y.; GATILOV, Y.V.; BAGRYANSKAYA, I.Y.; SHEVTSOV, S.A.; RYBALOVA, T.V. Stereochemistry of hydrogen peroxide - acetic acid oxidation of ursolic acid and related compounds. **Tetrahedron**, v. 50, p. 11459-11465, 1994.

TRACY, J.W.; WEBSTER Jr, L.T. Fármacos usados na quimioterapia das Infecções Parasitárias. In: HARDMAN, J.G.; LIMBIRD, L.E. (Ed.). **GOODMAN & GILMAN As Bases Farmacológicas da Terapêutica**. 10. ed. Rio de Janeiro: McGraw-Hill, 2003. p. 803-822.

TRAGER, W.; JENSEN, J.B. Human malarial parasites in continuous culture. **Science**, v. 193, p. 673-677, 1976.

TRAORE, F.; FAURE, R.; OLLIVIER, E.; GASQUET, M.; AZAS, N.; DEBRAUWER, L.; KEITA, A.; TIMON-DAVID, P.; BALANSARD, G. Structure and antiprotozoal activity of triterpenoid saponins from *Glinus oppositifolius*. **Planta Medica**, v. 66, 368-371, 2000.

TRAORE-KEITA, F.; GASQUET, M.; DI GIORGIO, C.; OLLIVIER, E.; DELMAS, F.; KEITA, A.; DUOMBO, O.; BALANSARD, G.; TIMON-DAVID, P. Antimalarial activity of four plants used in traditional medicine in Mali. **Phytotherapy Research**, v. 14, p. 45-47, 2000.

UNTERHALT, B. **Organisch-chemisches Praktikum für Pharmazeuten**. 2.ed. Stuttgart : Wissenschaftliche, 1986. p. 155.

VANGAPANDU, S.; JAIN, M.; KAUR, K.; PATIL, P.; PATEL, S.R.; JAIN, R. Recent advances in antimalarial drug development. **Medicinal Research Reviews**, v. 27, p. 65-107, 2007.

van AALTEN, D. M. F.; BYWATER, R.; FINDLAY, J. B. C.; HENDLICH, M.; HOOFT, R. W. W.; VRIEND, G. PRODRG, a program for generating molecular topologies and unique molecular descriptors from coordinates of small molecules. **Journal of Computer-Aided Molecular Design**, v. 10, p. 255-262, 1996.

van der SPOEL, D.; LINDAHL, E.; HESS, B.; GROENHOF, G.; MARK, A.E.; BERENDSEN, H.J.C. GROMACS: Fast, Flexible, and Free. **Journal of Computational Chemistry**, v. 26, p. 1701-1718, 2005.

VATHSALA, P.G.; PRAMANIK, A.; DHANASEKARAN, S.; DEVI, C.U.; PILLAI, C.R.; SUBBARAO, S.K.; GHOSH, S.K.; TIWARI, S.N.; SATHYANARAYAN, T.S.; DESHPANDE, P.R.; MISHRA, G.C.; RANJIT, M.R.; DASH, A.P.; RANGARAJAN, P.N.; PADMANABAN, G. Widespread occurrence of the *Plasmodium falciparum* chloroquine resistance transporter (*Pfcr*) gene haplotype SVMNT in *P. falciparum* malaria in India. **American Journal of Tropical Medicine and Hygiene**, v. 70, p. 256-259, 2004.

VENNERSTROM, J.L.; FU, H.N.; ELLIS, W.Y.; AGER, A.L.; WOOD, J.K.; ANDERSEN, S.L.; GERENA, L.; MILHOUS, W.K. Dispiro-1,2,4,5-tetraoxanes: a new class of antimalarial peroxides. **Journal of Medicinal Chemistry**, v. 7, p. 3023-3027, 1992.

VERLI, H.; GUIMARÃES, J.A. Molecular dynamics simulation of a decasaccharide fragment of heparin in aqueous solution. **Carbohydrate Research**, v. 339, p. 281-290, 2004.

VERLI, H.; GUIMARÃES, J.A. Insights into the induced fit mechanism in antithrombin–heparin interaction using molecular dynamics simulations. **Journal of Molecular Graphics and Modelling**, v. 24, p. 203-212, 2005.

- VILLIERS, A.K; KASCHULA, C.H.; EGAN, T.J.; MARQUES, H.M. Speciation and structure of ferriprotoporphyrin IX in aqueous solution: spectroscopic and diffusion measurements demonstrate dimerization, but not *l*-oxo dimer formation. **Journal of Biological Inorganic Chemistry**, v. 12, p. 101-117, 2007.
- VIPPAGUNTA, S.R.; DORN, A.; MARILE, H.; BHATTACHARJEE, A.K.; KARLE, J.M.; ELLIS, R.G.; VENNERSTROM, J.L. Structural specificity of chloroquine-hematin binding related to inhibition of hematin polymerization and parasite growth. **Journal of Medicinal Chemistry**, v. 42, p. 4630-4639, 1999.
- von SEIDLEIN, L.; DURAISINGH, M.T.; DRAKELEY, C.J.; BAILEY, R.; GREENWOOD, B.M.; PINDER, M. Polymorphism of the *Pfmdr1* gene and chloroquine resistance in *Plasmodium falciparum* in The Gambia. **Transactions of the Royal Society of Tropical Medicine and Hygiene**, v. 91, p. 450-453, 1997.
- WANG, B.; JIANG, Z.H. Studies on oleanolic acid. **Chinese Pharmaceutical Journal**, v. 27, p. 393-397, 1992.
- WANG, P.; READ, M.; SIMS, P.F.; HYDE, J.E. Sulfadoxine resistance in the human malaria parasite *Plasmodium falciparum* is determined by mutations in dihydropteroate synthetase and an additional factor associated with folate utilization. **Molecular Microbiology**, v. 23, p. 979-986, 1997.
- WERMUTH, C.G. Application strategies for primary structures-activity relationship exploration. In: WERMUTH, C.G. (Ed.). **The Practice of Medicinal Chemistry**. 2nd ed. Amsterdam: Academic, 2004. p. 289-300.
- WINSTANLEY, P.; WARD, S.; SNOW, R.; BRECKENRIDGE, A. Therapy of Falciparum Malaria in Sub-Saharan Africa: from Molecule to Policy. **Clinical Microbiology Reviews**, v. 17, p. 612-637, 2004.
- WHO, 2006a. <http://www.who.int/tdr/diseases/malaria/direction.htm>
- WHO, 2006b. <http://www.who.int/csr/drugresist/malaria/en/> .
- WHO, 2006c. <http://www.who.int/tdr/diseases/malaria/lifecycle.htm> .
- WILLIAMS, D.A.; LEMKE, T.L.; **FOYE'S Principles of Medicinal Chemistry**. 5. ed. Philadelphia: Lippincott Williams & Wilkins, 2002. p. 869-879.
- WONGSRICHANALAI, C.; PICKARD, A. L.; WERNSDORFER, W. H.; MESHNICK, S. R. Epidemiology of drug-resistant malaria. **The Lancet Infectious Diseases**, v. 2, p. 209-218, 2002.
- ZALIS, M.G.; PANG, L.; SILVEIRA, M.S.; MILHOUS, W.K.; WIRTH, D.F. Characterization of *Plasmodium falciparum* isolated from the Amazon region of Brazil: evidence for quinine resistance. **American Journal of Tropical Medicine and Hygiene**, v. 58, p. 630-637, 1998.

ZANDONALE, E.; GAUDIO, A.C. Proposição, validação e análise dos modelos que correlacionam estrutura química e atividade biológica. **Química Nova**, v. 24, p. 658-671, 2001.

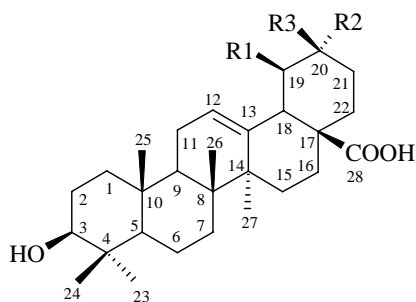
ZHENG, Q.; YIN, Q.; ZHAO, Y. The study on the interaction between seryl-histidine dipeptide and proteins by circular dichroism and molecular modeling. **Bioorganic & Medicinal Chemistry**, v.13, p. 2679-2689, 2005.

ZIEGLER, J.; CHANG, R.T.; WRIGHT, D.W. Multiple-antigenic peptides of histidine-rich protein II of *Plasmodium falciparum*: dendrimeric biomineralization templates. **Journal of the American Chemical Society**, v. 121, p. 2395-2400, 1999.

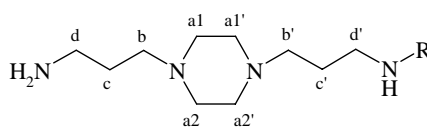
ZIEGLER, H.L.; FRANZYK, H.; SAIRAFIANPOUR, M.; TABATABAI, M.; TEHRANI, M.D.; BAGHERZADEH, K.; HÄGERSTRAND, H.; STÆRK, D.; JAROSZEWSKI, J.W. Erythrocyte membrane modifying agents and the inhibition of *Plasmodium falciparum* growth: structure-activity relationships for betulinic acid analogues. **Bioorganic & Medicinal Chemistry**, v.12, p. 119-127, 2004.

www.dndi.org. Access 11.05.07.

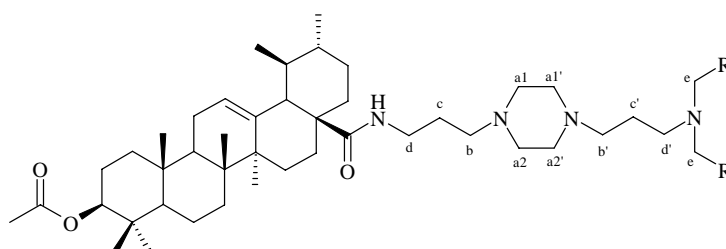
VIII.1. Structures numbering/Numérotation :



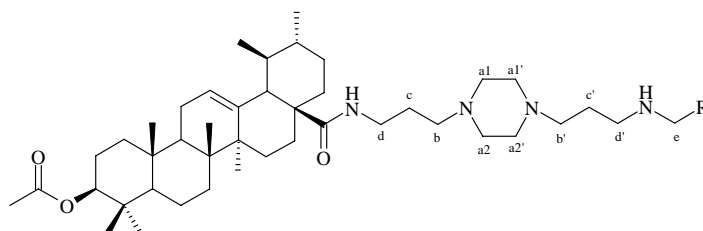
acide ursolique : R1= CH₃, R2=CH₃, R3=H
 acide oléanolique: R1=H, R2=CH₃, R3= CH₃



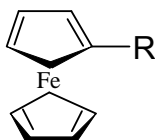
Dérivés 1,4-bis-(3-aminopropyl)piperazine



Dérivés piperaziniques de l'acide ursolique dialkylés

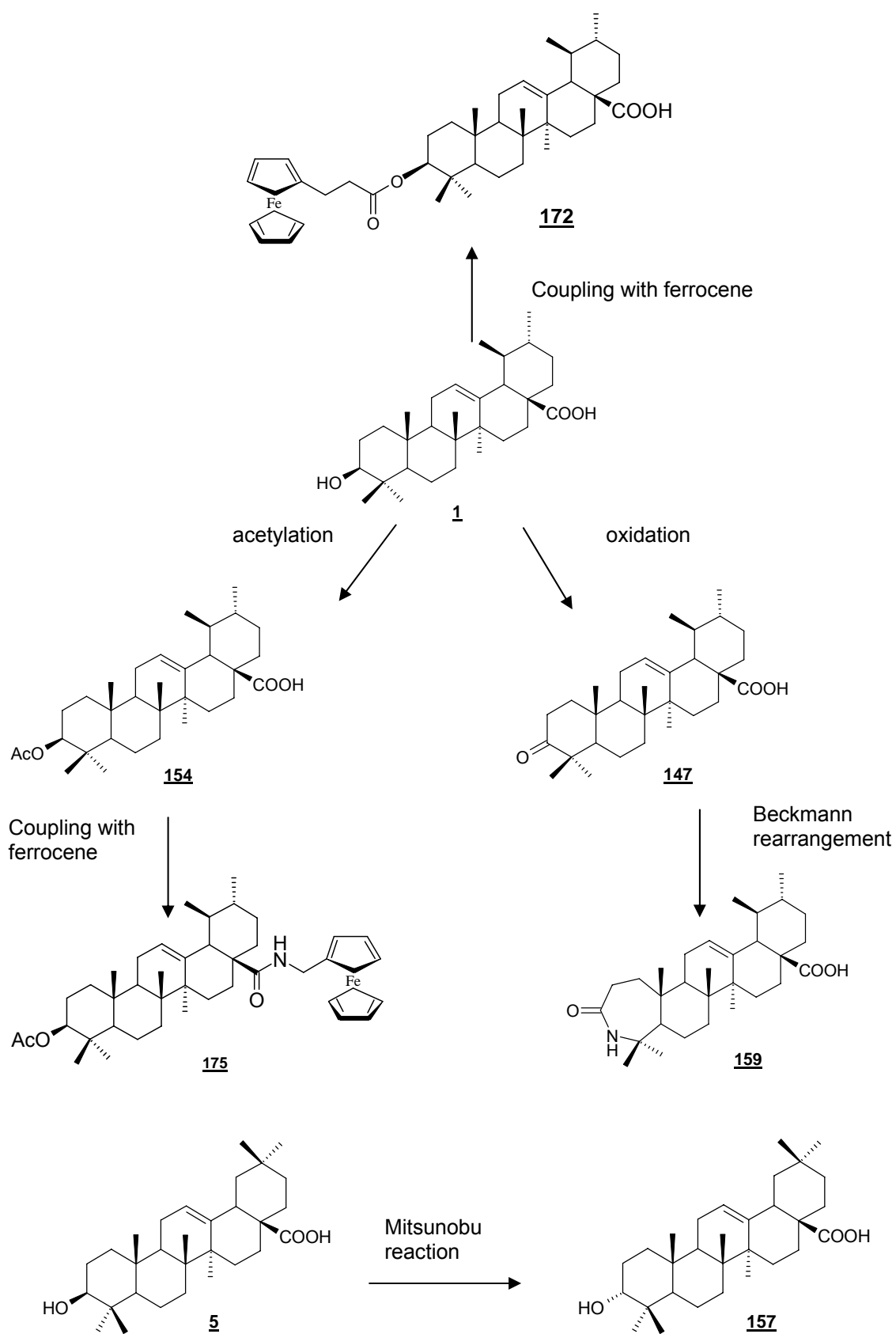


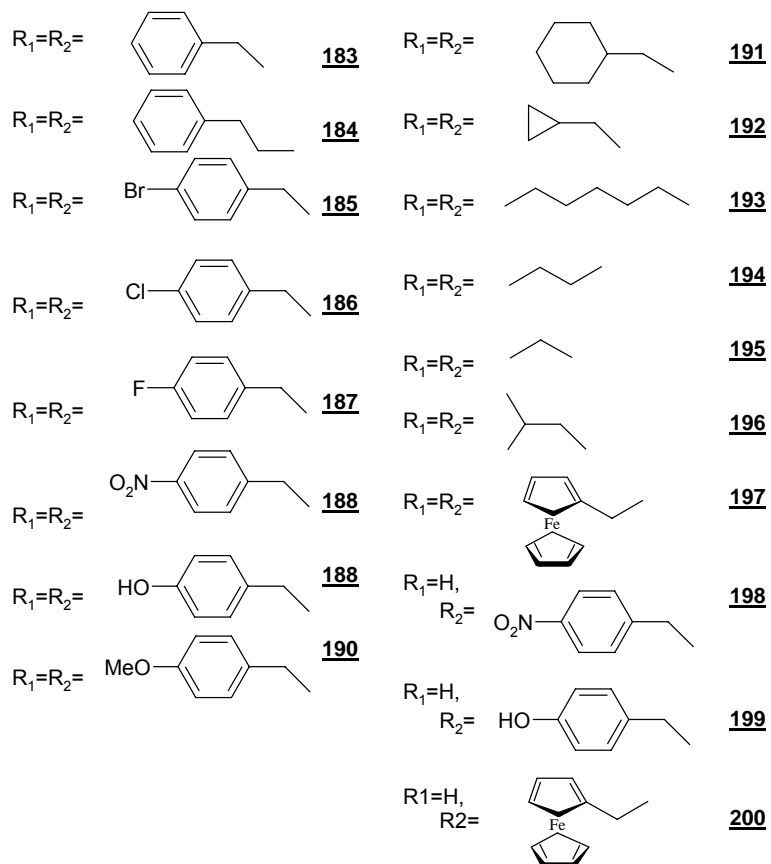
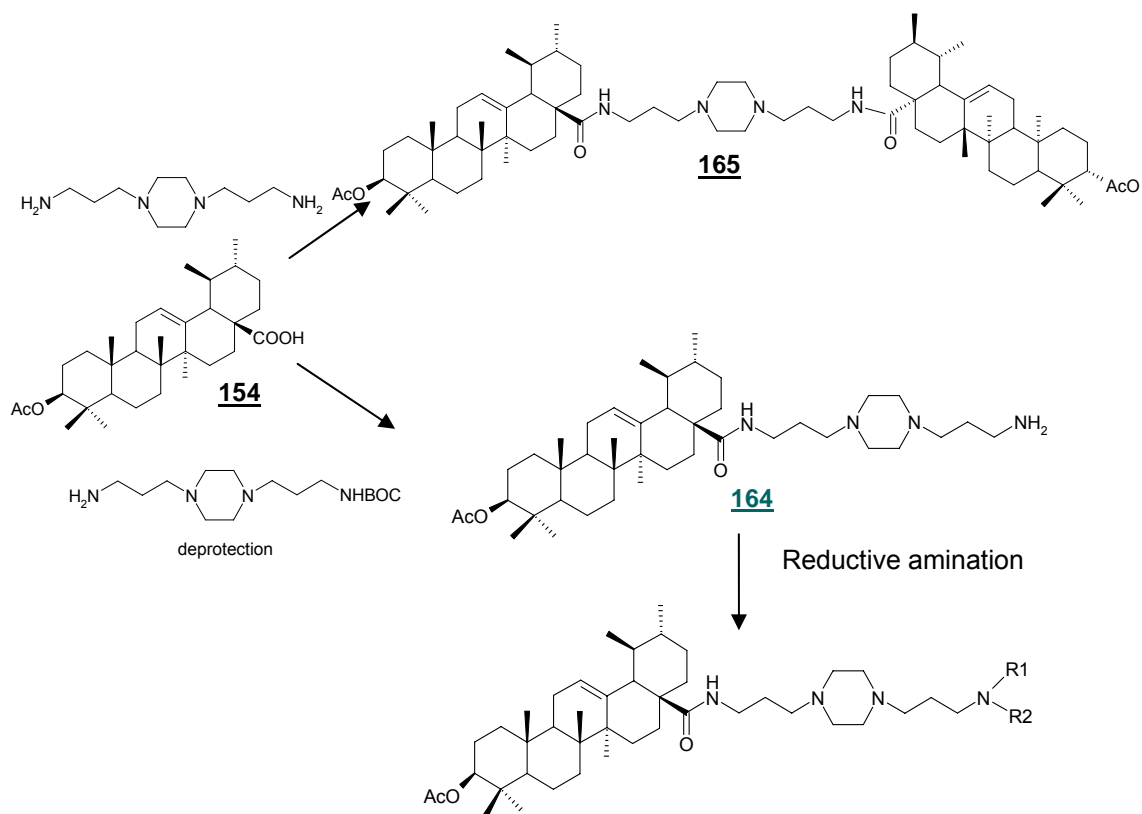
Dérivés piperaziniques de l'acide ursolique monoalkylés



Dérivés du ferrocène

VIII.2. General Reactions Scheme





IX BIOGRAPHY OF THE AUTHOR

CURRICULUM VITAE

Personal Data

Name : Simone Cristina Baggio Gnoatto
 Born : 03/10/1974 at Paim Filho/RS – Brazil
 Nationality : Brazilian
 Marital Status : Married
 Profession: Pharmacist
 Parents: Oracilda Baggio Gnoatto and Vitorino Gnoatto

Academic Background

2003 – 2007 Doctoral thesis in Pharmaceutical Sciences (in cotutela)
 Universidade Federal do Rio Grande do Sul (UFRGS), Brazil.
 Université de Picardie Jules Verne (UPJV), France.
 Research: Synthesis and antimalarial activity of triterpenoid derivatives from *Ilex*.
 Advisors: Prof. Grace Gosmann (Brazil) and Pr Pascal Sonnet (France).

2000 – 2002 Master of Sciences, Faculdade de Farmácia
 Universidade Federal do Rio Grande do Sul (UFRGS), Brazil.
 Research: Desenvolvimento de Metodologia Analítica para a Quantificação de Marcadores Químicos em Solução Extrativa e Extrato seco por Nebulização de *Ilex paraguariensis*.
 Advisor Prof. Valquiria Linck Bassani.

1993 – 1997 Pharmacy School at Universidade Federal do Rio Grande do Sul (UFRGS), Brazil.

Academic Fellowships

October 2006 – July 2007	Conselho Nacional de Desenvolvimento Científico e Tecnológico, Brazil - CNPq.
March 2004 – September 2006	Coordenação de Aperfeiçoamento de Pessoal de Nível Superior, Brazil - CAPES
December 2003 – February 2004	Conselho Nacional de Desenvolvimento Científico e Tecnológico, Brazil - CNPq.
2000 – 2002	Conselho Nacional de Desenvolvimento Científico e Tecnológico, Brazil - CNPq.
1996 – 1997	Conselho Nacional de Desenvolvimento Científico e Tecnológico, Brazil - CNPq.

Publications

1. GNOATTO, S.C.B., BASSANI, V.L., COELHO, G.C., SCHENKEL, E.P. Influência do método de extração nos teores de metilxantinas em erva-mate (*Ilex paraguariensis* A. St.-Hil., Aquifoliaceae). **Química Nova** (São Paulo) v.30, p. 304-307, 2007.
2. GNOATTO, S. C. B., SCHENKEL, E.P., BASSANI, V.L. HPLC Method to Assay Total Saponins in *Ilex paraguariensis* Aqueous Extract. **Journal of the Brazilian Chemical Society** (São Paulo) v.16, p. 723 - 726, 2005.
3. LACERDA, L.D, GNOATTO, S.C.B., SILVA, R.C., LINS, G., SILVA, A.L., GRAEBIN, C., KOBER, U.A., PISONI, D.S., SILVA, E.O., POHLMANN, A. Reações de Cicloadição: Uma Abordagem Teórica e Aplicações em Síntese Orgânica. **Caderno de Farmácia** (Porto Alegre) v.21, p. 11 - 29, 2005.
4. TAKETA, A.T.C., GNOATTO, S.C.B., GOSMANN, G., PIRES, V.S., SCHENKEL, E.P., GUILLAUME, D. Triterpenes from Brazilian *Ilex* Species and Their *in vitro* Antitrypanosomal Activity. **Journal of Natural Products**. v.67, p. 1697 - 1700, 2004.
5. ATHAYDE, M. L., SCHENKEL, E.P., GNOATTO, S.C.B., GOSMANN, G., GIBERTI, G.C., GUILLAUME, D. Triterpenes and saponins from *Ilex argentina* Leaves. **Acta Farmacéutica Bonaerense** (La Plata) v.20, p. 13 - 16, 2001.

AWARDED PRIZE

Best Oral Presentation: **Conception et synthèse de nouveaux dérivés de génines triterpéniques d'*Ilex* à visée antipaludique**, 2005. At XIV Rencontres Européennes du Groupement de Pharmacochimistes de l'Arc Atlantique GP2A, Angers, France.

Professional data

- | | |
|-------------|--|
| 1998 – 1999 | Pharmacist in pharmacy store. |
| 2002 – 2003 | Substitute teacher in Medicinal Chemistry at Faculdade de Farmácia, Universidade Federal do Rio Grande do Sul, Brazil. |